Colonization of a smooth surface by Pseudomanas aeruginosa : image analysis methods
by Andreas R Escher

A thesis submitted in partial fulfillment of the requirements for the degree of Doctor of Philosophy in Civil Engineering
Montana State University

Abstract:
Primary adsorption of bacteria to a clean substratum has generally been described by measuring net accumulation. Thus, the independent processes that contribute to the overall accumulation of biofilm, such as adsorption, desorption, cell multiplication, and erosion, cannot be considered separately to help to elucidate mechanisms of early colonization. With the use of image analysis techniques and additional software, these individual processes at the substratum in a continuous flow system have been measured directly. Additional parameters, such as cell movement and direction, orientation of the colony forming units (CFU), spatial distribution at the surface, and shape are also quantified with this technique. With the continuous flow system, the influences of operational parameters such as fluid shear stress, the bulk properties of the fluid, and the characteristic of the substratum can also be delineated in a fundamental manner. Two experimental variables, bulk CFU concentration and shear stress have been used to investigate early colonization under different conditions and to determine the rate controlling factor in biomass accumulation. In addition, a novel method for quantitative analysis of spatial distribution has been developed.

It was found that adsorption and desorption rates are independent of the surface concentration whereas growth and surface related processes are independent of bulk concentrations. At low surface concentration, P. aeruginosa tend to adsorb randomly. With increase in surface concentration the spatial distribution of adsorbing CFU becomes uniform indicating a formation of a repulsing area around adsorbed cells.

COLONIZATION OF A SMOOTH SURFACE BY PSEUDOMONAS AERUGINOSA: IMAGE ANALYSIS METHODS

by

Andreas R. Escher

A thesis submitted in partial fulfillment
of the requirements for the degree

of

Doctor of Philosophy

in

Civil Engineering

Montana State University
Bozeman, Montana

December 1986

APPROVAL

of thesis submitted by

Andreas R. Escher

This thesis has been read by each member of the thesis committee and has been found to be satisfactory regarding content, English usage, format, citations, bibliographic style, and is ready for submission to the College of Graduate Studies.

31 Dec '86 — Date

W. Elmachli — Chairperson, Graduate Committee

Approved for the Major Department

31 Dec '86 — Date

Theodore E. Lang — Head, Major Department

Approved for the College of Graduate Studies

1-12-87 — Date

M R Walker — Graduate Dean

STATEMENT OF PERMISSION TO USE

In presenting this thesis in partial fulfillment of the requirements for a doctoral degree at Montana State University, I agree that the Library shall make it available to borrowers under the rule of the Library. I further agree that copying of the thesis is allowable only for scholarly purposes, consistent with "fair use" as prescribed in the U.S. Copyright Law. Requests for extensive copying or reproduction of this thesis should be referred to University Microfilms International, 300 North Zeeb Road, Ann Arbor, Michigan 48106, to whom I have granted "the right to reproduce and distribute copies of the dissertation in and from microfilm and the right to reproduce and distribute by abstract in any format."

Signature: 

Date: 12/22/86

TABLE OF CONTENTS

Table of Contents (continued)

Table of Contents (continued)

LIST OF TABLES

LIST OF FIGURES

List of Figures (continued)

List of Figures (continued)

List of Figures (continued)

ABSTRACT

Primary adsorption of bacteria to a clean substratum has generally been described by measuring net accumulation. Thus, the independent processes that contribute to the overall accumulation of biofilm, such as adsorption, desorption, cell multiplication, and erosion, cannot be considered separately to help to elucidate mechanisms of early colonization. With the use of image analysis techniques and additional software, these individual processes at the substratum in a continuous flow system have been measured directly. Additional parameters, such as cell movement and direction, orientation of the colony forming units (CFU), spatial distribution at the surface, and shape are also quantified with this technique. With the continuous flow system, the influences of operational parameters such as fluid shear stress, the bulk properties of the fluid, and the characteristic of the substratum can also be delineated in a fundamental manner. Two experimental variables, bulk CFU concentration and shear stress have been used to investigate early colonization under different conditions and to determine the rate controlling factor in biomass accumulation. In addition, a novel method for quantitative analysis of spatial distribution has been developed.

It was found that adsorption and desorption rates are independent of the surface concentration whereas growth and surface related processes are independent of bulk concentrations. At low surface concentration, P. aeruginosa tend to adsorb randomly. With increase in surface concentration the spatial distribution of adsorbing CFU becomes uniform indicating a formation of a repulsing area around adsorbed cells.

INTRODUCTION

Microbial cells attach firmly to almost any surface submerged in aquatic environments. The immobilized cells grow, reproduce, and produce extracellular polymers which extend from the cell forming a matrix of molecular fibers which provide structure to the assemblage termed a biofilm. Biofilms are sometimes distributed relatively evenly over the wetted surface and other times are quite "patchy" in appearance. Biofilms can consist of a monolayer of cells covering only a fraction of the substratum or can be 300-400 mm thick as observed in algal mats. Biofilms are generally heterogenous, frequently containing more than one distinct microbial environment. For example, biofilms with aerobic as well as anaerobic environments are frequently observed. Consequently, the term biofilm does not necessarily reflect a surface accumulation which is uniform in time and/or space.

Relevance of Biofilms

Biofilms serve beneficial purposes in the natural environment as well as in some modulated or engineered biological systems. Biofilms are responsible for removal of

contaminants from natural streams and in wastewater treatment plants. Biofilms in natural waters frequently control water quality by influencing dissolved oxygen levels and serve as a sink for many toxic and/or hazardous materials. Biofilm reactors are used in some common fermentation processes (e.g. "quick" vinegar process) and are being considered more frequently for biotechnological applications.

On the negative side biofilms result in fouling. Fouling is the accumulation of a deposit on equipment surfaces which result in decreased performance and/or reduced equipment lifetime. Biofilms have been observed to increase fluid frictional resistance in water conduits and on ship hull surfaces. Microbial (as opposed to macrobial) films can significantly increase drag of a ship. Biofilm accumulation in pipes has been observed to reduce the flow rate by as much as 50% even when the film thickness was 0.1% of the pipe diameter (Characklis, 1973). Biofouling deposits decrease heat transfer in power plant condensers on shipboard as well as in land based power plants (Turakhia and Characklis, 1984). As a result, the power plant consumes more fuel to produce the same amount of power. The accumulation of biofilms has also been linked with accelerated corrosion of metallic surfaces, deterioration of

wooden structures, and degradation of concrete structures. Reduced performance may be observed in many other ways.

For a better understanding of biofilms it is essential not only to study fully developed biofilms but also the mechanisms of the buildup, i.e. the early colonization of surfaces by bacteria, the separation between adsorption and desorption, and between other, growth related processes.

Previous Research

Much of the emphasis on adsorption of microbial cells has concentrated on biological and chemical aspects of mechanisms with little emphasis on physical factors in the environment or concern about the rate of adsorption. Nor has much consideration been given to the influence of the initial events on the extent of subsequent biofilm accumulation or the biofilm composition.

In most, if not all reported research on microbial cell adsorption, net cell accumulation at the substratum is observed (Figure 1). Most of the microbial adsorption research has been conducted in quiescent (i.e., fluid velocity equals zero), closed (i.e., no input or output flows) systems. Such systems create a significant number of

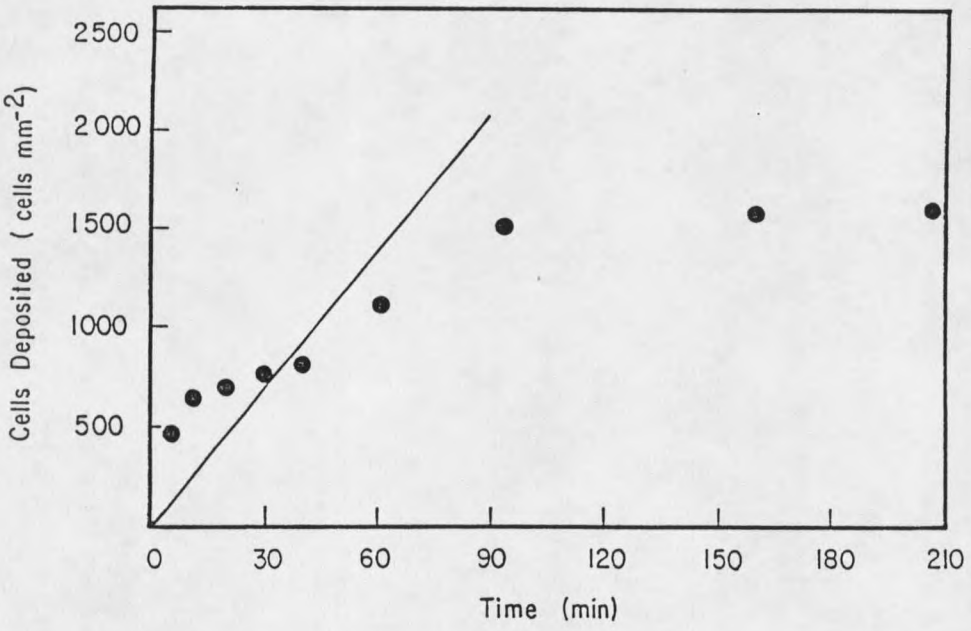

Figure 1. Experimental data from Powell and Slater (1983) for adsorption of Bacillus cereus to the surface of clean glass at a shear stress of 0.075 N m^{-2} and temperature of 53° C. The straight line represents the theoretical adsorption rate for non-motile cells calculated from Bowen et al. (1979).

experimental artifacts leading to rate data which are irrelevant to environmental and/or technical applications. Thus, open, continuous flow experimental systems will be described. The initial events in the accumulation of cells at the substratum consist of the following steps, each occurring with a characteristic rate:

1. Transport of the cell from the liquid phase to the substratum.

2. Cell adsorption to the substratum, a direct substratum-particle interaction.

3. Desorption of some of the adsorbed cells and their reentrainment in the liquid phase.

4. In some cases, microbial reproduction may contribute to the initial events.

These processes occur either in parallel or in series and, thus, the overall rate of cell accumulation at the substratum will be determined by the combination of the different rates. Variables such as fluid shear stress, liquid phase cell density, and nutrient concentration influence each individual process rate to a different extent and, therefore, influence net cell accumulation. Consequently, the process for cell accumulation in a tube enclosing turbulent flow will be very different from the one for a glass slide immersed in quiescent water, even though the net rate of accumulation may appear to be equal in both cases. Therefore, a closer look at each process is essential to develop a useful, predictive model for cell adsorption.

Goal of Research

The goal of the research is to determine the influence of different independent parameters, such as fluid dynamics,

biomass concentration in the bulk flow, surface characteristics (interface free energy), and cell physiology on early colonization of surfaces.

Objectives of Research

The specific objectives of the research related to early colonization of substrata are as follows:

1. Develop a method to directly measure the rate of different processes contributing to colonization.

2. Develop a method to observe individual "behavioral"[1] characteristics of the organisms at the substratum for elucidating mechanisms contributing to early colonization of surfaces.

3. Derive a mathematical model describing the accumulation of biomass during the early stage of biofilms accumulation.

---

[1] "Behavioral" characteristics include all the characteristics which can be observed but are not part of the kinetic system, such as shape, orientation, gliding at the substratum, and more.

BACKGROUND

Process Analysis

During the early events of fouling, biomass can be expressed as colony forming units (CFU), or cells. This distinction is essential since cells can adsorb in groups or as single cells. Moreover, not all the cells accumulate at the surface through transport alone. Cells can be produced at the substratum (growth), the number of cells per colony can change with time, or cells may glide away from their colony of origin to form a new colony. The following four processes must be distinguished (Figure 2) in terms of CFU:

Transport: This process is responsible for carrying the CFU to a point adjacent to the substratum. This step does not include the adsorption process.

Adsorption: This process is defined as the linking of the CFU with the substratum. The cell is adsorbed to the substratum only if it has a linkage to it and, hence, becomes immobilized for a finite time.

Desorption: Desorption is the breaking of the linkage of the CFU and its complete removal from the substratum. Desorption is the reverse of adsorption.

CFU - Separation: A CFU with more than one cell can split into two independent CFU. This process forms a new CFU at the substratum and, hence, contributes to the accumulation of CFU at the substratum. CFU-separation is a growth related process.

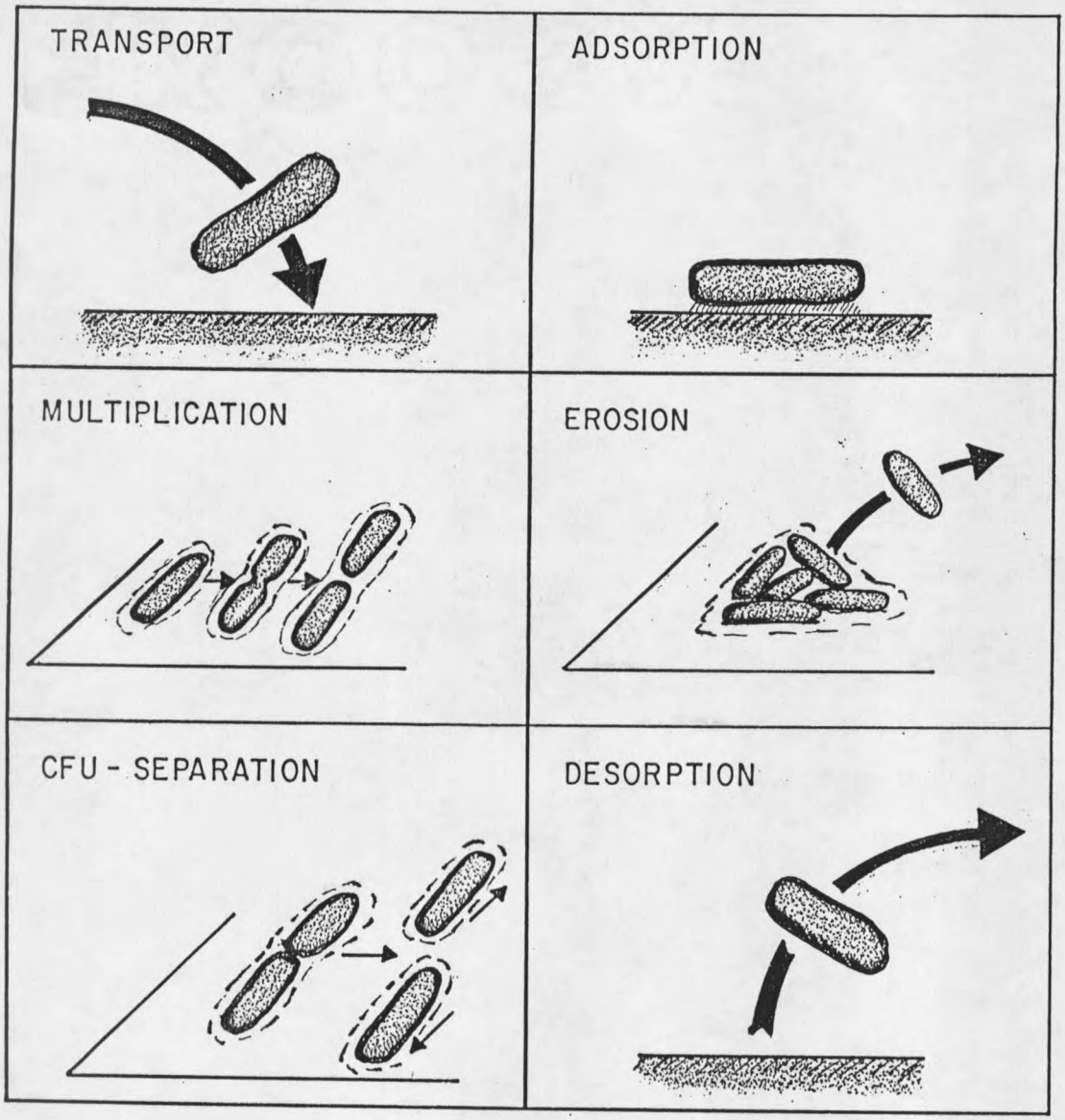

Figure 2. Definition of processes during early colonization of a substratum.

These four processes can be expressed in terms of cells by using the number of cells in each individual CFU. However, CFU - separation does not contribute to the accumulation in terms of cells. Two additional processes can be defined (after transport, adsorption, and desorption) when cell accumulation is considered:

> Multiplication: Multiplication is related to cellular growth, but only refers to those daughter cells which remain within the same CFU. Cells within a CFU multiply and increase the number of cells within this CFU. This does not change the accumulated number of CFU but does change the accumulated number of cells.
>
> CFU - Erosion: Cells within a CFU can "detach" and, hence, reduce the cell number of the CFU. This process is the reverse of multiplication.

Therefore, processes of early colonization can be separated into sorption- and growth-related which then can be expressed as rates. With these rates, mass balances for accumulation both in terms of CFU and cells can be accomplished:

$$\frac{d\,CFU}{dt} = + K_{ads} - K_{des} + K_{sep} \qquad 2.1$$

Accumulation CFU	Adsorption CFU	Desorption CFU	Separation CFU

$$\frac{d\ cell}{dt} = + K_{ads} - K_{des} + K_{mul} - K_{ero} \qquad 2.2$$

Accumulation cells	Adsorption cells	Desorption cells	Multiplication cells	Erosion cells

Equations 2.1 and 2.2 demonstrate the importance of measuring the different process rates for a better understanding of surface colonization mechanisms, since they reveal whether growth- or sorption-related processes dominate the accumulation.

Transport

For a better understanding of adsorption processes and comparison between adsorbed and suspended biomass, the transport process must be understood very well, both in terms of transport of biomass to the substratum and the transport of nutrients to the adsorbed biomass.

Currently, most of the information about kinetics of cellular adsorption and desorption has been derived from stagnant systems with no shear stress. The absence of flow or shear forces in natural and engineered systems is not common and, therefore, not of great practical interest. To define transport in quiescent systems is not an easy task,

since it depends on parameters , i.e. diffusivity, which can not be measured directly. Additionally, adsorption kinetics in stagnant systems are subject to artifacts produced by the combination of sedimentation and active adsorption rates. Some studies in flow systems have been published, focusing on net accumulation rates at the substratum. From the literature, it appears that it is essential to measure both adsorption and desorption rates independently. Figure 1 (Powell and Slater, 1983) illustrates the difficulty in determining adsorption rates from the accumulation alone. The data fit the theoretical calculated rates poorly. Measuring accumulation rates instead of adsorption can lead to artifacts since accumulation can include other processes, such as cellular multiplication at the substratum, which are not related to adsorption itself but which can be a major contribution to an increased accumulation.

Transport and Adsorption to the Substratum

Diffusivity: Under laminar flow conditions, particles are transported to the substratum by diffusion perpendicular to the flow. Microorganisms with a size of 1 to 4 μm^3 have a very small Brownian motion and, hence, a small Brownian diffusivity. Therefore, motility is of considerable importance during the processes of transport but has often

been neglected in adsorption studies. Jang and Yen (1985) calculated the non-Brownian diffusivity (motility) for different microorganisms to be in the range of $0.4 \cdot 10^{-3}$ to $5.6 \cdot 10^{-3}$ mm² s^{-1}, compared to the Brownian diffusivity of $50 \cdot 10^{-6}$ mm² t^{-1}. They used the following equation to calculate non-Brownian diffusion:

$$D_c = \frac{v_r \cdot d_r}{3 \cdot (1 - \alpha)} \qquad 2.3$$

D_c : diffusivity [L² t^{-1}]
v_r : velocity of motility [L t^{-1}]
d_r : free length of random run [L]
α : main cosine of angle of turn [-]

Under condition of no chemotaxis, α can be assumed to be zero. If motility is not considered as a contributing factor in the process of transport to the substratum, the transport rate might be underestimated 20 to 50 times. The non-Brownian diffusivity can be calculated from the velocity and the mean free path length. Vaituzi and Doetsch (1969) measured speeds up to 55.8 µm s^{-1} for Pseudomonas aeruginosa with "track photography". Their results suggest a mean free path length of random run in the range of 50 to 85 µm. These values yield a non-Brownian diffusivity (Equation 2.3) of 10^{-3} mm² s^{-1} for P aeruginosa.

Transport Rate to the Substratum: Good information is available for the transport and adsorption of inert particles to different substrata. Bowen et al. (1976) proposed an analysis with a first-order-reaction approximation for the surface-particle capture rate, which leads to an expanded Graetz solution. This solution converges well for relatively large Peclet numbers and proved to be accurate for inert particles adsorbing to charged surfaces. The resulting equation has the following form:

$$K_{CFU} = \frac{c_0 \cdot D_c}{h} \cdot \left[\frac{\left[\frac{2}{9K_1}\right]^{1/3}}{\Gamma\left[\frac{4}{3}\right] + \left[\frac{1}{\epsilon}\right] \cdot \left[\frac{2}{9K_1}\right]^{1/3}} \right] \qquad 2.4$$

K_{CFU} : Adsorption rate of CFU to the substratum [# L^{-2} t^{-1}]
c_0 : CFU concentration in bulk liquid [# L^{-3}]
D_c : Diffusivity of CFU [L^{-2} t^{-1}]
h : Half-thickness of channel [L]
K_1 : Dimensionless distance from channel inlet [-]
ϵ : Surface-particle capture factor [-]
Γ : Gamma function [$\Gamma(4/3) = 0.89338$]

In the special case where the surface-particle capture rate ϵ approaches infinity ($\epsilon=\infty$), Equation 2.4 becomes:

$$N_{CFU} = \frac{c_0 \cdot D_c}{h} \cdot \left[\frac{\left[\frac{2}{9K_1}\right]^{1/3}}{\Gamma\left[\frac{4}{3}\right]} \right] \qquad 2.5$$

N_{CFU} : Flux of CFU to Substratum [# L^{-2} t^{-1}]

The strength of this solution is that one can estimate the flux of particles to the substratum ($\epsilon=\infty$, Eq. 2.5) and obtain a discrete value for the surface-particle capture factor, independent of concentration and motility, for different substrata. In addition, a "sticking efficiency" can be calculated with Equations 2.4 and 2.5 by dividing adsorption rate by the CFU flux to the substratum.

Assay for Substratum Properties: The use of Equations 2.4 and 2.5 to describe transport and adsorption processes, especially the dimensionless factor ϵ, is a good analysis for studying the effects of different degrees of hydrophobicity of substrata (independent of concentration and diffusivity).

Fletcher and Marshall (1982) show an increase of accumulation with an increased hydrophobicity. They use the double-layer theory (DLVO) of the colloidal chemistry to explain these mechanisms, based on the calculated charge of the substratum measured with the bubble contact angle method

and the overall charge of the organisms. Van Pelt et al. (1985) showed that there is statistically seen a very poor correlation between the free surface energy and extent of accumulation. They propose as possible reasons for this poor correlation that accumulation as the measured value is not the most appropriate parameter to describe adsorption, that the free surface energy during the experiment is not the same as that previously measured, or that the mechanisms of adsorption are different depending on the free surface energy.

Van Pelt's first proposition is that the change in accumulation or the net adsorption is the result of adsorption minus desorption and, therefore, measurements of accumulation does not reflect the primary occurring process.

The second proposition is in accordance with the observation of the "conditioning film". This change of well defined surfaces due to exposure to water containing organic macro molecules has been described by Loeb and Neihof (1975), Baier and Weiss (1975), Abbott et al. (1983), and Little and Zsolnay (1986). They summarize the effect of a conditioning film that a solid surface in contact with liquids containing diverse organic macromolecules alter due to the formation of a monolayer of adsorbed macromolecules. This results in the following: hydrophobic surfaces become

hydrophilic, positively- and negatively-charged surfaces acquire a net negative charge and Zeta potentials, contact potentials, and critical surface tensions are increased.

The third proposition is that depending on the free surface energy cells use a different mechanism for adsorption. Fletcher and Marshall (1982) indicated the importance of proteins in the processes of adsorption. By adding Pronase they reduced the increase of accumulation. Paul and Jeffrey (1985) showed that for hydrophobic substrata, such as polystyrene, the protein linking is essential, whereas for hydrophilic substrata other adsorptive mechanisms dominate. Their result indicates that, indeed, different mechanisms of adsorption dominate depending on the free energy of the substratum.

Growth-Related Processes

Very little work has been done in regard to growth-related processes during early colonization of surfaces. Only two groups of studies are available:

1. The early phase of biofilm accumulation (Trulear, 1983; Turakhia, 1986).

2. Growth measurements with Image Analysis (Caldwell and Lawrence, 1986,).

Trulear and Turakhia determined growth rates in biofilms grown under constant shear stress and turbulent flow. During the first or second day after exposure of acrylic plastic surfaces to P. aeruginosa, the adsorbed biomass had a growth rate ($\mu \geq 0.65\ h^{-1}$) exceeding the maximum growth rate in suspension ($\mu_{max} \approx 0.5\ h^{-1}$). After this initial time, the measured overall growth rates were reduced to levels below the maximum rate in suspension. Their results do not indicate whether this increased initial activity is due to prior physiologic or genetic phenomena or due to analytical variations after adsorption. Data suggest that the process of adsorption is very selective for the "more active" organisms (cells with a high motility have a greater diffusivity).

Caldwell and Lawrence (1986) measured "behavior" of adsorbed P. fluorescens under laminar flow conditions. They observed different patterns of adsorption and subsequent growth at the substratum. Unfortunately, they do not state the shear stress of the liquid on the wall but only an average velocity. From the publication, shear stress cannot be calculated since the geometry is unknown. The growth rates measured do not answer all questions since the substrate concentration used were unusually high (1 g glucose l^{-1} and 100 mg glucose l^{-1}). The cells were grown in batch cultures and washed twice before being used in the

adsorption study. The measured specific growth rates are in the range of 0.42 h^{-1}.

Spatial Distribution

The spatial distribution of the CFU during adsorption can be of great value since it can determine whether the process is controlled by the adsorbing cells alone or a cell - substratum interaction (including the existing colonization). If the process is due to cells only, without any influence by the substratum's present state of colonization, a random distribution would be expected. If conditioning and occupation of the surface positively influences adsorption, then an aggregated distribution can be anticipated. A uniform distribution, conversely, results when the area around an existing CFU is blocked for adsorption indicating a negative influence. Classic Nearest Neighborhood Analysis cannot be used for this analysis since only distance to the single nearest neighbor is used ignoring the other adsorbed cells. An analysis is needed which accounts for the overall population density. An extensive description of a unique solution for spatial distribution analysis is presented in Appendix A.

Fluid Dynamics

Defined fluid dynamics is essential for adsorption studies under constant shear stress. Hydrodynamics control both transport and adsorption: Transport is a function of the loading rate and adsorption depends on shear stress. Due to this relationship, it is difficult to compare experimental results obtained under different hydrodynamic conditions without their precise definition. Two different flow patterns must be considered:

1. Turbulent flow
2. Laminar flow

Turbulent Flow

The nature of turbulent flow does not allow an easy determination of the velocity gradients near the wall. Depending on the Reynolds number of the flow and the roughness of the wall, a wide variety of velocity gradients and, thus, shear stresses are possible. Using the theory of the "viscous sublayer", within its limitations, i.e. smooth surface, it is possible to estimate the shear forces.

According to Prandtl, this viscous sublayer can be explained and estimated in the following way: Due to the viscosity of the liquid, the velocity at the wall is zero and the resulting shear forces in the liquid adjacent result in reduction of the velocity. This generates a layer with a viscous flow which extends into the flow with an increasing velocity up to the point where the flow starts to become fully turbulent. The transition from the boundary layer to the turbulent bulk flow is asymptotical. Therefore, the thickness of this layer cannot be determined unequivocally. Generally, the thickness of the layer is defined as the point where the theoretical flow velocity reaches 99% of the outer bulk velocity. In reality, this problem is complicated by the possible existence of three forms in the viscous sublayer: a laminar boundary layer, a transition region, and a turbulent boundary layer with a laminar sublayer. In addition, any disturbance of the substratum changes the development of the boundary layer. According to Dracos (1973), the shear stress at the wall can be estimated if the friction factor is known (flat plate):

Laminar boundary layer:

$$c_f = 0.66 \cdot \left[\frac{v_\infty \cdot x}{\mu} \right]^{-1/2} \qquad 2.6$$

c_f : friction factor [-]

v_∞ : mean bulk velocity [L t^{-1}]
x : length of layer development [L]
μ : viscosity [L^2 t^{-1}]

Turbulent boundary layer:

$$c_f = 0.059 \cdot \left[\frac{v_\infty \cdot x}{\mu} \right]^{-1/5} \qquad 2.7$$

with the c_f values of Equations 2.6 or 2.7 the shear force at the wall can be calculated:

$$\tau_0 = c_f \cdot \frac{1}{2} \cdot d \cdot v_\infty^2 \qquad 2.8$$

τ_0 : shear stress at wall [F L^{-2}]
d : density of liquid [F t^2 L^{-4}]

According to Equations 2.6 - 2.8, a turbulent flow with mean bulk velocity of 0.5 m s^{-1} will produce a shear stress of 0.34 N m^{-2} along a flat plate after a length of 10 m. This calculation for flat plates can, with caution, be used for larger diameters of pipes, especially if one assumes frequent irregularities and, hence, uses Equation 2.6 for the calculation of the friction factor.

Laminar Flow

Laminar flow is analytically much simpler than

turbulent flow. The velocity profile is parabolic and shear stress can be calculated according Newton's law:

$$\tau_{xy} = - \mu \frac{dv_y}{dx} \qquad 2.9$$

x : length axis of system
y : height

The boundary conditions for this system are fairly simple: both the wall velocity and the shear stress at the symmetry point are zero. There are no undefined boundary layers or troublesome asymptotic approaches as in turbulent flow.

CONCEPTUAL MODEL OF SURFACE COLONIZATION

The analysis of adsorption, desorption and growth related processes during the early colonization of a substratum cannot be considered in traditional terms of continuum mass balances. Rather, population balances, where the single observed particles are individual members of the total population must be used. For population balances, the probability of an event, in terms of the total population, is the key factor.

Population Balance in Terms of CFU

The population balance will be made in terms of Colony Forming Units (CFU), an individual observable particle which consists of one to many cells. Each CFU can be observed and treated individually with the image analyzing system.

Transport

Particles or cells are transported by momentum transport in the laminar flow parallel to the substratum. There is no momentum transport perpendicular to the

substratum. However, the particles or cells are transported to the surface by a diffusive random movement. Assuming that chemotaxis is absent, this diffusive transport is either a Brownian motion or the random motility of the cell itself. Hence, a Brownian and a "non-Brownian" diffusion is responsible for the transport to the substratum. The non-Brownian diffusion, which can be calculated with the average free path length and velocity of the random movement, can exceed the Brownian motion by orders of magnitude.

"Transport" does not define the physicochemical interaction of the particles with the substratum, but only the transport to the substratum. Particles might "hit" the substratum due to transport and come to a brief stop. But as long as they do not interact with the substratum, even if they are visible to the observer, they are not considered adsorbed. Transport depends on the total concentration of particles through the system and the particle diffusivity D_∞. The rate of transport is the number of particles transported to the substratum per unit area and per time.

Adsorption

Adsorption refers to a direct particle-substratum interaction. It does not include the transport to the substratum but only the direct interaction of a particle, which has been transported to the substratum, with the substratum. The probability of adsorption for a CFU transported to the substratum can be defined as "sticking efficiency". This probability may depend on surface characteristics of the particles and the substratum as well as the fluid shear stress at the surface. Last, but not least, the physiological state of organisms can influence adsorption.

The rate of adsorption, therefore, is a function of the rate of transport and the probability of adsorption and has units of particles per unit area per time.

Reversible versus Irreversible Adsorption

When CFU adsorb to a substratum, their linkage can be relatively weak, but strong enough to resist shear stress of the liquid for some time. Due to the poor connection, they have a probability to desorb after a short time. By

improving their linkage to the substratum with time, their probability of desorption decreases. Hence, as soon as their probability to desorb reaches zero, they are irreversibly adsorbed. During the period where their probability to desorb is greater than zero, they are "reversibly adsorbed". The time interval between adsorption and the time at which CFU's are either sheared off or irreversibly adsorbed, is the offset time of desorption for reversibly adsorbed CFU. This concept of reversibly adsorbed CFU and offset time is not the same as used in other experiments (Fletcher and Marshall, 1982), where the term "irreversibly adsorbed CFU" indicates the amount of CFU washed off after termination of an experiment. In this text, it is used to describe a mechanism during the process of adsorption. Therefore, the offset time is a specific time interval during the process of adsorption dependent on the physiology of the adsorbing CFU, shear stress, and substratum.

This concept can be used to describe kinetically the findings by Brash and Samak, 1978. They found that there is a dynamic equilibrium (turnover) between proteins in the bulk flow and adsorbed to the substratum. As soon the bulk concentration was reduced to zero, the surface concentration remained constant in a static equilibrium (no turnover),

indicating that the molecules went through the state from reversibly to irreversibly adsorbed.

Desorption

Desorption refers to an entire CFU detaching from the substratum and reentering the bulk liquid. The probability of desorption is more related to probability of adsorption than to the total number of CFU at the substratum, indicating that the chances for a CFU remaining at the substratum increases as its residence time increases (see reversible adsorption versus irreversible adsorption). Thus, the probability of desorption is not equal for all adsorbed CFU since a CFU improves its bonding to the substratum with time. The rate of desorption can be defined as the product of the probability of desorption (ß) with the rate of adsorption. This probability is a function of shear stress, physiological state of CFU, and characteristics of the substratum. Desorption offset time, t_{∞}, defines the time interval between the start of adsorption (t=0) and the first desorption event ($t=t_{\infty}$) in an experimental run.

CFU-Separation

CFU-separation is the separation of a CFU into two independent CFU's and is a process related to growth at the substratum. CFU-separation increases the number of CFU at the substratum but not the number of cells so it is important to the CFU population balance. Since all irreversibly adsorbed CFU have the same probability per time to separate, this probability is defined as a first order kinetic rate coefficient. The total rate expression of CFU-separation has the units of number of CFU per area and per time. The probability (not the rate) of CFU-separation depends on shear stress, substratum characteristics, and physiology of the CFU, but is independent of the CFU concentration at the substratum.

Other Processes at the Substratum

Adsorption, desorption, and CFU-separation are the only processes relevant to the description of the colonization processes in terms of CFU. However, the experimental system only permits observation of a limited substratum area and CFU can enter or exit the field of observation. Therefore, for experimental purposes, two additional processes have to

be considered: 1.) CFU entering and 2.) CFU exiting the field.

Population Balance in Terms of Cells

The number of cells per CFU can be calculated (area measurement and division by standard cell size) to obtain a population balance in terms of cells. All processes described in terms of CFU can be translated into terms of cells. As indicated before, CFU-separation does not contribute to the cell accumulation. However, other growth related processes contribute to the population balance in terms of cells.

Multiplication and Erosion

Multiplication is a growth related process at the substratum. Whenever a cell within a discrete CFU is growing and the newly formed daughter cell remains within the same CFU, the process of multiplication is observed. If the newly formed cell is lost immediately due to shear forces, no multiplication will be observed since this process describes only the formation of new cells which remain within the same CFU. In case an established cell

within a CFU (with more than one cell) detaches and reenters the bulk flow, the CFU is eroding. If a CFU erodes, it loses cells to the bulk flow without being removed itself.

The probabilities of multiplication and erosion are defined in the same way as CFU-separation. All the irreversibly adsorbed cells have the same probability for multiplication and subsequent erosion. The probability terms for both are defined as a probability per time (analog to first order kinetics). The rates for multiplication and erosion are expressed as number of cells per area per time.

Kinetic Expressions in Terms of CFU

The rate expressions of the model, conceptually described above, will be used in this section more explicitly to derive the kinetic equations of the population balance.

According to the previously described processes the "stoichiometry" of the CFU population balance can be written in the following way:

$$[CFU]_{bulk} \longleftrightarrow [CFU]_{rev} \longrightarrow [CFU]_{irrev} \qquad 3.1\ a$$

suspended biomass — reversible adsorbed biomass — irreversible

$$[CFU]_{tot} = [CFU]_{rev} + [CFU]_{irrev} \qquad 3.1\ b$$

Total adsorbed CFU — total reversibly adsorbed CFU — total irreversibly adsorbed CFU

Using these stoichiometric equations (3.1 a and 3.1 b), the kinetics and surface concentrations can be determined with the equations that follow.

Transport from Bulk Flow to Substratum

Deposition rate of colloidal particles from a laminar flow to the walls of a parallel plate, as described by Bowen et al. (1976) will be used for CFU. The local transport rate to the substratum is given by:

$$K_{CFU} = \frac{c_0 \cdot D_c}{h} \cdot \left[\frac{\left[\frac{2}{9K_1}\right]^{1/3}}{\Gamma\left[\frac{4}{3}\right] + \left[\frac{1}{\epsilon}\right] \cdot \left[\frac{2}{9K_1}\right]^{1/3}} \right] \qquad 3.2$$

K_{CFU} : Adsorption rate of CFU to the substratum [# CFU L^{-2} t^{-1}]
c_0 : CFU concentration in bulk liquid [# CFU L^{-3}]
D_c : Diffusivity of CFU [L^2 t^{-1}]
h : half-thickness of channel [L]
K_1 : dimensionless distance from channel inlet [-]
ϵ : surface-particle capture factor [-]
Γ : Gamma function [$\Gamma(4/3) = 0.89338$]

Equation 3.2 accounts for the CFU transport to the region ultimately adjacent to the substratum and also for the particle-substratum interaction (adsorption). K_1, the dimensionless length, is calculated with the following equation:

$$K_1 = \left(\frac{1}{Pe} \right) \cdot \left(\frac{8x}{3h} \right) \qquad 3.3$$

h : Half-thickness of channel [L]
x : Length from inlet [L]
Pe : Peclet number [-]

Peclet number describes the ratio of bulk velocity to convective velocity and is defined:

$$Pe = \frac{4 \cdot v_m \cdot h}{D_c} \qquad 3.4$$

v_m : Average velocity in channel [L t^{-1}]
D_c : Diffusivity [L^2 t^{-1}]

The non-Brownian diffusivity of bacteria (motility) (Equation 2.3) can be calculated with the free path length and the rate of motion in the random movement of bacteria (Jang and Yen, 1985):

$$D_c = \frac{v_r \cdot d_r}{3 (1 - \alpha)} \qquad 3.5$$

v_r : "linear swimming speed" [L t^{-1}]
d_r : mean traveling length of random run [L]
α : mean cosine of angle in random turn

If a non-chemotactic movement is assumed, α becomes equal to zero.

The upper limit of transport (without adsorption) can be calculated by assuming the surface-particle capture rate approaching infinity (i.e. $\epsilon = \infty$). This upper limit assumes that the substratum is an infinite sink for CFU with reduces Equation 3.2 to:

$$N_{CFU} = \frac{c_0 \cdot D_c}{h} \cdot \left[\frac{\left[\frac{2}{9K_1} \right]^{1/3}}{\Gamma \left[\frac{4}{3} \right]} \right] \qquad 3.6$$

N_{CFU} : Flux of CFU to substratum [# CFU L^{-2} t^{-1}]

Equation 3.6, assuming the substratum as a total sink, can only be used to determine the flux of CFU to the substratum. It should not be used for a mass balance within the bulk liquid!

Population Balance at Substratum

CFU from the bulk liquid adsorb at the substratum first as reversible and then as irreversible CFU (Equation 3.1). The population balance for the two groups can be written:

Reversible Adsorption (CFU):

$$\frac{d[CFU]_{rev}}{dt} = K_{CFU} - K_{Cdes} - K_{Ctran} \qquad 3.7$$

accumulation — adsorption — desorption — transformation

[CFU] : CFU concentration at substratum [# CFU L^{-2}]
K_{Cdes} : Desorption Rate CFU [# CFU L^{-2} t^{-1}]
K_{Ctran}: Transformation from reversible to irreversible adsorbed CFU [# CFU L^{-2} t^{-1}]

Irreversible Adsorption (CFU):

$$\frac{d[CFU]_{irrev}}{dt} = K_{Ctran} + k_{sep} \cdot [CFU]_{irrev} \qquad 3.8$$

accumulation — transformation — CFU-separation

k_{sep} : Probability of separation [t^{-1}]

Total CFU:

$$\frac{d[CFU]_{tot}}{dt} = \frac{d[CFU]_{rev}}{dt} + \frac{d[CFU]_{irrev}}{dt} \qquad 3.9$$

Equation 3.7 can be integrated in the following way with the boundary conditions:

$t=0 \longrightarrow [CFU]_{rev}=0$ and $t \leq t_r \longrightarrow K_{cdes}, K_{ctran} = 0$ (t=0 : first observation of adsorption). This boundary condition leads to a discontinuous function with respect to t:

$$[CFU]_{rev} = \begin{cases} K_{CFU} \cdot t & t \leq t_r \\ (K_{CFU} \cdot t) - (K_{cdes} + K_{ctran}) \cdot (t - t_r) & t \geq t_r \end{cases} \qquad 3.10$$

t_r : Offset time of reversible adsorption $[t^{-1}]$

The rates K_{cdes} and K_{ctran} (for $t \geq t_r$) can be expressed by the probability term β_c for desorption:

$$[CFU]_{rev} = K_{CFU} \cdot [\, t - \{\beta_c + (1-\beta_c)\} \cdot (\, t - t_r \,)\,] \qquad 3.11$$

If β_c is independent of time, then the population balance of reversible adsorbed CFU in Equation 3.11 can (for $t \geq t_r$) be reduced to:

$$[CFU]_{rev} = K_{CFU} \cdot t_r \qquad 3.12$$

Equation 3.12 states that the number of reversibly adsorbed CFU per area is independent of time.

The population balance for the irreversible CFU (Eq. 3.8) can be integrated with the boundary conditions: $t=t_r$ ——> $[CFU]_{irrev}=0$. This boundary condition stands for the assumption that, for any time smaller than t_r no transformation from CFU_{rev} to CFU_{irrev} will occur. This assumption leads to a discontinuous function for $[CFU]_{irrev}$ with the break point $t=t_r$:

$$[CFU]_{irrev} = \begin{cases} 0 & t \leq t_r \\ \left[\frac{K_{ctran}}{k_{sep}}\right] \cdot \left[e^{k_{sep}(t-t_r)} - 1 \right] & t \geq t_r \end{cases} \qquad 3.13$$

In Equation 3.13 the term for K_{ctran} can be replaced with the probability term:

$$K_{ctran} = K_{CFU} \cdot (1 - \beta_c) \qquad 3.14$$

which puts irreversible accumulation into a direct relationship to the adsorption rather than the transformation rate.

According to Equation 3.1 b, Equations 3.12 and 3.13 can be combined for total CFU, using the assumption of Equation 3.14:

$$[CFU]_{tot} = \begin{cases} K_{CFU} \cdot t & t \leq t_r \\ (K_{CFU}) \cdot \left[t_r + \left[\frac{1-\beta_c}{k_{sep}} \cdot \left[e^{k_{sep}(t-t_r)} - 1 \right] \right] \right] & t \geq t_r \end{cases} \qquad 3.15$$

This equation describes the kinetics in terms of total CFU.

Kinetic Expressions in Terms of Cells

Since the cell number for each individual CFU can be measured, all the events in term of CFU can be translated into terms of cells. Additionally, a change in cells per individual CFU can be observed. Hence, the processes of cell multiplication and erosion can also be defined. CFU-separation, a process which does not contribute to the change of total cells adsorbed, is omitted.

Transport from Bulk to Substratum

Transport can be defined in the same way as for CFU (Eq. 3.2):

$$K_x = \frac{c_x \cdot D_c}{h} \cdot \left[\frac{\left[\frac{2}{9K_1}\right]^{1/3}}{\Gamma\left[\frac{4}{3}\right] + \left[\frac{1}{\epsilon}\right] \cdot \left[\frac{2}{9K_1}\right]^{1/3}} \right] \qquad 3.16$$

K_x : Adsorption rate of cells [# cell L^{-2} t^{-1}]
c_x : cell concentration in bulk liquid [# cell L^{-3}]
D_c : Diffusivity of CFU [L^2 t^{-1}]
h : half-thickness of channel [L]
K_1 : dimensionless distance from channel inlet [-]
ϵ : surface-particle capture factor [-]

The main difference between Equation 3.2 and Equation 3.16 is the difference of concentration. As is the case for Equation 3.2, Equation 3.16 represents the rate of adsorption. The dimensionless distance K_1 is the same for both equations, since the initial measurement is made in terms of CFU and then translated into cells. Hence, Equation 3.3 - 3.5 are unchanged. The rate of transport (not adsorption) can be defined in analogy to Equation 3.6:

$$N_x = \frac{c_x \cdot D_c}{h} \cdot \left[\frac{\left[\frac{2}{9K_1}\right]^{1/3}}{\Gamma\left[\frac{4}{3}\right]} \right] \qquad 3.17$$

N_x : flux of cells to substratum [# cell L^{-2} t^{-1}]

Population Balance at Substratum

Cells at the substratum undergo a transformation from reversibly to irreversibly adsorbed cells. The population balances for cells are similar to those for CFU (Eq.3.7 - 3.9).

Reversible Adsorption (cells):

$$\frac{d[x]_{rev}}{dt} = K_x - K_{xdes} - K_{xtran} \qquad 3.17$$

[x] : Cell concentration at substratum [# cell L^{-2} t^{-1}]
K_x : Adsorption rate cells [# cell L^{-2} t^{-1}]
Kxdes: Desorption rate cells [# cell L^{-2} t^{-1}]
K_{xtran}: Transformation rate irreversible adsorp. [# cell L^{-2} t^{-1}]

Irreversible Adsorption (cells):

$$\frac{d[x]_{irrev}}{dt} = K_{xtran} + (k_{mult} - k_{eros}) \cdot [x]_{irrrev} \qquad 3.18$$

k_{mult} : Multiplication rate [t^{-1}]

$k_{erosion}$: Erosion rate $[t^{-1}]$

Total cells:

$$\frac{d[x]_{tot}}{dt} = \frac{d[x]_{rev}}{dt} + \frac{d[x]_{irrev}}{dt} \qquad 3.19$$

where [x] is the cell concentration at the substratum, K_{xdes} the desorption, and K_{xtran} the transformation rate to irreversible adsorbed cells. With the boundary conditions: $t=0 \longrightarrow [x]_{rev}=0$ and $t \leq t_r \longrightarrow K_{xdes}=0$, $K_{xtran}=0$. This boundary condition leads to a discontinuous function in respect of t:

$$[x]_{rev} = \begin{cases} K_x \cdot t & t \leq t_r \\ (K_x \cdot t) - (K_{xdes} + K_{xtran}) \cdot (t - t_r) & t \geq t_r \end{cases} \qquad 3.20$$

If the probability β_x of desorption is independent of time then Equation 3.20 can for the case of $t \geq t_r$ simplified (analogous to Eq.11 and 12) to:

$$[x]_{rev} = K_x \cdot t_r \qquad 3.21$$

With that simplification, $[x]_{rev}$ becomes independent of time.

For the irreversible adsorbed cells Equation 3.13 can be adapted after combining k_{multi} and $k_{erosion}$ in Equation 3.18:

$$k_{xnet} = k_{mult} - k_{eros} \qquad 3.22$$

Then Equation 3.13 becomes:

$$[x]_{irrev} = \begin{cases} 0 & t \leq t_r \\ \left[\frac{K_{xtran}}{k_{xnet}}\right] \cdot \left[e^{k_{xnet}(t-t_r)} - 1\right] & t \geq t_r \end{cases} \qquad 3.23$$

Using an analogous step to Equation 3.14 and combining Equations 3.20 - 3.23, the Equation for the total cell concentration at the substratum can be written as it has been done in Equation 3.15 for CFU:

$$[x]_{tot} = \begin{cases} K_x \cdot t & t \leq t_r \\ (K_x) \cdot \left[t_r + \left[\frac{1-\beta_x}{k_{xnet}} \cdot \left[e^{k_{xnet} \cdot (t-t_r)} - 1\right]\right]\right] & t \geq t_r \end{cases} \qquad 3.24$$

Thus, with Equation 3.15 and 3.24 it is possible to estimate the accumulation of both CFU and cells at the substratum with time.

Sticking Efficiency

Sticking efficiency is a parameter frequently used to describe the ratio of adsorption rates to the flux to the substratum. Thus, it is an overall probability of adsorption. The sticking efficiency is not identical to the Surface-Particle Capture Factor ϵ, but rather a function of it. In terms of CFU, the sticking efficiency can be described by the ratio of Equations 3.2 to 3.7, and in terms of cells by the ratio of Equations 3.16 to 3.17:

$$\Phi = \frac{\Gamma\left[\frac{4}{3}\right]}{\Gamma\left[\frac{4}{3}\right] + \left[\frac{1}{\epsilon}\right] \cdot \left[\frac{2}{9K_1}\right]^{1/3}} \qquad 3.25$$

Φ	:	Sticking efficiency [-]
ϵ	:	Surface-particle capture factor [-]
K_1	:	Dimensionless distance from channel inlet [-]
Γ	:	Gamma function [$\Gamma(4/3) = 0.89338$]

Thus, the sticking efficiency Φ has a range of zero to one. Sticking efficiency, Φ, is the probability that a CFU being transported to the substratum will adsorb. The surface-particle capture factor ϵ is part of the extended Graetz solution for a mass balance of the bulk liquid and the substratum in terms of adsorption.

Summary of the Conceptual Model

The model describes the population balance for both CFU and cells at the substratum. The parameters used in this model can vary with cell concentration in the bulk liquid and shear stress at the substratum. All relevant parameters in this model, with the exception of the non-Brownian diffusivity, can be measured experimentally or calculated with the method described in "Kinetic Results". Non-Brownian diffusivity can be estimated with literature values and direct observations.

EXPERIMENTAL SYSTEM AND METHODS

Experimental System

The experimental system consists of a chemostat system, a rectangular capillary tube, and an image analyzer similar to the system described by Powell and Slater (1983):

Microbial cells grown in continuous culture (chemostat) provide continuous inoculum for the experimental system with minimal variation in cell physiological state and cell concentration throughout an experiment. Prior to beginning the experiment, cell concentration in the chemostat is measured by direct count. The cell size distribution is also determined for calculating cell numbers per CFU.

The desired cell concentration at the capillary entrance is obtained by dilution in the mixing chamber. The effluent from the mixing chamber is pumped through the rectangular capillary (Wale Apparatus) at a constant rate using a non-pulsing gear pump. The inside surface of the rectangular capillary is the substratum in these experiments and the processes occurring at this surface are monitored continuously by a video camera mounted on the microscope.

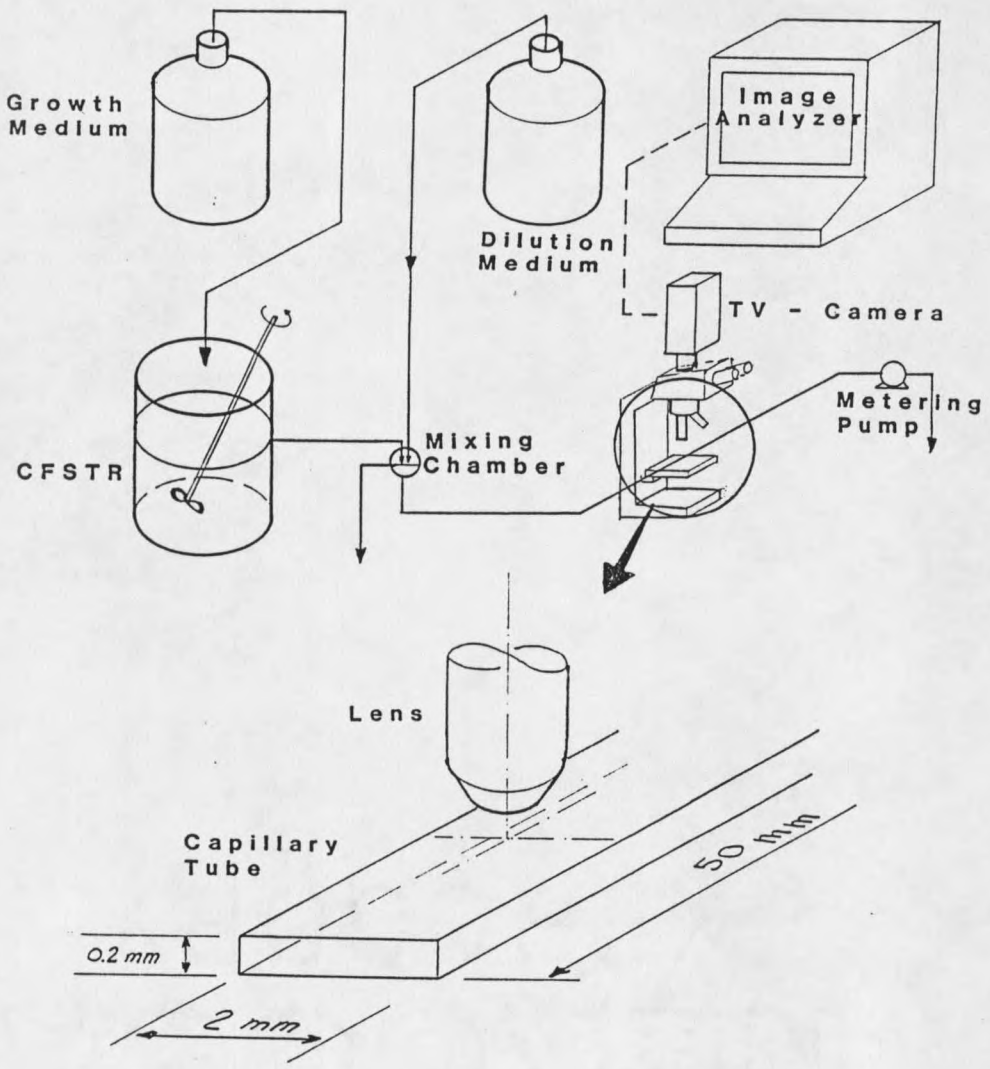

Figure 3. Schematic of the system.

The video signal is transmitted to the image analyzer which then converts the grey image into a binary image. The image analyzer accumulates this image into a "tracking" image which is similar to a multiple exposure and displays all of the images simultaneously in different colors on the screen.

A single binary image of the specimen is stored on disk at constant time intervals (e.g., every five minutes) for later analysis. After every tenth binary image stored (50 minutes), the tracking image formed during this period is also stored. A micro-irregularity in the substratum (1 - 3 µm) is used as a reference point to focus the microscope, set the detection levels, and to measure and correct for drift of the specimen during the experiment.

Image Analyzer

The Image analyzer used in this setup is the Cambridge Q10, equipped with an image analyzer unit (68000 processor) and four independent binary image planes (storage of four complete binary images within the RAM - memory), and CP-M controlling unit (64 K RAM). It digitizes grey images in a grey scale from 0 (black) to 64 (white) in variable slices into a binary image with 512 * 480 pixels. Logical operations of the binary images from one image plane to another are possible, as well as manual editing of the image with a digitizer pad. Binary images (34 K) can be stored onto disks (640 K) for later analysis. Two different kinds of image measurements are possible:

a) Field measurements are made on an overall basis, including number of features, area coverage, average feature size and more.

b) Feature measurements are made on each individual feature detected within the image. They include coordinates, area, length, width, orientation, shape (roundness), perimeter, etc. Each type of measurements can be called independently for further calculations.

In addition to the display and output of the measurements, the image analyzer can perform limited statistical analysis on the measurements. Up to eight different distribution histograms can be calculated at the same time. The instrument has two different routines, one in compiled C (high level machine language) and one in M-Basic. The image analyzer has a communication link for data transfer to an IBM-compatible computer.

Modification of the Programs

The standard Basic program package, consisting of 15 interactive subroutines, has been modified in several places to make the machine useful to study adsorption processes. During the booting up of the analyzer, one disk drive can be selected solely for the storage of images. A new subroutine (Phase F) has been written to create "tracking images" and to store real images as well as the tracking images. This

subroutine uses the same variables as the standard routine, version 2.10 (copyrighted by Olympus-Cambridge). Hence, all the parameters used in this subroutine can be defined in the Setup Section of the Image Analyzer. Subroutine Phase 4 has been modified with a logical switch to recall images stored on disk instead of detecting of a new binary image. In the user function subroutine (Phase A), results of the image measurement are stored in form of random access files (RAF) for later analysis in the sorting routine ("assembly of CFU"). This form has been selected because space requirements for these RAF files are less than for normal ASCII-files, and input-output operations are performed more quickly.

Data Collection and Analysis

Image Collection

During an experimental run, the only data manipulation is done in the form of creating and storing binary images. Two different kinds of images are collected, the real image and the tracking image. The latter is comparable to a photographic multiple exposure with an additional depiction every second (see Figure 4). This tracking image serves two purposes: to visualize the movement of the CFU at the substratum during the entire experiment, and to determine

the total area fraction covered by CFU during the entire period, including the "tracks". The tracks, however, are not real trails in the sense of footprints left by the CFU but rather the artificial visualization of the path.

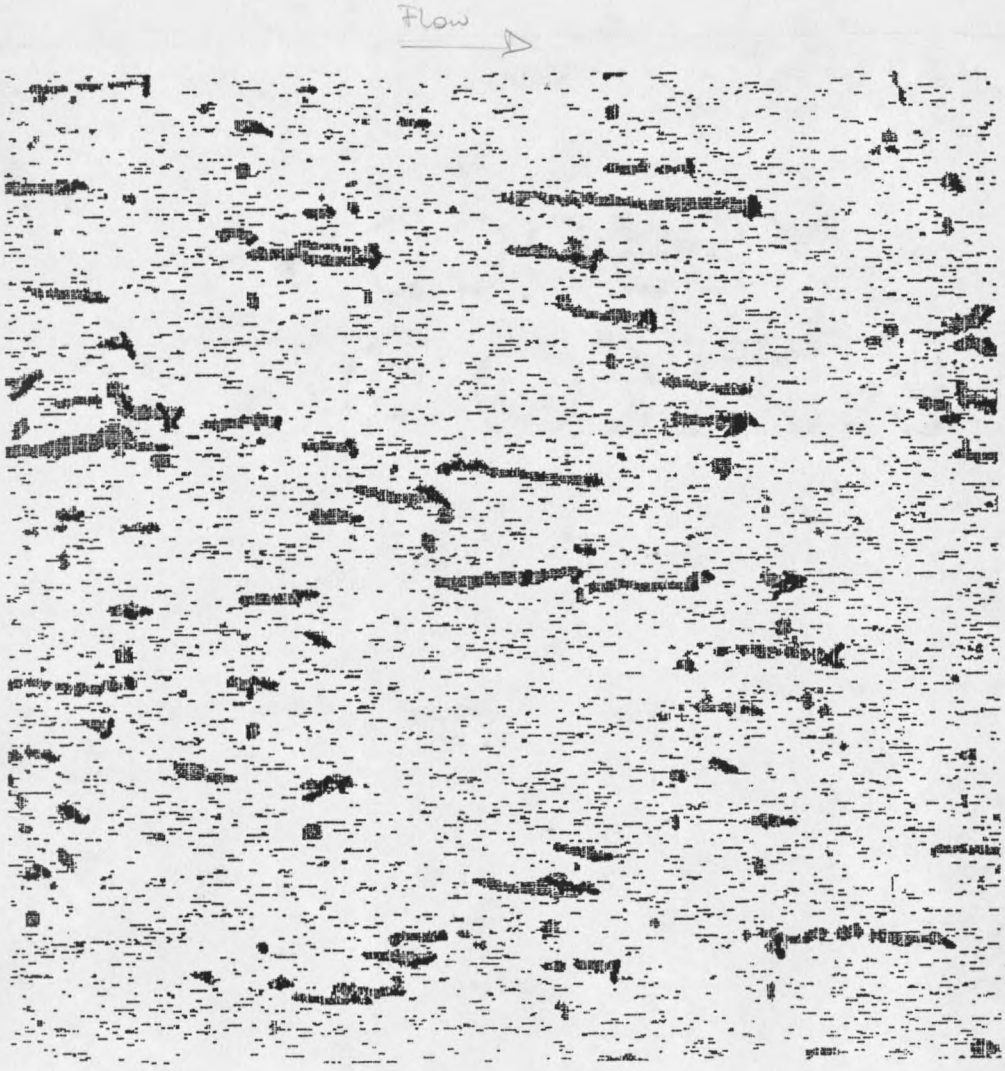

Figure 4. Tracking Image. 1.0 N m^{-2}, 10^6 cells/ml. Flow direction from left to right. The grayish areas are the tracks of the colonies and the dark areas within the tracks the colony forming units (CFU). The streaks are markings of "hits" by CFU transported to the substratum without adsorbing. Size of observed image: 150 · 150 µm

Fixpoint Calculation

After completion of the real time experiment and prior to the analysis of the single images, the movement of the fixpoint has to be calculated. This step requires that the fixpoint be isolated from all the other CFU within the image. The easiest way to achieve this task is by manually editing the image of the total tracks for the track of the fixpoint alone. Then, with a logical exclusion, the feature of the fixpoint for each image can be separated and measured individually. The measurements include the true midpoint coordinates which are stored in a data file. This routine can be done either before or within the analysis routine.

Image Analysis

Once the coordinates of the fixpoint have been calculated, it is then possible to analyze the images for the CFU. For each CFU detected, the following measurements are done:

X- and Y- coordinates of each detected CFU (feature count point),

Minimum and maximum X- and Y- values of the CFU to calculate the true midpoint corrected for the drift of the specimen holder,

Area,

Length,

Width,

Orientation of the length axis,

Shape (roundness).

At the same time, the cell number per CFU is calculated to obtain a cell number per CFU distribution for the analyzed field. In this routine, the results will be corrected for the possible drift of the specimen holder during the experimental run using the fixpoint coordinates. All the data obtained are stored on disk in form of random access files for further analysis. Up to this point, the evaluation of the data is done in a two dimensional way with the coordinates as the two dimensions.

Data Assembly

In this routine, data will sorted and assembled for each CFU with time as the third dimension. This can either be done with the image analyzer or with an IBM compatible system. In the image analyzer, the tracking image provides a criterion for the continuation of a CFU with time. As

long as the routine finds a data point in the next image, within the same track, it will use it as the continuing point of the same CFU. If it finds two possible points for continuation, it selects the closer of the two to the last analyzed point, and labels the other as a potential daughter CFU (CFU-separation). Within the image analyzer, this routine is relatively slow since it requires frequent interactions with the image analyzer unit and multiple image handling.

The routine within an IBM-compatible computer uses a less rigid criterion for the evaluation of the continuation. Instead of using the tracks, it uses a range (4 by 6 μm) within which a continuation is allowed. If it finds two possibilities to continue, it selects the closer one and labels the other a possible daughter-CFU (CFU-separation). Since this system can use a hard disk setup and a machine language version of the programs, this routine is much faster in an IBM-compatible system than in the Image Analyzer.

Both systems reevaluate possible CFU-separations during the assembly process. If the mother-CFU does not decrease in size during a possible division, the separation will be rejected.

Other than the above differences, the sorting routine performs the same functions in the two systems. In addition to the three dimensional analysis this routine calculates the neighbor analysis, the dimensionless nearest neighbor distance, the influence number (not dimensionless), and the dimensionless influence number. Additionally, this routine calculates the movements and directions of the CFU at the surface and monitors changes in cell numbers per CFU. The latter will be used to determine the number of events of cell multiplications with time at the surface as well as erosion of CFU. The organization of these data files is listed in Appendix B. Since accumulation of both CFU and cells can be influenced by colonies moving into and out of the field, the program identifies those new appearances close to the image frame. The calculation by this routine can be summarized in the following way:

1. Calculation of the values for each CFU, including first and last observations.

2. Determination whether each CFU adsorbed, separated, or migrated into the field, and whether they desorbed, or migrated out of the field.

3. Calculation of movement and direction for each CFU.

4. Conversion of the area of each CFU into cells per CFU and calculation of the events of adsorption, desorption, multiplication and erosion in terms of cells at the surface.

5. Calculation of the neighborhood analysis during the first observation of each CFU.

Subsequently, the sorting routine builds several data files with a summary of data obtained. These files are in form of ASCII - files which can be translated into a format for Super Calc spread sheets and other statistical software.

Method of Analysis and Chemostat Operation

Direct Cell Count

Cell concentration in the bulk flow of the capillary tube was one of the main parameters of the experimental series. Therefore, it was necessary to use a fast and accurate method to determine the cell concentration of the chemostat effluent. The method of Hobbie et al. (1976) was adapted to use the Image Analyzer for counting. The filters used were evenly hydrophilic, so that surfactant treatment could be omitted. Thus, the filters retained the irgalan black much better under the high energy illumination than surfactant-treated filters. Counting the cells with the Image Analyzer facilitated and significantly improved the analysis. 10 fields on each filter were counted and the average of these counts used to determine the cell concentration. Standard errors of the counts per filter were in the range of 7 to 12%, significantly lower than the error by the manual method. Replicates of several filters with the same sample (count of three filters per sample)

yielded for the average values per filter a standard error of less than 10%. Chemostat effluent samples were sonicated prior to the count to break up aggregation of the cells. A sub-sample (75 µl) was suspended in three ml 0.01% acridine orange (AO) for at least 5 min. It appears to be noteworthy to mention that cells from chemostat cultures appear mainly orange, whereas bacteria from natural environments (very low growth rate) are often green. Since orange cells are much better detected by the Image Analyzer than green ones (in contrast to direct count by eye) it can be necessary to heat the sample before staining to change green fluorescens to orange (denaturalizing of protein).

Cell Size Distribution

Cell size for single cells and the total population of the chemostat effluent were measured with the image analyzer prior to the experimental series to determine the cell number per adsorbed CFU in the capillary analysis. For this analysis white light phase contrast was used with a microscope magnification of 40•1.5. Single cells for the size distribution were selected manually, whereas all cells were accepted for the size distribution of the total population.

Mounting of Capillary Tube

Capillary tubes (Wale Apparatus) were precleaned by combustion (500°C) for several hours (over night) to remove all organic contamination in the inside. They were connected to $^1/_{16}$ inch diameter high pressure nylon tubing (6 cm) with heat-shrink PVC tubing (2 cm, diameter nominally $^1/_{16}$ inches). The connections were sealed and secured with silicon glue dispensed out of a tuberculin syringe (1 ml), and then heat fitted with hot air. This procedure to connected the flat capillary tubes tightly to the round tubing (no leaks on the microscope stage).

Chemostat Operation

A New Brunswick Bioflow C30 with a volume of 330 ml and a flow rate of 1.0 ml min^{-1} was used as chemostat. Thus, the dilution rate and growth rate was 0.18 h^{-1}. Temperature was maintained at 25° ± ½° C. Growth was carbon-limited with glucose as sole carbon source (44.4 mg l^{-1} as TOC). C to N ratio was 10 and C to P ratio 15. Phosphorus was used to buffer the system at pH 6.8. Calcium concentration was 50 mg l^{-1} as $CaCO_3$ (added sterile after heat sterilization to prevent precipitation in form of calcium phosphate).

Magnesium chloride concentration was 7.5 mg l^{-1}. Micronutrients were added according to Trulear (1983). The dilution liquid had the identical composition as the growth medium except that no organic carbon was present. The chemostat could be operated continuously for up to five days without heavy wall growth. Effluent glucose was measured colorimetrically with a specific enzyme reaction (Trulear, 1983).

RESULTS

Progression of Experiments

The results are based on 15 experiments, 9 at 0.5 N m^{-2} and two each at 0.75, 1.0, and 1.25 N m^{-2}. CFU concentration in the bulk flow of the capillary tube ranged from $1.1 \cdot 10^6$ to $11.2 \cdot 10^6$ CFU ml^{-1}. Each experiment lasted 300 min for colonization, and images were taken at 5 min intervals.

The extent of surface colonization by CFU under different conditions and the total surface coverage by tracks is displayed in Figures 5, 6, and 7 (not real tracks but artificial display of tracks; see "Image Collection"). The small dark areas are the colonies and the grayish, larger fields are the "tracks". The figures of the tracks were generated over a period of 300 minutes, and the colonies are the ones observed at 300 minutes after beginning of the experiment. Figures 5 and 6 are from experiments at 0.5 N m^{-2} with $1.1 \cdot 10^6$ and $10 \cdot 10^6$ CFU ml^{-1} respectively. Shear stress during colonization in Figure 7 was 1.25 N m^{-2} and CFU concentration $12.2 \cdot 10^6$ CFU ml^{-1}.

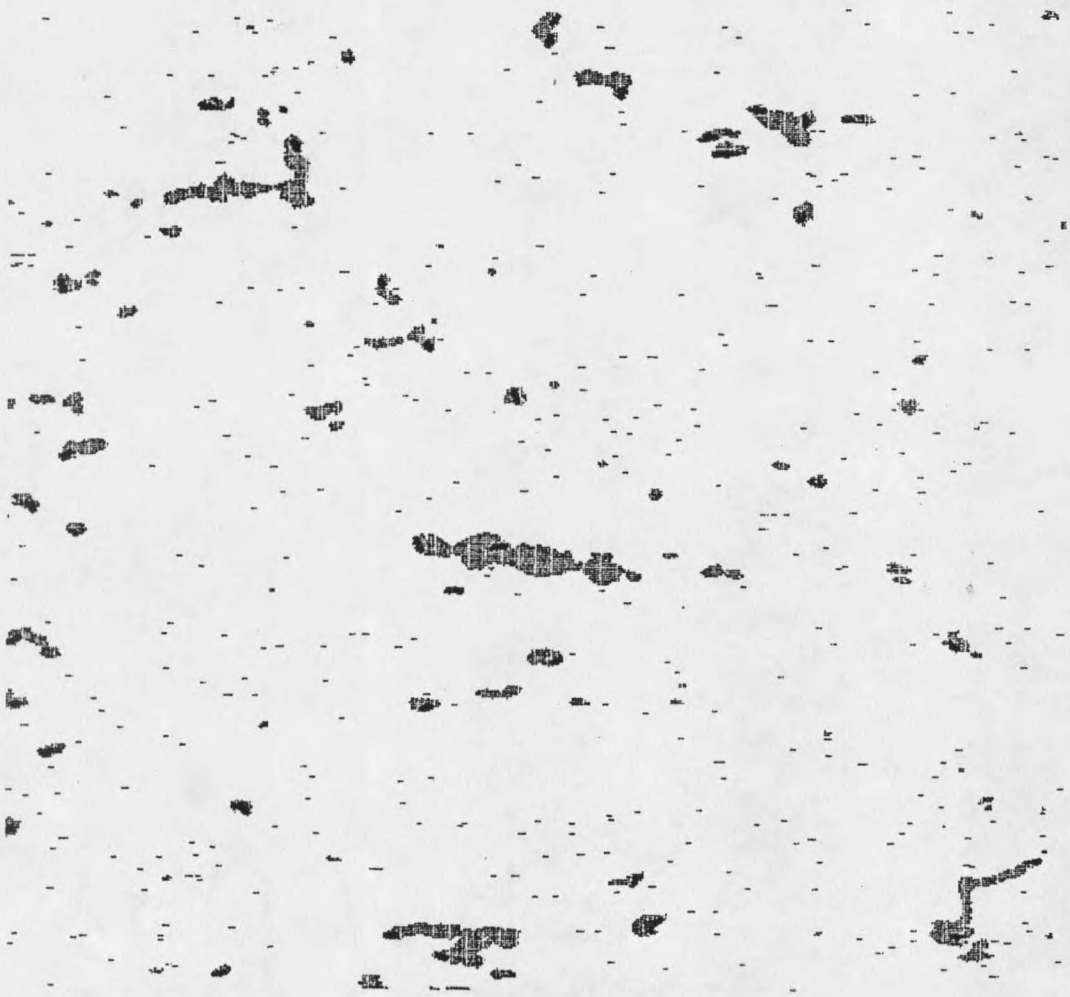

Figure 5. Tracking Image: 0.5 N m^{-2}, $1.1 \cdot 10^6$ CFU ml^{-1}, flow from left to right. The grayish areas are the tracks of the colonies and the dark within the tracks are the colonies (after 300 min). Size of observed area:150·150 µm. Area coverage by CFU: 0.35%, by tracks: 3.325%

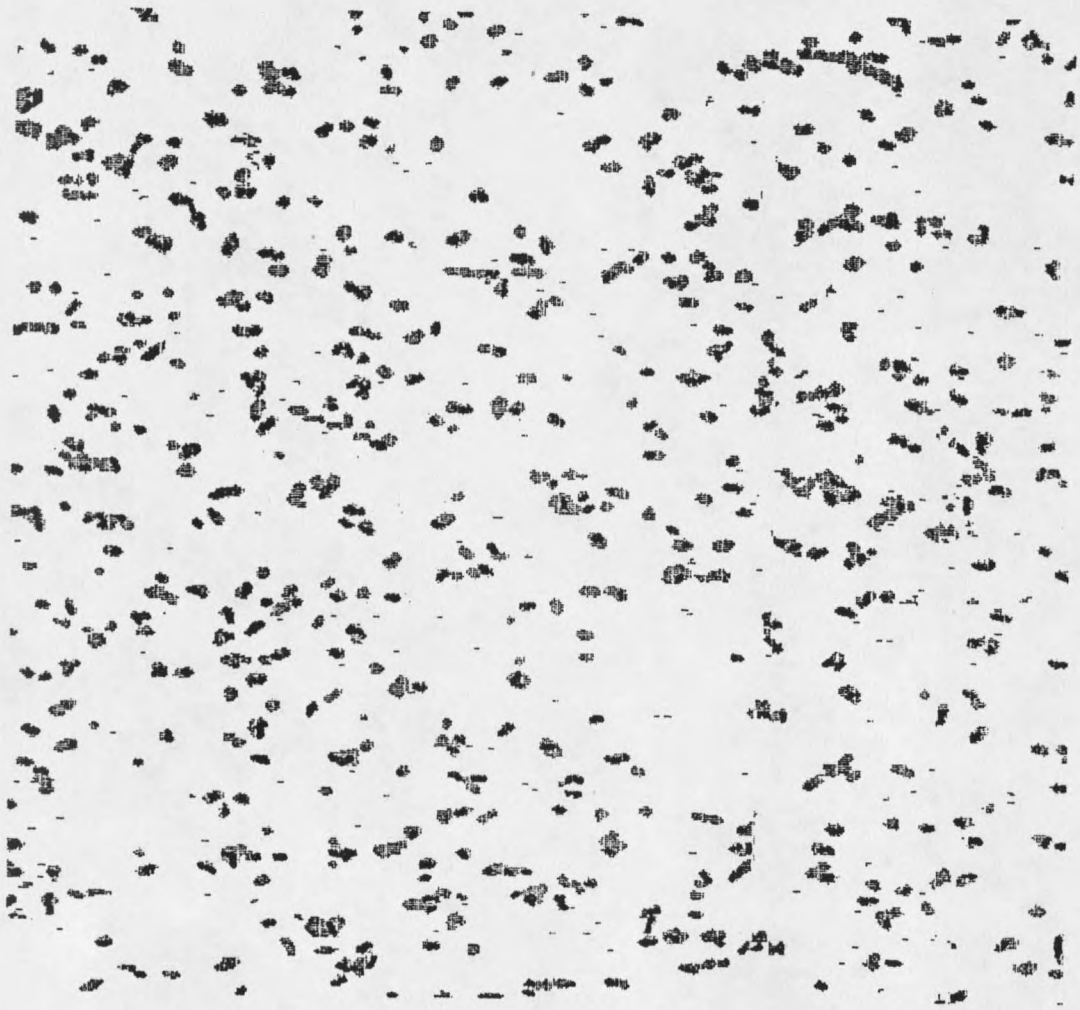

Figure 6. Tracking Image: 0.5 N m^{-2}, $10 \cdot 10^6$ CFU ml^{-1}, flow from left to right. The grayish areas are the tracks of the colonies and the dark within the tracks are the colonies (after 300 min). Size of observed area:150·150 µm. Area coverage by CFU: 3.04%, by tracks: 11.3%

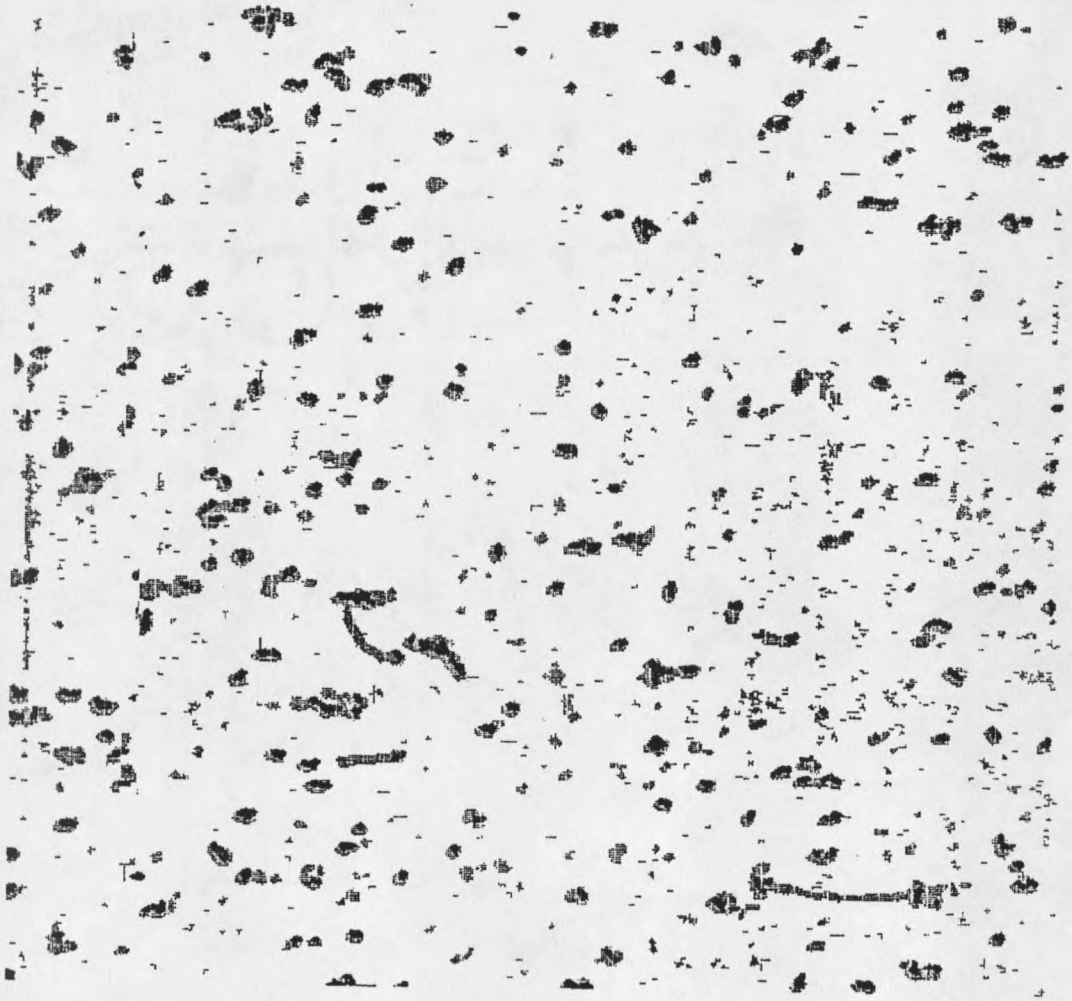

Figure 7. Tracking Image: 1.25 N m^{-2}, 12.2·10^6 CFU ml^{-1}, flow from left to right. The grayish areas are the tracks of the colonies and the dark within the tracks are the colonies (after 300 min). Size of observed area:150·150 µm. Area coverage by CFU: 1.9%, by tracks: 8.46%

The results can be grouped in three classes:

1. Kinetic measurements
2. Behavioral distributions
3. Spatial distributions

Kinetic measurements describe the events at the substratum, i.e. events of adsorption, desorption, and growth related processes during the observation time interval (5 min) and their rates. The results describe the kinetics of substratum colonization.

"Behavioral" characteristics of each CFU observed, include size during first and last observation, age during last observation, movement, orientation, net growth, and so on. These results are not useful for kinetic analysis but help to elucidate the processes involved during the early colonization of a substratum.

The third group, spatial distribution, determines the degree of interaction of each CFU during its first observation with other CFU already established. This analysis is uncommon but very powerful in establishing mechanisms of adsorption in terms of spatial distribution.

Kinetic Results

The events of colonization on a glass substratum during the first 300 min can be presented in terms of CFU (Figure 8a), and areal coverage (Figure 8b). Adsorption kinetics can also be demonstrated in terms of cells (Figure 8c). Growth related processes are displayed in Figure 8c. Accumulation of biomass and areal coverage are presented as measured, but adsorption, desorption, and growth related processes are shown cumulative, i.e. the number of observed events were added to the number of the previous events. The slope of data displayed in this manner is equal to the rate. Thus, an increase of the slope indicates an increase of the rate.

Directly Measured Results

All results are presented in the Tables 9 to 23 (Appendix C). Each table represents an entire experimental series, whereas Figures 41 to 55 (Appendix D) represent the same results in graphic form. The summarized results are displayed in Tables 1 to 3. The nomenclature is in accordance to ones used in the conceptual model. Adsorption rate is a function of CFU concentration in the bulk flow

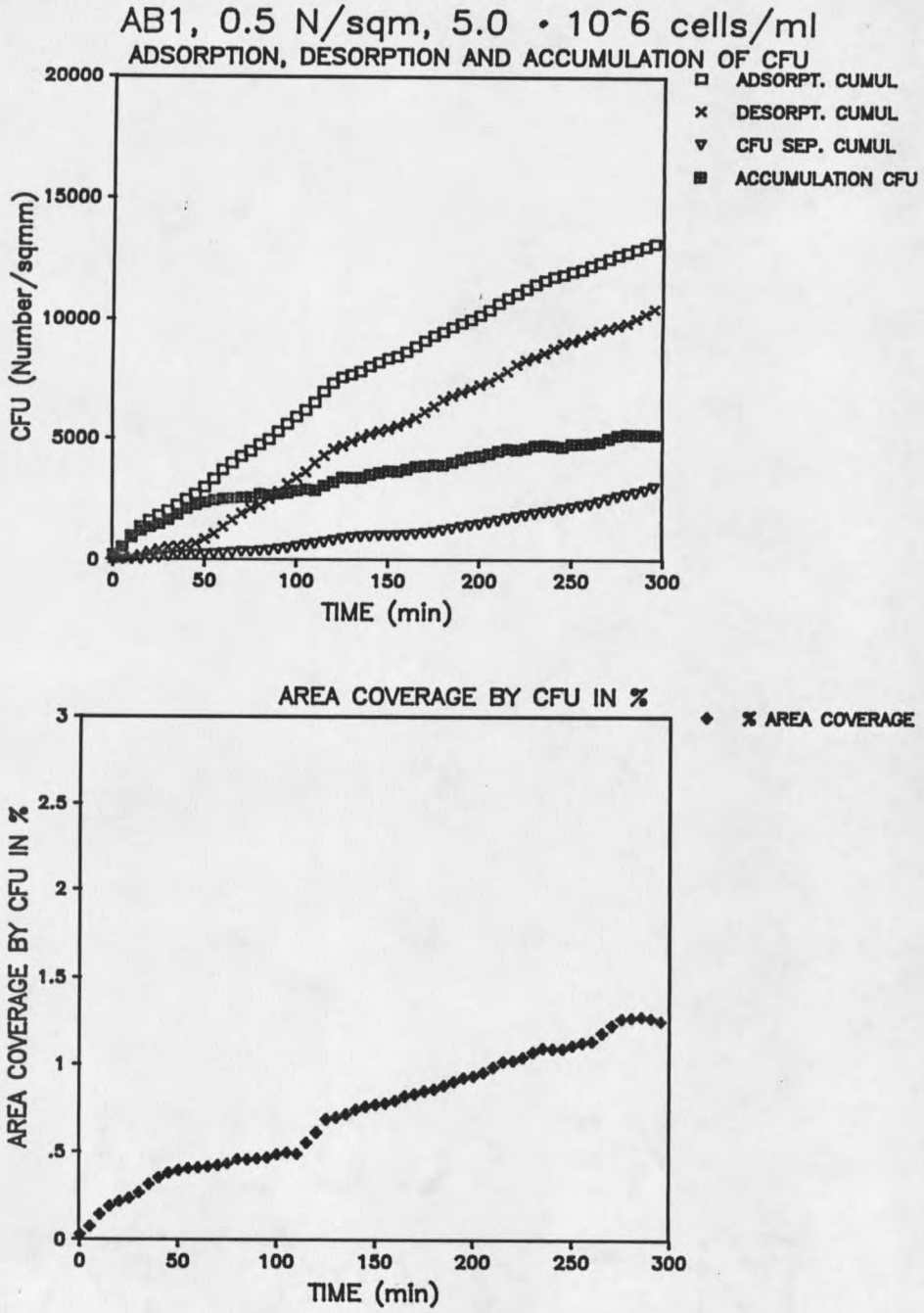

Figure 8. Typical progression of colonization in terms of CFU (8a) and area coverage (8b) during 300 min. of a smooth glass substratum. Shear stress: 0.5 N m^{-2}

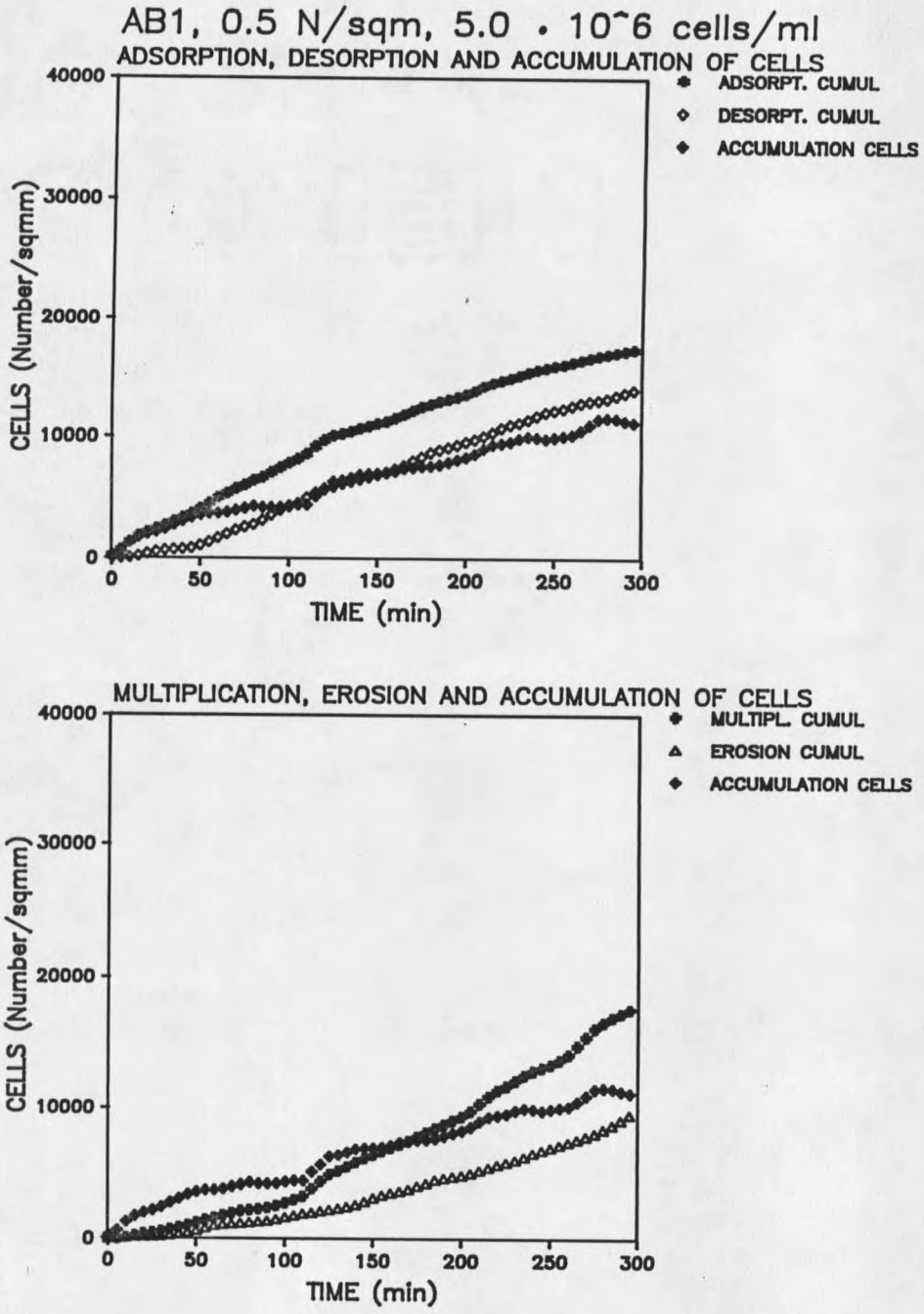

Figure 8. Typical progression of colonization in terms of cells. Adsorption related processes (8c) and growth related Processes (8d)

(Figure 9a and 9b). The linear regressions in these figures is calculated in Table 1 and presented as "Slope" and "intercept". Thus, the assumption of a direct proportionality between adsorption rate and bulk CFU concentration as stated in Equations 3.2 and 3.16 is valid. Figure 10a displays the desorption rates at the same shear stress for CFU and Figure 10b for cells. Data from these figures suggest that all regressions of the rates with cell concentration have their origin through the zero points of the coordinate system.

Growth related processes, such as CFU-separation, cell multiplication, and erosion for a shear stress of 0.5 N m^{-2} are displayed in Figure 11, 12a and 12b respectively. These first order rates do not show a correlation with cell concentration in the bulk flow, which is in accordance with Equations 3.8 and 3.18.

Shear Stress: 0.5 N m^{-2}

ZERO ORDER KINETICS, Rate [# min^{-1} mm^{-2}]

Series #	CFU/ml	Adsorption CFU	Desorption CFU	Adsorption Cell	Desorption Cell
AA1	1.1e6	8.18 ± 2.46	7.54 ± 4.17	14.38 ± 2.46	11.37 ± 5.81
AB3	1.1e6	5.99 ± 2.38	2.34 ± .90	10.43 ± 4.28	3.73 ± 1.47
AA4	1.92e6	13.52 ± 4.53	10.07 ± 4.82	16.20 ± 5.5	10.92 ± 4.97
AB2	2.45e6	19.34 ± 3.48	10.24 ± 4.63	30.18 ± 3.62	15.26 ± 6.80
AA3	2.75e6	20.50 ± 6.28	11.11 ± 5.29	34.33 ± 10.29	16.70 ± 7.89
AC2	3.64e6	27.29 ± 3.75	11.11 ± 8.24	47.61 ± 3.2	15.12 ± 8.83
AC1	4.7e6	35.34 ± 13.44	27.11 ± 23.95	46.29 ± 16.75	27.11 ± 23.95
AB1	5e6	43.45 ± 5.51	36.81 ± 15.04	57.51 ± 6.61	50.80 ± 29.15
AA2	1e7	71.68 ± 26.40	57.20 ± 31.75	135.66 ± 47.48	107.03 ± 58.56
Slope		7.39e-6 ± 8.26e-7	6.18e-6 ± 1.54e-6	1.36e-5 ± 1.86e-6	1.12e-5 ± 2.80e-6
Intercept		.423 ± 2.16	-3.146 ± 4.03	-5.779 ± 4.87	-12.122 ± 7.33

FIRST ORDER KINETIC COEFFICIENT [h^{-1}] in respect to surface concentration

Series #	CFU/ml	CFU-Separation	Multipl. (Cells)	Erosion (Cells)
AA1	1.1e6	.239 ± .225	.712 ± .431	.474 ± .386
AB3	1.1e6	.015 ± .045	.306 ± .204	.212 ± .262
AA4	1.92e6	.074 ± .107	.638 ± .337	.482 ± .397
AB2	2.45e6	.067 ± .061	.581 ± .243	.394 ± .129
AA3	2.75e6	.055 ± .071	.556 ± .336	.290 ± .130
AC2	3.64e6	.048 ± .044	.392 ± .084	.254 ± .068
AC1	4.7e6	.039 ± .043	.433 ± .238	.286 ± .130
AB1	5e6	.180 ± .084	.550 ± .208	.294 ± .106
AA2	1e7	.193 ± .107	.593 ± .191	.360 ± .209
Average		.099 ± .076	.559 ± .124	.391 ± .104

Table 1. Summary of directly measured rates at 0.5 N m^{-2} shear stress. Slope and intercept are the linear regressions used in Figures 9 and 10 to show the proportionality of the rates with bulk CFU concentration.

Shear Stress : 0.75 N m^{-2}

ZERO ORDER KINETICS, Rate [# min^{-1} mm^{-2}]

Series #	CFU/ml	Adsorption CFU	Desorption CFU	Adsorption Cell	Desorption Cell
AB4	2.65e6	18.82 ± 6.99	10.21 ± 4.87	27.33 ± 9.47	13.44 ± 6.32
AC3	6.3e6	42.61 ± 15.93	21.50 ± 10.18	74.17 ± 27.2	27.86 ± 10.87
Slope		6.52e-6	3.09e-6	1.28e-5	3.95e-6
Intercept		1.548	2.013	-6.677	2.971

FIRST ORDER KINETIC COEFFICIENT [h^{-1}] in respect to surface concentration

Series #	CFU/ml	CFU-Separation	Multipl. (Cells)	Erosion (Cells)
AB4	2.65e6	.065 ± .061	.457 ± .191	.210 ± .114
AC3	6.3e6	.012 ± .030	.431 ± .097	.321 ± .081
Average		.039	.444	.266

Shear Stress : 1.0 N m^{-2}

ZERO ORDER KINETICS, Rate [# min^{-1} mm^{-2}]

Series #	CFU/ml	Adsorption CFU	Desorption CFU	Adsorption Cell	Desorption Cell
AB5	6.75e6	31.75 ± 4.01	22.17 ± 12.33	56.01 ± 8.81	36.99 ± 21.22
AC4	8.71e6	41.33 ± 16.86	26.78 ± 15.21	73.86 ± 33.82	39.92 ± 20.38
Slope		4.89e-6	2.35e-6	9.11e-6	1.49e-6
Intercept		-1.242	6.294	-5.463	26.899

FIRST ORDER KINETIC COEFFICIENT [h^{-1}] in respect to surface concentration

Series #	CFU/ml	CFU-Separation	Multipl. (Cells)	Erosion (Cells)
AB5	6.75e6	.126 ± .098	.455 ± .199	.229 ± .132
AC4	8.7e6	.055 ± .062	.433 ± .132	.301 ± .099
Average		.091	.444	.265

Table 2. Summary of directly measured rates at 0.75 and 1.0 N m^{-2}. Slope and intercept describe the proportionality between the rates and the bulk CFU concentration.

Shear Stress : 1.25 N m^{-2}

ZERO ORDER KINETICS, Rate [# min^{-1} mm^{-2}]

Series #	CFU/ml	Adsorption CFU	Desorption CFU	Adsorption Cell	Desorption Cell
AB6	6.9e6	19.69 ± 2.71	11.76 ± 3.56	30.42 ± 3.74	15.69 ± 4.75
AC5	1.22e7	51.76 ± 22.57	17.36 ± 10.76	80.40 ± 30.38	28.85 ± 12.35
Slope		6.05e-6	1.06e-6	9.43e-6	2.48e-6
Intercept		-22.062	4.469	-34.648	-1.443

FIRST ORDER KINETIC COEFFICIENT [h^{-1}] in respect to surface concentration

Series #	CFU/ml	CFU-Separation	Multipl. (Cells)	Erosion (Cells)
AB6	6.9e6	.057 ± .059	.563 ± .234	.345 ± .149
AC5	1.22e7	.034 ± .044	.572 ± .247	.370 ± .183
Average		.046	.568	.358

Table 3. Summary of directly measured rates at 1.25 N m^{-2}. Slope and intercept describe the proportionality between the rates and the bulk CFU concentration.

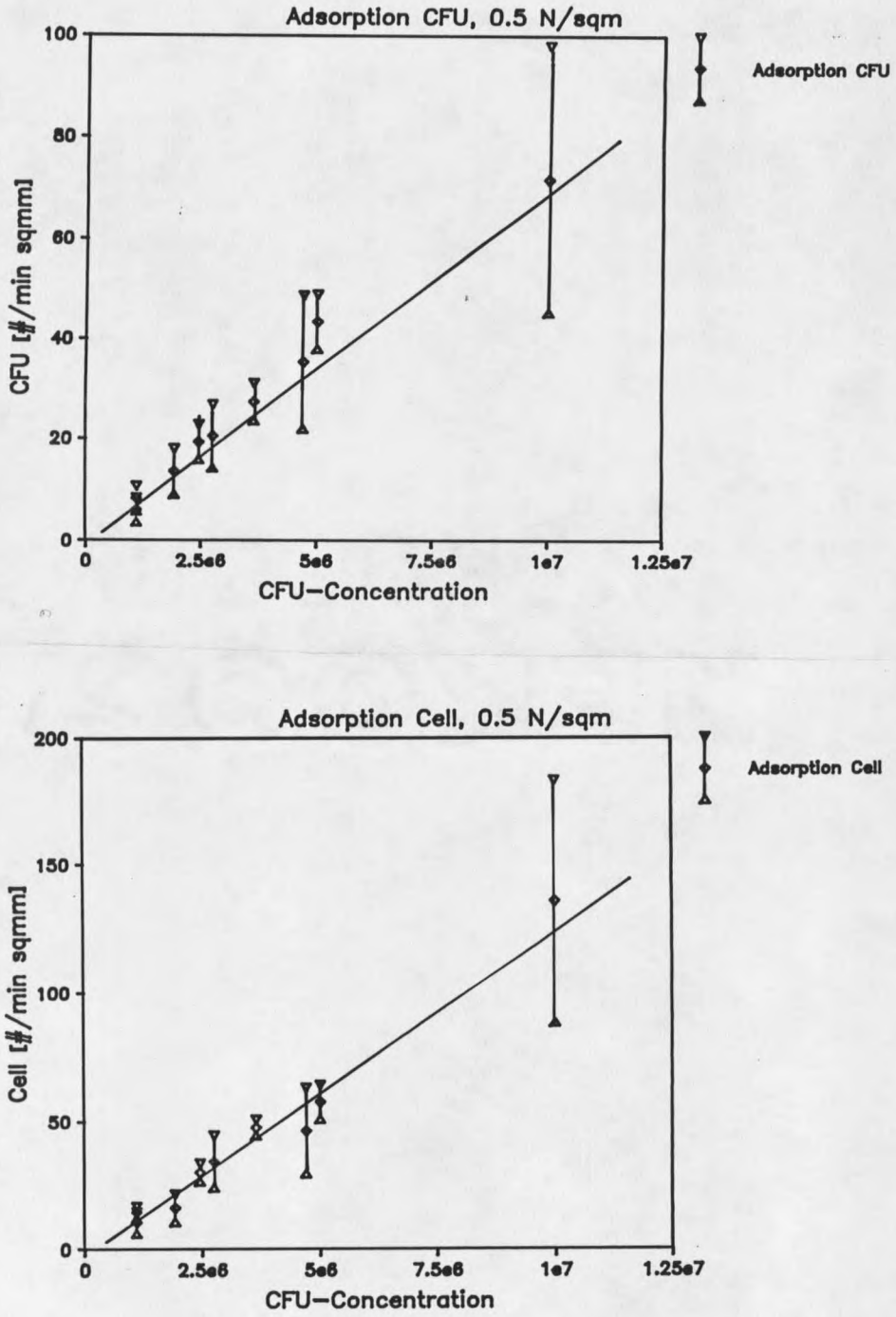

Figure 9. Adsorption rates plotted against cell concentration in the bulk flow for CFU (9a) and for cells (9b). Shear stress: 0.5 N m^{-2}. The slope and intercept of the regressions are presented in Table 1.

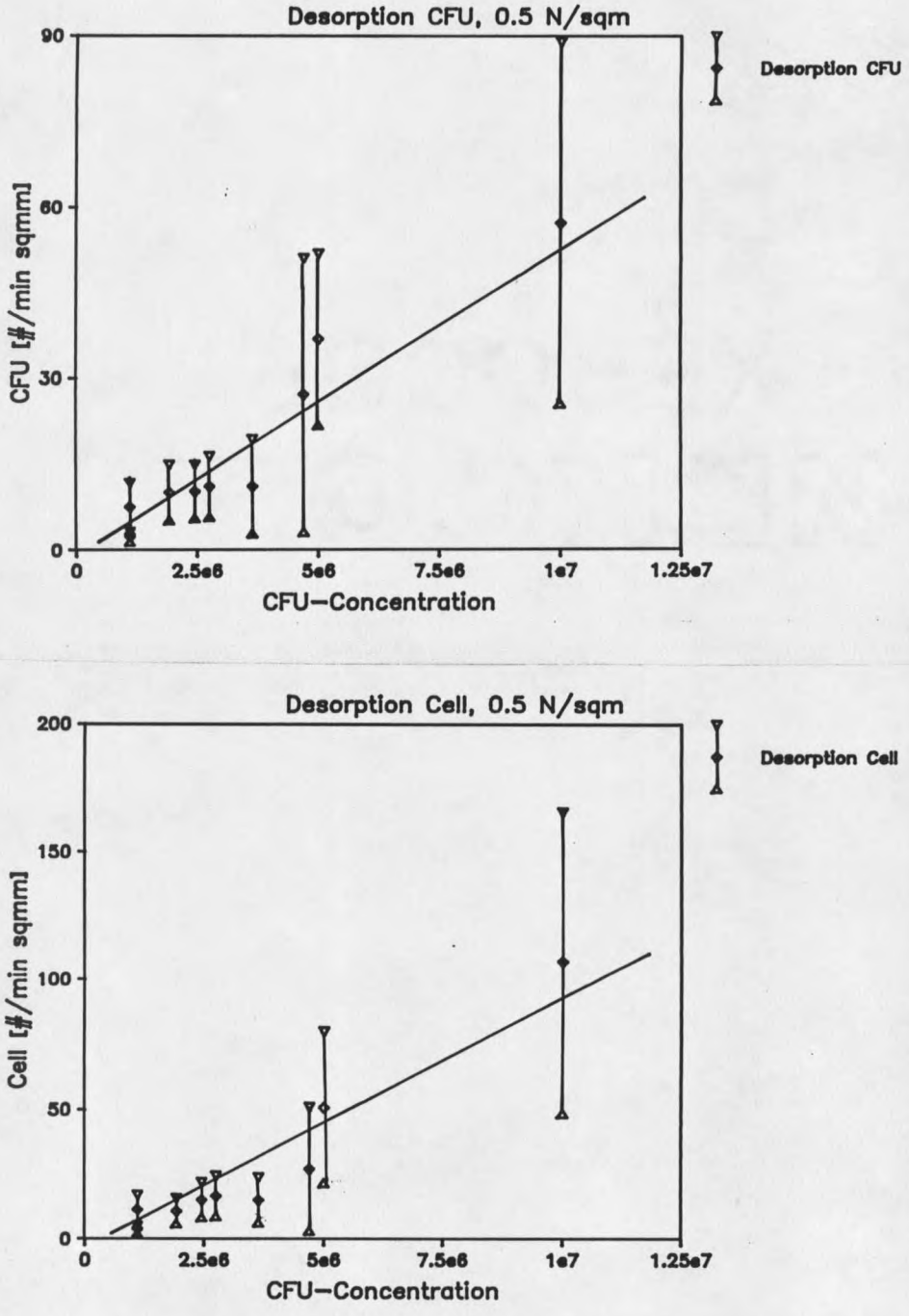

Figure 10. Desorption rates plotted against cell concentration in the bulk flow for CFU (10a) and for cells (10b). Shear stress: 0.5 N m^{-2}. The slope and intercept of the regressions are presented in Table 1.

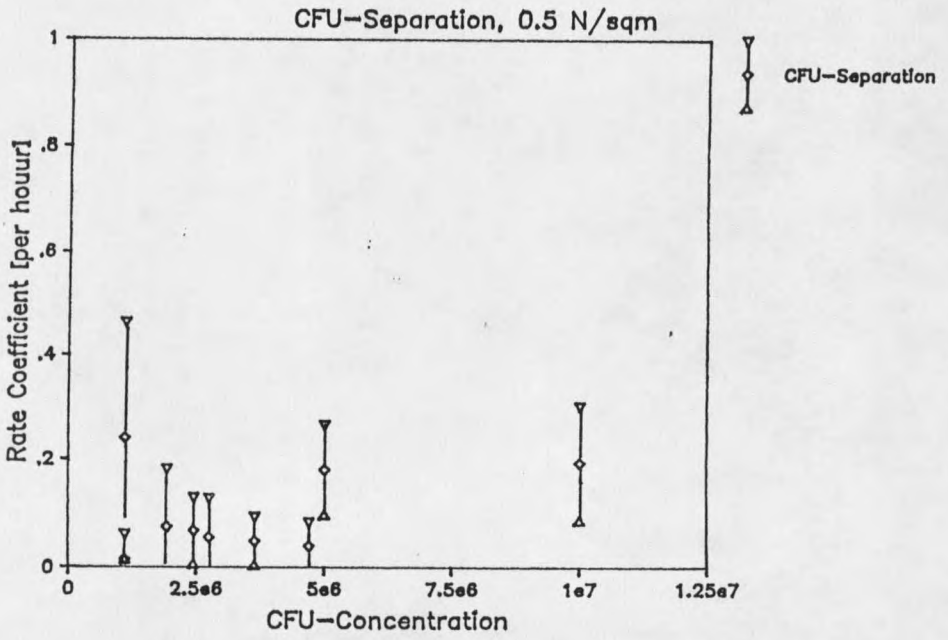

Figure 11. CFU-separation as a first order rate plotted against cell concentration in the bulk flow. Shear stress: 0.5 N m^{-2}. Average rate coefficient is 0.099 ± 0.076 h^{-1}.

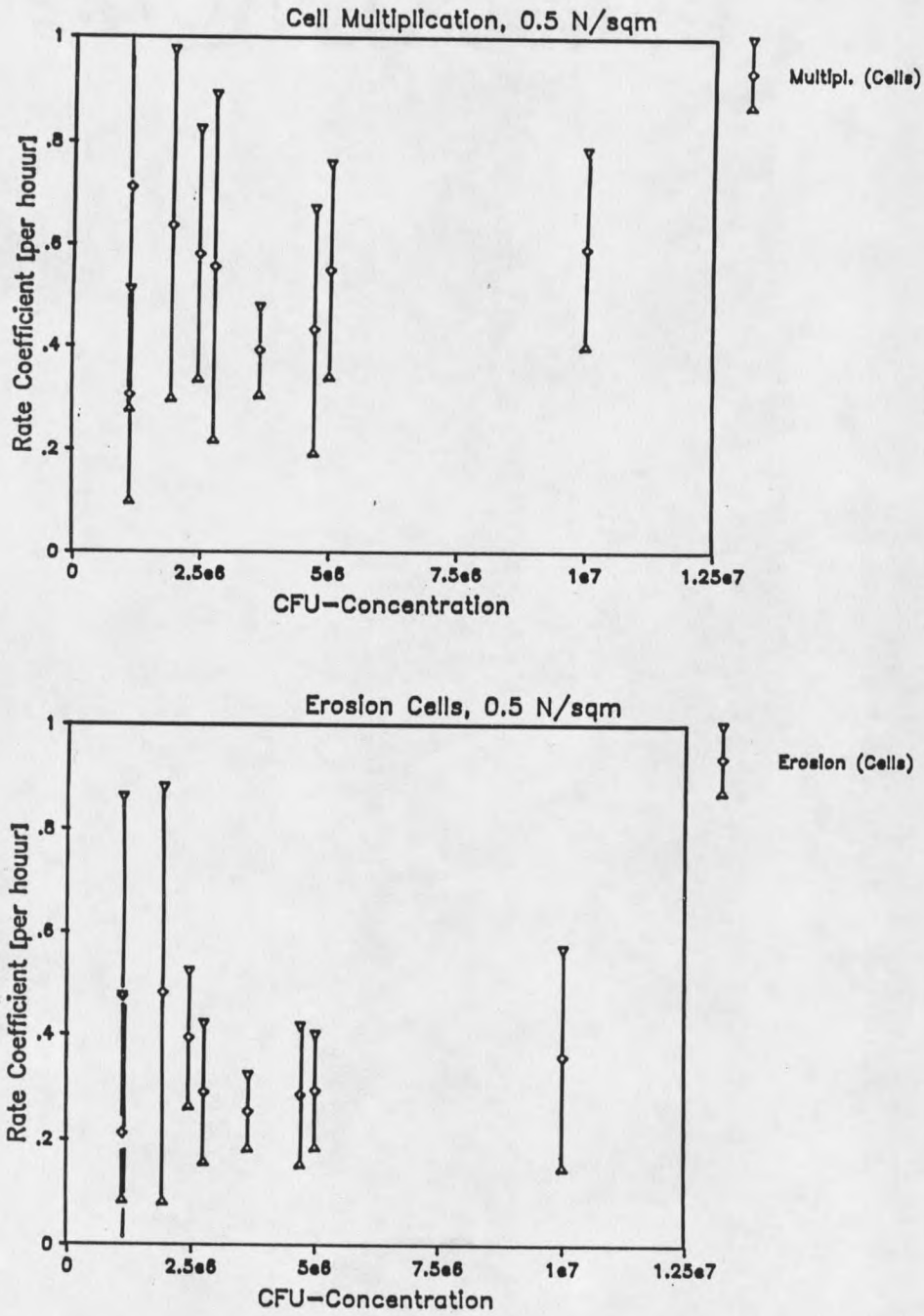

Figure 12. First order rate coefficient for cell multiplication (12a) and cell erosion (12b) plotted against cell concentration in the bulk flow. Shear Stress: 0.5 N m^{-2}.

Derived Results

Derived results cannot be measured directly in the experiments, but are calculated from direct measurements, such as the probabilities for desorption and erosion, surface-particle capture factors, and offset time. The derived results are presented in Tables 24 to 38 in Appendix E, and rates are summarized in Tables 4 to 7:

Shear Stress : 0.5 N m^{-2}

Series #	CFU/ml	Desorption		Erosion	Adsorption		Transport CFU		Offset Time	
		ß CFU	ß Cell	δ Cell	∈ CFU	∈ Cell	Rate	Σ	t_r (CFU)	t_r (Cell)
AA1	1.1e6	92.81	79.04	76.68	.01125	.01991	964.06	.0085	48.99	53.52
AB3	1.1e6	39.02	35.73	75.69	.00822	.01438	964.06	.0062	48.58	51.11
AA4	1.92e6	74.50	67.61	63.50	.01065	.01278	1682.72	.0080	37.21	44.67
AB2	2.45e6	52.94	50.57	67.84	.01195	.01874	2147.22	.0090	69.93	78.66
AA3	2.75e6	54.22	48.65	58.32	.01128	.01900	2410.15	.0085	35.74	41.89
AC2	3.64e6	40.73	31.75	54.94	.01134	.01992	3190.16	.0086	50.21	65.38
AC1	4.7e6	76.71	58.56	41.13	.01138	.01494	4119.16	.0086	42.41	55.50
AB1	5e6	84.70	88.32	77.11	.01317	.01748	4382.09	.0099	35.81	44.83
AA2	1e7	79.35	78.90	74.21	.01087	.02067	8764.17	.0082	62.89	68.40
Average		66.11	59.90	65.49	.01112	.01754		.0084	47.97	56.00
Standard Error		8.90	6.38	3.74	.00004	.00079		.00004	31.42	11.28

Table 4. Summary of derived rates calculated for 0.5 N m^{-2}.

Shear Stress : 0.75 N m^{-2}

Series #	CFU/ml	Desorption ß CFU	ß Cell	Erosion δ Cell	Adsorption ∈ CFU	∈ Cell	Transport CFU Rate	$\bar{x}$	Offset Time t_r (CFU)	t_r (Cell)
AB4	2.65e6	54.25	49.71	61.30	.01073	.01563	2658.6	.0071	57.42	60.25
AC3	6.3e6	50.54	37.56	47.71	.01021	.01787	6320.46	.0067	33.86	47.06
Average		52.40	43.64	54.51	.01047	.01675		.0069	45.64	53.66
Standard Error		1.32	4.29	4.83	.00018	.00079		.00015	20.51	10.31

Table 5. Summary of derived rates calculated for 0.75 N m^{-2}.

Shear Stress : 1.0 N m^{-2}

Series #	CFU/ml	Desorption ß CFU	ß Cell	Erosion δ Cell	Adsorption ∈ CFU	∈ Cell	Transport CFU Rate	$\bar{x}$	Offset Time t_r (CFU)	t_r (Cell)
AB5	6.75e6	70.82	66.05	74.81	.00699	.01254	7453.46	.0042	65.36	64.81
AC4	8.7e6	64.79	54.05	57.41	.00716	.01283	9606.68	.0043	52.12	62.66
Average		67.81	60.05	66.11	.00708	.01269		.0043	58.74	63.74
Standard Error		2.15	4.24	6.17	.00006	.00010		.00005	25.54	7.82

Table 6. Summary of derived rates calculated for 1.0 N m^{-2}.

Shear Stress : 1.25 N m^{-2}

Series #	CFU/ml	Desorption ß CFU	ß Cell	Erosion δ Cell	Adsorption ∈ CFU	∈ Cell	Transport CFU Rate	$\bar{x}$	Offset Time t_r (CFU)	t_r (Cell)
AB6	6.9e6	59.26	51.56	66.20	.00429	.00664	82707.4	.0024	34.03	32.56
AC5	1.22e7	33.54	35.88	59.06	.00639	.00994	14511	.0036	55.05	66.43
Average		46.40	43.72	62.63	.00534	.00829		.0030	44.54	49.50
Standard Error		9.10	5.54	2.60	.00074	.00117		.00043	11.02	12.39

Table 7. Summary of derived rates calculated for 1.25 N m^{-2}.

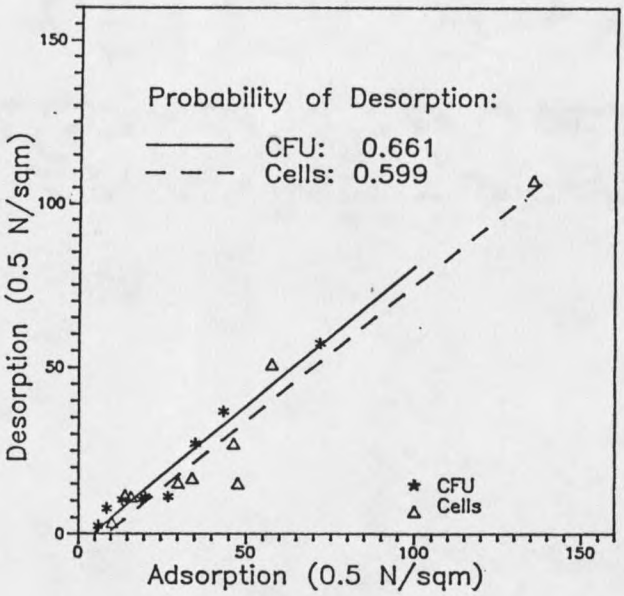

Figure 13. Correlation between desorption and adsorption at 0.5 N/m². The slope of the regression is equal to the probability of desorption in terms of adsorption.

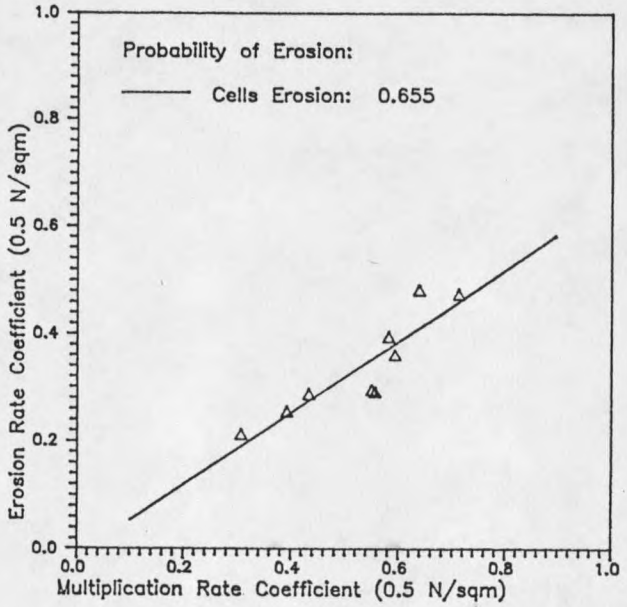

Figure 14. Correlation between erosion and multiplication at 0.5 N/m². The slope of the regression is equal to the probability of erosion in terms of multiplication

The probabilities of desorption and erosion as derived terms are directly related to their positive counter parts, adsorption and multiplication. The relatively good fit (Figure 13 and 14) indicates that these rates are rather dependent their positive counter rate than the bulk flow concentration. Offset time is calculated from the slopes and intercepts of adsorption and desorption. It is defined as the time difference between the beginning of adsorption and the "offset" beginning of desorption. This time interval is a function of the conditioning of the substratum and the residence time distribution, but it appears to be independent of the bulk CFU concentration (Figure 15).

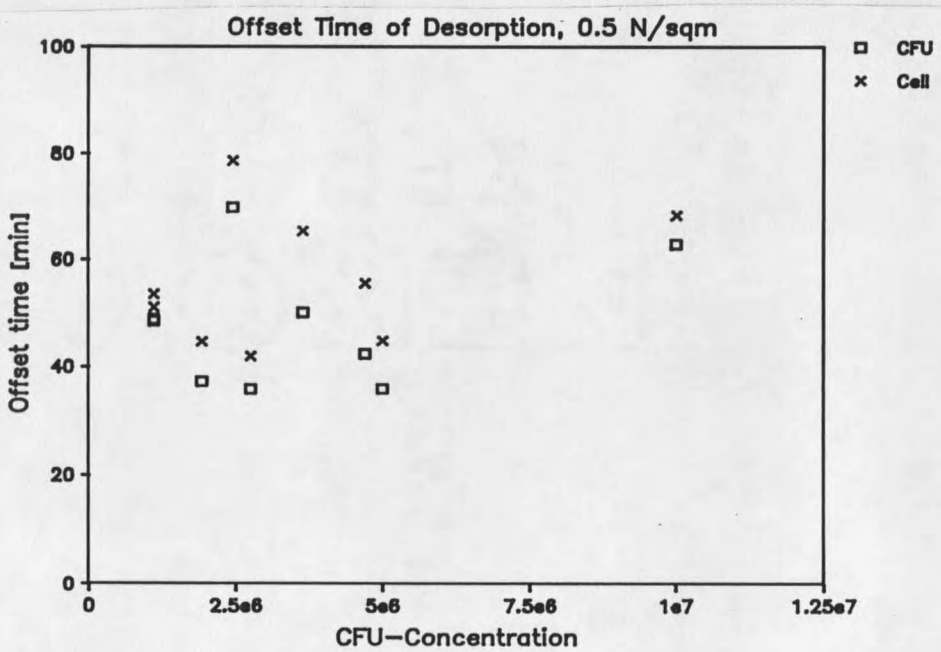

Figure 15. Correlation between offset time and bulk CFU concentration.

Behavioral Distribution

Results in this section represent measurements obtained from individual CFU and are not necessary related to the kinetics of colonization of substrata, i.e. events per unit time and area. The "behavioral" characteristics, measured and presented in this section, describe activities of CFU at the substratum such as movement, orientation of CFU during adsorption, cells per CFU, net growth, and more. The data, presented in distribution histograms, represent a defined subset of the data base. The criteria for the subset depend on the specific behavioral characteristics.

Data of individual CFU have been combined from several experiments and organized depending on shear stress. This reduces the number of distributions and increases the number of samples per distribution. Distributions representing 0.5 N m^{-2} are presented in this section and a complete set in Appendix F. Eight distributions per shear stress have been calculated.

Residence Time

Two different distributions for residence time have been calculated: 1. Total residence time, and 2. finite residence time. The difference between the two is the criterion for rejecting a CFU.

For the total residence time distribution all CFU have been incorporated where adsorption has been observed including those which exceeded the last image. Hence, the residence time for these CFU could have been longer since their desorption has not been observed prior to termination of the experiment (Figure 16 a).

For the finite residence time distribution only those CFU have been included where adsorption and desorption has been observed. In contrast to the total residence time distribution, this distribution represents the residence time of the reversibly adsorbed CFU, since both adsorption and desorption of these CFU have been observed. The difference between reversibly adsorbed and total CFU is reflected in the level of acceptance: 371 of 884 CFU were characterized in the finite compared to 815 of 884 CFU in the total residence time distribution. The probability of remaining at the substratum decreases with time. For

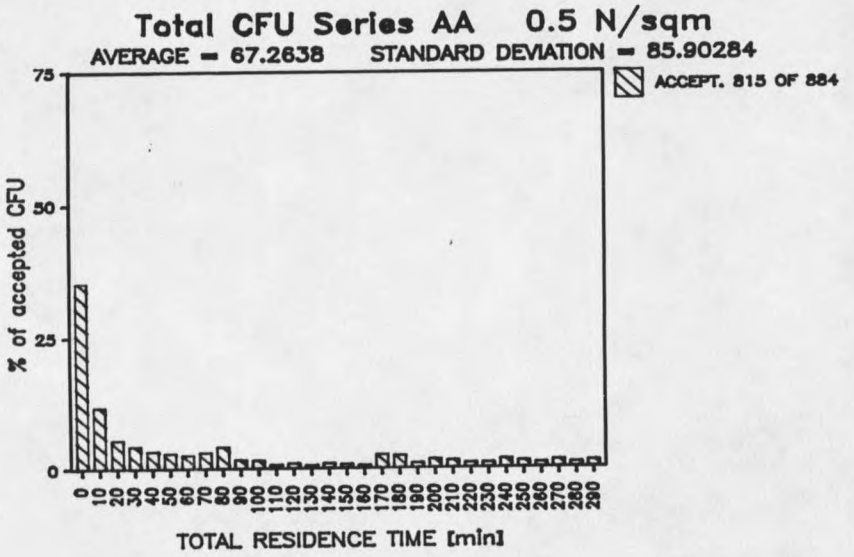

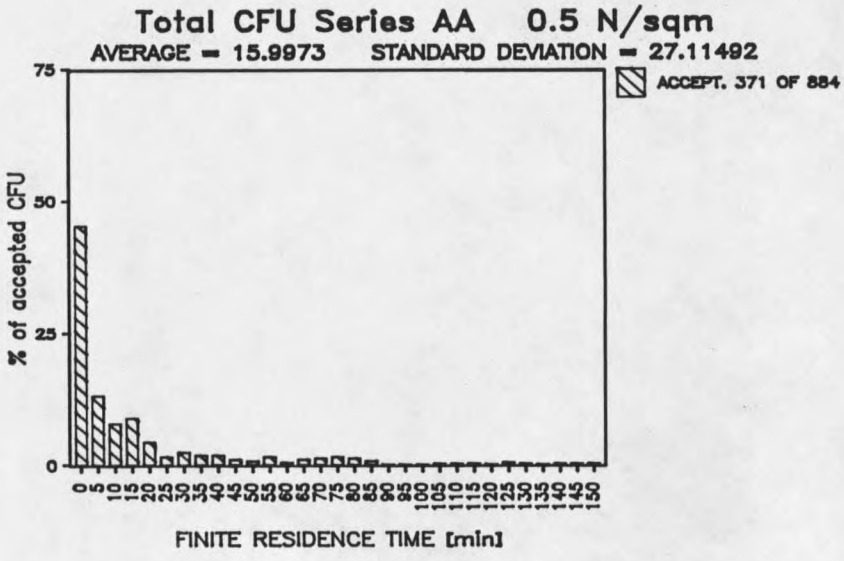

Figure 16. Residence time distribution Series AA (0.5 N m^{-2}). a: Total residence time distribution representing all CFU AA except the ones entering or exiting. b. Finite residence time of series AA. Only CFU were accepted where adsorption and desorption has directly been observed (no daughter-CFU, entering, exiting, or CFU exceeding last image of the experiments). This distribution represents for reversibly adsorbed CFU the probability in respect to time to remain at the substratum.

example, the probability of desorbing between zero and five minutes at 0.5 N m^{-2} is 48%, between five and ten minutes it reduces to 12% and so on.

Orientation of CFU During Adsorption

The distribution of CFU orientation at its first observation after adsorption is presented in Figure 17. Only CFU were included where adsorption was observed (no entry and no daughter-CFU). This distribution shows two peaks, one at 0° degree and one at 90° (flow direction 90°). In some case CFU length orientation could not be measured unequivocally and the image analyzer reported their orientation as 0°. About 25 to 30% of the CFU with a 0° orientation were identified as being squared or round (no valid measurement of orientation). That leaves about 30 to 35% of the CFU with a true 0° orientation. Therefore, it can be concluded that CFU either adsorb perpendicular or parallel to the flow direction with a very small probability for any values in between (Figure 17).

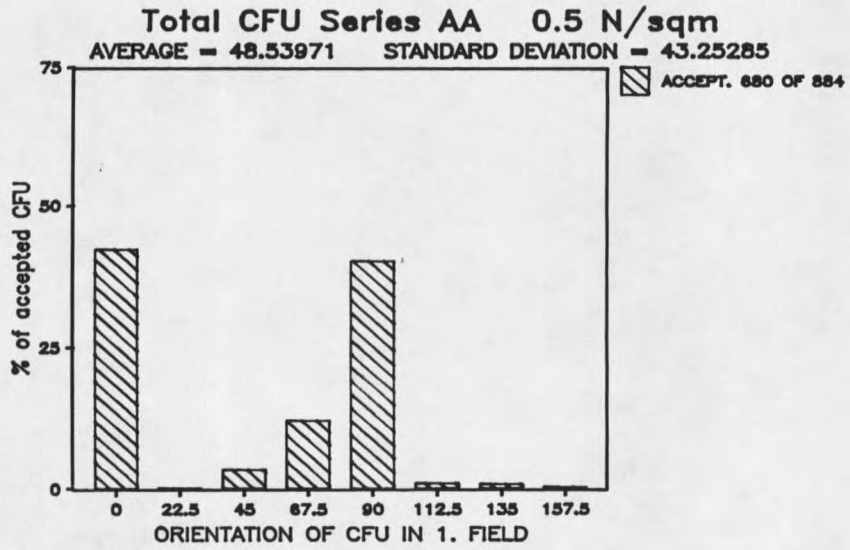

Figure 17. Orientation of adsorbing CFU at substratum. Only adsorbing CFU have been accepted for this distribution. Direction of flow: 90°

Motility at Substratum

Motility at the substratum was measured for all CFU which were observed for at least 15 minutes (three images). Figure 18 a displays the rate of gliding on the substratum. Rates of gliding less that 0.1 μm min^{-1} do not necessarily express motility. They can represent a change of location of the center point due to growth or resolution of the image analyzer. Figure 18 b shows the distribution of direction of gliding. CFU which were stationary are represented with a direction of 0° (flow direction 90°). Moving CFU have a

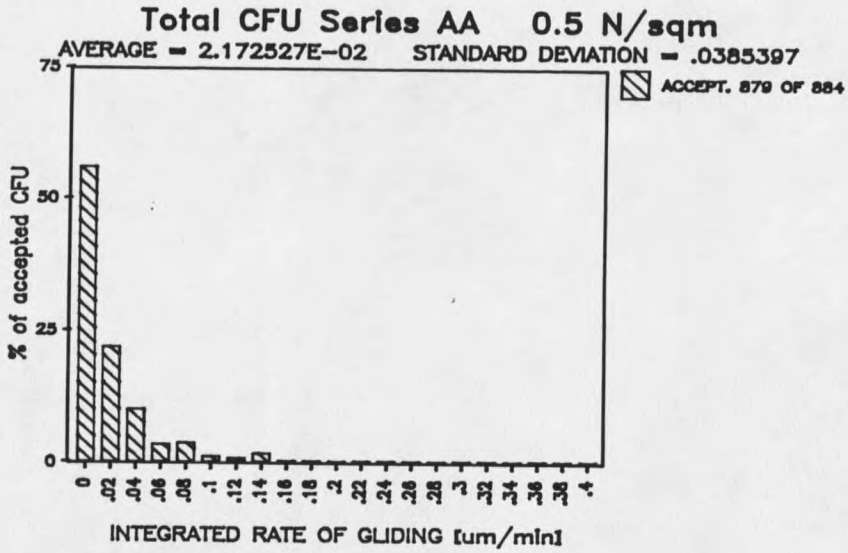

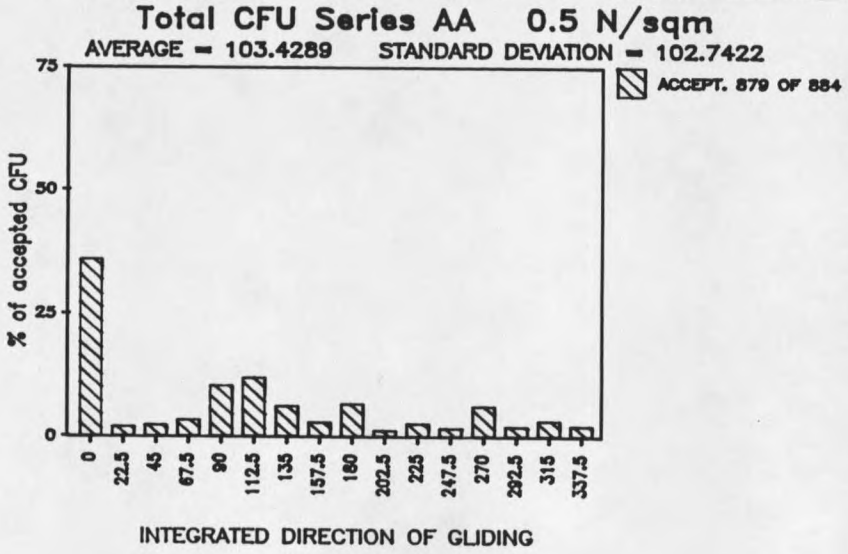

Figure 18. Integrated movement at substratum. a: Integrated rate of gliding of CFU in Series AA. Minimum residence time for this distribution is 15 min. b: Integrated direction of gliding of CFU at substratum. 0° degree direction is associated with no motion. Direction of flow: 90°.

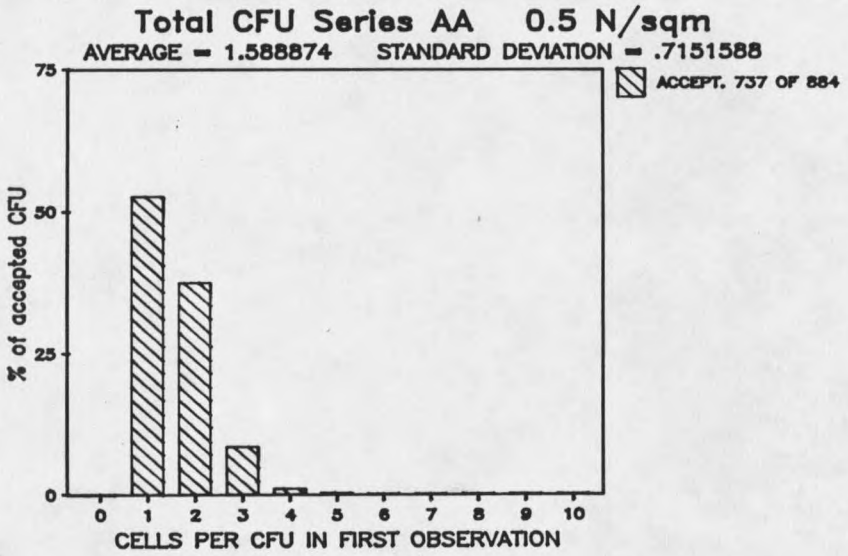

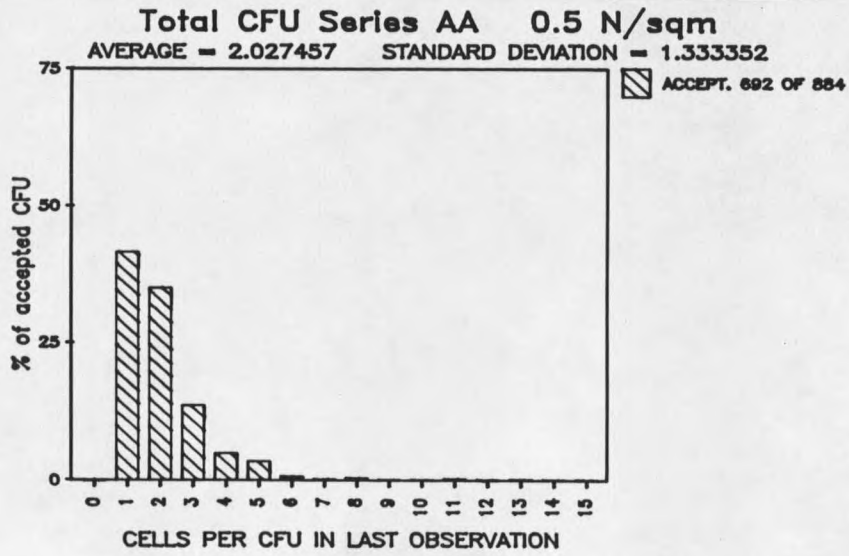

Figure 19. Cells per CFU (Series AA). a: Number of cells per CFU during first observation. b: Number of cells per CFU during last observation.

general gliding direction with the flow. This is also indicated in the tracking images (Figures 5 to 7).

Cell Number per CFU

The number of cells per CFU has been measured for both the first and the last observation (Figures 19 a and b). These values have been calculated from area measurement of each CFU and division by standard single cell size (rounded to the next integer value). All CFU have been accepted for this requirement except for daughter-CFU, and entering/ exiting CFU. The comparison of the two plots indicates a growth of the CFU during their observed residence time.

Spatial Distribution of CFU during Adsorption

Spatial distribution has been calculated for all adsorbing CFU. Daughter-CFU and entering CFU have been excluded. Calculation of spatial distribution was made according to the analysis presented in Appendix A. Figure 20 displays the spatial distribution for adsorbing cells of the experimental series AA2. All results of experimentally measured spatial distributions are presented in Appendix G.

Spatial distributions of adsorbing CFU are calculated with the frequency of two indices of interaction with established colonies:

> The relative neighbor distance is the index representing the width of "empty field" around the adsorbing CFU. Thus, the relative neighbor distance is an index describing non-interaction between the adsorbing CFU and the established colonies. The relative neighbor distance is a dimensionless number which is calibrated to be 1000 for a perfect uniform distribution.
>
> The dimensionless influence number is the index representing the influence of established colonies on the adsorbing CFU. The more dense the colonies, the greater is the influence number. Thus, the influence number represents an index describing interaction between adsorbing CFU and established colonies. This number is dimensionless and has a value close to 10 for a perfect uniform distribution.

This spatial distribution analysis results in a three dimensional graph of the two indices with frequency as the third dimension. The distributions of the experimental values (solid lines) are standardized with calibration distributions generated with computer simulations (dotted lines). The calibration distributions are presented in Figure 20 with dotted lines: uniform distribution (left,top), true random (center), and aggregated (bottom, right). The contour lines have been generated with the 10% to 90% values of the summations of the two indices. Therefore, the center represents the median value of the frequencies, and the contour lines enclose data point

frequencies in intervals of 20%. Thus, data of series AA2 can be interpreted as following:

> The median of adsorbing CFU has a spatial distribution similar to * 40% of true random with a trend to uniform distribution.
>
> 10% of adsorbing CFU have a spatial distribution similar to 25% of true random distribution with a trend to aggregated distribution.
>
> 10% of adsorbing CFU have a spatial distribution similar to the median of the calibration for uniform distribution.
>
> The entire distribution of adsorbing CFU of Series AA2 is a random distribution with a clear trend to uniform distribution.

This three-dimensional frequency analysis allows a quantitative description of the distribution in terms of the median value, the width of distribution, and the extreme values.

The figures of the spatial distributions (Appendix G) indicate that the distributions at low CFU concentration in the bulk flow and, thus, a low surface concentration have a wide range of variance. The higher the surface concentration the narrower will be the variance of distribution. At the same time the median shifts towards a uniform distribution. The measured distributions show a clear trend towards uniformity compared with the calibration

distribution. This indicates, that the neighborhood of established colonies is blocked for new adsorption.

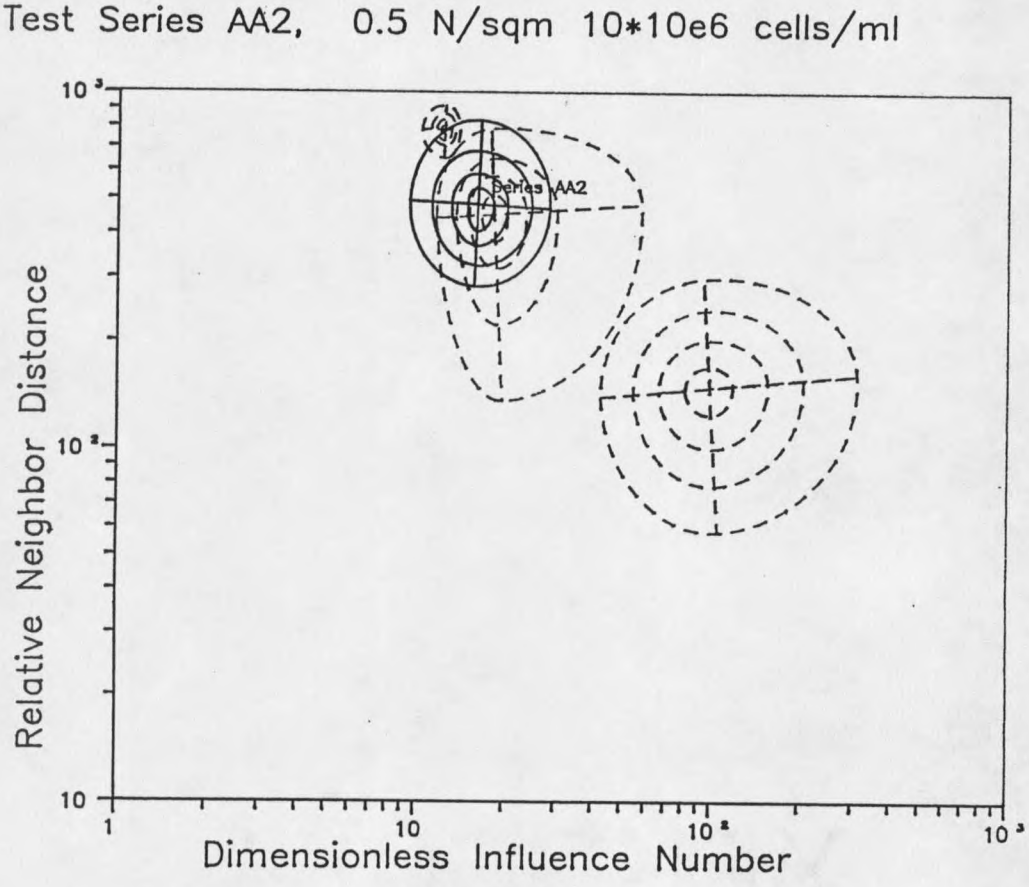

Figure 20. Spatial distribution of adsorbing CFU of Series AA2. The measured distribution (solid lines) is superimposed on the calibration distributions (dotted lines). The calibration distributions in the upper left is for uniform, in the center for true random, and in the lower right for aggregated distributions.

DISCUSSION

Sorption-Related Processes

Sorption related processes comprise adsorption and desorption, hence processes which carry biomass from the bulk liquid to the substratum and vice versa.

In the Results section, it was noted that adsorption rates are proportional to the CFU concentration in the bulk flow and also a function of shear stress (Tables 1 to 3). Depending on two independent variables does not facilitate comparison of adsorption rates obtained under different conditions. Nevertheless, using the definition of Equation 3.2 in terms of CFU and Equation 3.16 in terms of cells, it is possible to separate a factor representing the surface-liquid interaction. In the experimental system used (two variables: CFU concentration in bulk flow, and shear stress) this surface-particle capture factor ϵ depends on shear stress only. With Equation 3.25, it is possible to express a sticking efficiency Φ as a function of ϵ and the dimensionless length of the system. This sticking efficiency is the ratio of adsorption rate to flux to the substratum. In addition, this dimensionless factor can be recalculated for systems documented in literature.

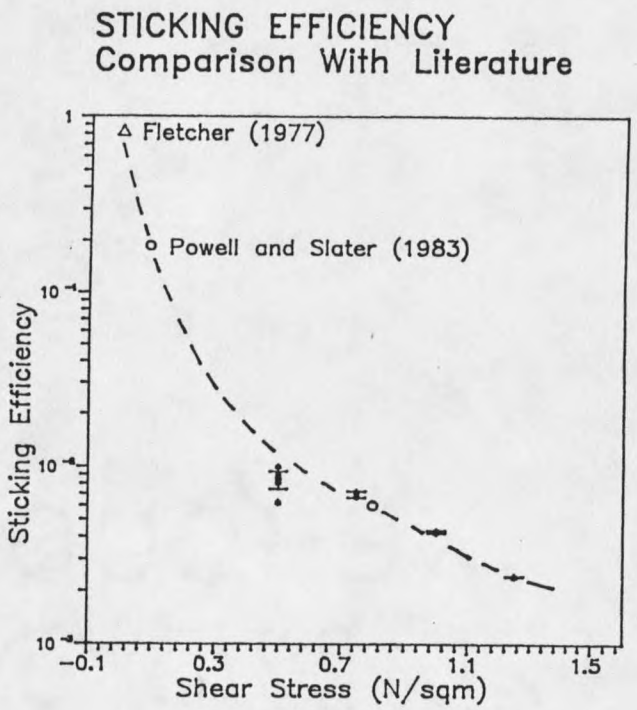

Figure 21. Sticking efficiency Φ in comparison with data from Fletcher (1977) and Powell and Slater (1983).

Figure 21 displays the sticking efficiency of the experiments in relation to values documented in literature. Data obtained by Fletcher (1977) are from a stagnant system, where sedimentation might have been the main contributing transport mechanism. Powell and Slater's (1983) data were obtained in a flow through system comparable to the one used. From Figure 21 it becomes evident that, indeed, shear stress is controlling the adsorption processes. This can also be seen from the Figures 22 and 23. These figures display the surface-particle capture factors ϵ both in terms of CFU and cells at the substratum.

In the Results section it was shown that desorption can be expresses in terms of adsorption. Both rates were found to follow the characteristics of zero order kinetics. This indicates that these processes are, for the length of experiments (5 hours), independent of the accumulation of CFU at the substratum. The independence of desorption can be explained by the concept of reversible and irreversible adsorption. CFU adsorbing to the substratum have a distinct probability to desorb within some time or become irreversibly adsorbed. The probability of desorption, as opposed the rate of desorption, is independent of shear stress (65.9 ± 17.6%). Figure 24 displays probability of desorption in terms of CFU and Figure 25 in terms of cells. The slight trend of a lower probability with increased shear is statistically not significant. Hence, probability of desorption is independent of shear stress. The solid line represents the mean and the dotted lines the 95% confidence interval.

The time interval for reversible adsorption which is sometimes referred to as the "critical residence time" is not a fixed time of x minutes but rather a "critical residence time probability" (see Figure 14b). This time probability is a function of shear stress. Since the frequency is a power function of residence time, the product

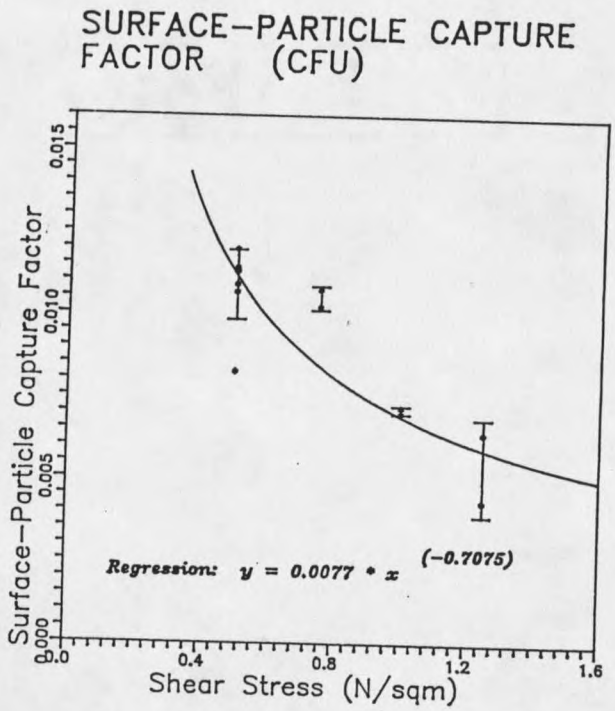

Figure 22. Surface-particle capture factor ϵ for CFU in relation to shear stress.

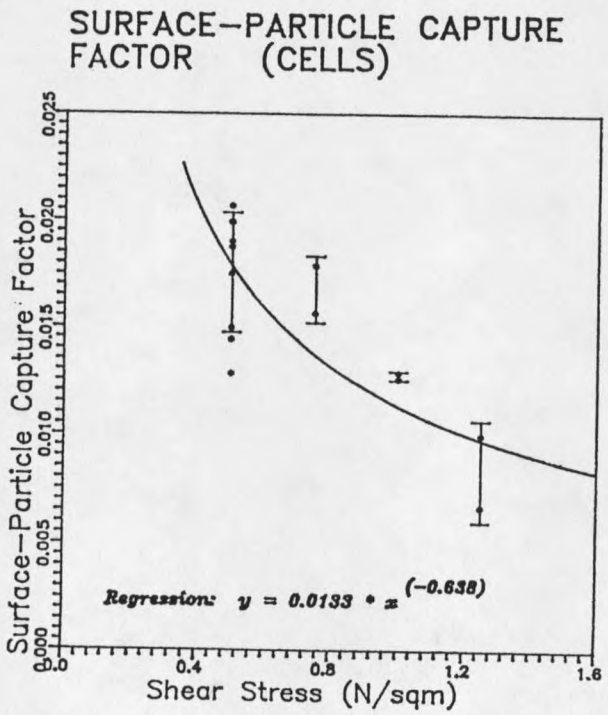

Figure 23. Surface-particle capture factor ϵ for cells in relation to shear stress.

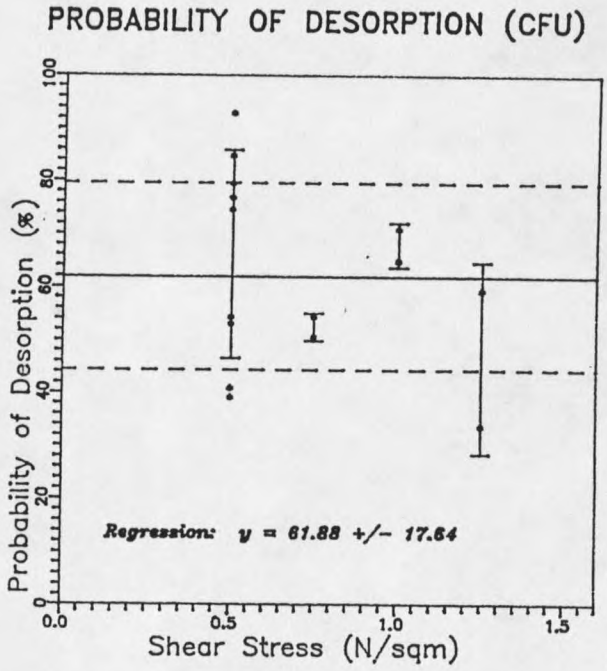

Figure 24. Probability of desorption of CFU in terms of adsorption.

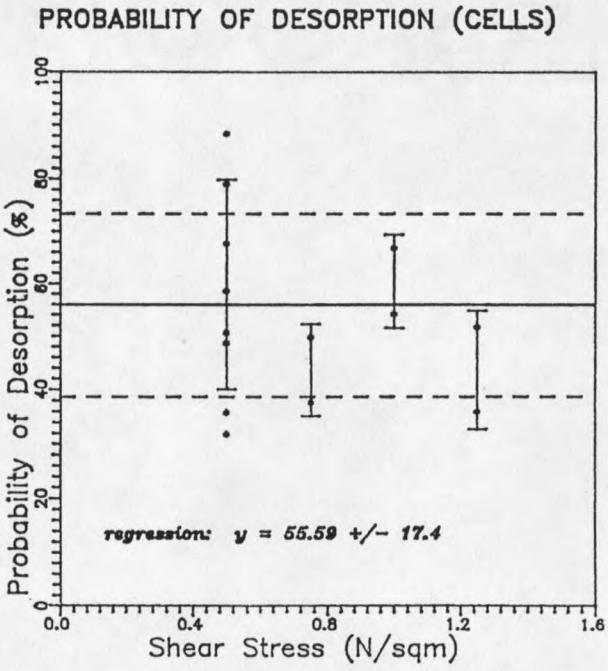

Figure 25. Probability of desorption in terms of cell.

of residence time and frequency is constant (see Table 8) but varies with shear stress. This dependency is presented in Figure 26.

Shear Stress [N m^{-2}]	Residence Time Probability [%·min]	Standard Error
0.5	59.6	± 35.7
0.75	50.7	± 29.8
1.0	39.3	± 23.2
1.25	37.0	± 26.4

Table 8. Residence time probability for reversibly adsorbed CFU under different shear stresses.

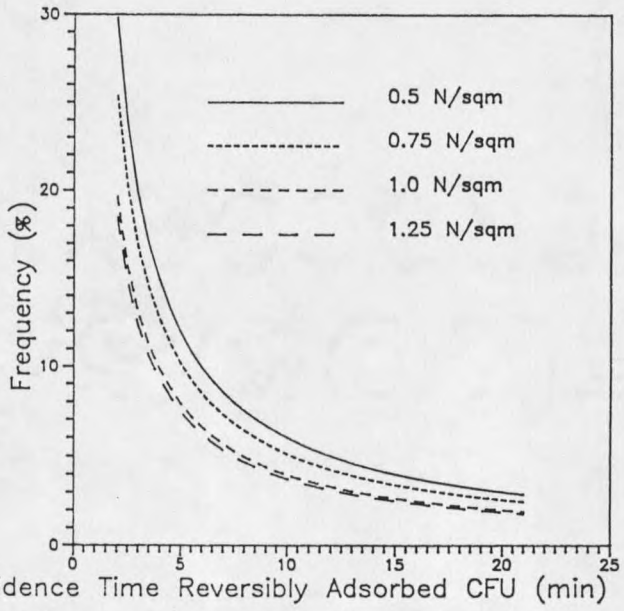

Figure 26. Comparison of residence time of reversibly adsorbed CFU as a function of shear stress.

Offset Time of Desorption

The offset time has a very poor correlation with shear stress which indicates its independence of it. Data suggest that the offset time is neither a function of the residence time of reversibly adsorbed biomass nor a function of bulk CFU concentration. The offset time is much longer than the average residence time of reversibly adsorbed CFU. Therefore, it must be the result of the conditioning of the substratum and, hence, a function of the probability to transform from reversible to irreversible adsorption, which might be much greater in the beginning of an experiment than later on. This is indicated by a "ramp" or a low desorption rate during the period of offset time (Figure 8). Indeed, CFU adsorbing very early (first 5 to 15 min) to an almost clean substratum have a probability of close to one to transform to irreversibly adsorbed CFU, whereas CFU's adsorbing later have a probability of about 0.4. This can be translated into the following assumption of two phases of conditioning: 1. Conditioning by organic macromolecules, 2. Conditioning by colonies established at substratum. Thus, the average values from Tables 4 to 7 are used to describe this time interval.

Growth Related Processes

Growth related processes, such as CFU-separation, multiplication, and erosion, are processes restricted to the biomass immobilized at the substratum.

CFU-Separation

CFU-separation rates were found to follow a first-order kinetic in terms of CFU at the substratum. One could speculate that CFU-separation should depend on shear stress. CFU separation rate decreases slightly with increased shear stress (Figure 27). This might be the result of a weakening of bonding within the CFU, permitting daughter CFU to glide away from the mother CFU under low shear stress. Under increased stress, this frail connection can break and the disconnected part can reenter the bulk flow. The trend of decreased rates of CFU-separation with increased shear stress is not clearly significant.

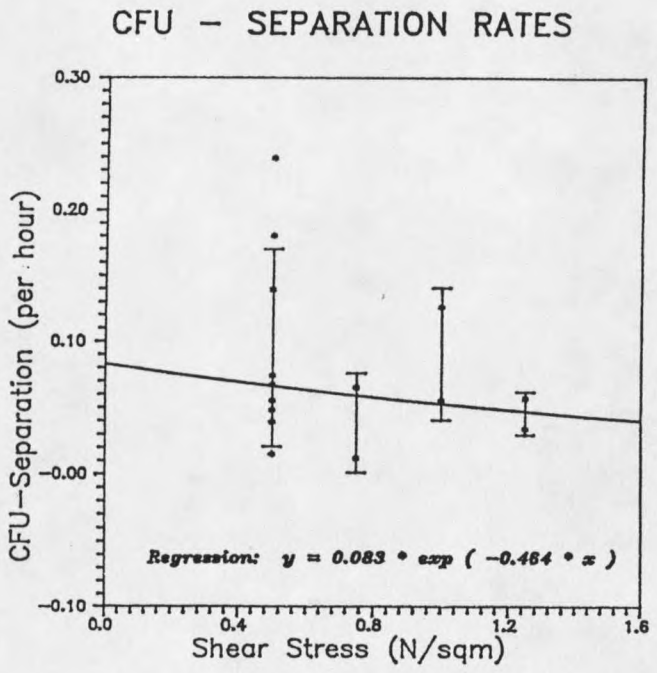

Figure 27. CFU-separation rates as a function of shear stress.

Multiplication Rates

Multiplication rates measured were in the range of 0.4 to 0.6 h^{-1}, significantly higher than the growth rate in the chemostat (0.18 h^{-1}) but within the range of maximum growth rate μ_{max} for P. aeruginosa. This increased rate can be attributed to several reasons:

CFU adsorbing to the substratum are in the process of cell division during adsorption. Thus, the measured multiplication rate is not the growth rate but represents only the in situ observation of cells multiplying. In this case, the concept

of growth rate based on a generation time is not fulfilled.

Due to immobilization of the biomass and the flux of nutrients along the substratum, the organisms "see" more nutrients than they did in the chemostat (no diffusive boundary layer). Still, the observed rate is greater than the normally measured maximum growth rate (0.45 h^{-1}).

Due to the selective process of adsorption (sticking efficiency $\Phi \leq 0.008$) only highly active cells are adsorbing. If "activity" is expressed in a higher motility, too, then these cells have an advantage over others to adsorb.

Figure 28 displays the measured multiplication rates. The solid line represents the total experimental average and the dotted lines the 95% confidence interval.

Erosion

Erosion rates can be described best with a first order kinetic in terms of cells at the substratum. Data suggest that erosion rates of cells appear to be related to multiplication rates. The more new cells are formed within CFU, the larger the number of cells which can erode. Figure 29 displays the measured erosion rates. Erosion as a probability is displayed in Figure 30. The solid line represents the total experimental average and the doted lines the 95% confidence interval.

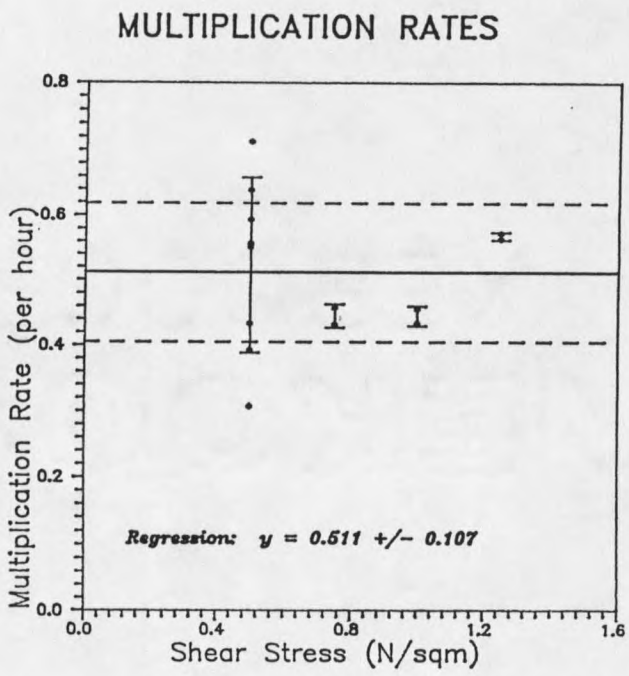

Figure 28. Multiplication rates of cells at the substratum. The solid line represents the total average and the dotted line the 95% confidence interval.

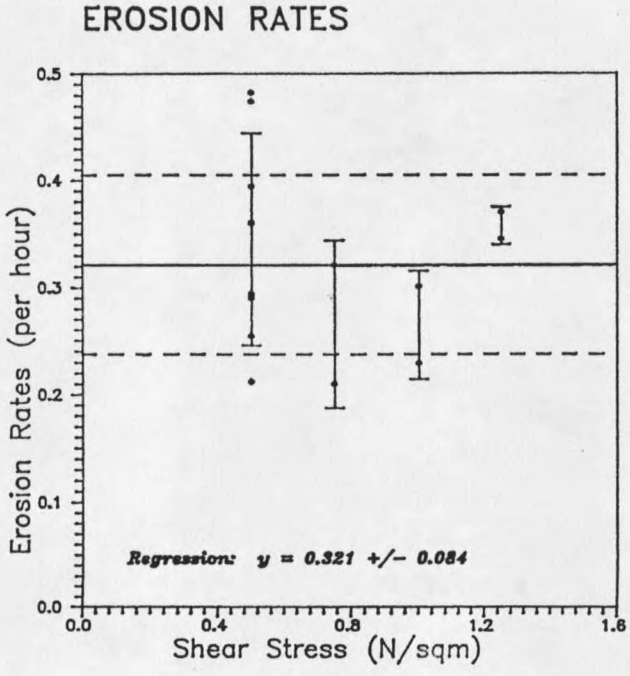

Figure 29. Erosion rates of cells within colonies.

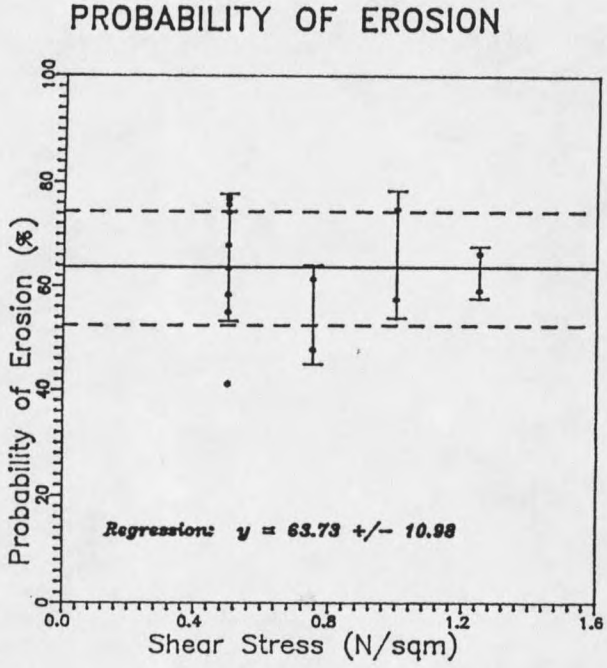

Figure 30. Probability of erosion of cells in colonies as a function of multiplication.

Summary of Kinetic Results

The results indicate that under the experimental conditions sorption related processes are dependent on shear stress and bulk CFU concentration, whereas growth related processes are a direct function of the surface concentration. Sorption related processes follow a zero order kinetic and growth related processes are first order rates in respect to accumulation at substratum.

Kinetic data obtained can be used in the model developed before. The parameters used will be described in Equations 6.1 to 6.10 where τ is the shear stress in N m^{-2}:

Surface-Particle Capture Factor: ϵ [-]

$$\epsilon_{CFU} = 0.0070 \cdot \tau^{(-0.684)} \quad 6.1$$

$$\epsilon_{cell} = 0.0133 \cdot \tau^{(-0.638)} \quad 6.2$$

Probability of Desorption: β [-]

$$\beta_{CFU} = 61.88 \pm 17.64 \quad 6.3$$

$$\beta_{cell} = 55.59 \pm 17.40 \quad 6.4$$

CFU-Separation Rates: k_{sep} [h^{-1}]

$$k_{sep} = 0.083 \cdot e^{(-0.464 \cdot \tau)} \quad 6.5$$

Multiplication Rates (cells): k_{mult} [h^{-1}]

$$k_{mult} = 0.511 \pm 0.107 \quad 6.6$$

Erosion Rates (cells): k_{eros} [h^{-1}]

$$k_{eros} = 0.321 \pm 0.084 \quad 6.7$$

Probability of Erosion: δ [-]

$$\delta = 63.73 \pm 10.98 \quad 6.8$$

Offset Time: t_r [h]

$$t_{r_{CFU}} = 0.82 \qquad 6.9$$

$$t_{r_{cell}} = 0.93 \qquad 6.10$$

Simulation with the Kinetic Results

The kinetic results can be used to simulate accumulation of cells over an extended time (10 hours). The simulation uses equations defined in section "Conceptual Model" for a population balance in terms of cells. Figure 31 displays a simulation with constant shear stress (0.5 N m^{-2}) and a variation of CFU concentration in the bulk flow. The simulations are displayed as lines. Accumulation of cells from Series AB1 is marked with dots to compare the simulation with the actually measured values. The result of this series is presented in Figures 8 and 9. The simulation with a CFU concentration of 5 * 10^6 CFU ml^{-1} has a cell concentration at the substratum in a similar range as the experiment. All the simulations show at the beginning the same increased accumulation as the real experiments (see Figure 8a).

The simulation suggests that accumulation under constant shear stress is proportional to the CFU

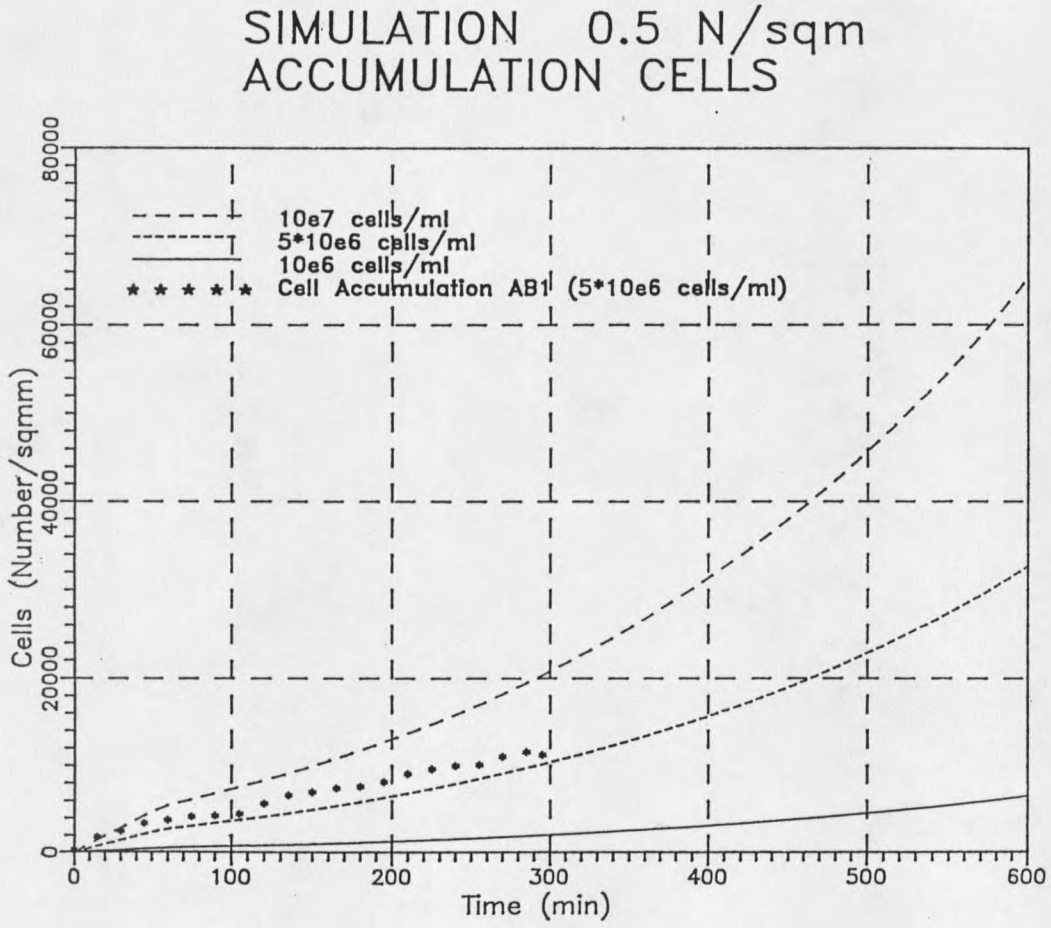

Figure 31. Simulation of accumulation of cells under constant shear stress and a variation in CFU concentration in the bulk flow. The simulation is compared with the cell accumulation of Series AB1.

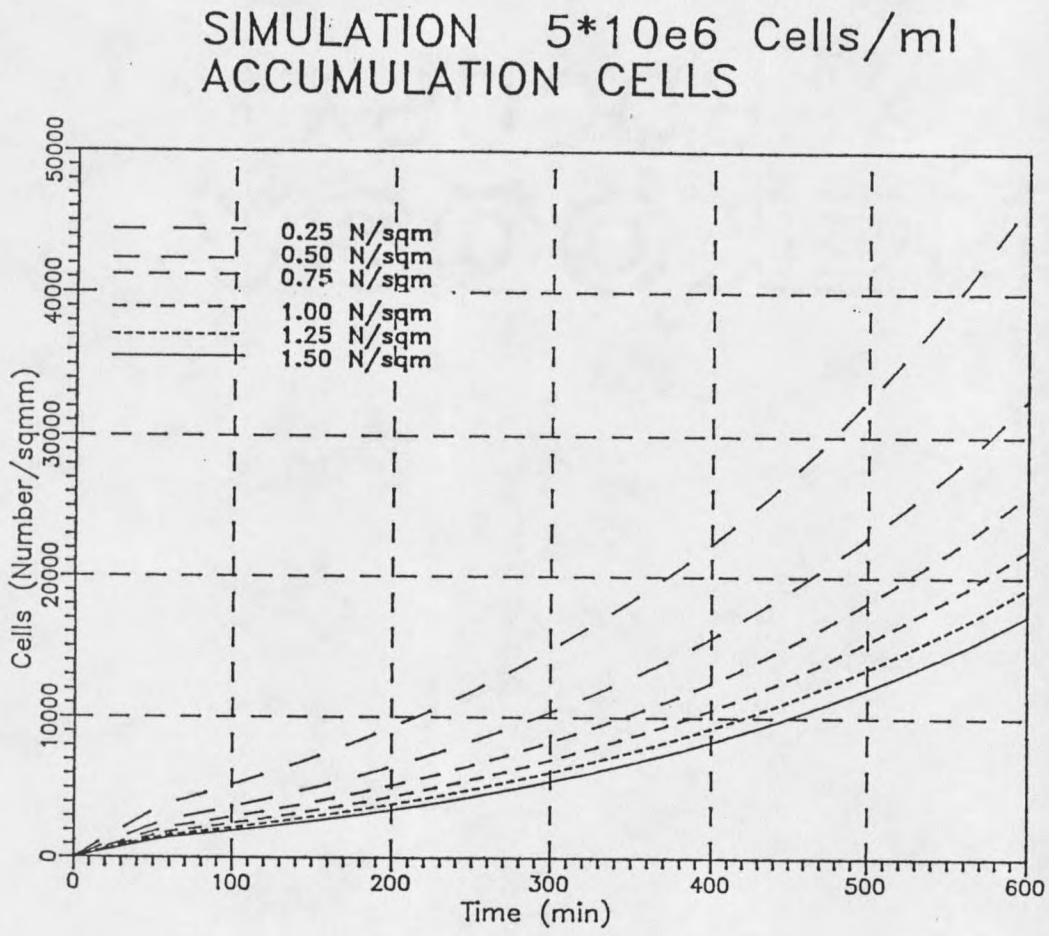

Figure 32. Simulation of accumulation of cells under constant CFU concentration in the bulk flow and a variation in shear stress.

concentration in the bulk flow. It appears that sorption related processes are important, but that after about 100 minutes growth related processes start to contribute to the accumulation increasingly. The degree of contribution is, however, an indirect function of the CFU concentration, and, thus, of adsorption. This becomes evident in a simulation with a variation of shear stress and a constant CFU concentration in the bulk flow. At low shear, adsorption is greater than at high shear stress, resulting in a more rapid accumulation of cells at the substratum. The simulation suggests that, although growth related processes start to control accumulation after about 100 minutes, the influence of CFU concentration dictates the extent of accumulation with time.

Spatial Distribution

Spatial distributions show a similar trend for all shear stresses: At low CFU concentration in the bulk flow, spatial distribution for adsorbing CFU is generally a random distribution with an extreme broad variance. Some of the observed CFU have a distribution pattern as if they were aggregated and others as if they were in a uniform distribution (compared to the calibration distribution). With increase of CFU concentration in the bulk flow and, thus increase of the surface concentration, the variation of

the distribution becomes narrower and shifts toward a uniform distribution. Data suggest that below a CFU concentration of $2.75 \cdot 10^6$ per ml at 0.5 N m^{-2} the distribution has a wide variance with a median value of random distribution. Above this concentration the median value moves toward uniform distribution, and no values can be found with a distribution pattern as aggregated. Hence, adsorbing CFU start to develop a uniform distribution pattern under higher surface concentration. This change of pattern is most probably related to a variation of the "conditioning" around the established colonies. Apparently, colonies form a "protected field" around themselves which reduces the probability for new CFU to adsorb into it. This field can either be formed due to an increased localized negative charge or due to some excretions of the colonies. The size of this field is narrow and allows enough free space at the substratum for continuous adsorption. However, this phenomenon can explain the observed reduction of adsorption rates with time under high CFU concentration in the bulk flow.

A similar pattern of change from random to uniform distribution has been observed in surface colonization by larvae of the barnacle Elminius modestus (Crisp, 1981). In difference to bacterial colonization, barnacle larvae actively seek their location for irreversible attachment by

migrating over the surface n searching for an empty location. This suggest that even distributions are a common phenomenon in surface colonization, both for bacteria and marine invertebrate.

CONCLUSION

The work presented uses a novel technique to measure early colonization of a smooth substratum. Several steps in the analysis of colonization processes have been developed for this work and have not been used before. Several conclusions with respect to the method and the experimental results have been derived:

1. The method of using an image analyzer allows direct measurement of essential independent processes contributing to colonization of surfaces.

2. Behavioral characteristics of the organisms at the substratum, such as growth, rate and direction of motion, orientation, and more, can be measured *in situ*.

3. The method provides for a novel quantitative analysis of spatial distributions of organisms during adsorption.

4. Sorption related processes depend on shear stress and bulk CFU concentration, whereas growth related processes depend on surface concentration alone (under the experimental conditions).

5. Sorption related processes are zero order rates, whereas growth related processes are first order rates with respect to surface concentration.

6. Although growth related processes are dominant within a short time, the extent of accumulation depends heavily on adsorption processes.

7. Analysis of spatial distribution shows that established colonies of *P. aeruginosa* produce a "protected field" around themselves, reducing the probability for new CFU to closely adsorb.

NOMENCLATURE/SYMBOLS

Nomenclature

Adsorption: This process is defined as the linking of the CFU with the substratum. The CFU is adsorbed to the substratum only if it has a linkage to it and, hence, becomes immobilized for a finite time.

Brownian diffusivity: Diffusivity due to Brownian motion.

CFU: Colony Forming Unit. It comprises one to several cells and formes a single colony.

CFU-separation: A CFU with more than one cell can split into two independent CFU. This process forms a new CFU at the substratum and, hence, contributes to the accumulation of CFU at the substratum. CFU-separation is a growth related process.

Desorption: This is the breaking of the linkage of a CFU and its complete removal from the substratum. Desorption is the reverse of adsorption.

Erosion: Cells within a CFU can "detach" and reduce the cell number of the CFU. This process is the reverse of multiplication.

Foot prints: Extracellular polymeric substances left at the substratum after detachment of biomass. It can be made visible with stains (fluorescens microscopy) or with scanning electron microscopy.

Gliding: Slow movement of the cells at the substratum due to the plasto-viscosity of the bonding under shear stress.

Growth: Cell separation due to metabolic activity of the biomass. Commonly, growth rates are defined in respect to generation intervals.

Hits: CFU transported to the substratum without adsorption. Hits can be detected with the image analyzer as a single line of "activated" pixels. The CFU is out of the focal plane during the scans of the other lines.

Multiplication: Event of observed cell separation at the substratum. Multiplication rates are not the

same as growth rates since they are the measured frequency of cell divisions which might have been initiated prior to adsorption.

Non-Brownian diffusivity: Diffusivity due to motility of the cells.

Offset time: Time difference between initial adsorption and beginning of desorption. This time interval depends to a large degree on the change of the conditioning of the substratum during the early stage of an experiment.

Tracks: Artificial image generated with the image analyzer. Tracking images are comparable to a multiple exposure photography and display the movement of the colonies at the substratum.

Transport: This process is responsible for carrying the CFU to a point adjacent to the substratum. This step does not include the adsorption process.

Symbols

[CFU]	:	CFU concentration at substratum [# CFU L^{-2}]
[x]	:	Cell concentration at substratum [# cell L^{-2} t^{-1}]
ϵ	:	Surface-particle capture factor [-]
# CFU	:	Number of counted CFU in field [-]
α	:	mean cosine of angle in random turn
β	:	Probability of desorption
δ	:	Probability of erosion
Γ	:	Gamma function [$\Gamma(4/3) = 0.89338$]
μ'	:	Growth rate [h^{-1}]
μ	:	viscosity [L^2 t^{-1}]
Φ	:	Sticking efficiency
τ_0	:	shear stress at wall [F L^{-2}]
A	:	Area of observed field [L^2]
c_0	:	CFU concentration in bulk liquid [# CFU L^{-3}]
c_f	:	friction factor [-]
c_x	:	cell concentration in bulk liquid [# cell L^{-3}]
d	:	density of liquid [F t^2 L^{-4}]
d	:	Nearest neighbor distance [L]
D	:	Relative nearest Neighbor distance [-]

d'	:	normal distance between points of uniform distribution [L]
D_m	:	Diffusivity of CFU [L^2 t^{-1}]
d_r	:	mean traveling length of random run [L]
E	:	Energy measured in observation point [e L^{-2}]
e	:	"Radiating energy" of point source [e]
h	:	Half-thickness of channel [L]
I	:	Dimensionless influence number [-]
K_1	:	dimensionless distance from channel inlet [-]
K_{cdes}	:	Desorption Rate CFU [# CFU L^{-2} t^{-1}]
K_{CFU}	:	Adsorption rate of CFU to the substratum [# CFU L^{-2} t^{-1}]
K_{ctran}	:	Transformation from reversible to irreversible adsorbed CFU [# CFU L^{-2} t^{-1}]
k_{ero}	:	Erosion rate [t^{-1}]
k_{mult}	:	Multiplication rate [t^{-1}]
k_{sep}	:	Probability of separation [t^{-1}]
K_x	:	Adsorption rate cells [# cell L^{-2} t^{-1}]
K_x	:	Adsorption rate of cells [# cell L^{-2} t^{-1}]
Kxdes	:	Desorption rate cells [# cell L^{-2} t^{-1}]
K_{xtran}	:	Transformation rate irreversible adsorption [# cell L^{-2} t^{-1}]
N_{CFU}	:	Flux of CFU to substratum [# CFU L^{-2} t^{-1}]
N_x	:	flux of cells to substratum [# cell L-2 t^{-1}]
Pe	:	Peclet number [-]
r	:	Distance between observed CFU and colonies [L]
r	:	Distance of observation point to point source [L]
t_r	:	Offset time of reversible adsorption [t^{-1}]
v_m	:	mean bulk velocity [L t^{-1}]
v_m	:	Average velocity in channel [L t^{-1}]
v_r	:	velocity of motility [L t^{-1}]
v_r	:	"linear swimming speed" [L t^{-1}]
x	:	Length from inlet [L]
x	:	length of layer development [L]
x	:	length axis of system
y	:	height

LITERATURE CITED

LITERATURE CITED

Baier, R.E. and L. Weiss, (1975) "Demonstration of the Involvement of Adsorbed Proteins in Cell Growth on Solid Surfaces." In: Applied Chemistry at Protein Interfaces (Gould R.F., ed.) Advances in Chemistry Series 145, Amer. Chemical Soc. Washington, D.C., pp 300-307.

Bowen, B.D., S. Levine, and N. Epstein, (1976) "Fine Particle Deposition in Laminar Flow Through Parallel-Plate and Cylindrical Channels." Journal of Colloid Interface Science, Vol. 54 (3), pp 375-390.

Brash, J.L. and Q.M. Samak, (1978) "Dynamics of Interaction Between Human Albumin and Polyethylene Surface." Journal of Colloid Interface Science, Vol. 65 (3), pp 495-504.

Caldwell, D.E. and J.R. Lawrence (1986) "Growth Kinetics of Pseudomonas fluorescens Microcolonies within the Hydrodynamic Boundary Layers of Surface Micro-Environments." Microbial Ecology, Vol. 12, pp 299-312.

Characklis, W.G. (1973) "Attached Microbial Growth - II. Frictional Resistance due to Microbial Slimes." Water Research, Vol. 7, pp 81-87.

Crisp, D.J. (1981) "Overview of Research on Marine Invertebrate Larvae, 1940-1980". In: Marine Biodeterioration: Interdisciplinary Study. (J.D. Costlow and R.C. Tipper, eds.) Naval Institute Press, Annapolis, MD.

Dracos, Th. (1973) "Hydraulic." Vorlesung, Verlag der Fachvereine, ETH Zürich.

Fletcher, M. (1977) "The Effects of Culture Concentration and Age, Time,and Temperature on Bacterial Attacment to Polystyrene." Canadian Journal of Microbiology, Vol. 23, pp 1-6.

Fletcher, M. and K.C. Marshall (1982) "Bubble Contact Angle Method for Evaluating Substratum Interfacial Characteristics and Its Relevance to Bacterial Attachment." Applied and Environmental Microbiology, Vol. 44 (1), pp 148-192.

Hobbie, J.E., R.J. Daley, and S. Jasper (1976) "Use of Nuclepore Filters for Counting Bacteria by Fluorescence Microscopy." Applied and Environmental Microbiology, Vol. 33 (5), pp 1225-1228.

Jang, L.K. and T.F. Yen (1985) "A Theoretical Model of Convective Diffusion of Motile and Non-Motile Bacteria Toward Solid Surfaces." In: Microbes and Oil Recovery (Vol. 1) (Zajic and Donaldson, ed.) International Bioresources Journal, pp 226-246.

Little, B.J. and A. Zsolnay (1986) "Chemical Fingerprinting of Adsorbed Organic Materials on Metal Surfaces." Journal of Colloid and Interface Science, in press.

Loeb G.I. and R.A.Neihof, (1975) "Marine Conditioning Films." In: Applied Chemistry at Protein Interfaces (Gould R.F., ed.) Advances in Chemistry Series 145, Amer. Chemical Soc. Washington, D.C., pp 319-335.

Nelson C.H., J.A. Robinson, and W.G. Characklis (1985) "Bacterial Adsorption to Smoth Surfaces: Rate, Extent, and Spatial Pattern." Biotechnology and Bioengineering, Vol. 27, pp 1662-1667.

Paul, J.H. and W.H. Jeffrey (1985) "Evidence for Separate Adhesion Mechanisms for Hydrophilic and Hydrophobic Surfaces in Vibrio proteolytica." Applied and Environmental Microbiology, Vol. 50 (2), pp 431-437.

Powell, M.S. and N.K.H. Slater (1983) "The Deposition of Bacterial Cells from Laminar Flows onto Solid Surface." Biotechnology and Bioengineering, Vol. 25, pp 891-900.

Turakhia, M.H. (1986) "The Influence of Calcium on Biofilm Processes." Ph.D Thesis. Montana State University.

Turakhia, M.H. and W.G. Characklis (1984) "Fouling of Heat Exchange Surfaces: Measurement and Diagnosis." Heat Transfer Engineering, Vol. 5, pp 93-101.

Trulear, M.G. (1983) "Cellular Reproduction and Extracellular Polymer Formation in the Development of Biofilms." Ph.D. Thesis. Montana State University.

Vaituzi, Z. and R.N. Doetsch (1969) "Motility Tracks: Technique for Quantitative Study of Bacterial Movement." Applied and Environmental Microbiology, Vol. 17, pp 584-588.

Van Pelt, A.W.J., A.H. Weerkamp, M. Uyen, H.J. Busscher, H.P de Jong, and J. Arends (1985) "Adhesion of Streptococcus sanguis CH3 of Polymer with Different Surface Free Energy." Applied and Environmental Microbiology, Vol. 49 (5), pp 1270-1275.

APPENDICES

APPENDIX A

THEORY OF SPATIAL DISTRIBUTION

SPATIAL DISTRIBUTION

The only study of spatial distribution of colony forming units at a substratum deals with the final distribution (after completion of the experiment, Nelson et al., 1985). The analysis of spatial distribution during the process of adsorption would, however, give important information about the interaction between the current status of colonization and the CFU being adsorbed. This is important to eliminate effects of CFU-separation and migration at the substratum.

If the present colonization, due to adsorption-, growth-, and other processes influences the spatial probability of adsorption, then this would be reflected in the spatial distribution pattern of the colonies at the time of adsorption.

Three different interactions between the established and the newly adsorbing CFU's are possible:

1. No influence.
2. Positive influence.
3. Negative influence.

No Influence

If present colonization does not influence the spatial probability of adsorption, a CFU transported to the substratum can adsorb wherever it is in respect to other established CFU. Hence, the resulting spatial distribution pattern for adsorbing CFU will be a random distribution.

Positive Influence

If existing colonies at the substratum are conditioning the area surrounding themselves in a way that it favors adsorption of new CFU, i.e. locally increasing the positive surface charge or rendering it more "sticky", then the probability for CFU transported to the substratum increases to adsorb close to established colonies, resulting in a buildup of aggregates. This would yield in an aggregated spatial distribution for the adsorbing CFU.

Negative Influence

If the existing colonization changes the conditioning of the substratum inhibiting adsorption of new CFU in this

area (increased relative negative charge) then the probability to adsorb close to existing colonies is reduced. This yields in a uniform distribution for the adsorbing CFU, maintaining a distinct distance between each other.

THEORY OF QUANTITATIVE SPATIAL DISTRIBUTION

The only study documented is based on the counted frequency of CFU per observation area (Nelson et al., 1985). It uses a probability function to determine the range of counted CFU per field in a direct cell count of colonized substrata and compares it to the actually found values. The disadvantage of this method is, that it is highly dependent on the criterium of field selection (subjective influence of random selection) and on the number of counted CFU per field. The denser the population the less sensitive is this method. In addition, it does not describe the extent of interaction or non-interaction, it gives only a statistical probability for random- against non-random distribution (uniform or aggregated).

For a more accurate analysis of the spatial distribution a different approach has to be selected. Since the analysis of adsorption provides the coordinates of each CFU at any given time, including during adsorption, it is

possible to calculate the geometrical characteristics (distance between the CFU's at the substratum) during adsorption and with that "spatial interaction indices".

Spatial Interaction Indices

The hypothesis of spatial interaction during the process of adsorption assumes that the measured spatial distribution reflects the interaction of established colonies and newly adsorbing CFU. Therefore, one should be able to obtain for each newly adsorbing CFU an index of interaction and non-interaction in respect to established colonies to describe its spatial arrangement. These indices have to be normalized and independent of the actual number of colonies per unit area (variable with time) and observed field size.

Relative Nearest Neighbor Distance

The concept of dimensional Nearest Neighbor Distance has sometimes been used to describe nucleation in crystallography or cluster formation. But its application to general spatial distributions could not be found. Since it is a dimensional value, it is highly sensitive to the

number of specimens, i.e. CFU, pre area. This distance, however, can be used to describe the minimum diameter of an idealized "empty field" around each CFU. Hence, the greater this minimum diameter is, the greater is this empty field or the degree of non-interaction with the neighboring CFU.

This distance to the nearest neighbor can be normalized and then be used as an index for "no-interaction" by dividing through the theoretical distance d', which is the calculated distance of a uniform hexagonal distribution of the same number of specimens per area (arranged as a "honeycomb", the densest possible arrangement):

$$d' = \sqrt{\frac{2 \cdot A}{(\#\,CFU) \cdot \sqrt{3}}} \qquad A.1$$

d' : normal distance between points of uniform distribution [L]
A : Area of observed field [L²]
CFU: Number of counted CFU in field [-]

$$D = \frac{d}{d'} \qquad A.2$$

D : Relative nearest Neighbor distance [-]
d : Nearest neighbor distance [L]

This relative nearest neighbor distance D, defining the empty relative space, is an index for non-interaction. In this work the resulting relative nearest neighbor number has been multiplied by 1000. Hence, a relative nearest neighbor

number D of less than 1000 indicates that the degree of non-interaction is smaller than it would be for a perfect uniform distribution. If D is 1000 or greater it indicates a high degree of non-interaction as found in uniform distributions.

Relative Influence Number

This number is an index for interaction. It uses an analogy of energy levels from different point sources. The further apart the sources are and the less numerous they are the less will be the energy level in the point of observation. It can be calculated in the following way:

$$E = \sum_{i}^{n-1} \frac{e}{r_i^2} \qquad \text{A.3}$$

e : "Radiating energy" of point source [e]
E : Energy measured in observation point [e L^{-2}]
r : Distance of obaservation point to point source [L]

This concept can be used to define a degree of influence originating from each CFU at the substratum. This influence decreases with the square of the distance r. The strength of influence can be calculated for each point (Equation A.3). This "influence level" can be made dimensionless by substituting e as emitted energy by the total area divided

by the number of observed CFU, which is the theoretical average free field associated with each CFU:

$$I = \sum_{i}^{n-1} \frac{A}{(\#\ CFU) \cdot r_i^2} \qquad A.4$$

I	:	Dimensionless influence number [-]
A	:	Area of observed field [L^2]
r	:	Distance between observed CFU and colonies [L]
# CFU:		Total number of colonies in field [-]

This relative influence number I is the index of interaction of the observed CFU by all established colonies in the field. The lower the index the less is the influence.

The advantage of these two indices is that they can clearly discriminate between the two extremes of spatial distributions, the uniform and the aggregated distribution. In a uniform distribution the relative nearest neighbor distance D is highly sensitive and in case of aggregated the sensitive index is the influence number I.

CALIBRATION OF SPATIAL DISTRIBUTION

Since this analysis is undocumented, it is necessary to calibrate it with a series of simulations and to test it before it can be used for the analysis of experimental

results. Three distinct different characteristics have been used to generate the calibration distributions : true random distribution, uniform distribution, and aggregated distribution. Figures 33 to 35 display examples of these calibration distributions. The uniform calibration distribution has a small randomness of 15% of d' (Equation A.1) to display a frequency field instead of a single point[1]. The criteria of the aggregated distribution have been that the centers of the aggregates have to be at least 30% of the field width apart from each other, and that the location of each particle within the aggregate has a random value of 15% of the field width, i.e. clear separation of each aggregate. The random distribution has been randomly generated over the entire field.

Ten fields of each distribution have been computer generated with the according criteria for statistical analysis of the calibration (each field is different). The indices of interaction and non-interaction, the influence number respectively the relative nearest neighbor distance, has then been calculated according to Equations A.1 to A.4. The points close to the border of the field (border 10% of field width) have been excluded in the analysis of their

---

1 In a 100% pure uniform distribution both indices do not vary at all. Hence, their frequency would be reduced into a single point.

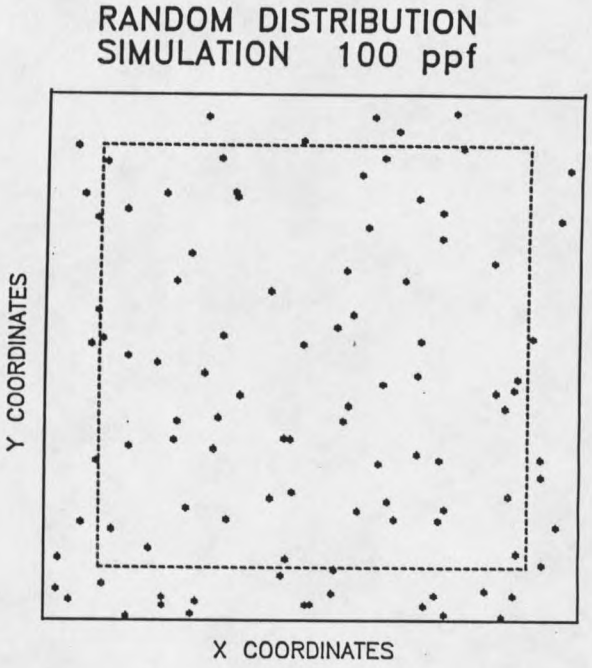

Figure 33. Example of a true random distribution for calibration.

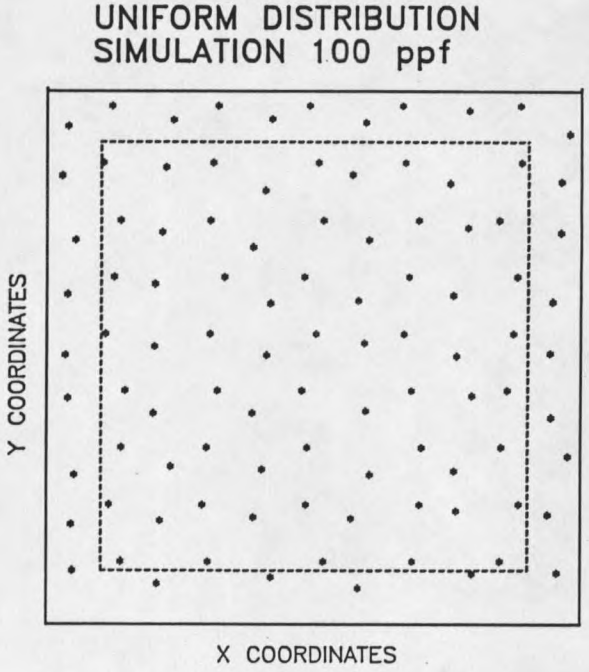

Figure 34. Example of a uniform distribution for calibration. A small degree of randomness has been imposed. The particles are arranged in a hexagonal system, the densest packing possible.

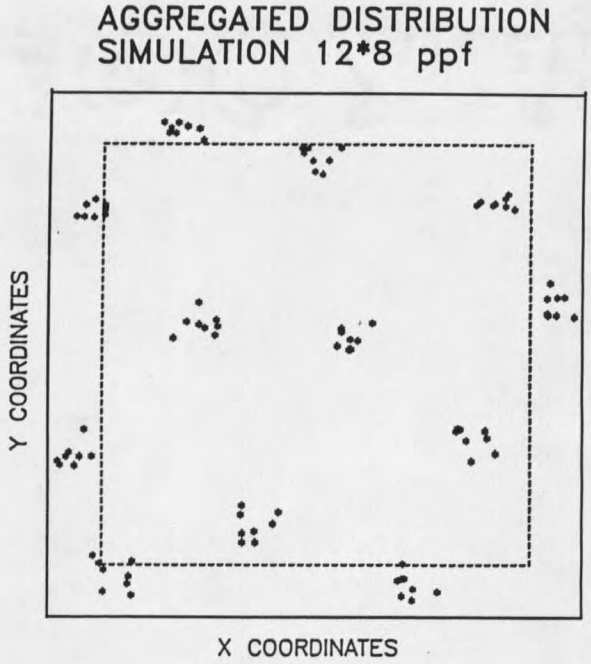

Figure 35. Example of aggregated distribution for calibration.

indices to eliminate a "border influence". This is indicated with a dotted line in Figures 33 to 35.

Since this problem with two indices yields a statistical distribution in three dimension (third dimension: frequency) the orientation of the frequency has to be determined by a regression through the index pairs. Because this regression is in the shape of an exponential function, it can be linearized by using the logarithms of the two indices. After this first transformation, a linear regression through the logarithms of the two values has been calculated, and a new coordinate system (x',y') parallel to the slope of the regression has been superimposed. All data

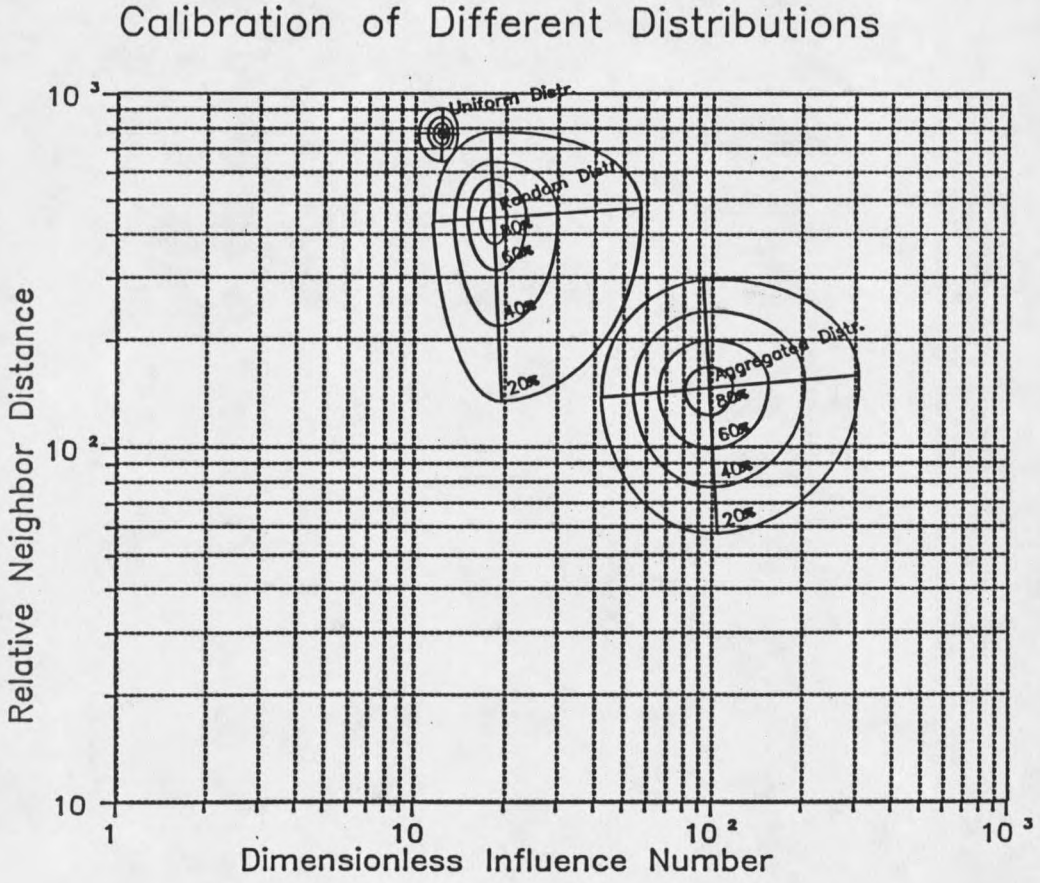

Figure 35. Frequency contour plot of the calibration distributions.

points have been translated into the new coordinate system and the data sorted for a summation curve. This coordinate transformation allows a minimizing of the size of the frequency field. The 10%- through the 90% levels of both x'- and y' coordinates gave the coordinates in the initial coordinate system for the frequency contour plot. The circle formed by the 10%- and the 90% values defines a field containing 80% of all measured values. In Figure 35 this boundary line is called the 20% border line. The frequency

contour plot for each calibration distribution has been calculated and plotted in log-scale (Figure 35). Figure 36 displays the same values as Figure 35 in linear scale to show that transformation of the indices into their logarithms give a good linearization of the problem.

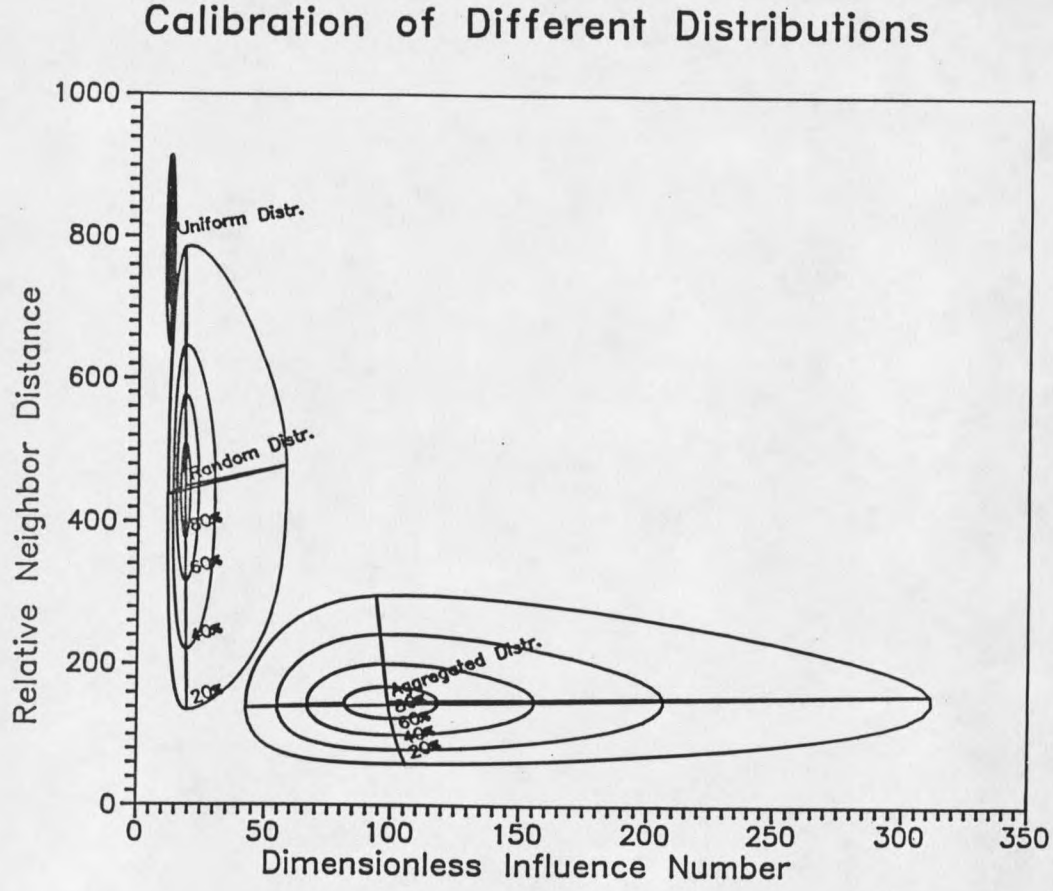

Figure 36. Frequency contour plot (Figure 35) displayed in linear scaling.

TEST OF THE SPATIAL DISTRIBUTION

Several tests of the distribution analysis have been performed. First it has been tested whether the distributions are independent of particle (50) numbers per field. Ten fields with half the number of particles compared to the calibration have been generated and analyzed for both uniform and random distributions. No difference could be found compared to the calibration. This test suggest that the two indices are independent of the number of particles per field.

Three test distributions with ten fields for each have been generated with a different pattern than the calibration distribution. One of the test distributions has been based on a uniform, and two on an aggregated distribution. Compared to the calibration distribution, they had a much greater degree of randomness. Hence, their frequencies of indices are between true random and the relative calibration distribution. Figures 37, 39, and 41 are examples of these distributions.

Uniform Test Distribution

This test distribution (Figure 37) has a 10 times higher degree of randomness than the uniform calibration distribution (Figure 33). In a visual comparison it appears that this distribution is closer to a random- than a uniform distribution except that a very short nearest neighbor distance for few particles, as found in true random patterns, is missing, but it has some "empty spots" in the field, too. Plotting the frequency contour plot (Figure 38) of this distribution shows that 20% of the points have distribution indices similar to the median of the uniform

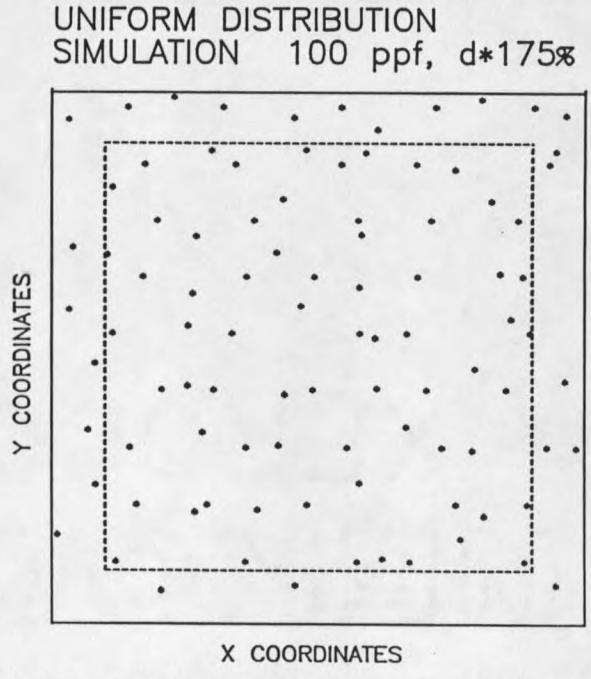

Figure 37. Example of a uniform test distribution.

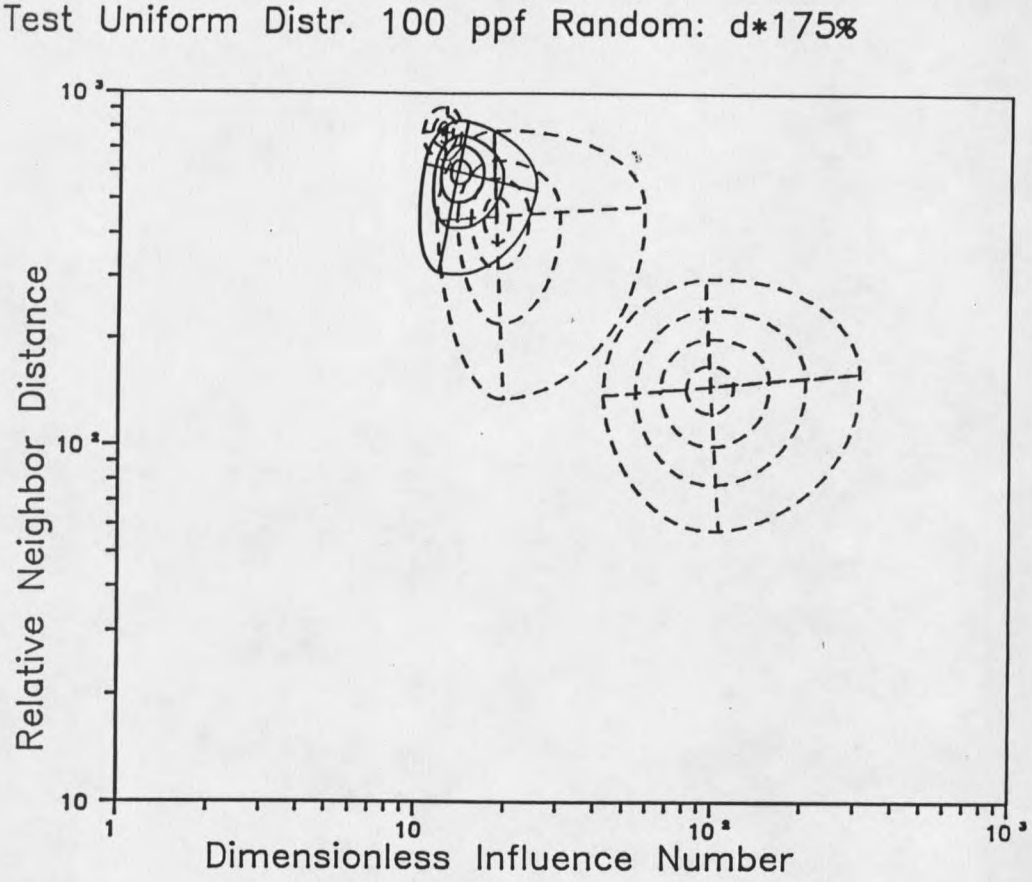

Figure 38. Frequency contour plot of the uniform test distribution.

calibration, and about 20% are similar to a true random. The median of the test distribution is between random and uniform but clearly not either one.

Aggregated Test Distribution 1.

This test has been generated with five centers and 20 particles per center (Figure 39). The degree of randomness

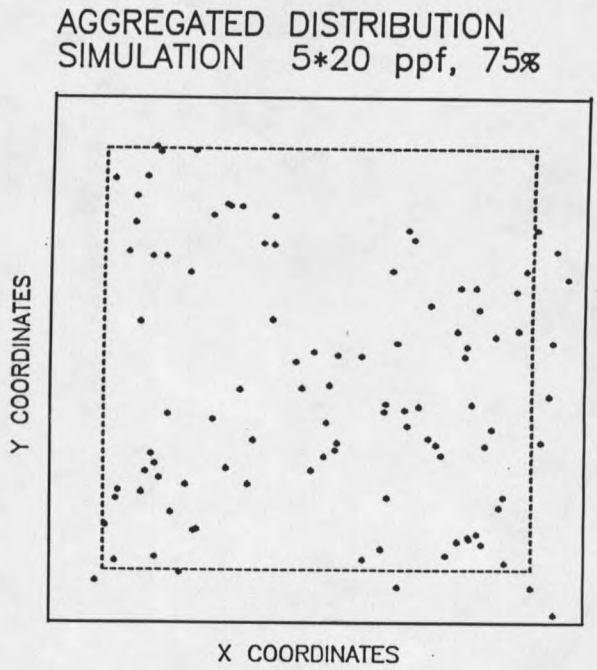

Figure 39. Example of aggregated test distribution 1.

around the centers of aggregates has been increased to 75% of the field width, and the centers have been placed randomly. Hence, it is possible that the aggregates can overlap each other. The randomness in this test distribution is clearly visible. However, the frequency of points close to each other is much greater than in a true random distribution. The comparison of the frequency contour plot with the calibration (Figure 40) shows that the median of this distribution is similar to 40% of the true random distribution. The entire distribution covers a wide range from nearly uniform to highly aggregated.

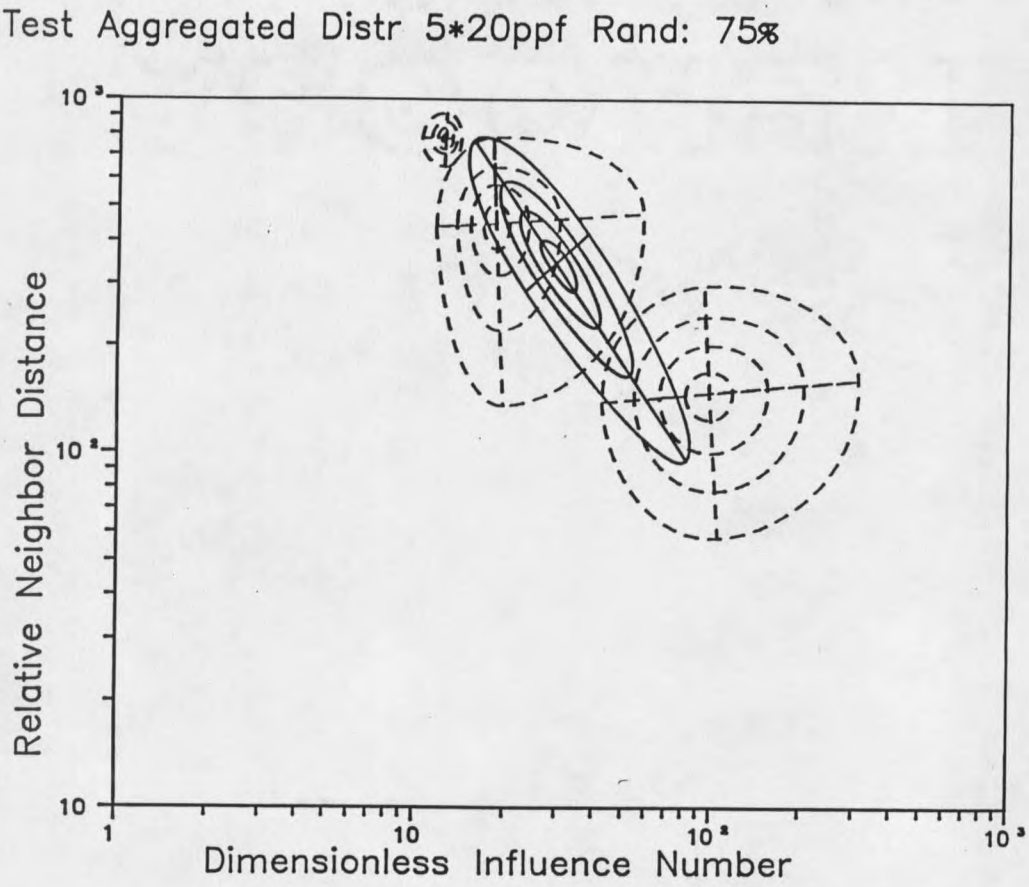

Figure 40. Frequency contour plot of aggregated test distribution 1.

Aggregated Test Distribution 2.

The generation of this distribution used 33 centers and three particles per field (Figure 41). In addition, the centers had to be 10% of the field width apart from each other, and the particles had the same random distance (10% of field width). Therefore, an overlap of the aggregates as it was found in Figure 39 was excluded. Each aggregate can

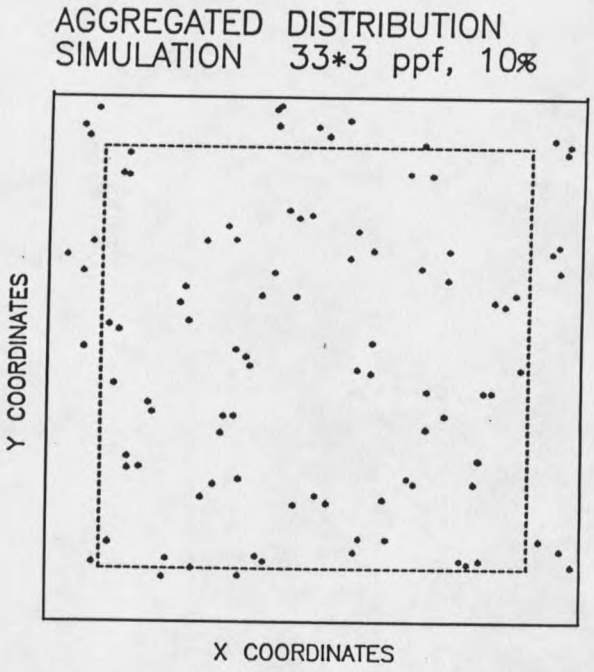

Figure 41. Example of aggregated test distribution 2.

easily be defined, but overall it appears that this distribution has a fairly even density of particles over the entire field. The frequency contour plot of this distribution (Figure 42) indicates that it is clearly an aggregated distribution, especially in terms of the index for non-interaction, the relative nearest neighbor distance. The median of the index of interaction, the dimensionless influence number, is about half of that of the calibration distribution, which is in good accordance with the number of particle per aggregate (three instead of eight).

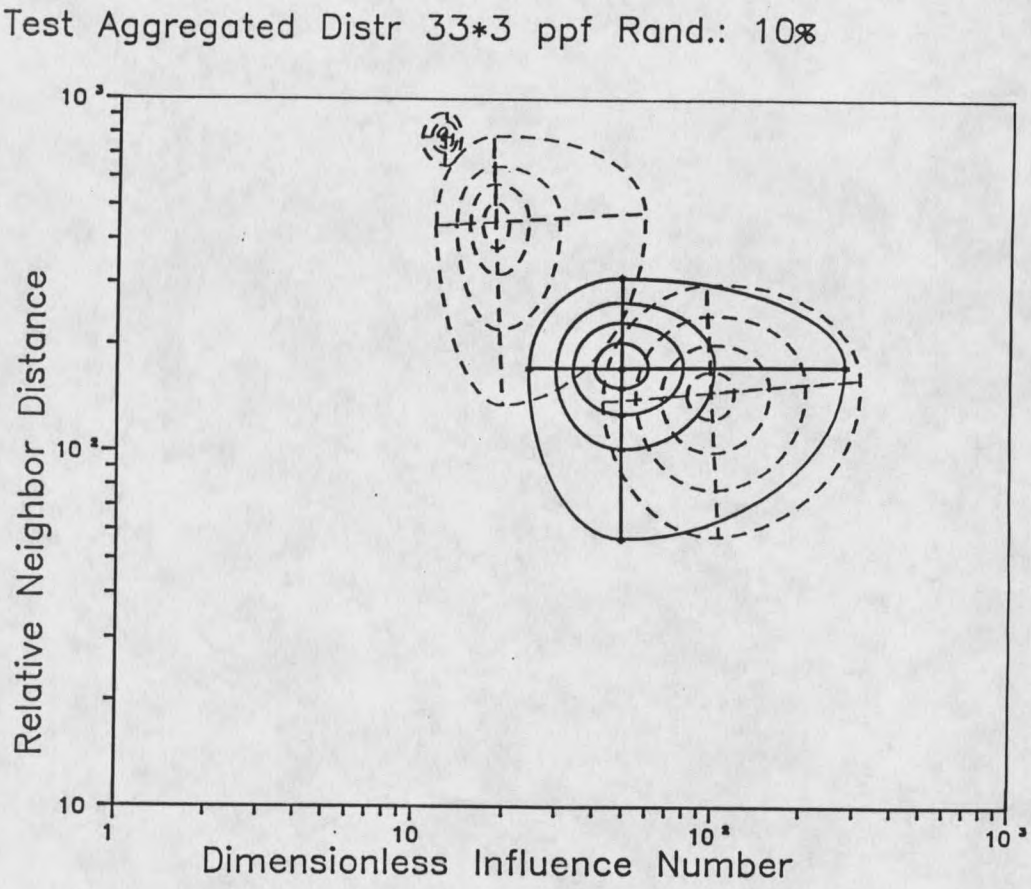

Figure 42. Frequency contour plot of aggregated test distribution 2.

Conclusion of the Test Distributions

The tests show that the indices for the spatial distributions are to a large extend independent of the number of particles per field and the field dimension, and they are a useful tool to describe the characteristics of the distribution pattern. Some refinements can be included, such as variance analysis and others which would allow an

analysis of skewness or "double-humps" in the frequency contour plot. But the task of this part of the work was to define a base for a measurable system to describe spatial distributions during the process of adsorption.

APPENDIX B

ORGANIZATION OF DATA FILES

ORGANIZATION OF DATA FILES

All data files are comma separated ASCII sequential files. The file identifier determines the experimental series.

The following files are created within the sorting routine:

1.	1SUMDATA.XXX	Summary of events per field.
2.	1CFUSUMM.XXX	Summary of each observed CFU.
3.	1CFUSEPA.XXX	Summary of CFU-separation.
4.	1CFUENDF.XXX	Summary of CFU observed in last field of the experiments.
5.	1CFUDETA.XXX	Summary of cell erosion of each CFU.
6.	1CFUEXIT.XXX	Summary of CFU exiting the field.

Data Organization

1SUMDATA.XXX:

One line contains 21 entries. Each image analyzed will be represented in one line. It is a summary of the number of events observed during an experiment, containing the values of number of adsorptions, desorptions, multiplications, and so on.

1. experimental time (from beginning of experiment).
2. time interval between this and the earlier image.
3. counted events of adsorption in terms of CFU.
4. counted events of desorption in terms of CFU.
5. counted events of entries in terms of CFU.
6. counted events of exits in terms of CFU.
7. counted events of CFU-separation in terms of CFU.
8. number of CFU in this field (accumulation)
9. area coverage in this field.

10. counted events of adsorption in terms of cells.
11. counted events of desorption in terms of cells.
12. counted events of entries in terms of cells.
13. counted events of exits in terms of cells.
14. counted events of CFU-separation in terms of cells.
15. counted events of cell multiplications in terms of cells.
16. counted events of erosions in terms of cells.
17. number of cells in this field (accumulation).
18. counted events of total increase in terms of CFU.
19. counted events of total decrease in terms of CFU.
20. counted events of total increase in terms of cells.
21. counted events of total decrease in terms of cells.

1CFUSUMM.XXX

One line has 15 entries, each CFU is represented in one line. It is a summary of each observed CFU, and contains all relevant data to describe the CFU's "behavior".

1. CFU number.
2. CFU name index: 1 - normal, 2 - entry, 3-exit, 4 - daughter, 6 - daughter exit.
3. Field of first observation.
4. Field of last observation.
5. Age of CFU at last observation.
6. Relative nearest neighbor number during adsorption.
7. Areal density influence number during adsorption (non dimensionless).
8. Dimensionless areal density number during adsorption.
9. Orientation of length axis of CFU in first observation (flow direction: 90°).
10. Integrated rate of gliding at substratum from first to last observation [µm/min]
11. Integrated direction of the gliding in 10 in degrees.
12. Cells per CFU during firs observation.
13. Cells per CFU in last observation.
14. Net growth (13-12), calculated as growth rate [h^{-1}].
15. Total number of cells eroded from CFU.

1CFUSEPA.XXX

Separation of CFU, in order of fields. Each line has 9 entries, and each event of separation has one line.

1. CFU number of daughter CFU.
2. Field number of separation.
3. Dummy variable.
4. Cells of "mother" CFU prior to separation.
5. Cells formed in "mother" CFU prior to separation.
6. Distance moved by "mother" CFU prior to separation.
7. Time interval to 6 in min.
8. Age of "mother" CFU prior to separation.
9. Time "mother" CFU exceeds after separation.

1CFUENDF.XXX

Summary for each CFU observed in the last field of the experiment. Each line has 4 entries and each CFU detected in the last field has 1 line.

1. CFU number.
2. Field number of the last field.
3. CFU index (1 : normal, 2 : daughter)
4. age of CFU [min].

1CFUDETA.XXX

Summary for each event of erosion of cells from a CFU in order of fields. Each line has 10 entries and each event of erosion has 1 line.

1. CFU number.
2. Field number of observation.
3. Number of erosion events for this CFU prior to this erosion.
4. Number of cells eroded in this event.
5. Number of cells in this CFU prior to this erosion.
6. Net growth of CFU prior to this erosion.
7. Distance moved prior to this erosion.
8. Time interval to 7.
9. Age of CFU prior to erosion.
10. Age of CFU after erosion.

1CFUEXIT.XXX

Summary of CFU exiting the Field. Each line has 4 entries and each CFU exiting has 1 line.

1. CFU number.
2. Field number of exit.
3. index of CFU (1 : normal, 2 : daughter)
4. Age of CFU at last observation.

APPENDIX C

TABLES OF DIRECTLY MEASURED RESULTS

Series: AA1
Shear Stress: 0.5 $N \cdot m^{-2}$
Cell Concentration: $1.1 \cdot 10^6$ $cells \cdot ml^{-1}$

ZERO ORDER KINETICS [$\#\cdot min^{-1}\cdot mm^{-2}$]	RATE (slope)	Y-INTERCEPT	X-INTERCEPT	r^2	CONFIDENCE INTERVAL (95%) ± Rate	± Y-Interc.
Adsorption CFU	8.18	-10.68	1.30	1.00	2.64	8.48
Desorption CFU	7.54	-379.40	50.30	1.00	4.17	39.61
CFU Separation	3.83	-347.50	90.62	1.00	1.70	31.23
Entry CFU	0.22	15.36	-69.00	0.46	0.07	3.74
Exit CFU	0.57	-24.32	42.39	0.88	0.20	5.10
Accumulation CFU	4.20	43.76	-10.42	0.99	1.10	11.42
Adsorption Cell	14.38	64.20	-4.46	1.00	2.46	11.10
Desorption Cell	11.37	-557.60	49.05	1.00	5.81	61.34
Entry Cell	0.60	27.76	-46.34	0.50	0.18	9.98
Exit Cell	1.18	-51.61	43.62	0.90	0.42	10.02
Multiplication Cell	18.38	-1289.65	70.16	1.00	8.97	122.11
Erosion Cell	10.06	-462.71	45.99	1.00	5.40	51.21
Accumulation Cell	10.50	-51.70	4.93	0.98	2.76	33.55
Area Coverage	0.0012	-0.0074	6.3122	0.9855	0.0003	0.0032

FIRST ORDER KINETICS RATE COEFFICIENT (in terms of accumulation) [h^{-1}]	Rate	± Std. Dev.
Multiplication Cell	0.712	0.431
Erosion Cell	0.474	0.386
Desorption CFU	0.766	0.701
Desorption Cell	0.587	0.673
CFU Separation	0.239	0.225

NEGATIVE RATES IN TERMS OF THEIR POSITIVE EQUIVALENTS [%]		Time Offset [min]
Desorption CFU	92.18	48.99
Desorption Cells	79.04	53.52
CFU Separation		89.31
Erosion Cell 0. Order	54.73	-24.17
Erosion Cell 1. Order	76.68	

Table 9. Directly measured results of series AA1.

Series: AA2
Shear Stress: 0.5 $N \cdot m^{-2}$
Cell Concentration: $10 \cdot 10^6$ $cells \cdot ml^{-1}$

ZERO ORDER KINETICS [#·min⁻¹·mm⁻²]	RATE (slope)	Y-INTERCEPT	X-INTERCEPT	r^2	CONFIDENCE INTERVAL (95%) ± Rate	± Y-Interc.
Adsorption CFU	71.86	-1311.83	18.25	0.99	26.40	221.23
Desorption CFU	57.02	-4627.23	81.15	1.02	31.75	384.35
CFU Separation	27.97	-2112.11	75.51	1.03	19.22	169.44
Entry CFU	3.10	-222.38	71.70	0.98	1.33	23.51
Exit CFU	15.86	-998.97	62.99	1.02	10.16	89.47
Accumulation CFU	34.79	906.06	-26.04	0.92	9.14	226.81
Adsorption Cell	135.66	-2429.47	17.91	0.99	47.48	444.69
Desorption Cell	107.03	-9238.21	86.31	1.03	58.56	750.00
Entry Cell	4.97	-302.04	60.75	0.99	2.30	32.43
Exit Cell	30.97	-2394.30	77.31	1.02	17.17	204.13
Multiplication Cell	179.43	-12051.47	67.16	1.03	155.93	979.79
Erosion Cell	108.79	-7505.13	68.99	1.03	81.76	617.23
Accumulation Cell	88.73	1481.38	-16.69	0.94	23.31	530.78
Area Coverage	0.0096	0.1628	-16.8796	0.9342	0.0025	0.0582

FIRST ORDER KINETICS RATE COEFFICIENT (in terms of accumulation) [h^{-1}]	Rate ± Std. Dev.
Multiplication Cell	0.593 0.191
Erosion Cell	0.360 0.209
Desorption CFU	0.355 0.230
Desorption Cell	0.264 0.194
CFU Separation	0.193 0.107

NEGATIVE RATES IN TERMS OF THEIR POSITIVE EQUIVALENTS [%]		Time Offset [min]
Desorption CFU	79.35	62.89
Desorption Cells	78.90	68.40
CFU Separation		57.25
Erosion Cell 0. Order	60.63	1.83
Erosion Cell 1. Order	74.21	

Table 10. Directly measured results of series AA2.

Series: AA3
Shear Stress: 0.5 $N \cdot m^{-2}$
Cell Concentration: $2.75 \cdot 10^6$ $cells \cdot ml^{-1}$

ZERO ORDER KINETICS [#·min⁻¹·mm⁻²]	RATE (slope)	Y-INTERCEPT	X-INTERCEPT	r^2	CONFIDENCE INTERVAL (95%) ± Rate	± Y-Interc.
Adsorption CFU	20.50	-634.39	30.95	0.95	6.28	124.39
Desorption CFU	11.11	-741.19	66.69	1.00	5.29	73.25
CFU Separation	1.86	-205.42	110.54	0.82	0.64	26.57
Entry CFU	0.12	40.58	-338.92	0.42	0.03	2.21
Exit CFU	0.55	-38.60	69.72	0.61	0.18	10.17
Accumulation CFU	11.55	-183.52	15.88	0.93	3.04	69.31
Adsorption Cell	34.33	-1109.24	32.31	0.93	10.29	239.13
Desorption Cell	16.70	-1239.08	74.20	1.00	7.89	116.74
Entry Cell	0.21	52.81	-246.84	0.18	0.06	4.61
Exit Cell	0.95	-58.47	61.83	0.54	0.30	19.45
Multiplication Cell	36.61	-2734.06	74.67	0.97	14.97	296.32
Erosion Cell	16.68	-991.49	59.43	0.98	7.17	113.57
Accumulation Cell	35.26	-1145.43	32.48	0.90	9.27	262.67
Area Coverage	0.0039	-0.1291	33.2004	0.8968	0.0010	0.0300

FIRST ORDER KINETICS RATE COEFFICIENT (in terms of accumulation) [h⁻¹]	Rate	± Std. Dev.
Multiplication Cell	0.556	0.336
Erosion Cell	0.290	0.130
Desorption CFU	0.434	0.302
Desorption Cell	0.253	0.172
CFU Separation	0.055	0.071

NEGATIVE RATES IN TERMS OF THEIR POSITIVE EQUIVALENTS [%]		Time Offset [min]
Desorption CFU	54.22	35.74
Desorption Cells	48.65	41.89
CFU Separation		79.59
Erosion Cell 0. Order	45.56	-15.24
Erosion Cell 1. Order	58.32	

Table 11. Directly measured results of series AA3.

Series: AA4
Shear Stress: 0.5 $N \cdot m^{-2}$
Cell Concentration: $1.92 \cdot 10^6$ $cells \cdot ml^{-1}$

ZERO ORDER KINETICS [$\#\cdot min^{-1}\cdot mm^{-2}$]	RATE (slope)	Y-INTERCEPT	X-INTERCEPT	r^{2}	CONFIDENCE INTERVAL (95%) ± Rate	± Y-Interc.
Adsorption CFU	13.52	-583.07	43.14	0.97	4.53	73.50
Desorption CFU	10.07	-809.02	80.35	1.01	4.82	72.55
CFU Separation	1.56	-169.30	108.47	0.94	0.60	16.88
Entry CFU	0.00	0.00	0.00	0.00	0.00	0.00
Exit CFU	0.00	0.00	0.00	0.00	0.00	0.00
Accumulation CFU	5.77	-112.96	19.57	0.98	1.52	20.10
Adsorption Cell	16.20	-603.98	37.29	0.97	5.50	79.64
Desorption Cell	10.95	-897.49	81.96	1.00	4.97	83.07
Entry Cell	0.00	0.00	0.00	0.00	0.00	0.00
Exit Cell	0.00	0.00	0.00	0.00	0.00	0.00
Multiplication Cell	12.59	-798.68	63.45	0.98	5.36	89.44
Erosion Cell	7.17	-270.94	37.79	0.97	2.98	40.34
Accumulation Cell	10.86	-277.75	25.58	0.97	2.85	46.86
Area Coverage	0.0012	-0.0298	25.3751	0.9677	0.0003	0.0049

FIRST ORDER KINETICS RATE COEFFICIENT (in terms of accumulation) [h^{-1}]	Rate	± Std. Dev.
Multiplication Cell	0.638	0.337
Erosion Cell	0.482	0.397
Desorption CFU	0.683	0.282
Desorption Cell	0.434	0.189
CFU Separation	0.074	0.107

NEGATIVE RATES IN TERMS OF THEIR POSITIVE EQUIVALENTS [%]		Time Offset [min]
Desorption CFU	74.50	37.21
Desorption Cells	67.61	44.67
CFU Separation		65.33
Erosion Cell 0. Order	56.95	-25.66
Erosion Cell 1. Order	63.50	

Table 12. Directly measured results of series AA4.

Series: AB1
Shear Stress: 0.5 $N \cdot m^{-2}$
Cell Concentration: $5.0 \cdot 10^6$ $cells \cdot ml^{-1}$

ZERO ORDER KINETICS [$\#\cdot min^{-1}\cdot mm^{-2}$]	RATE (slope)	Y-INTERCEPT	X-INTERCEPT	r^2	CONFIDENCE INTERVAL (95%) ± Rate	± Y-Interc.
Adsorption CFU	43.45	1297.57	-29.86	0.99	5.51	56.81
Desorption CFU	36.81	-219.01	5.95	0.99	15.04	84.15
CFU Separation	10.86	-535.72	49.35	0.99	5.42	59.58
Entry CFU	3.24	-264.62	81.63	1.01	1.54	23.65
Exit CFU	4.50	-186.82	41.54	0.96	1.79	28.25
Accumulation CFU	14.22	1333.93	-93.82	0.95	3.74	71.20
Adsorption Cell	57.51	1818.27	-31.61	0.99	6.61	68.46
Desorption Cell	50.80	-671.08	13.21	1.00	29.15	134.56
Entry Cell	6.37	-604.31	94.87	1.00	2.81	53.38
Exit Cell	7.65	-296.51	38.76	0.92	2.75	56.73
Multiplication Cell	68.05	-3596.03	52.84	1.01	45.76	342.15
Erosion Cell	34.94	-1852.42	53.02	1.00	19.53	187.49
Accumulation Cell	35.83	1300.59	-36.30	0.99	9.41	96.02
Area Coverage	0.0040	0.1384	-34.7387	0.9889	0.0010	0.0096

FIRST ORDER KINETICS RATE COEFFICIENT (in terms of accumulation) [h^{-1}]	Rate	± Std. Dev.
Multiplication Cell	0.550	0.208
Erosion Cell	0.294	0.106
Desorption CFU	0.649	0.326
Desorption Cell	0.500	0.294
CFU Separation	0.180	0.084

NEGATIVE RATES IN TERMS OF THEIR POSITIVE EQUIVALENTS [%]		Time Offset [min]
Desorption CFU	84.70	35.81
Desorption Cells	88.32	44.83
CFU Separation		79.21
Erosion Cell 0. Order	51.34	0.18
Erosion Cell 1. Order	77.11	

Table 13. Directly measured results of series AB1.

Series: AB2
Shear Stress: 0.5 $N \cdot m^{-2}$
Cell Concentration: $2.45 \cdot 10^6$ $cells \cdot ml^{-1}$

ZERO ORDER KINETICS [$\#\cdot min^{-1}\cdot mm^{-2}$]	RATE (slope)	Y-INTERCEPT	X-INTERCEPT	r^2	CONFIDENCE INTERVAL (95%) ± Rate	± Y-Interc.
Adsorption CFU	19.34	372.78	-19.28	1.00	3.48	21.49
Desorption CFU	10.24	-518.58	50.65	0.98	4.63	61.28
CFU Separation	2.82	-165.07	58.56	0.99	1.34	17.45
Entry CFU	0.64	61.40	-96.29	0.71	0.17	5.95
Exit CFU	1.29	-96.01	74.24	0.79	0.44	17.10
Accumulation CFU	12.63	580.01	-45.93	0.97	3.32	52.23
Adsorption Cell	30.18	586.39	-19.43	0.99	3.62	29.66
Desorption Cell	15.26	-904.06	59.23	0.98	6.80	100.10
Entry Cell	1.19	54.44	-45.73	0.70	0.34	12.48
Exit Cell	2.34	-183.03	78.37	0.78	0.78	32.23
Multiplication Cell	50.53	-2561.46	50.69	1.01	34.23	248.35
Erosion Cell	35.58	-1976.76	55.55	1.00	18.20	204.35
Accumulation Cell	31.02	658.29	-21.22	0.98	8.15	87.63
Area Coverage	0.0034	0.0653	-19.1055	0.9895	0.0009	0.0080

FIRST ORDER KINETICS RATE COEFFICIENT (in terms of accumulation) [h^{-1}]	Rate ± Std. Dev.	
Multiplication Cell	0.581	0.243
Erosion Cell	0.394	0.129
Desorption CFU	0.228	0.154
Desorption Cell	0.155	0.112
CFU Separation	0.067	0.061

NEGATIVE RATES IN TERMS OF THEIR POSITIVE EQUIVALENTS [%]		Time Offset [min]
Desorption CFU	52.94	69.93
Desorption Cells	50.57	78.66
CFU Separation		77.83
Erosion Cell 0. Order	70.41	4.87
Erosion Cell 1. Order	67.84	

Table 14. Directly measured results of series AB2.

Series: AB3
Shear Stress: 0.5 $N \cdot m^{-2}$
Cell Concentration: $1.1 \cdot 10^{6}$ $cells \cdot ml^{-1}$

ZERO ORDER KINETICS [$\# \cdot min^{-1} \cdot mm^{-2}$]	RATE (slope)	Y-INTERCEPT	X-INTERCEPT	r^2	CONFIDENCE INTERVAL (95%) ± Rate	± Y-Interc.
Adsorption CFU	5.99	-76.87	12.84	1.00	2.38	13.93
Desorption CFU	2.34	-143.54	61.42	0.94	0.90	18.84
CFU Separation	0.23	-28.31	123.59	0.74	0.08	3.99
Entry CFU	0.39	-38.18	98.34	0.88	0.14	4.69
Exit CFU	0.39	-5.47	13.92	0.91	0.13	2.63
Accumulation CFU	3.89	2.95	-.76	0.99	1.02	8.68
Adsorption Cell	10.43	-129.94	12.46	1.00	4.28	23.22
Desorption Cell	3.73	-236.81	63.57	0.95	1.47	29.29
Entry Cell	0.58	-58.50	100.63	0.87	0.21	7.16
Exit Cell	0.61	-.53	0.86	0.85	0.19	4.86
Multiplication Cell	9.24	-817.75	88.48	1.01	4.31	71.26
Erosion Cell	7.51	-734.60	97.88	0.99	3.17	66.90
Accumulation Cell	8.35	-22.80	2.73	0.99	2.19	18.71
Area Coverage	0.0009	-0.0061	6.5659	0.9893	0.0002	0.0022

FIRST ORDER KINETICS RATE COEFFICIENT (in terms of accumulation) [h^{-1}]	Rate	± Std. Dev.
Multiplication Cell	0.306	0.204
Erosion Cell	0.212	0.262
Desorption CFU	0.240	0.239
Desorption Cell	0.181	0.186
CFU Separation	0.015	0.045

NEGATIVE RATES IN TERMS OF THEIR POSITIVE EQUIVALENTS [%]		Time Offset [min]
Desorption CFU	39.02	48.58
Desorption Cells	35.73	51.11
CFU Separation		110.75
Erosion Cell 0. Order	81.20	9.40
Erosion Cell 1. Order	75.69	

Table 15. Directly measured results of series AB3.

Series: AB4
Shear Stress: 0.75 $N \cdot m^{-2}$
Cell Concentration: $2.65 \cdot 10^6$ $cells \cdot ml^{-1}$

ZERO ORDER KINETICS [$\#\cdot min^{-1}\cdot mm^{-2}$]	RATE (slope)	Y-INTERCEPT	X-INTERCEPT	r^2	CONFIDENCE INTERVAL (95%) ± Rate	± Y-Interc.
Adsorption CFU	18.82	-104.36	5.54	1.00	6.99	31.00
Desorption CFU	10.21	-642.99	62.97	1.00	4.87	65.34
CFU Separation	2.92	-315.09	107.98	0.96	1.14	30.54
Entry CFU	0.71	84.31	-118.10	1.12	0.13	2.44
Exit CFU	0.30	-16.60	54.89	0.88	0.11	2.88
Accumulation CFU	12.44	211.74	-17.02	0.99	3.27	27.44
Adsorption Cell	27.33	-150.87	5.52	1.00	9.47	49.79
Desorption Cell	13.44	-883.78	65.77	0.99	6.32	88.74
Entry Cell	1.78	98.73	-55.48	0.90	0.39	8.35
Exit Cell	1.08	-70.43	65.04	0.90	0.39	10.49
Multiplication Cell	37.24	-2490.26	66.87	1.02	22.14	218.94
Erosion Cell	17.66	-1136.92	64.37	1.00	8.83	110.66
Accumulation Cell	33.95	-318.93	9.39	0.99	8.92	56.81
Area Coverage	0.0037	-0.0322	8.7605	0.9952	0.0010	0.0058

FIRST ORDER KINETICS RATE COEFFICIENT (in terms of accumulation) [h^{-1}]	Rate	± Std. Dev.
Multiplication Cell	0.457	0.191
Erosion Cell	0.210	0.114
Desorption CFU	0.251	0.127
Desorption Cell	0.154	0.096
CFU Separation	0.056	0.061

NEGATIVE RATES IN TERMS OF THEIR POSITIVE EQUIVALENTS [%]		Time Offset [min]
Desorption CFU	54.25	57.42
Desorption Cells	49.17	60.25
CFU Separation		102.44
Erosion Cell 0. Order	47.42	-2.49
Erosion Cell 1. Order	61.30	

Table 16. Directly measured results of series AB4.

Series: AB5
Shear Stress: 1.0 $N \cdot m^{-2}$
Cell Concentration: $6.75 \cdot 10^6$ $cells \cdot ml^{-1}$

ZERO ORDER KINETICS [$\# \cdot min^{-1} \cdot mm^{-2}$]	RATE (slope)	Y-INTERCEPT	X-INTERCEPT	r^2	CONFIDENCE INTERVAL (95%) ± Rate	± Y-Interc.
Adsorption CFU	31.31	288.62	-9.22	0.99	4.01	23.00
Desorption CFU	22.17	-1244.63	56.14	1.01	12.33	122.70
CFU Separation	9.65	-959.98	99.52	1.01	4.30	81.89
Entry CFU	0.35	-3.76	10.65	0.48	0.11	7.06
Exit CFU	3.27	-133.07	40.68	0.99	1.58	16.64
Accumulation CFU	16.63	525.60	-31.60	0.98	4.37	49.81
Adsorption Cell	56.01	406.98	-7.27	1.00	8.81	48.33
Desorption Cell	36.99	-2128.77	57.54	1.01	21.22	204.56
Entry Cell	0.67	-45.01	66.88	0.52	0.21	14.48
Exit Cell	4.89	-185.52	37.90	0.99	2.34	24.27
Multiplication Cell	60.68	-4144.98	68.31	1.00	30.12	393.41
Erosion Cell	29.11	-1844.55	63.37	1.00	13.91	186.48
Accumulation Cell	46.08	405.67	-8.80	0.99	12.11	113.64
Area Coverage	0.0051	0.0326	-6.4000	0.9873	0.0013	0.0131

FIRST ORDER KINETICS RATE COEFFICIENT (in terms of accumulation) [h^{-1}]	Rate	± Std. Dev.
Multiplication Cell	0.465	0.199
Erosion Cell	0.229	0.132
Desorption CFU	0.394	0.174
Desorption Cell	0.295	0.174
CFU Separation	0.126	0.098

NEGATIVE RATES IN TERMS OF THEIR POSITIVE EQUIVALENTS [%]		Time Offset [min]
Desorption CFU	70.82	65.36
Desorption Cells	66.05	64.81
CFU Separation		108.74
Erosion Cell 0. Order	47.97	-4.94
Erosion Cell 1. Order	74.81	

Table 17. Directly measured results of series AB5.

Series: AB6
Shear Stress: 1.25 $N \cdot m^{-2}$
Cell Concentration: $6.9 \cdot 10^6$ $cells \cdot ml^{-1}$

ZERO ORDER KINETICS [$\# \cdot min^{-1} \cdot mm^{-2}$]	RATE (slope)	Y-INTERCEPT	X-INTERCEPT	r^2	CONFIDENCE INTERVAL (95%) ± Rate	± Y-Interc.
Adsorption CFU	19.69	681.43	-34.60	0.98	2.71	30.81
Desorption CFU	11.67	6.65	-.57	0.97	3.56	37.47
CFU Separation	2.47	-201.91	81.63	1.01	1.17	18.09
Entry CFU	0.00	0.00	0.00	0.00	0.00	0.00
Exit CFU	1.22	-3.50	2.87	0.93	0.38	6.53
Accumulation CFU	9.17	493.03	-53.75	0.95	2.41	46.18
Adsorption Cell	30.42	1024.93	-33.69	0.98	3.74	40.64
Desorption Cell	15.69	17.70	-1.13	0.97	4.75	52.06
Entry Cell	0.00	0.00	0.00	0.00	0.00	0.00
Exit Cell	2.15	-80.35	37.36	0.78	0.70	24.68
Multiplication Cell	49.62	-3206.28	64.61	1.02	33.81	274.91
Erosion Cell	32.37	-2263.54	69.92	1.01	17.43	203.00
Accumulation Cell	29.28	285.62	-9.75	0.99	7.69	63.31
Area Coverage	0.0032	0.0261	-8.1012	0.9913	0.0008	0.0068

FIRST ORDER KINETICS RATE COEFFICIENT (in terms of accumulation) [h^{-1}]	Rate ± Std. Dev.	
Multiplication Cell	0.563	0.234
Erosion Cell	0.345	0.149
Desorption CFU	0.507	0.419
Desorption Cell	0.336	0.377
CFU Separation	0.057	0.059

NEGATIVE RATES IN TERMS OF THEIR POSITIVE EQUIVALENTS [%]		Time Offset [min]
Desorption CFU	59.26	34.03
Desorption Cells	51.56	32.56
CFU Separation		116.23
Erosion Cell 0. Order	65.24	5.31
Erosion Cell 1. Order	66.20	

Table 18. Directly measured results of series AB6.

Series: AC1
Shear Stress: 0.5 $N \cdot m^{-2}$
Cell Concentration: $4.7 \cdot 10^6$ $cells \cdot ml^{-1}$

ZERO ORDER KINETICS [$\#\cdot min^{-1}\cdot mm^{-2}$]	RATE (slope)	Y-INTERCEPT	X-INTERCEPT	r^2	CONFIDENCE INTERVAL (95%) ± Rate	± Y-Interc.
Adsorption CFU	35.34	-885.48	25.06	0.99	13.44	120.26
Desorption CFU	27.11	-1821.57	67.19	1.03	23.95	145.73
CFU Separation	1.71	-153.12	89.66	1.00	0.76	13.84
Entry CFU	0.00	0.00	0.00	0.00	0.00	0.00
Exit CFU	1.72	-184.83	107.32	0.97	0.69	17.14
Accumulation CFU	10.71	415.93	-38.85	0.99	2.81	27.65
Adsorption Cell	46.29	-541.26	11.69	0.99	16.75	114.63
Desorption Cell	27.11	-1821.57	67.19	1.03	23.95	145.73
Entry Cell	0.00	0.00	0.00	0.00	0.00	0.00
Exit Cell	2.29	-247.34	107.94	0.95	0.89	24.16
Multiplication Cell	33.39	-1297.31	38.85	1.00	17.59	157.83
Erosion Cell	22.55	-925.91	41.06	1.00	12.29	107.70
Accumulation Cell	30.90	518.28	-16.77	1.00	8.12	41.56
Area Coverage	0.0034	0.0526	-15.3664	0.9969	0.0009	0.0044

FIRST ORDER KINETICS RATE COEFFICIENT (in terms of accumulation) [h^{-1}]	Rate	± Std. Dev.
Multiplication Cell	0.433	0.238
Erosion Cell	0.286	0.130
Desorption CFU	0.623	0.219
Desorption Cell	0.256	0.087
CFU Separation	0.039	0.043

NEGATIVE RATES IN TERMS OF THEIR POSITIVE EQUIVALENTS [%]		/Time Offset [min]
Desorption CFU	76.71	42.14
Desorption Cells	58.56	55.50
CFU Separation		64.60
Erosion Cell 0. Order	67.52	2.21
Erosion Cell 1. Order	41.13	

Table 19. Directly measured results of series AC1.

Series: AC2
Shear Stress: 0.5 $N \cdot m^{-2}$
Cell Concentration: $3.64 \cdot 10^6$ $cells \cdot ml^{-1}$

ZERO ORDER KINETICS [$\#\cdot min^{-1}\cdot mm^{-2}$]	RATE (slope)	Y-INTERCEPT	X-INTERCEPT	r^2	CONFIDENCE INTERVAL (95%) ± Rate	± Y-Interc.
Adsorption CFU	27.29	348.02	-12.75	0.99	3.75	25.82
Desorption CFU	11.11	-416.25	37.45	1.01	8.24	45.96
CFU Separation	3.48	-312.51	89.90	0.99	1.50	29.03
Entry CFU	0.00	0.00	0.00	0.00	0.00	0.00
Exit CFU	1.58	-136.02	85.93	0.93	0.60	15.66
Accumulation CFU	18.70	446.52	-23.88	0.98	4.91	54.60
Adsorption Cell	47.61	604.98	-12.71	0.99	3.20	19.69
Desorption Cell	15.12	-796.17	52.67	1.01	8.83	79.40
Entry Cell	0.00	0.00	0.00	0.00	0.00	0.00
Exit Cell	3.57	-357.11	99.95	0.95	1.37	36.73
Multiplication Cell	64.77	-5088.74	78.57	1.01	31.87	452.85
Erosion Cell	36.33	-2554.09	70.30	1.00	17.66	242.22
Accumulation Cell	54.76	-212.62	3.88	1.00	14.39	78.85
Area Coverage	0.0060	-0.0325	5.3753	0.9959	0.0016	0.0089

FIRST ORDER KINETICS RATE COEFFICIENT (in terms of accumulation) [h^{-1}]	Rate	± Std. Dev.
Multiplication Cell	0.392	0.084
Erosion Cell	0.254	0.068
Desorption CFU	0.214	0.103
Desorption Cell	0.118	0.056
CFU Separation	0.048	0.044

NEGATIVE RATES IN TERMS OF THEIR POSITIVE EQUIVALENTS [%]		Time Offset [min]
Desorption CFU	40.73	50.21
Desorption Cells	31.75	65.38
CFU Separation		102.65
Erosion Cell 0. Order	56.10	-8.27
Erosion Cell 1. Order	54.94	

Table 20. Directly measured results of series AC2.

Series: AC3
Shear Stress: 0.75 $N \cdot m^{-2}$
Cell Concentration: $6.3 \cdot 10^6$ $cells \cdot ml^{-1}$

ZERO ORDER KINETICS [$\# \cdot min^{-1} \cdot mm^{-2}$]	RATE (slope)	Y-INTERCEPT	X-INTERCEPT	r^{2*}	CONFIDENCE INTERVAL (95%) ± Rate	± Y-Interc.
Adsorption CFU	42.61	-1301.42	30.54	0.99	15.93	163.32
Desorption CFU	21.50	-1384.53	64.40	1.00	10.18	139.74
CFU Separation	1.12	-142.49	127.56	0.65	0.37	22.75
Entry CFU	2.68	-136.85	51.05	1.00	1.43	14.42
Exit CFU	3.19	-153.58	48.14	0.98	1.41	19.04
Accumulation CFU	22.99	-325.63	14.16	0.99	6.04	50.89
Adsorption Cell	74.17	-2057.54	27.74	0.99	27.20	277.71
Desorption Cell	27.86	-2083.92	74.80	0.95	10.87	241.76
Entry Cell	4.58	-250.45	54.73	0.94	1.76	34.77
Exit Cell	6.36	-483.03	75.92	0.96	2.53	53.95
Multiplication Cell	62.05	-4760.64	76.73	0.98	26.55	481.95
Erosion Cell	46.69	-3670.48	78.62	0.99	20.37	359.70
Accumulation Cell	61.44	-1063.57	17.31	0.99	16.14	138.07
Area Coverage	0.0068	-0.1245	18.2354	0.9895	0.0018	0.0160

FIRST ORDER KINETICS RATE COEFFICIENT (in terms of accumulation) [h^{-1}]	Rate	± Std. Dev.
Multiplication Cell	0.431	0.097
Erosion Cell	0.321	0.081
Desorption CFU	0.432	0.148
Desorption Cell	0.206	0.075
CFU Separation	0.012	0.030

NEGATIVE RATES IN TERMS OF THEIR POSITIVE EQUIVALENTS [%]		Time Offset [min]
Desorption CFU	50.45	33.86
Desorption Cells	37.56	47.06
CFU Separation		97.02
Erosion Cell 0. Order	75.25	1.89
Erosion Cell 1. Order	47.71	

Table 21. Directly measured results of series AC3.

Series: AC4
Shear Stress: 1.0 $N \cdot m^{-2}$
Cell Concentration: $8.7 \cdot 10^6$ $cells \cdot ml^{-1}$

ZERO ORDER KINETICS [$\# \cdot min^{-1} \cdot mm^{-2}$]	RATE (slope)	Y-INTERCEPT	X-INTERCEPT	r^2	CONFIDENCE INTERVAL (95%) ± Rate	± Y-Interc.
Adsorption CFU	41.33	-979.86	23.71	0.99	16.86	127.66
Desorption CFU	26.78	-2030.40	75.83	1.02	15.21	170.63
CFU Separation	3.75	-375.35	100.17	0.86	1.32	47.73
Entry CFU	0.33	49.21	-150.49	0.84	0.07	2.52
Exit CFU	2.46	-146.61	59.66	0.84	0.84	26.94
Accumulation CFU	19.16	211.87	-11.06	0.99	5.03	45.19
Adsorption Cell	73.86	-1333.04	18.05	1.00	33.82	183.44
Desorption Cell	39.92	-3221.78	80.71	1.01	20.38	276.62
Entry Cell	0.72	176.64	-243.83	-1.87	0.09	2.94
Exit Cell	5.52	-486.64	88.22	0.86	1.95	65.37
Multiplication Cell	64.47	-4251.10	65.94	1.03	50.11	350.52
Erosion Cell	47.90	-3363.67	70.23	1.03	33.88	274.10
Accumulation Cell	52.60	281.19	-5.35	0.98	13.82	162.50
Area Coverage	0.0058	0.0304	-5.2725	0.9834	0.0015	0.0170

FIRST ORDER KINETICS RATE COEFFICIENT (in terms of accumulation) [h^{-1}]	Rate	± Std. Dev.
Multiplication Cell	0.433	0.132
Erosion Cell	0.301	0.099
Desorption CFU	0.410	0.163
Desorption Cell	0.236	0.122
CFU Separation	0.055	0.062

NEGATIVE RATES IN TERMS OF THEIR POSITIVE EQUIVALENTS [%]		Time Offset [min]
Desorption CFU	64.79	52.12
Desorption Cells	54.05	62.66
CFU Separation		76.46
Erosion Cell 0. Order	74.29	4.29
Erosion Cell 1. Order	57.41	

Table 22. Directly measured results of series AC4.

Series: AC5
Shear Stress: 1.25 $N \cdot m^{-2}$
Cell Concentration: 12.2 10^6 $cells \cdot ml^{-1}$

ZERO ORDER KINETICS [$\# \cdot min^{-1} \cdot mm^{-2}$]	RATE (slope)	Y-INTERCEPT	X-INTERCEPT	r^2	CONFIDENCE INTERVAL (95%) ± Rate	± Y-Interc.
Adsorption CFU	51.76	-469.66	9.07	1.00	22.57	93.98
Desorption CFU	17.36	-1113.17	64.12	1.02	10.76	98.49
CFU Separation	2.26	-227.69	100.66	0.93	0.86	24.04
Entry CFU	0.22	-29.35	133.12	0.43	0.07	6.60
Exit CFU	2.30	-44.32	19.28	0.95	0.83	12.08
Accumulation CFU	17.30	226.30	-13.08	0.98	4.54	52.43
Adsorption Cell	80.40	-1022.70	12.72	0.99	30.38	196.42
Desorption Cell	28.85	-2283.35	79.15	0.98	12.35	227.42
Entry Cell	1.07	-142.13	132.62	0.45	0.34	30.93
Exit Cell	4.49	-136.30	30.32	0.94	1.64	28.50
Multiplication Cell	73.07	-5104.62	69.85	1.00	35.68	484.20
Erosion Cell	47.79	-3213.26	67.24	1.00	23.26	311.29
Accumulation Cell	56.23	-626.34	11.14	0.99	14.77	144.90
Area Coverage	0.0062	-0.0745	12.0275	0.9883	0.0016	0.0153

FIRST ORDER KINETICS RATE COEFFICIENT (in terms of accumulation) [h^{-1}]	Rate ± Std. Dev.
Multiplication Cell	0.572 0.247
Erosion Cell	0.370 0.183
Desorption CFU	0.336 0.157
Desorption Cell	0.198 0.125
CFU Separation	0.034 0.044

NEGATIVE RATES IN TERMS OF THEIR POSITIVE EQUIVALENTS [%]		Time Offset [min]
Desorption CFU	33.54	55.05
Desorption Cells	35.88	66.43
CFU Separation		91.59
Erosion Cell 0. Order	65.39	-2.61
Erosion Cell 1. Order	59.09	

Table 23. Directly measured results of series AC5.

APPENDIX D

FIGURES OF KINETIC RESULTS

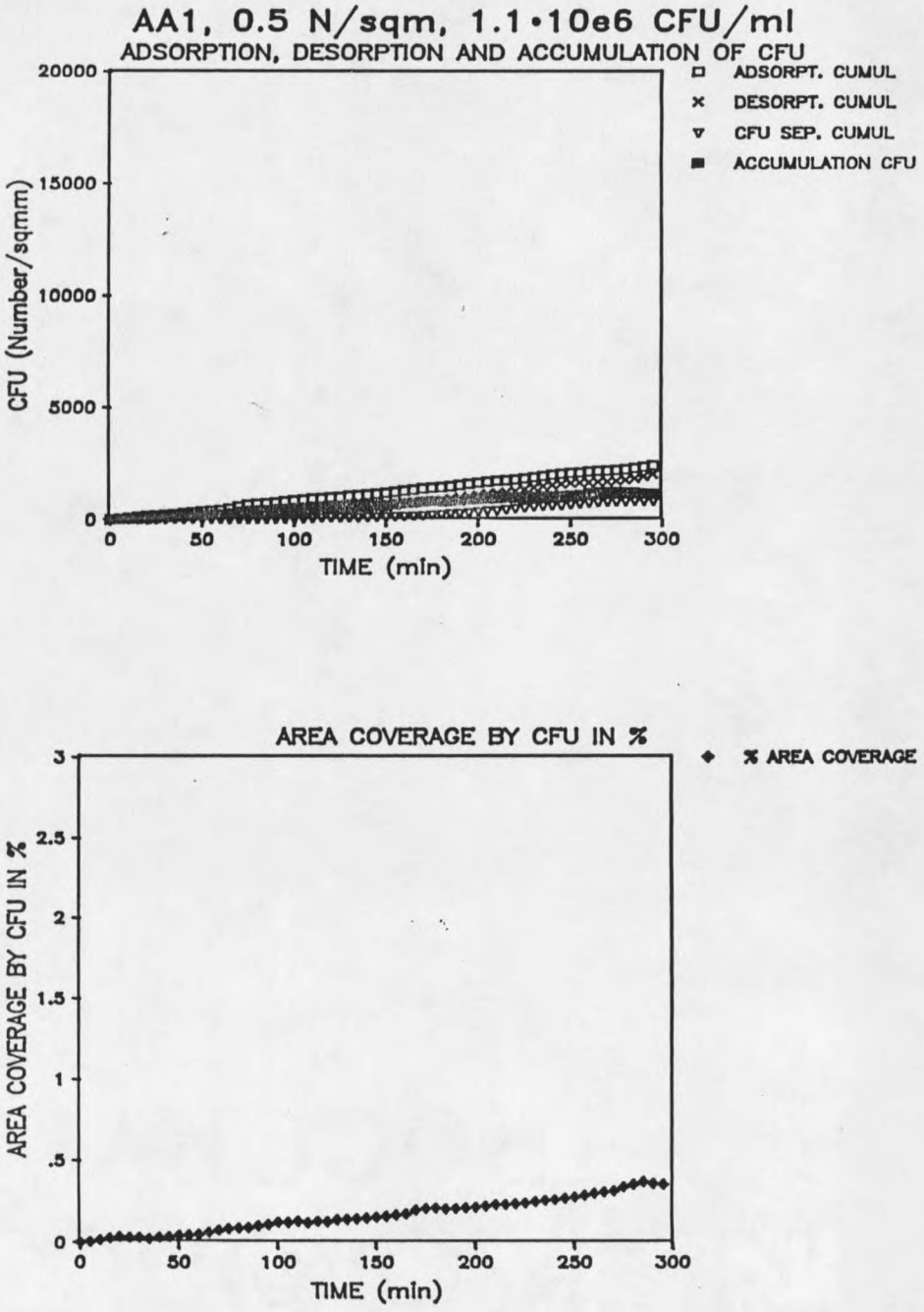

Figure 43. Progression of colonization (Series AA1) in terms of CFU (a) and area coverage (b).

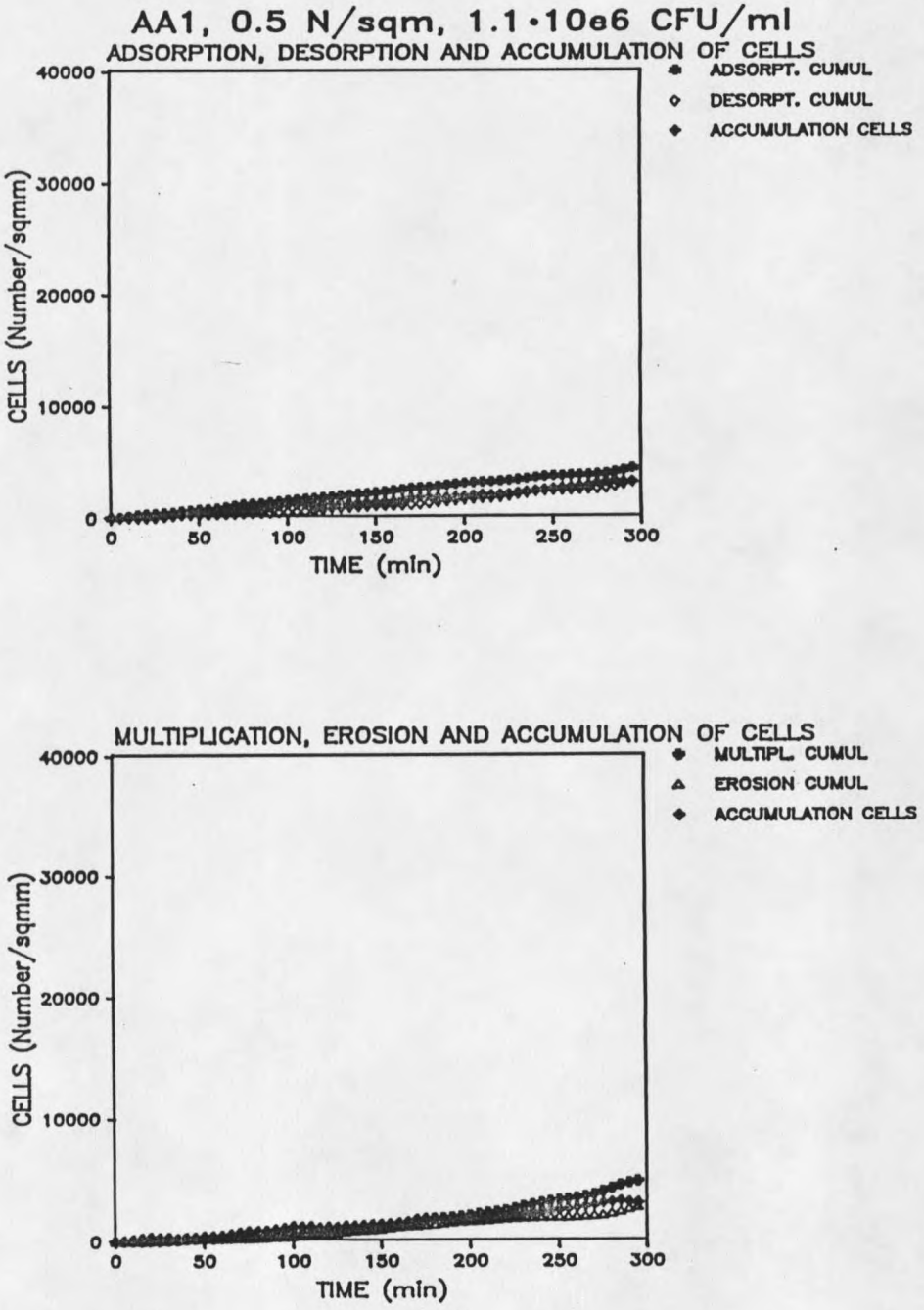

Figure 44. Progression in terms of cells (Series AA1). Sorption related processes (a) and growth related processes (b).

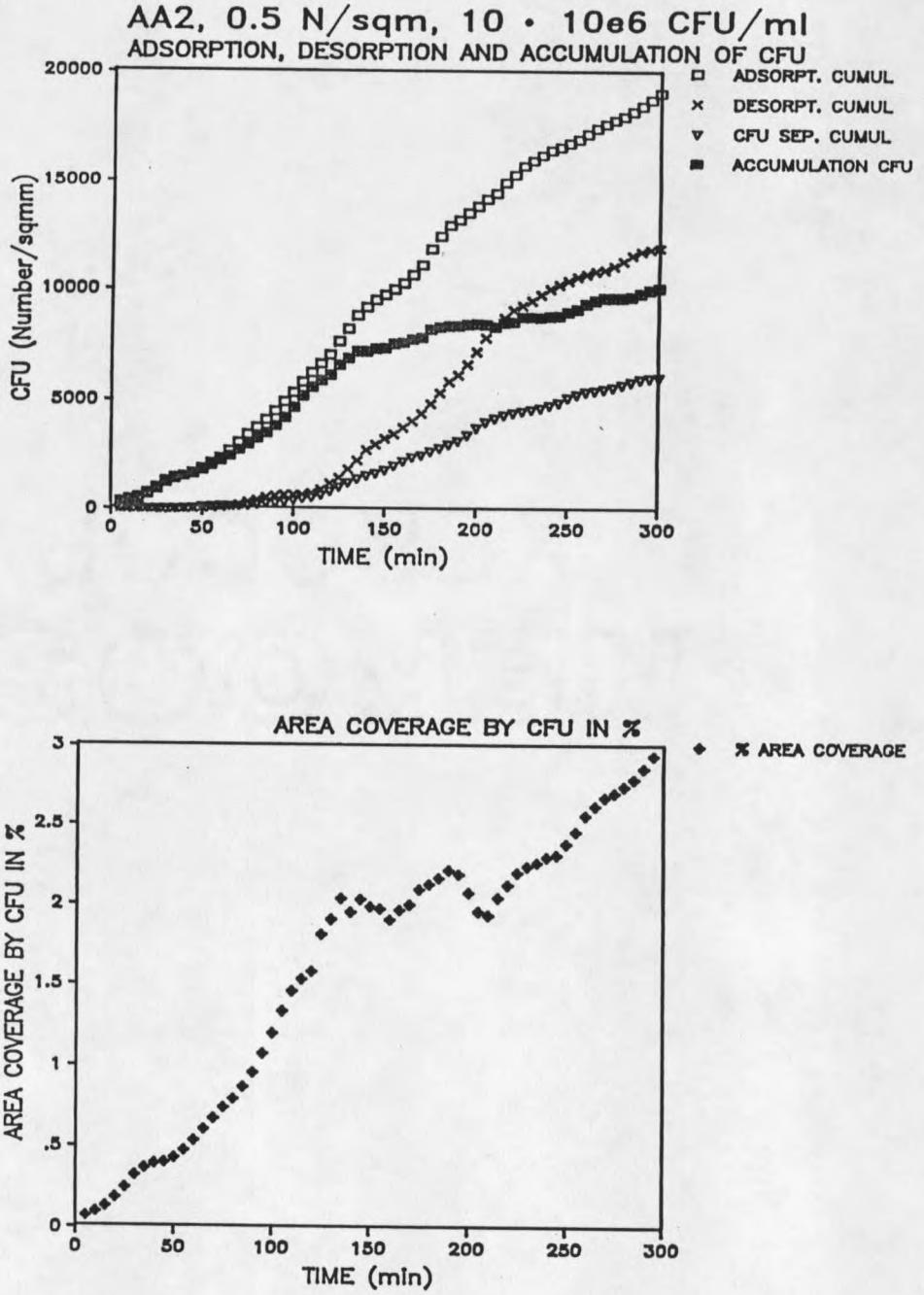

Figure 45. Progression of colonization (Series AA2) in terms of CFU (a) and area coverage (b).

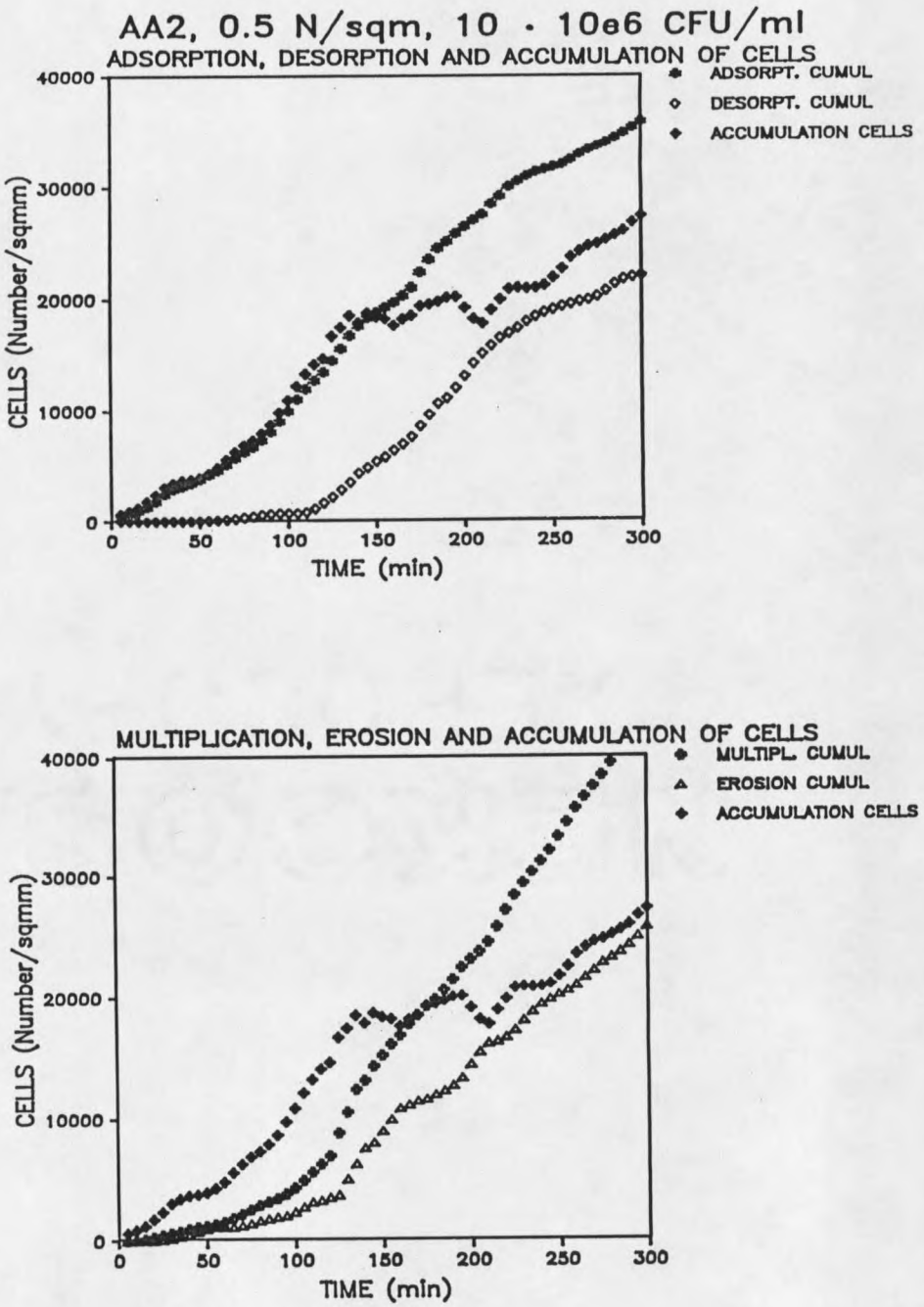

Figure 46. Progression in terms of cells (Series AA2). Sorption related processes (a) and growth related processes (b).

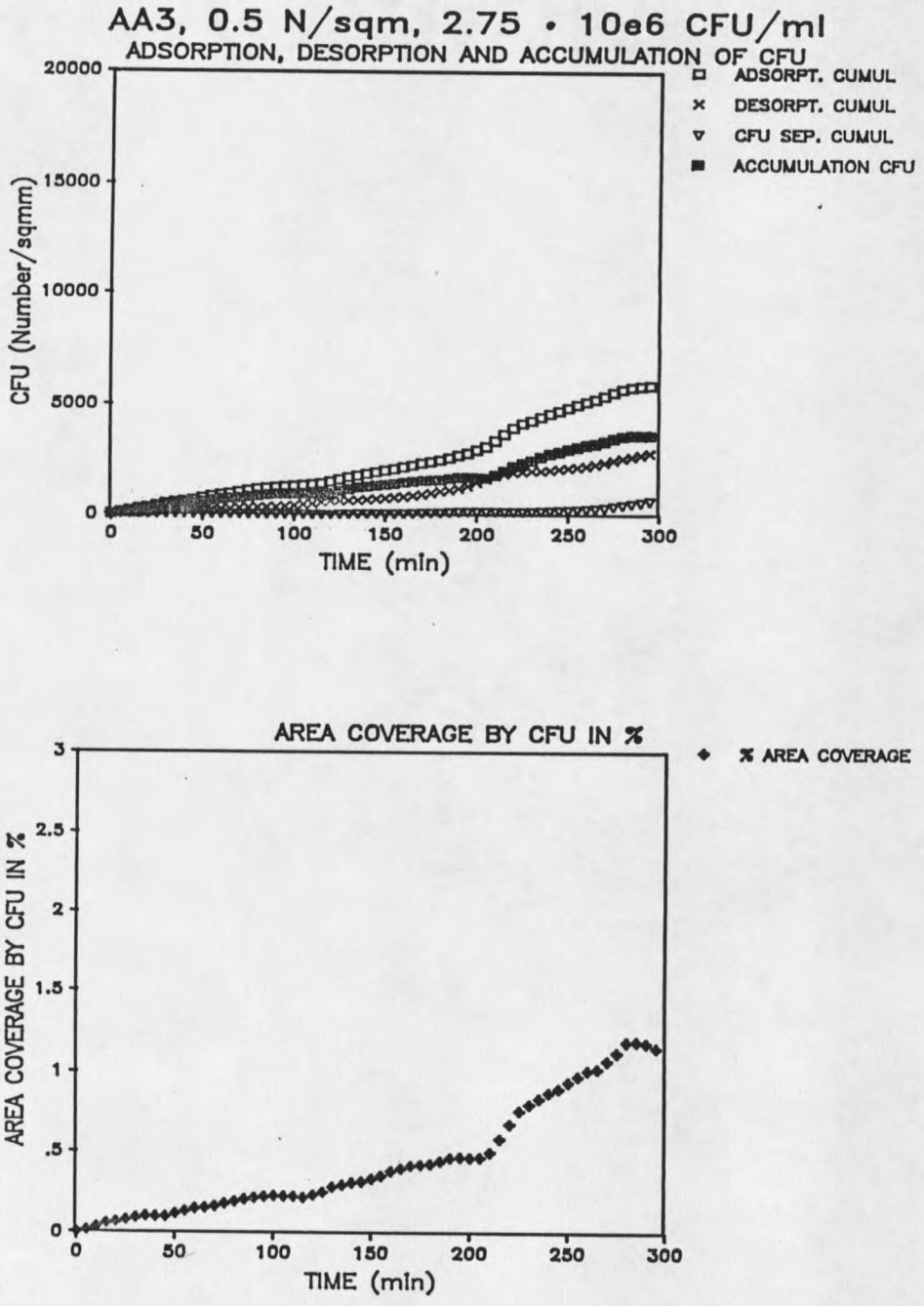

Figure 47. Progression of colonization (Series AA3) in terms of CFU (a) and area coverage (b).

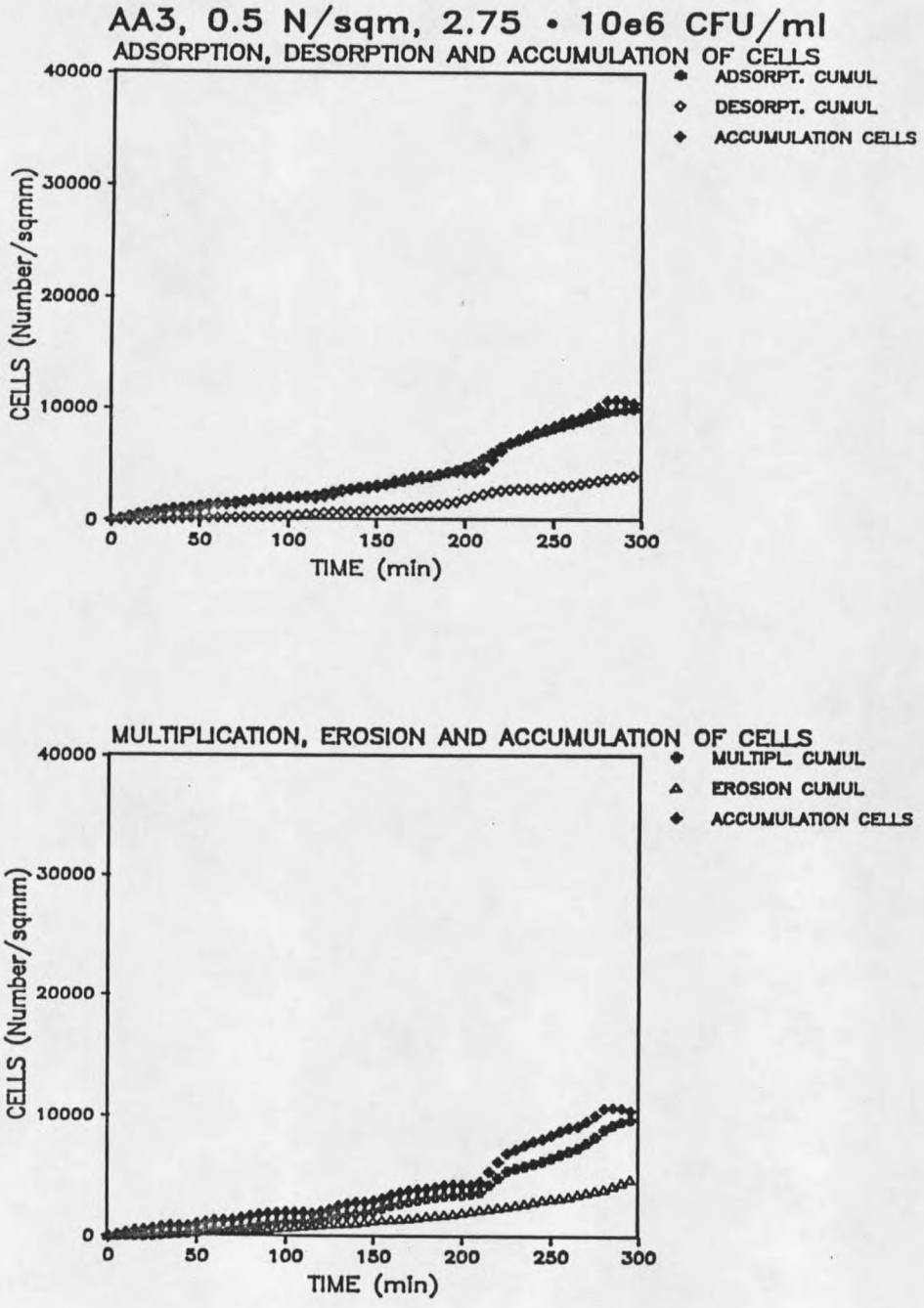

Figure 48. Progression in terms of cells (Series AA3). Sorption related processes (a) and growth related processes (b).

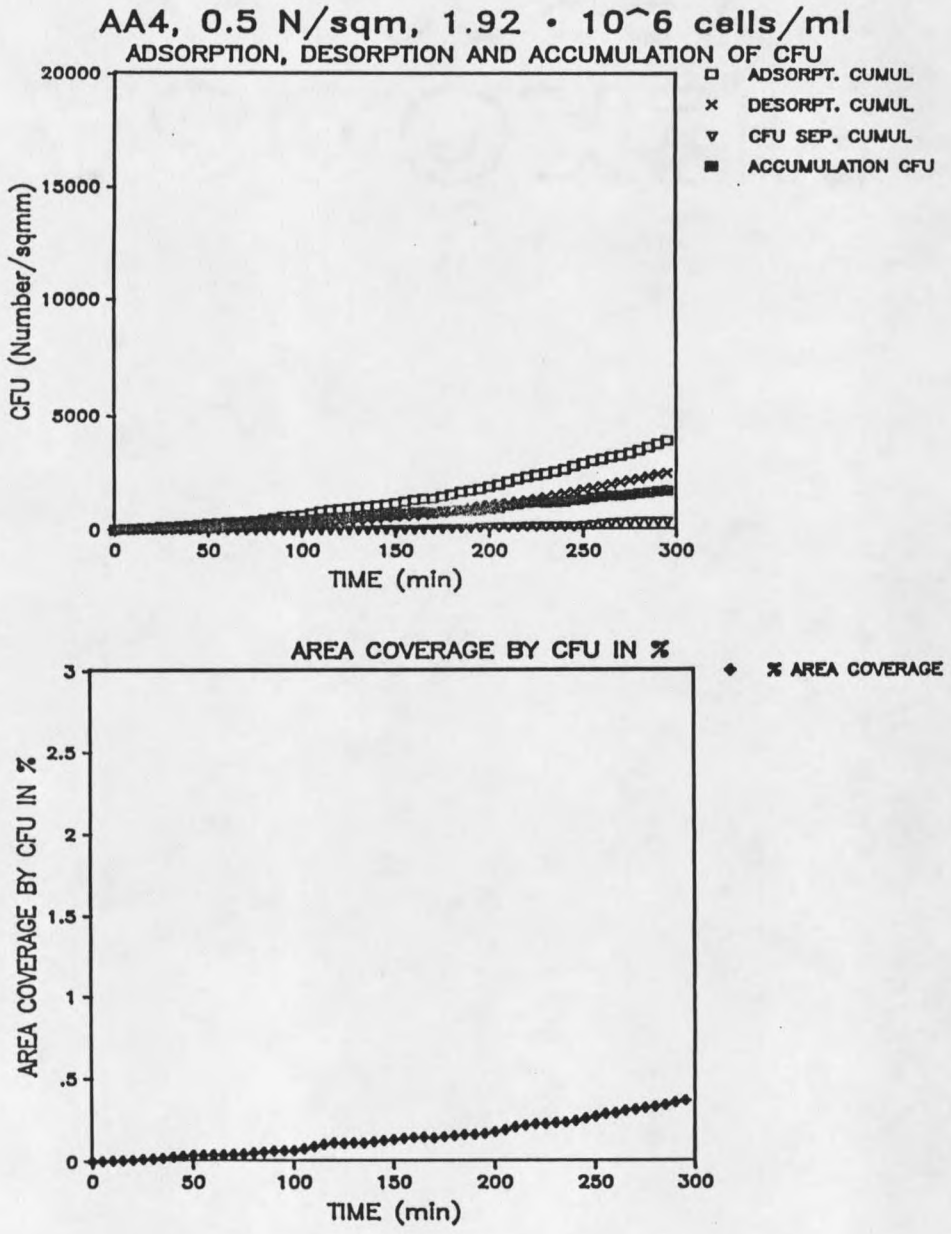

Figure 49. Progression of colonization (Series AA4) in terms of CFU (a) and area coverage (b).

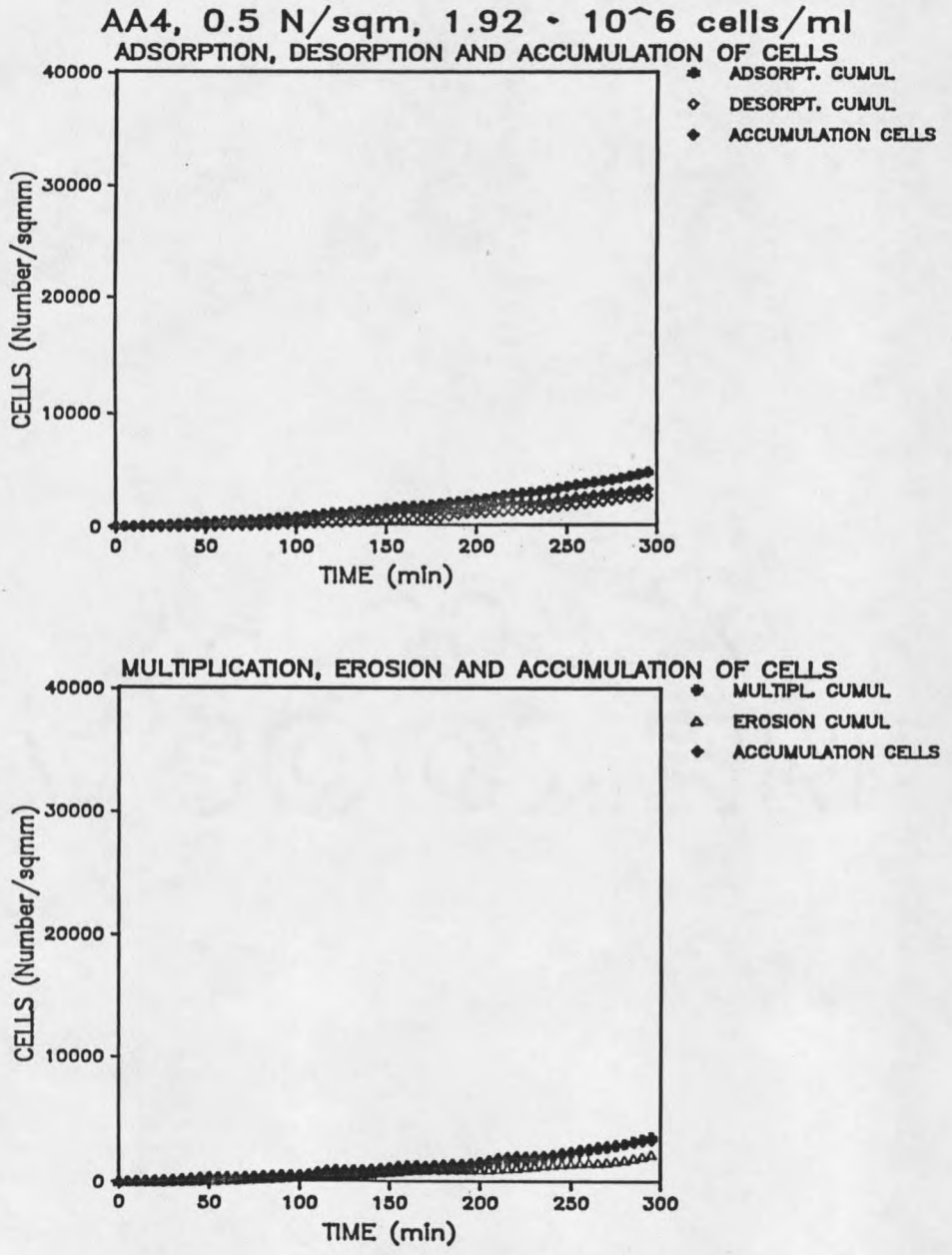

Figure 50. Progression in terms of cells (Series AA4). Sorption related processes (a) and growth related processes (b).

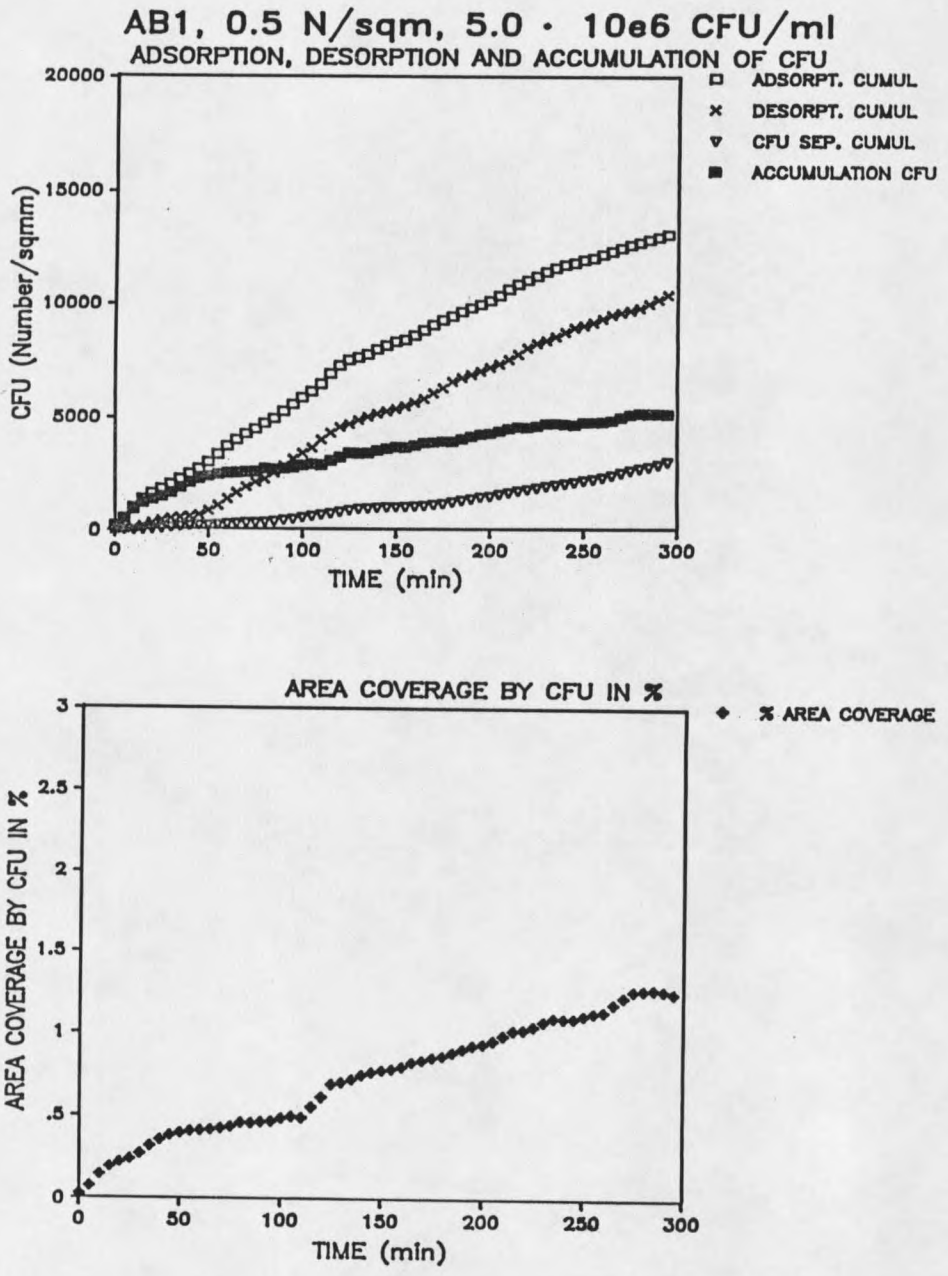

Figure 51. Progression of colonization (Series AB1) in terms of CFU (a) and area coverage (b).

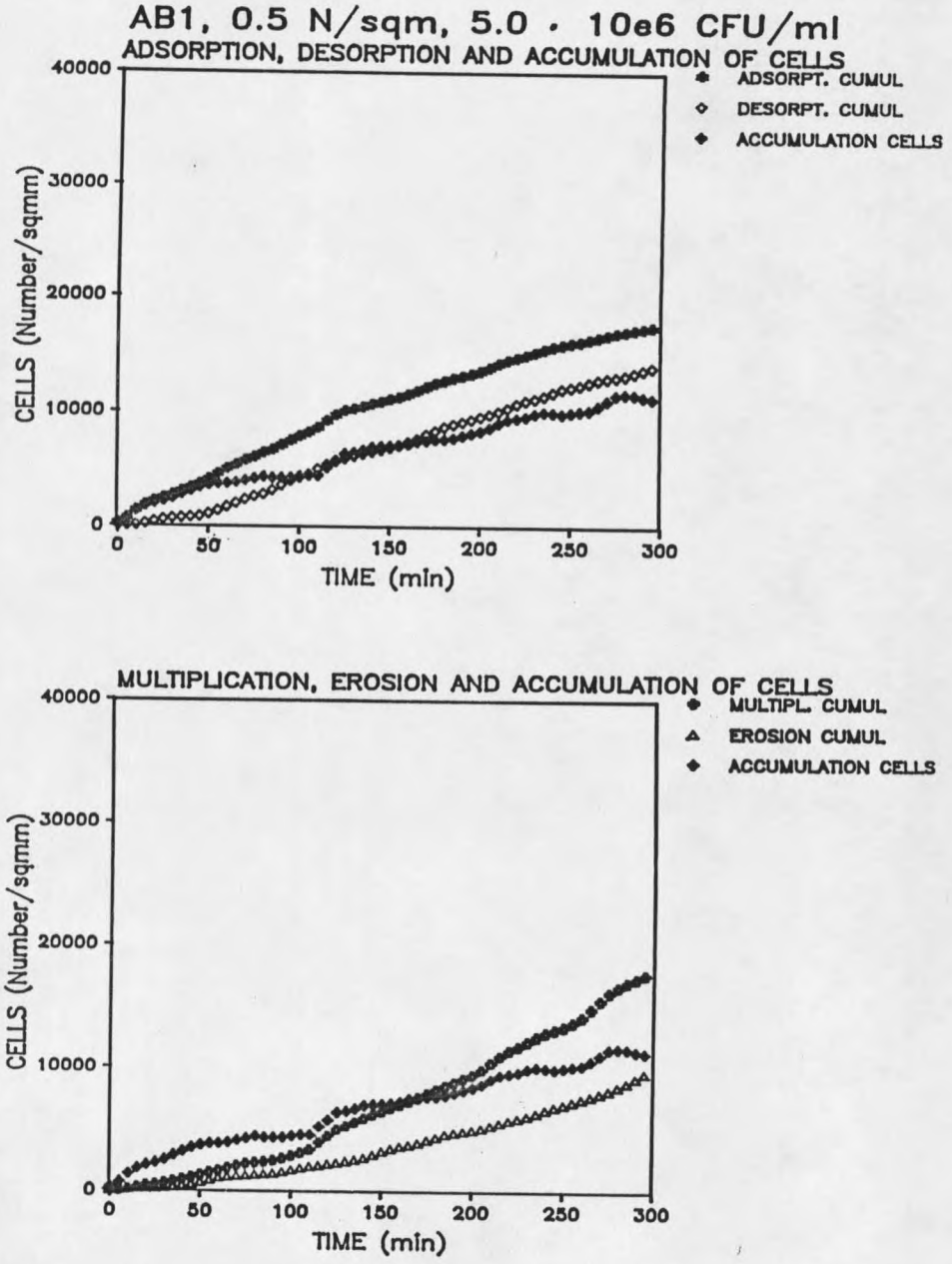

Figure 52. Progression in terms of cells (Series AB1). Sorption related processes (a) and growth related processes (b).

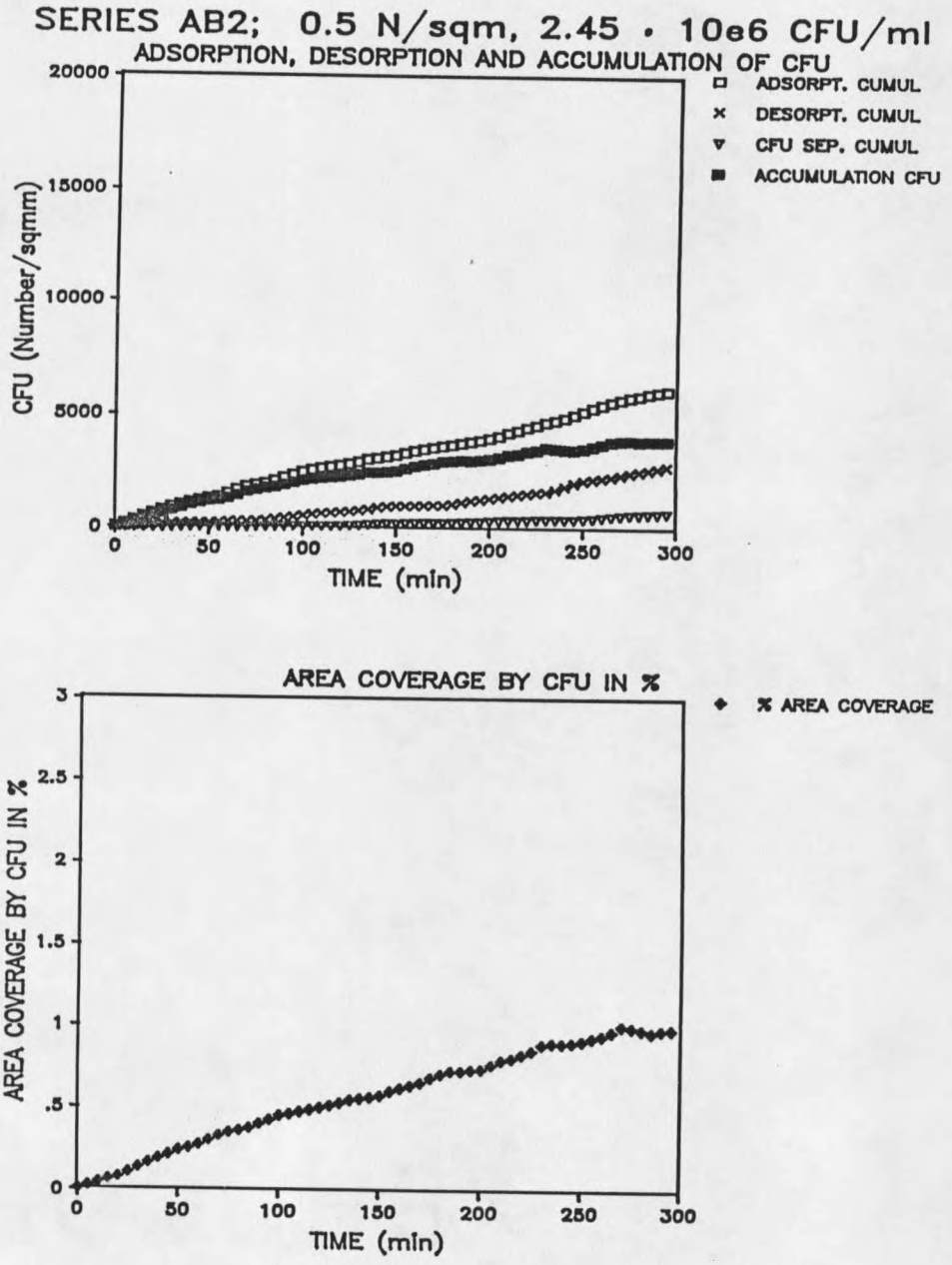

Figure 53. Progression of colonization (Series AB2) in terms of CFU (a) and area coverage (b).

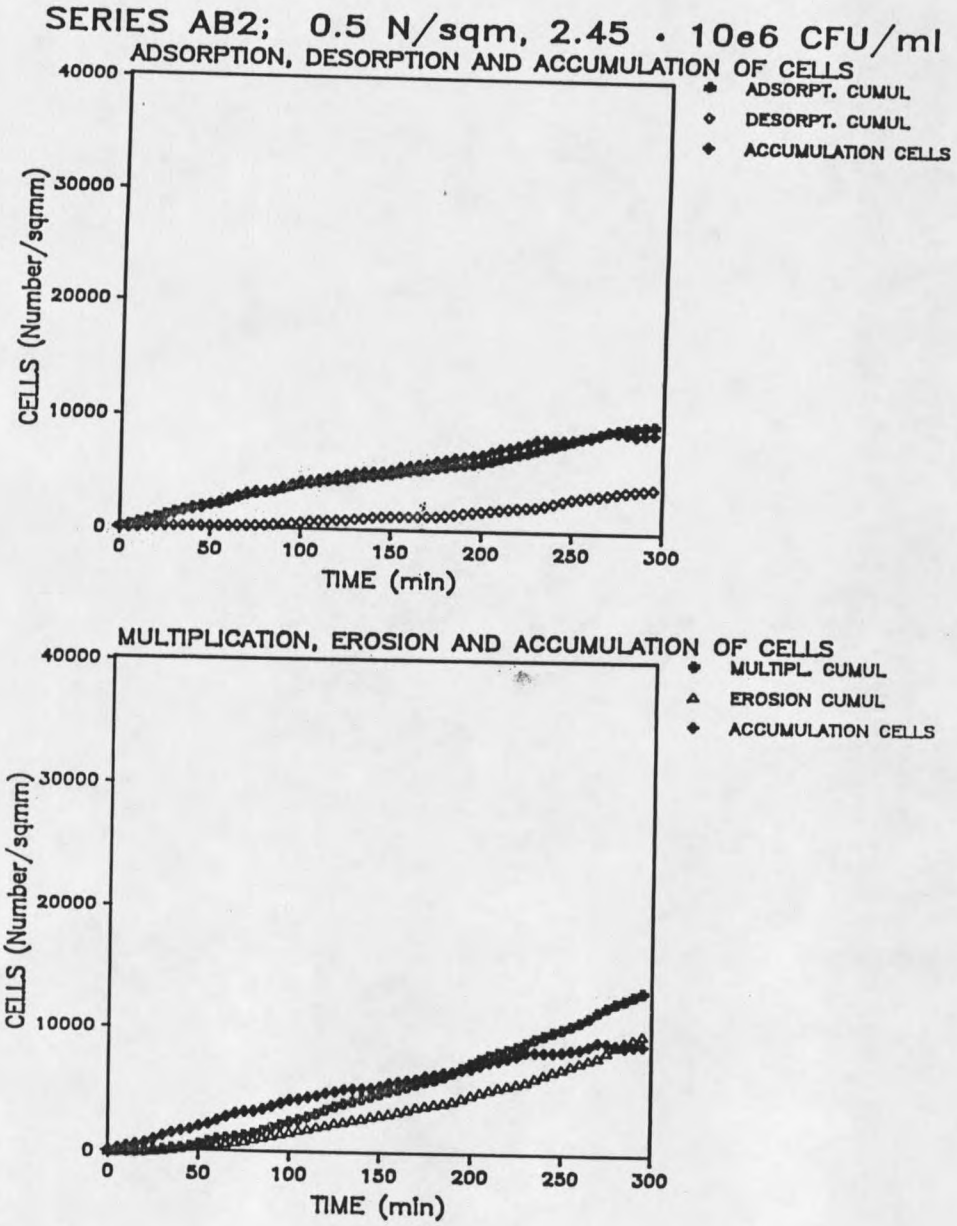

Figure 54. Progression in terms of cells (Series AB2). Sorption related processes (a) and growth related processes (b).

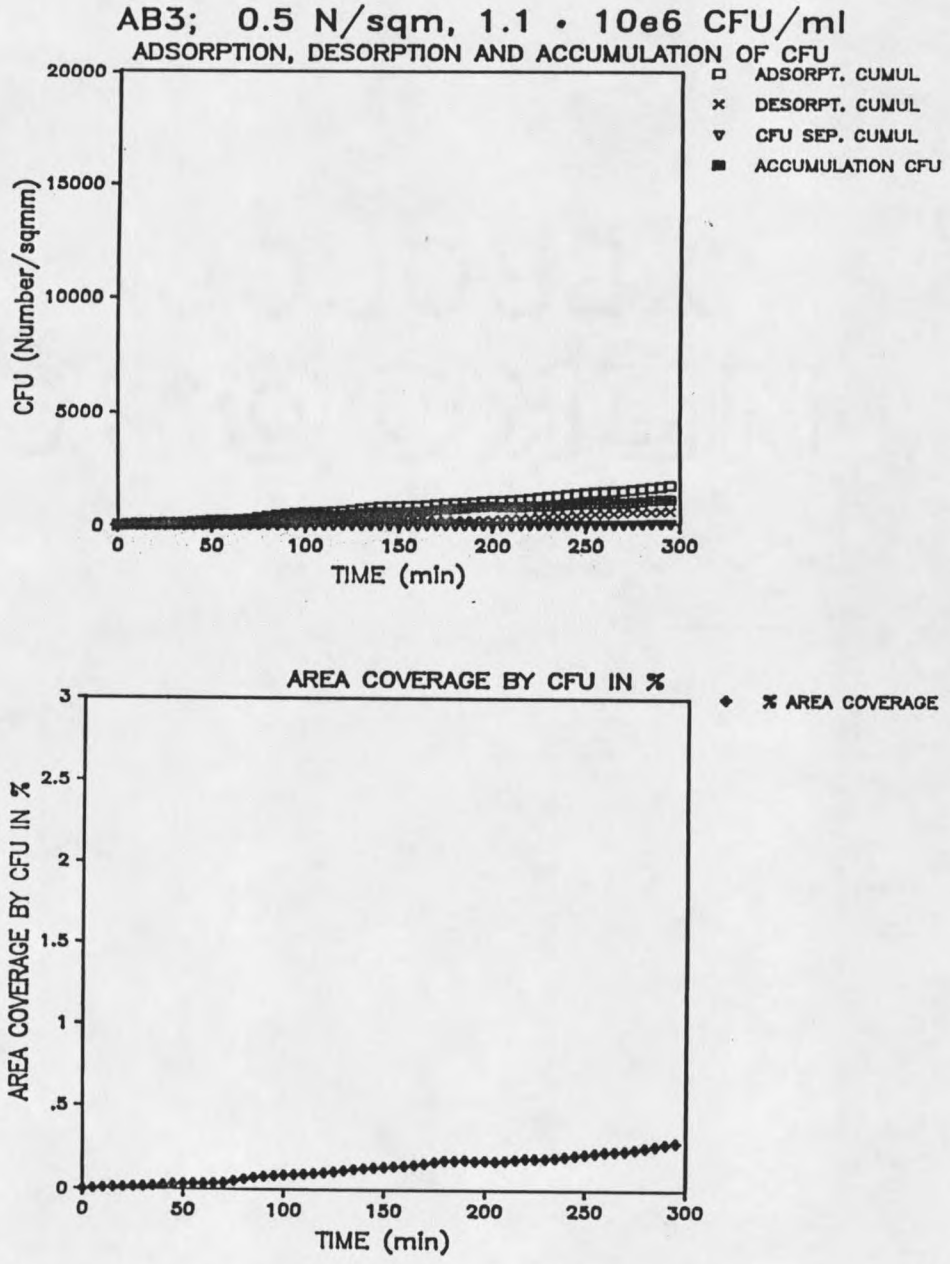

Figure 55. Progression of colonization (Series AB3) in terms of CFU (a) and area coverage (b).

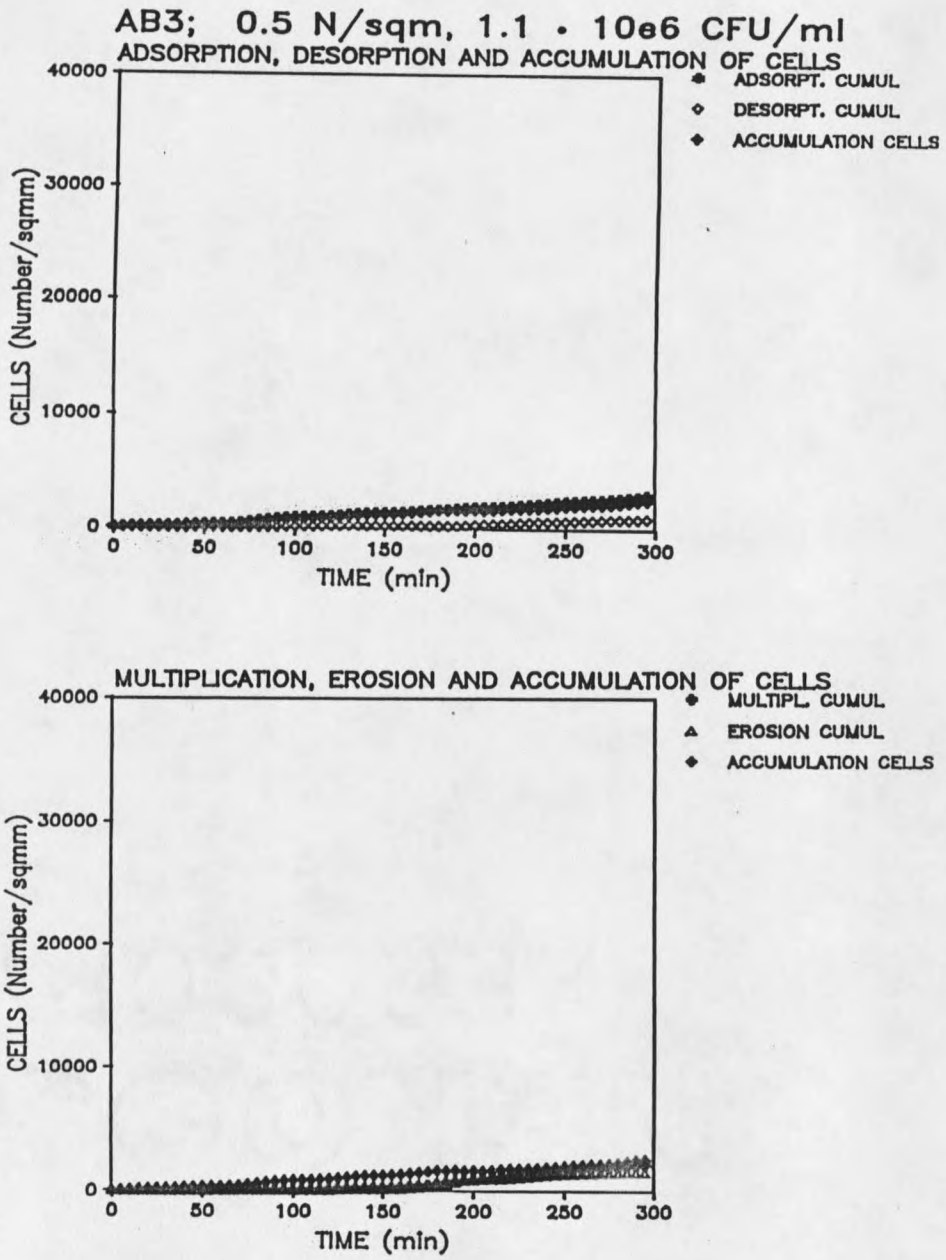

Figure 56. Progression in terms of cells (Series AB3). Sorption related processes (a) and growth related processes (b).

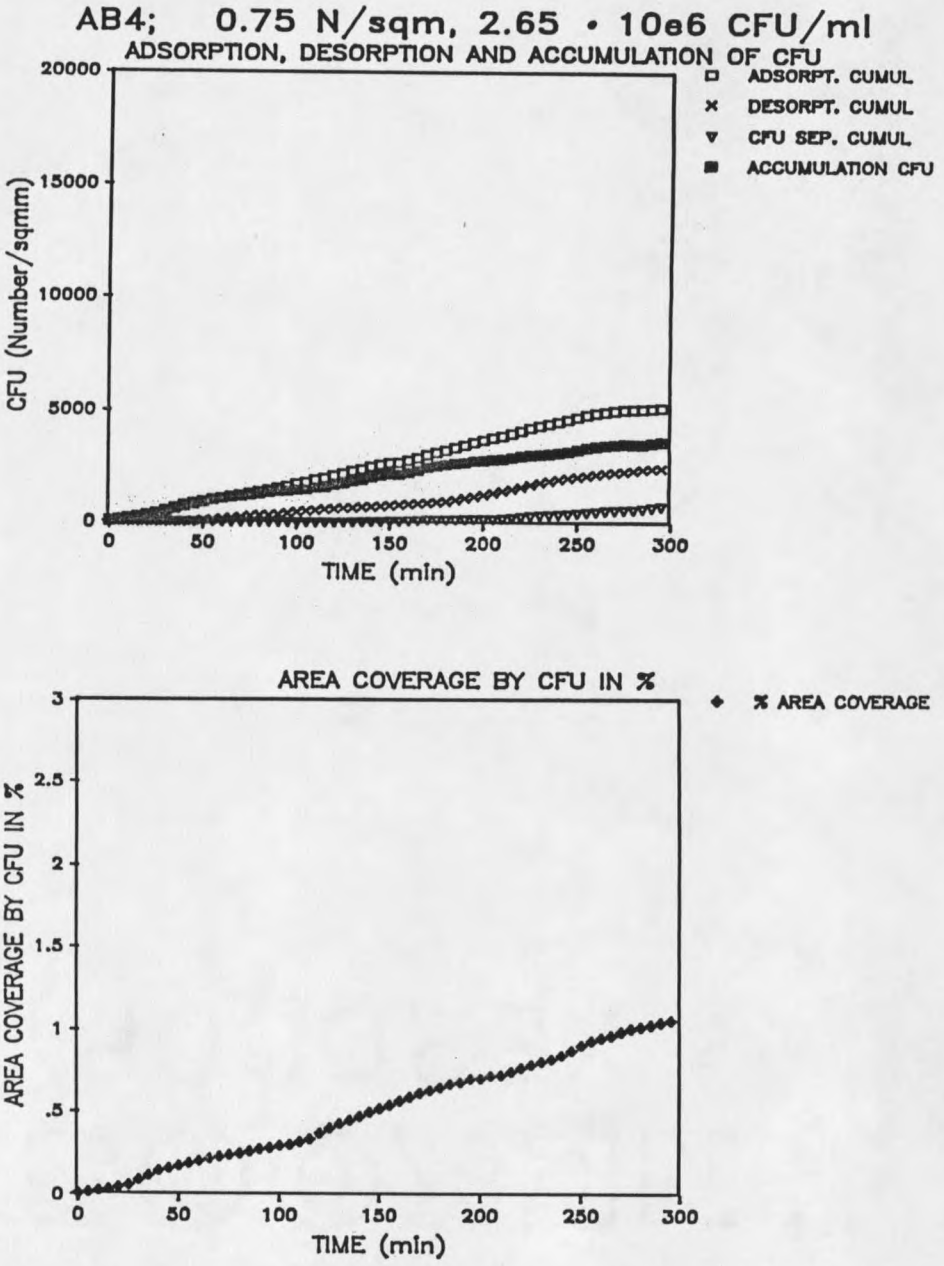

Figure 57. Progression of colonization (Series AB4) in terms of CFU (a) and area coverage (b).

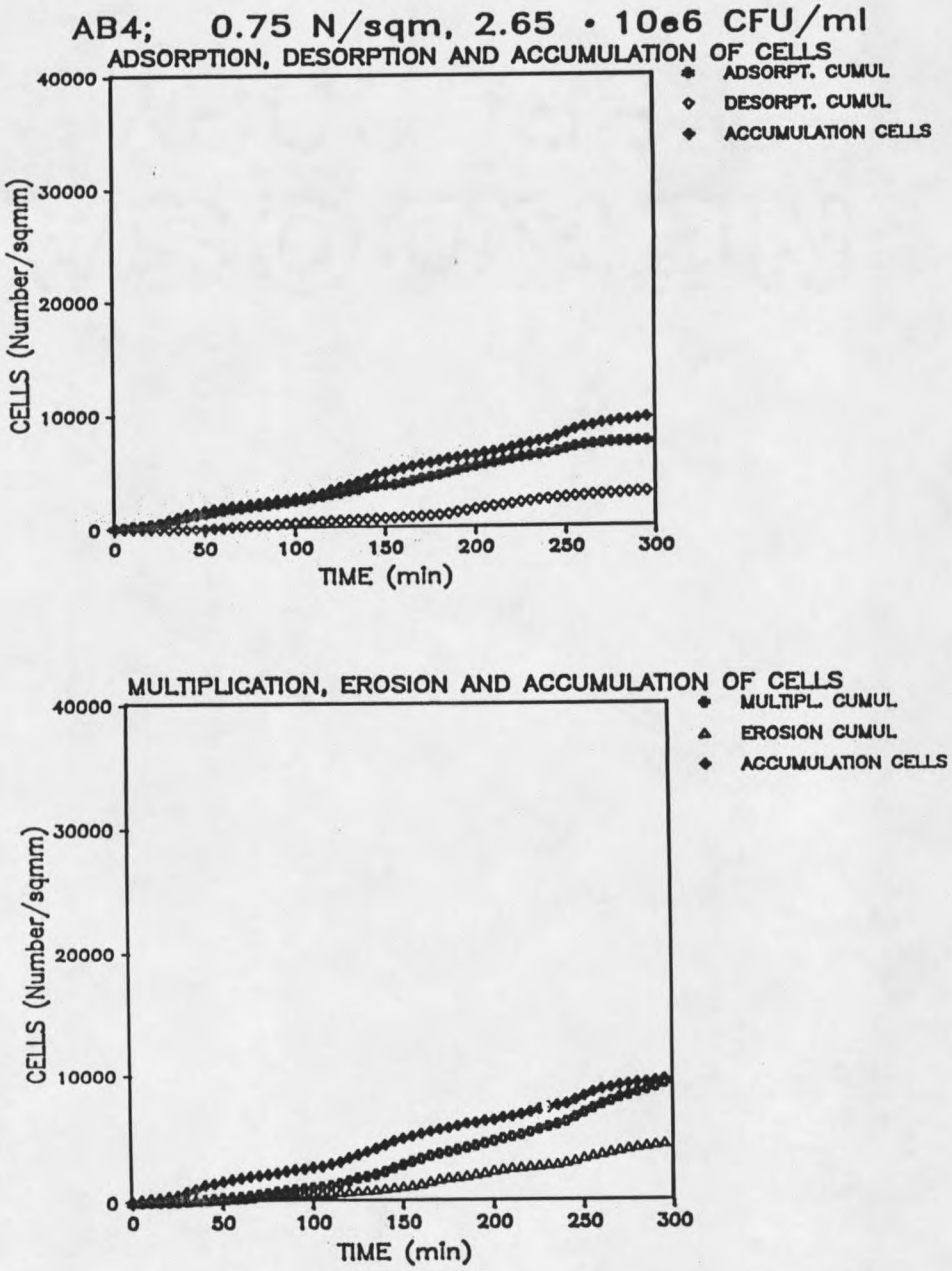

Figure 58. Progression in terms of cells (Series AB4). Sorption related processes (a) and growth related processes (b).

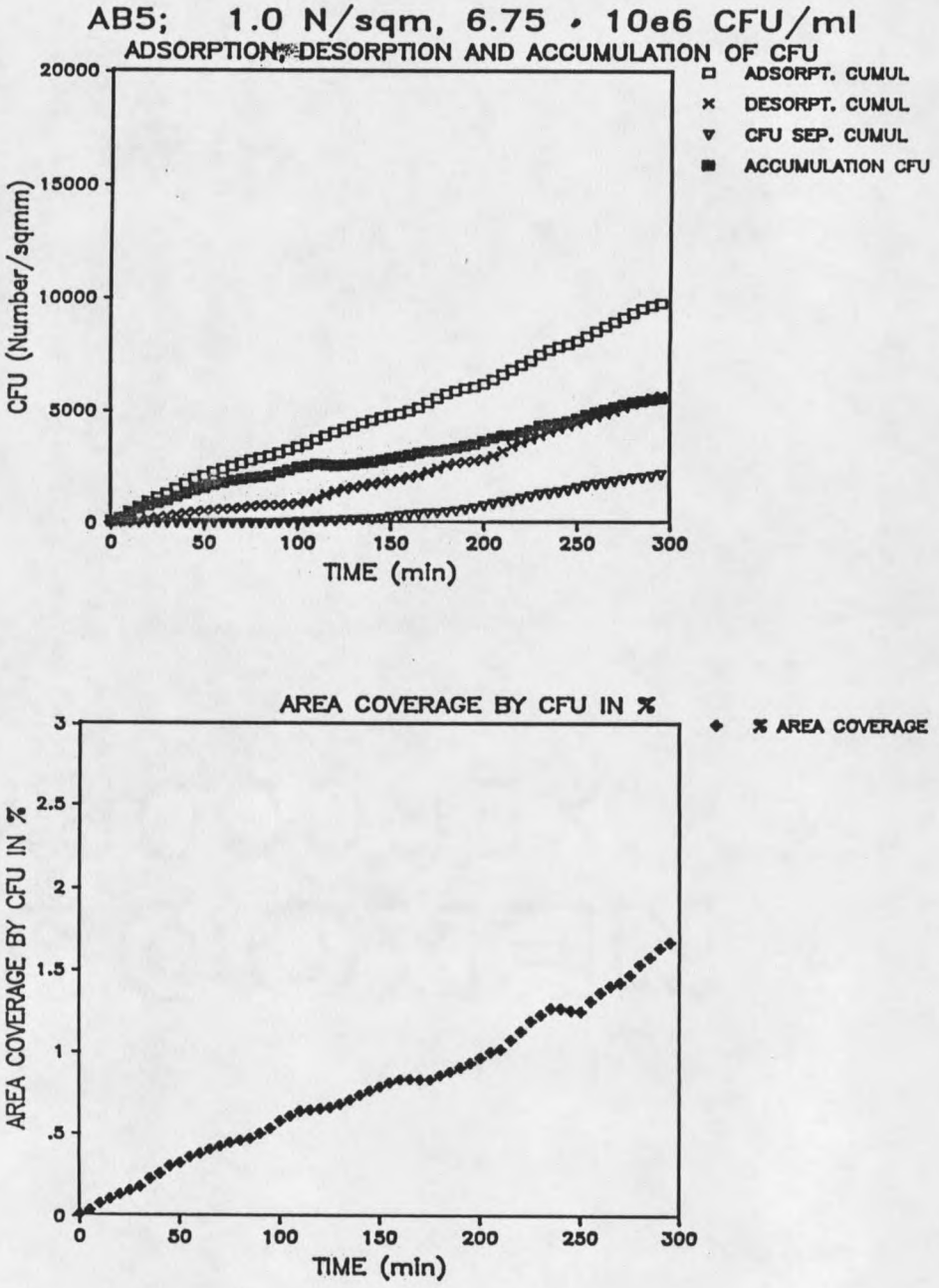

Figure 59. Progression of colonization (Series AB5) in terms of CFU (a) and area coverage (b).

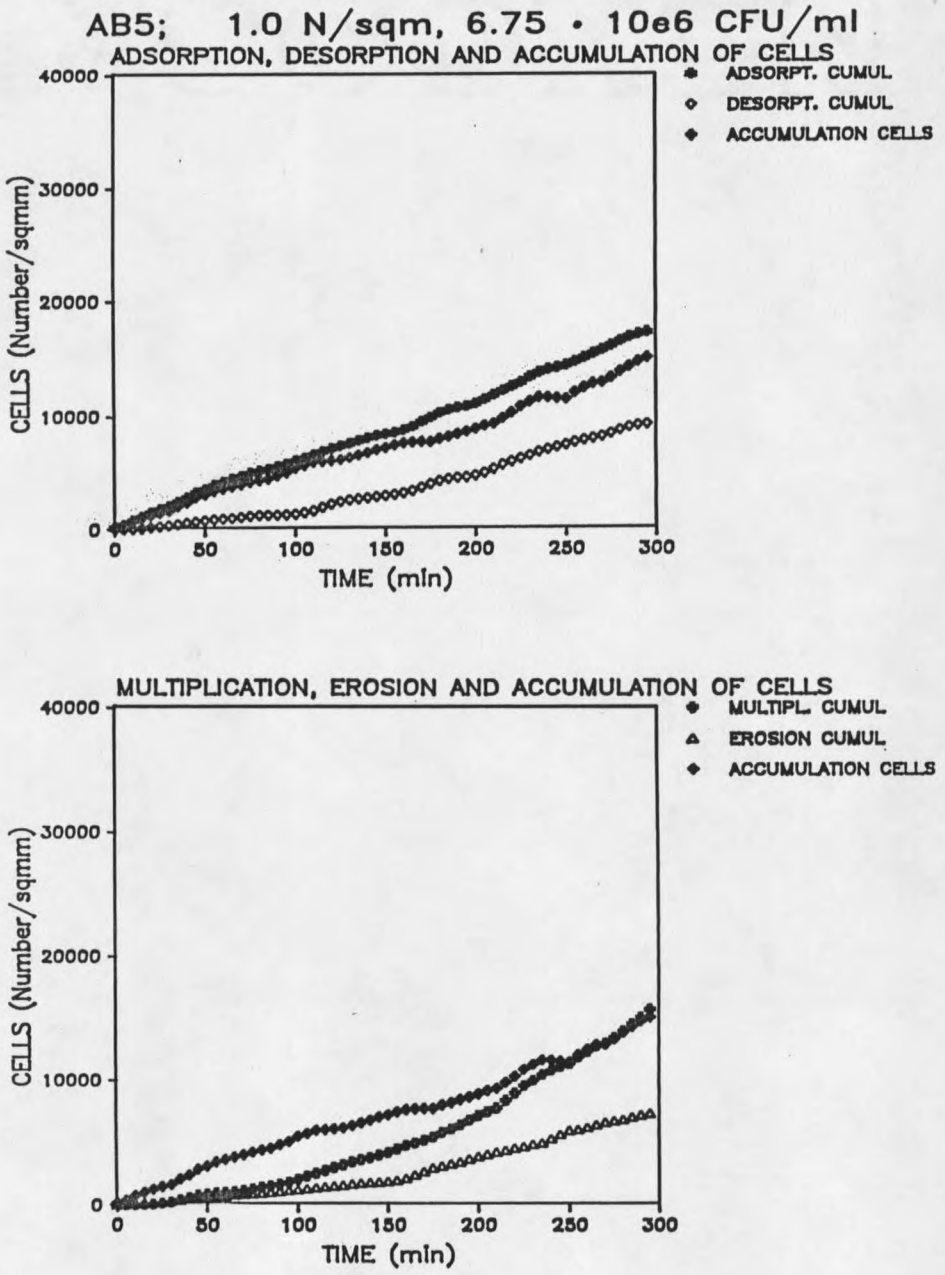

Figure 60. Progression in terms of cells (Series AB5). Sorption related processes (a) and growth related processes (b).

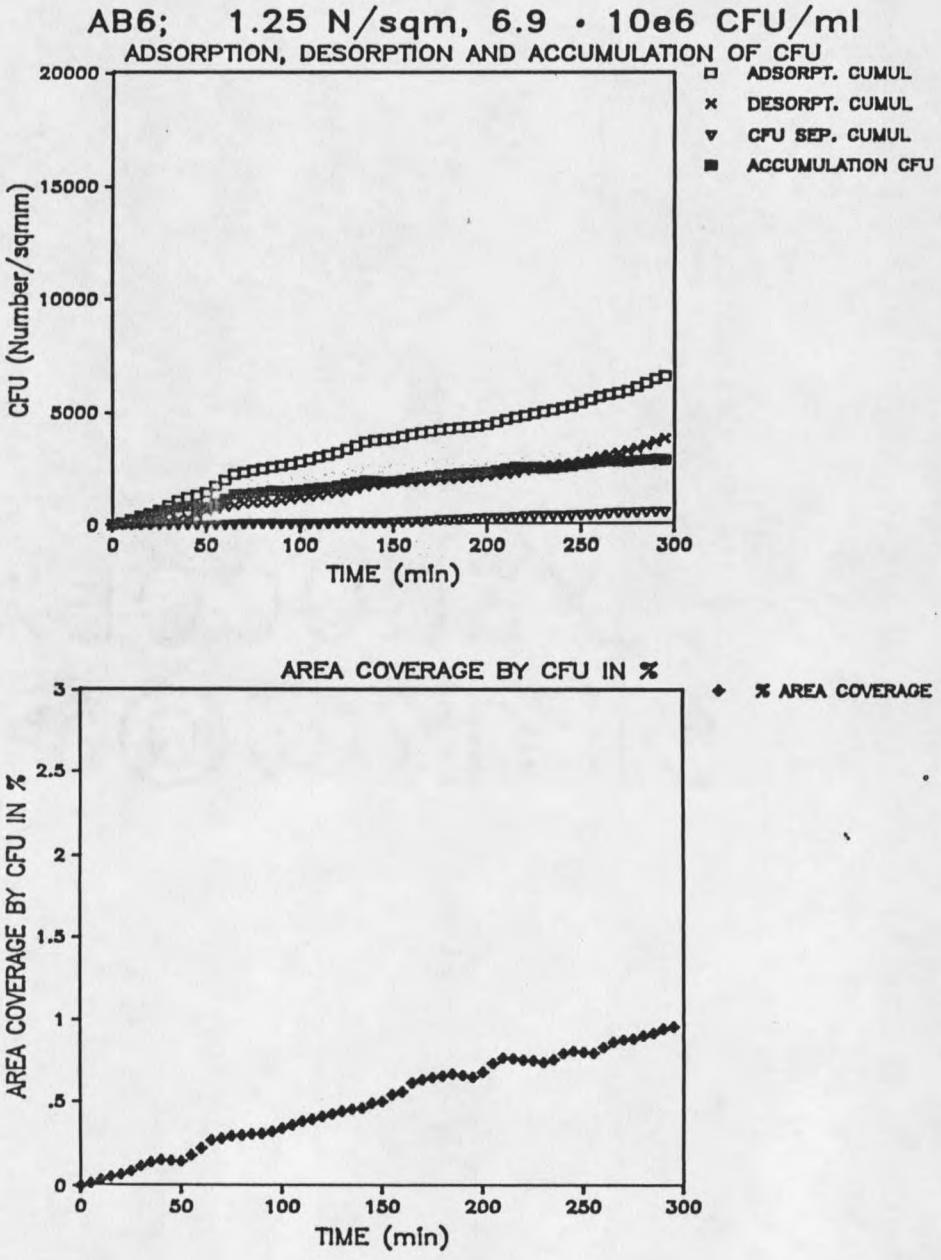

Figure 61. Progression of colonization (Series AB6) in terms of CFU (a) and area coverage (b)]

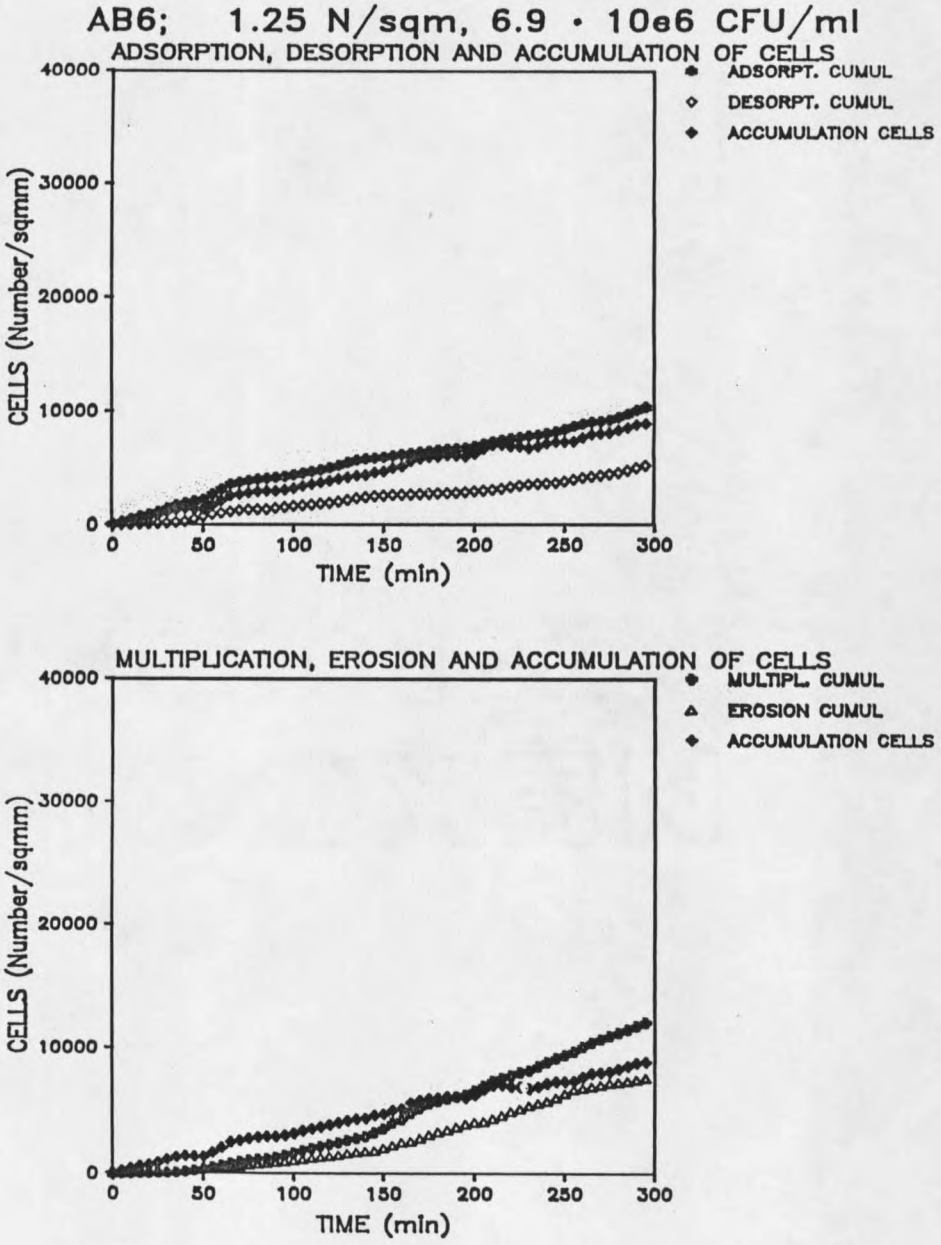

Figure 62. Progression in terms of cells (Series AB6). Sorption related processes (a) and growth related processes (b).

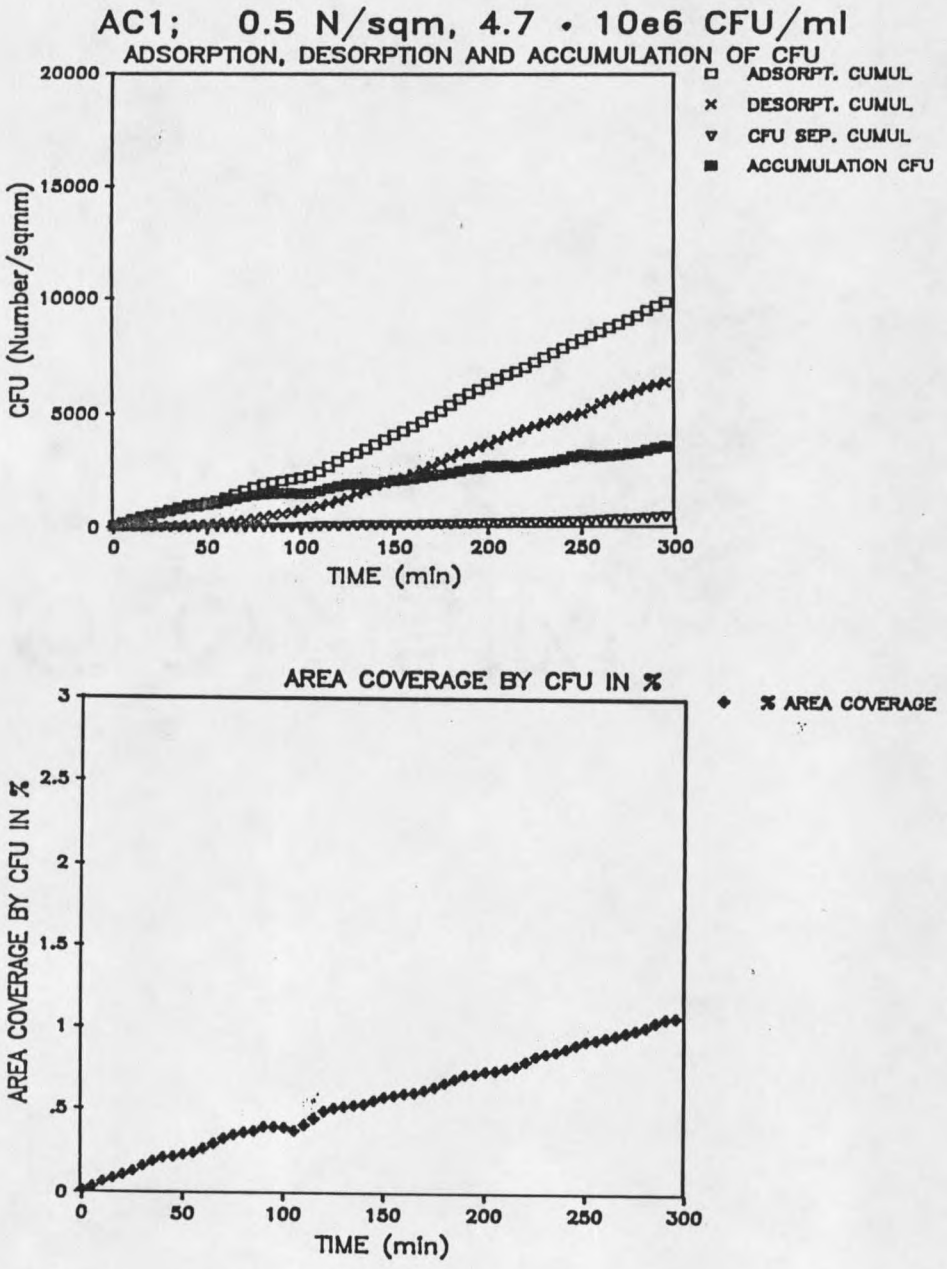

Figure 63. Progression of colonization (Series AC1) in terms of CFU (a) and area coverage (b).

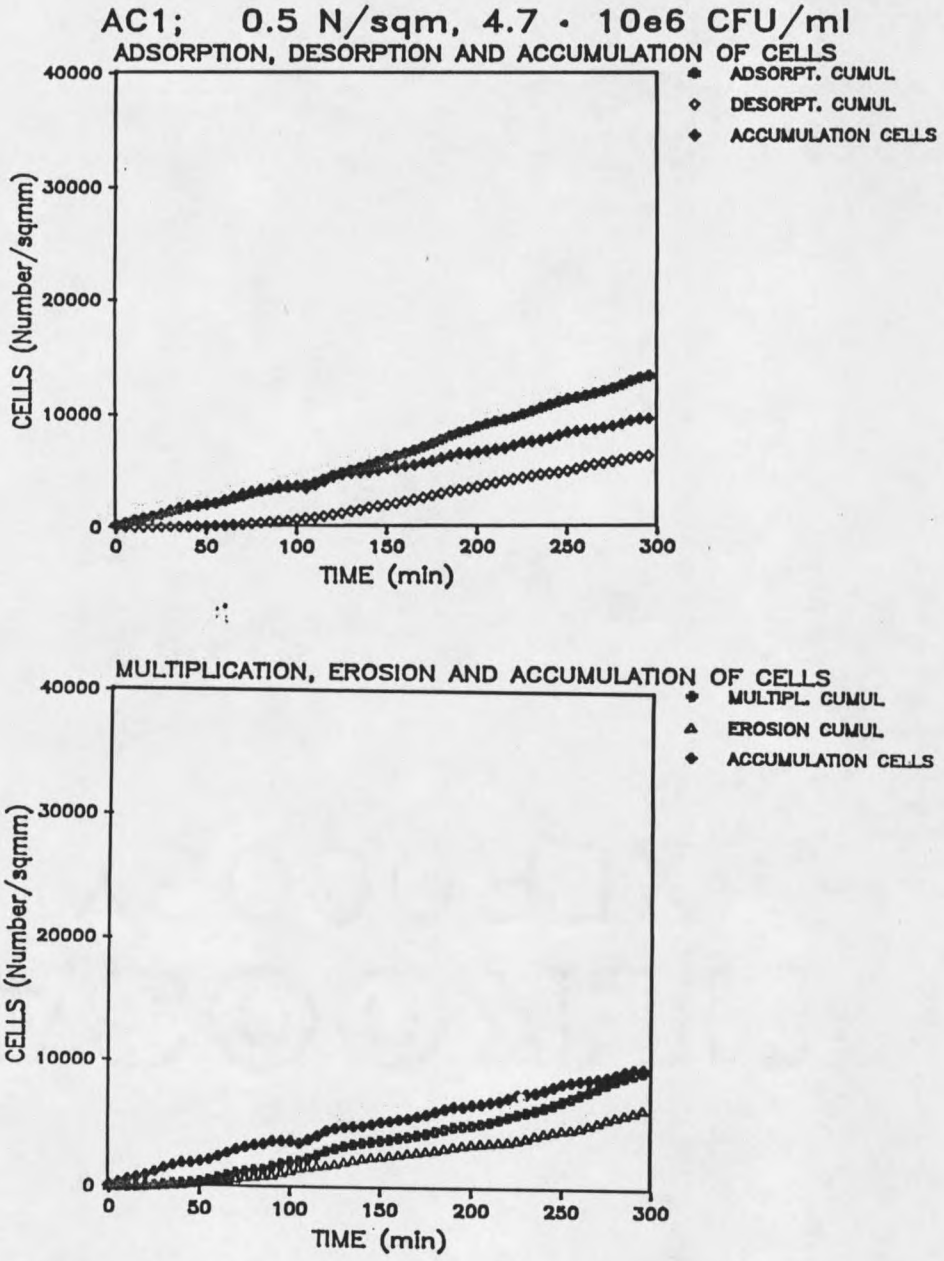

Figure 64. Progression in terms of cells (Series AC1). Sorption related processes (a) and growth related processes (b).

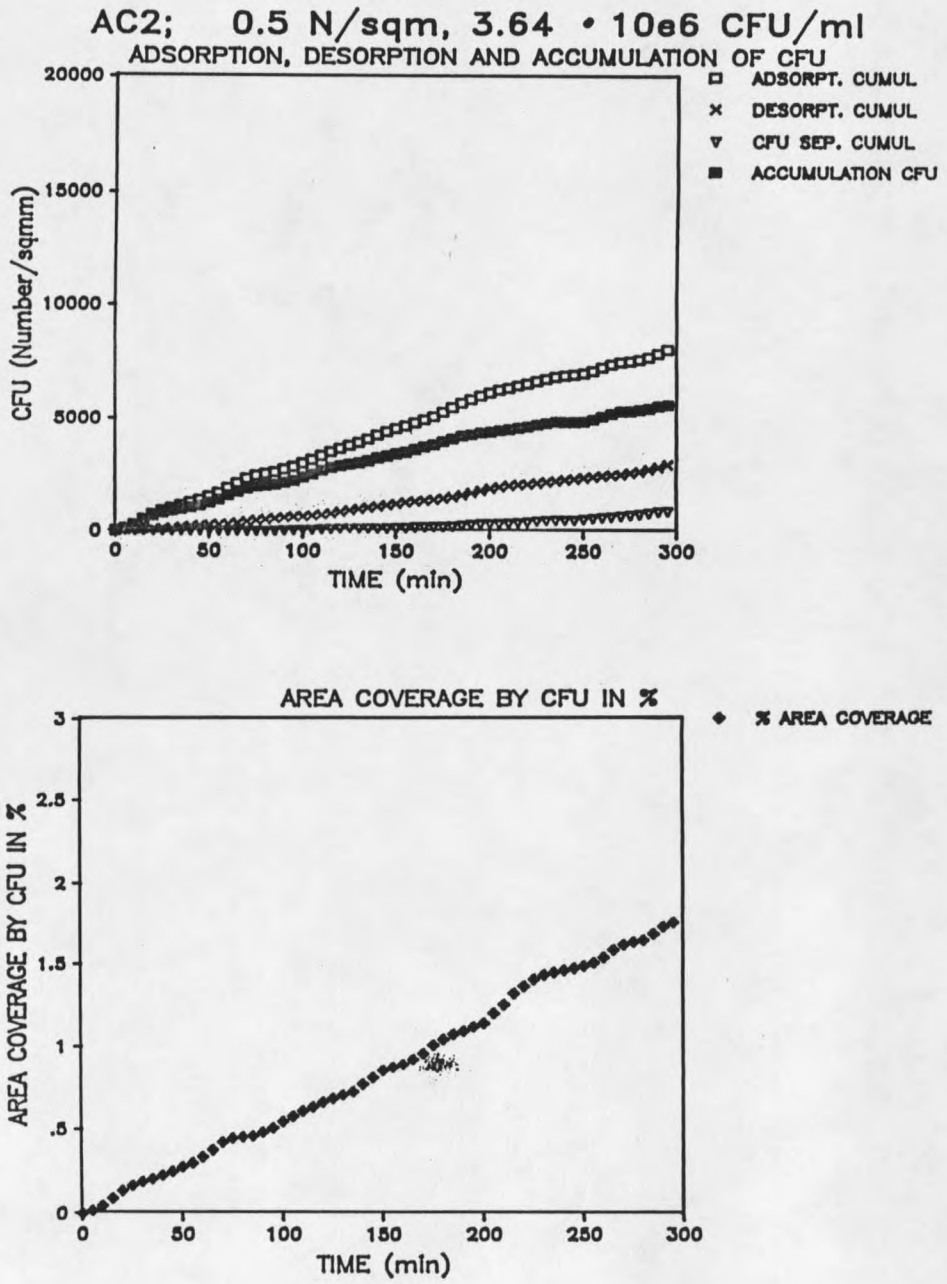

Figure 65. Progression of colonization (Series AC2) in terms of CFU (a) and area coverage (b).

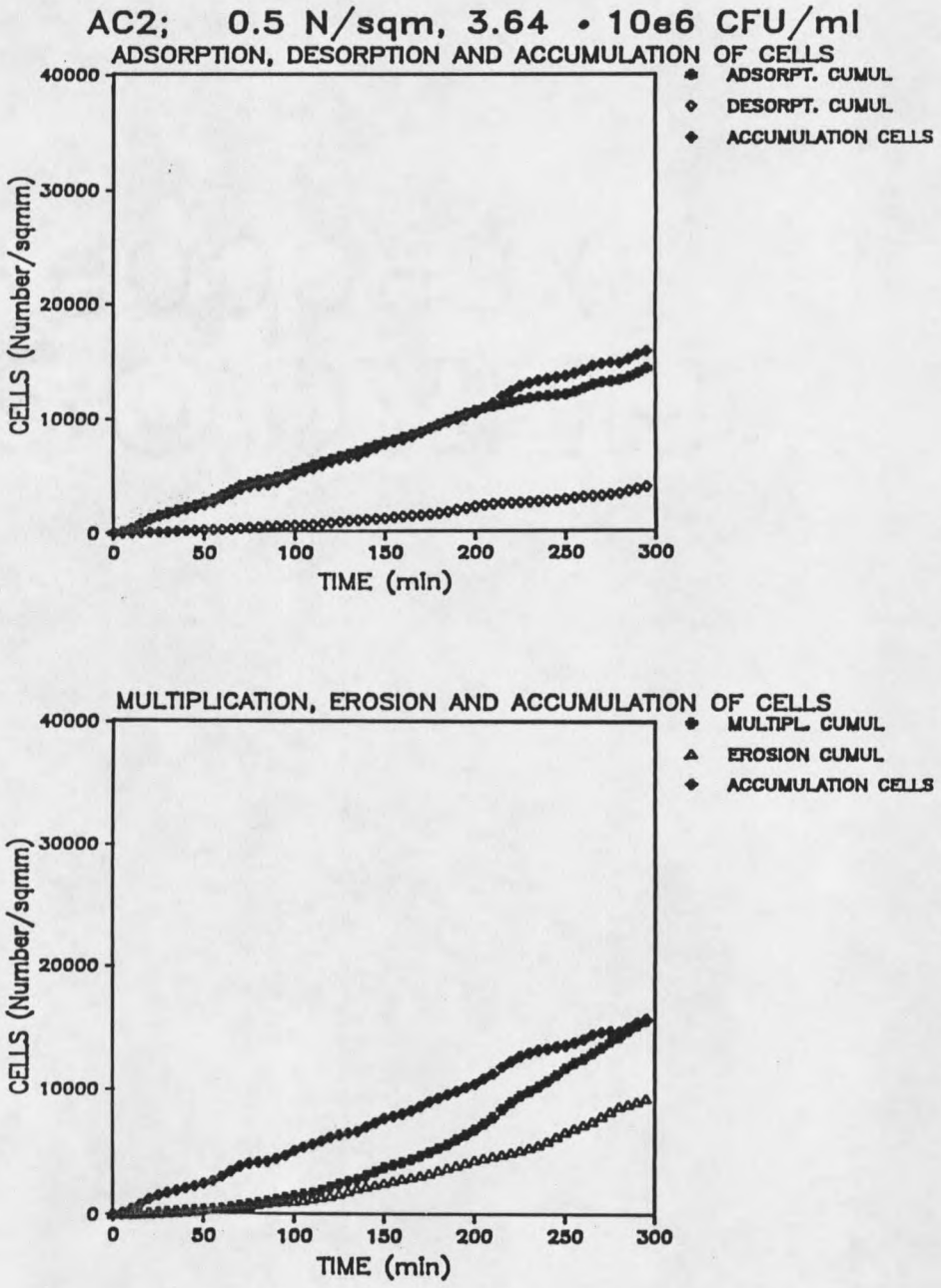

Figure 66. Progression in terms of cells (Series AC2). Sorption related processes (a) and growth related processes (b).

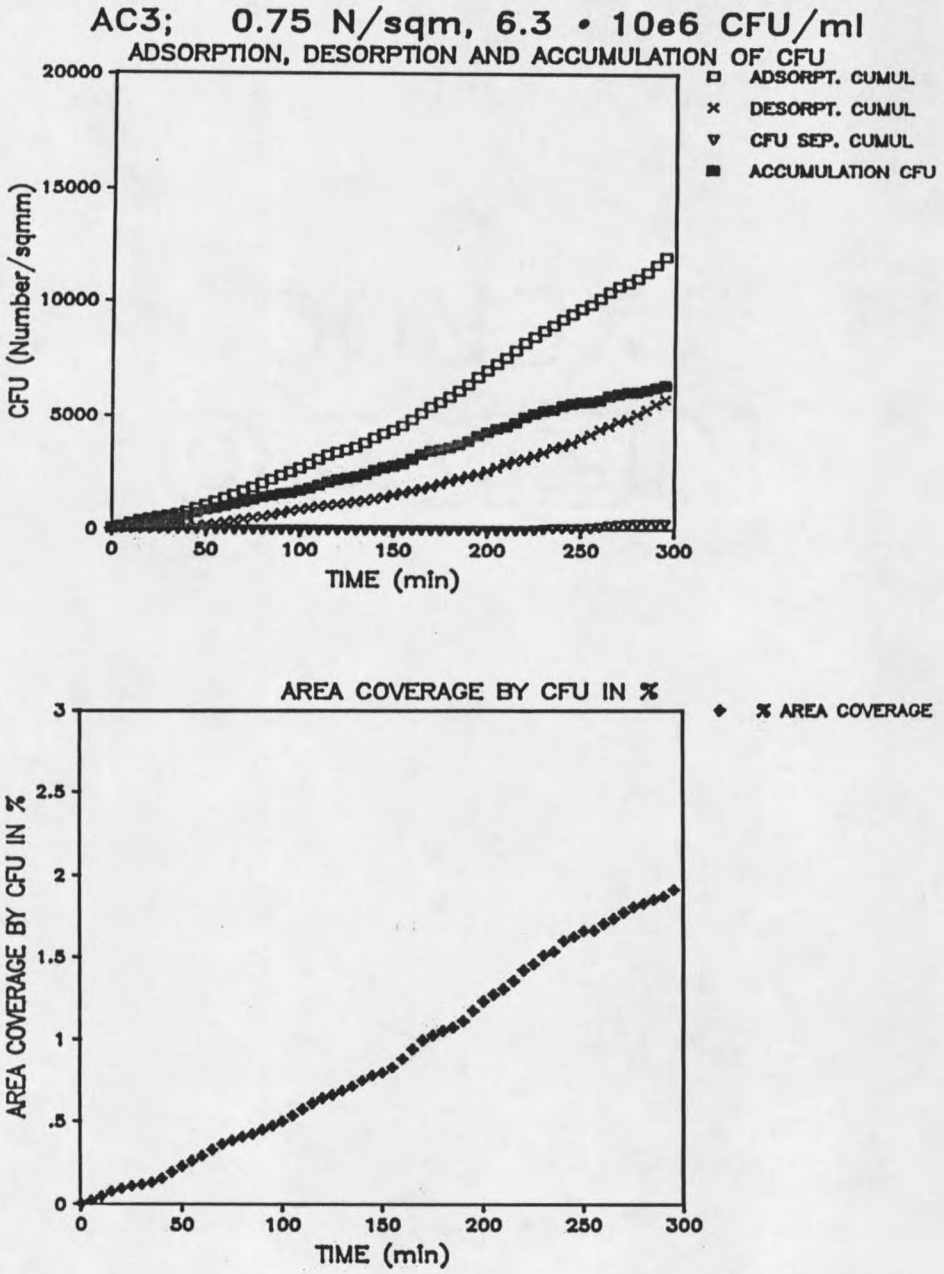

Figure 67. Progression of colonization (Series AC3) in terms of CFU (a) and area coverage (b).

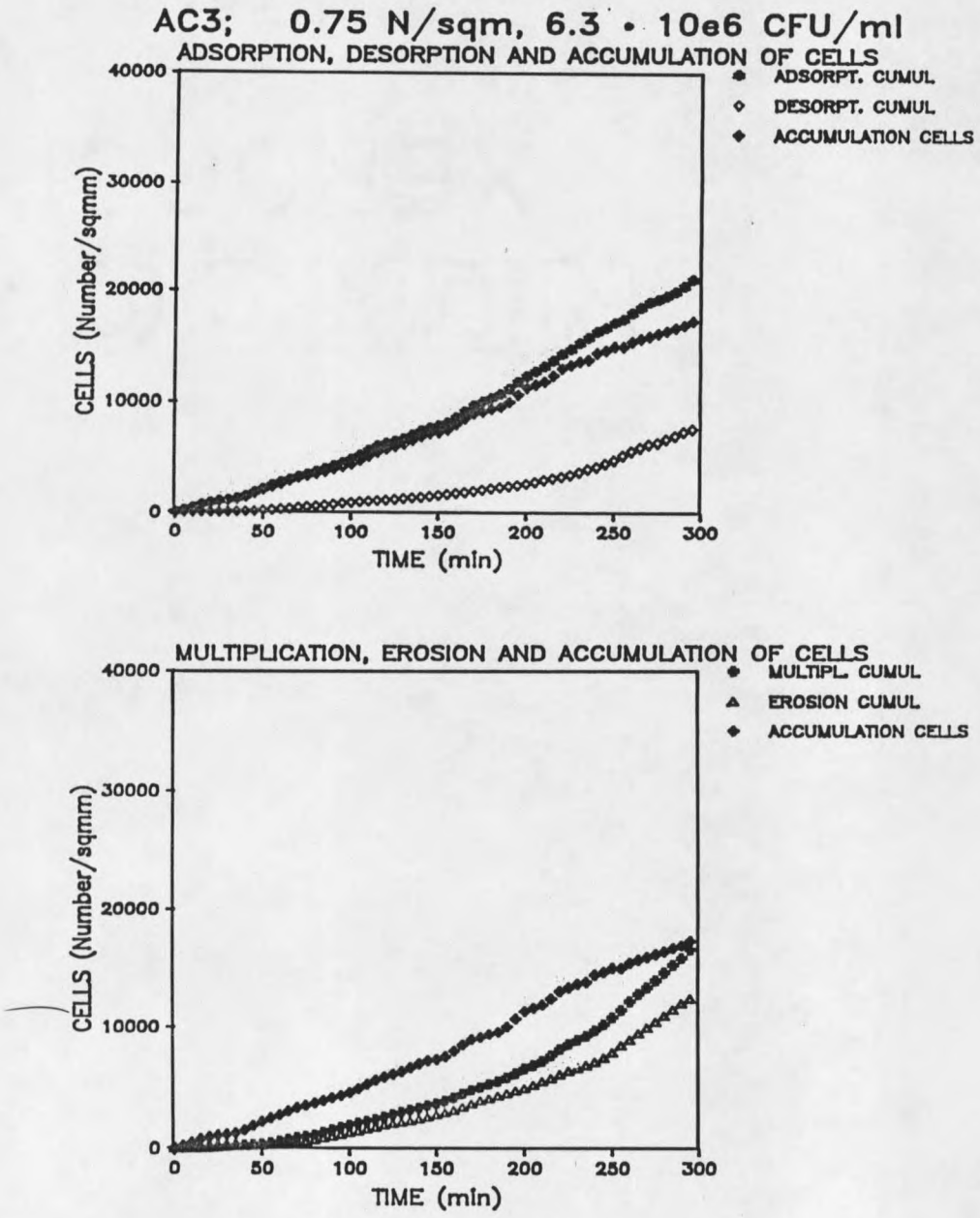

Figure 68. Progression in terms of cells (Series AC3). Sorption related processes (a) and growth related processes (b).

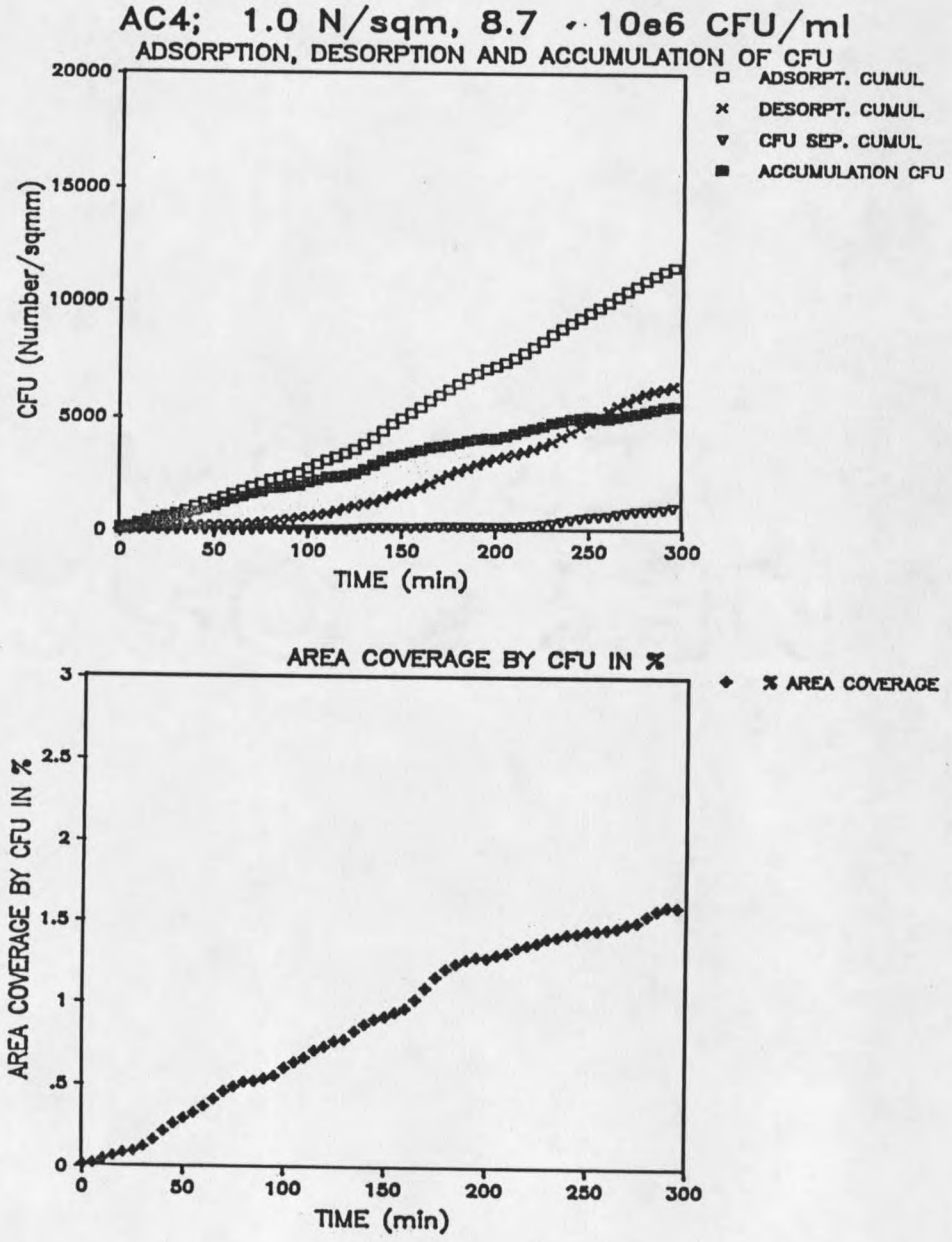

Figure 69. Progression of colonization (Series AC4) in terms of CFU (a) and area coverage (b).

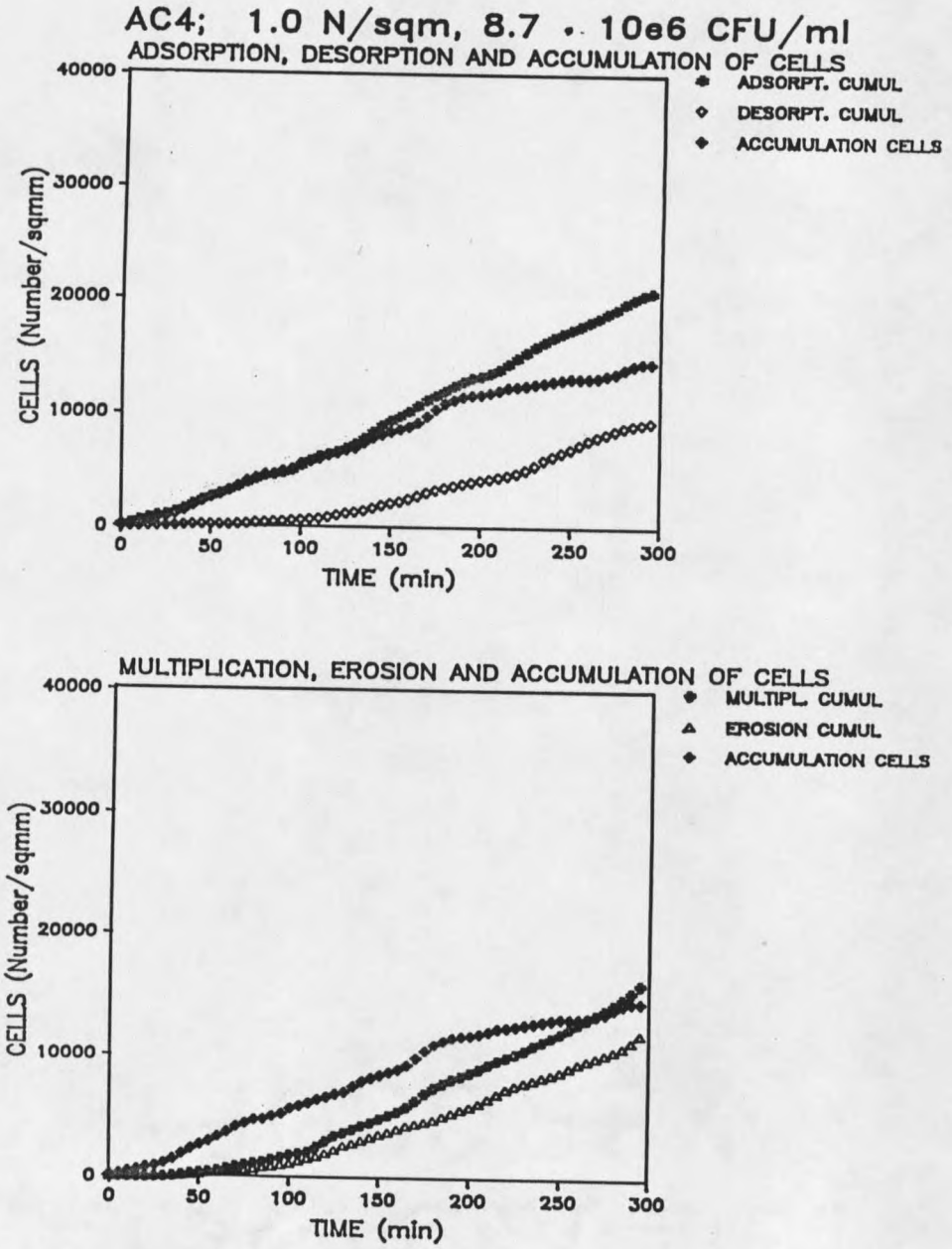

Figure 70. Progression in terms of cells (Series AC4). Sorption related processes (a) and growth related processes (b).

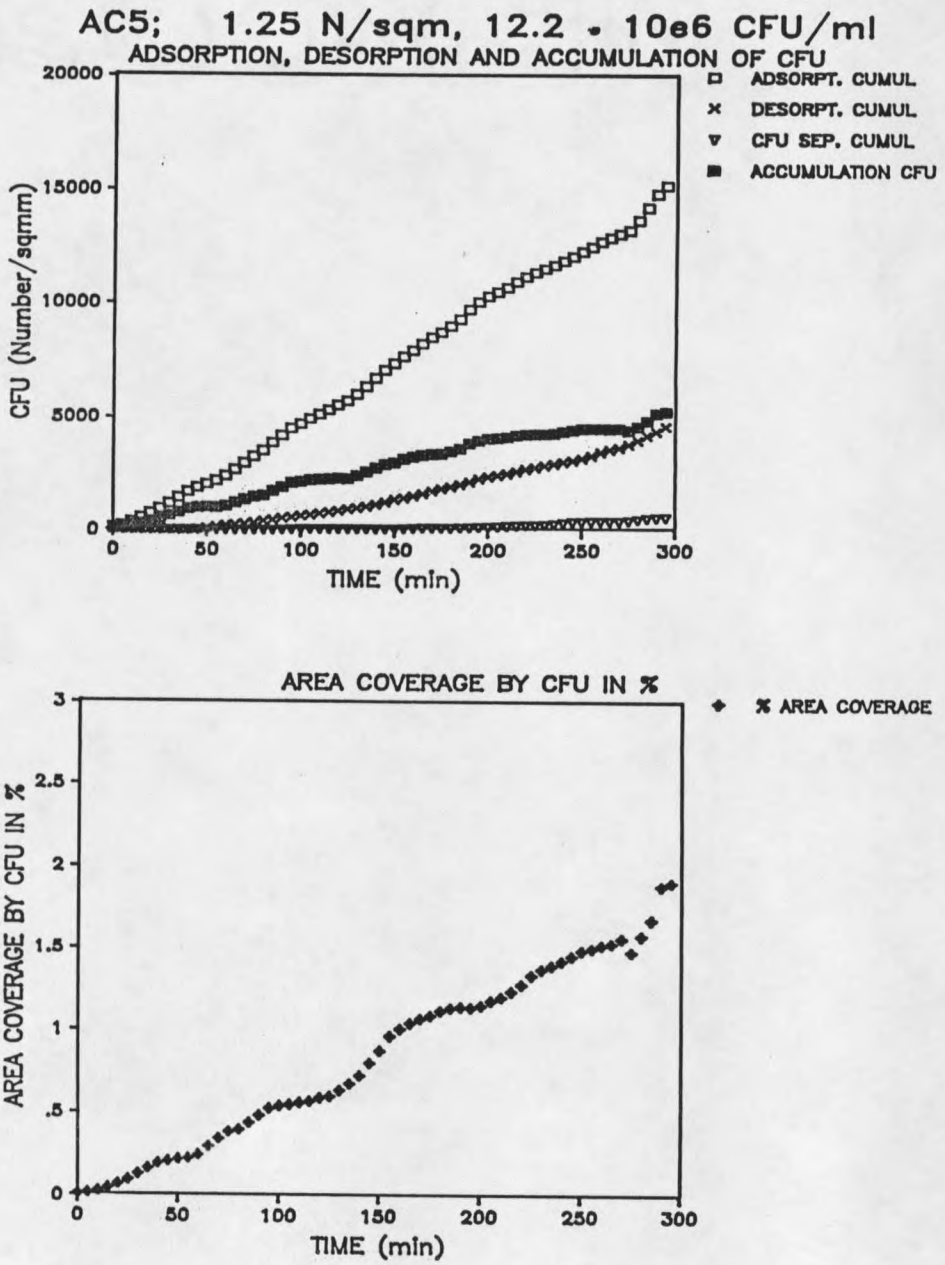

Figure 71. Progression of colonization (Series AC5) in terms of CFU (a) and area coverage (b).

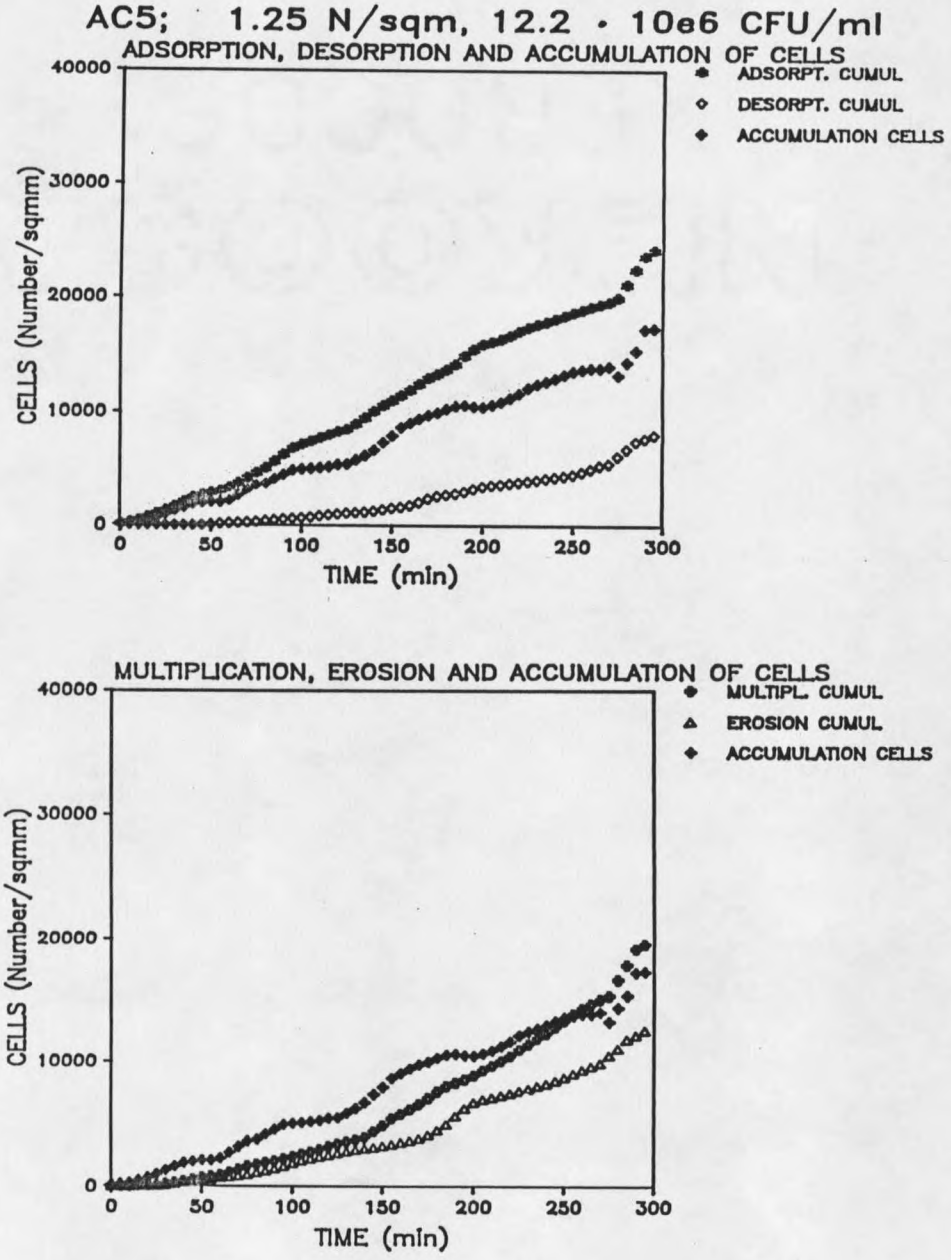

Figure 72. Progression in terms of cells (Series AC5). Sorption related processes (a) and growth related processes (b).

APPENDIX E

TABLES OF DERIVED RESULTS

Analysis of Adsorption	Series AA1	
CFU Conc. [#/ml] (· 10^6)	1.10	
Shear Stress [N·m^{-2}]:	.50	
Observed Adsorption CFU [#·mm^{-1}·min^{-1}]	8.18	
Observed Ads. Cells [#·mm^{-1}·min^{-1}]	14.38	
Other Important Parameters:		
Geometry of tube [mm]:		
Width:	4.00	
Half Height:	.09	
Transport Parameters:		
Diffusivity [mm^2·s^{-1}]	10^{-3}	
Viscosity [N·s·m^{-1}]	10^{-3}	
Adsorption and Transport CFU		
Adsorption coefficient ϵ:		.01125
Transport rate:		964.06
Ratio Transp./ Adsorpt. [%]		.85
Adsorption and Transport Cells		
Adsorption coefficient ϵ:		.01991
Transport rate:		964.06
Ratio Transp./ Adsorpt. [%]		1.49

Table 24. Derived results of series AA1.

Analysis of Adsorption	Series AA2	
CFU Conc. [#/ml] (· 10^6)	10.00	
Shear Stress [N·m^{-2}]:	.50	
Observed Adsorption CFU [#·mm^{-1}·min^{-1}]	71.86	
Observed Ads. Cells [#·mm^{-1}·min^{-1}]	135.66	
Other Important Parameters:		
Geometry of tube [mm]:		
Width:	4.00	
Half Height:	.09	
Transport Parameters:		
Diffusivity [mm^2·s^{-1}]	10^{-3}	
Viscosity [N·s·m^{-1}]	10^{-3}	
Adsorption and Transport CFU		
Adsorption coefficient ϵ:		.01087
Transport rate:		8764.17
Ratio Transp./ Adsorpt. [%]		.82
Adsorption and Transport Cells		
Adsorption coefficient ϵ:		.02067
Transport rate:		8764.17
Ratio Transp./ Adsorpt. [%]		1.55

Table 25. Derived results of series AA2.

Analysis of Adsorption	Series AA3	
CFU Conc. [#/ml] (• 10^6)	2.75	
Shear Stress [N•m^{-2}]:	.50	
Observed Adsorption CFU [#•mm^{-1}•min^{-1}]	20.50	
Observed Ads. Cells [#•mm^{-1}•min^{-1}]	34.33	
Other Important Parameters:		
Geometry of tube [mm]:		
Width:	4.00	
Half Height:	.09	
Transport Parameters:		
Diffusivity [mm^2•s^{-1}]	10^{-3}	
Viscosity [N•s•m^{-1}]	10^{-3}	

Adsorption and Transport CFU	
Adsorption coefficient ϵ:	.01128
Transport rate:	2410.15
Ratio Transp./ Adsorpt. [%]	.85

Adsorption and Transport Cells	
Adsorption coefficient ϵ:	.01900
Transport rate:	2410.15
Ratio Transp./ Adsorpt. [%]	1.42

Table 26. Derived results of series AA3.

Analysis of Adsorption	Series AA4	
CFU Conc. [#/ml] (• 10^6)	1.92	
Shear Stress [N•m^{-2}]:	.50	
Observed Adsorption CFU [#•mm^{-1}•min^{-1}]	13.52	
Observed Ads. Cells [#•mm^{-1}•min^{-1}]	16.20	
Other Important Parameters:		
Geometry of tube [mm]:		
Width:	4.00	
Half Height:	.09	
Transport Parameters:		
Diffusivity [mm^2•s^{-1}]	10^{-3}	
Viscosity [N•s•m^{-1}]	10^{-3}	

Adsorption and Transport CFU	
Adsorption coefficient ϵ:	.01065
Transport rate:	1682.72
Ratio Transp./ Adsorpt. [%]	.80

Adsorption and Transport Cells	
Adsorption coefficient ϵ:	.01278
Transport rate:	1682.72
Ratio Transp./ Adsorpt. [%]	.96

Table 27. Derived results of series AA4.

Analysis of Adsorption	Series AB1	
CFU Conc. [#/ml] (· 10^6)	5.00	Adsorption and Transport CFU
Shear Stress [N·m^{-2}]:	.50	
		Adsorption coefficient ∈: .01317
Observed Adsorption CFU [#·mm^{-1}·min^{-1}]	43.45	Transport rate: 4382.09
Observed Ads. Cells [#·mm^{-1}·min^{-1}]	57.51	Ratio Transp./ Adsorpt. [%] .99
Other Important Parameters:		Adsorption and Transport Cells
Geometry of tube [mm]:		
Width:	4.00	Adsorption coefficient ∈: .01748
Half Height:	.09	Transport rate: 4382.09
		Ratio Transp./ Adsorpt. [%] 1.31
Transport Parameters:		
Diffusivity [mm^2·s^{-1}]	10^{-3}	
Viscosity [N·s·m^{-1}]	10^{-3}	

Table 28. Derived results of series AB1.

Analysis of Adsorption	Series AB2	
CFU Conc. [#/ml] (· 10^6)	2.45	Adsorption and Transport CFU
Shear Stress [N·m^{-2}]:	.50	
		Adsorption coefficient ∈: .01195
Observed Adsorption CFU [#·mm^{-1}·min^{-1}]	19.34	Transport rate: 2147.22
Observed Ads. Cells [#·mm^{-1}·min^{-1}]	30.18	Ratio Transp./ Adsorpt. [%] .90
Other Important Parameters:		Adsorption and Transport Cells
Geometry of tube [mm]:		
Width:	4.00	Adsorption coefficient ∈: .01874
Half Height:	.09	Transport rate: 2147.22
		Ratio Transp./ Adsorpt. [%] 1.41
Transport Parameters:		
Diffusivity [mm^2·s^{-1}]	10^{-3}	
Viscosity [N·s·m^{-1}]	10^{-3}	

Table 29. Derived results of series AB2.

Analysis of Adsorption	Series AB3	
CFU Conc. [#/ml] (· 10^6)	1.10	
Shear Stress [N·m^{-2}]:	.50	
Observed Adsorption CFU [#·mm^{-1}·min^{-1}]	5.99	
Observed Ads. Cells [#·mm^{-1}·min^{-1}]	10.43	
Other Important Parameters:		
Geometry of tube [mm]:		
Width:	4.00	
Half Height:	.09	
Transport Parameters:		
Diffusivity [mm^2·s^{-1}]	10^{-3}	
Viscosity [N·s·m^{-1}]	10^{-3}	
Adsorption and Transport CFU		
Adsorption coefficient ϵ:		.00822
Transport rate:		964.06
Ratio Transp./ Adsorpt. [%]		.62
Adsorption and Transport Cells		
Adsorption coefficient ϵ:		.01438
Transport rate:		964.06
Ratio Transp./ Adsorpt. [%]		1.08

Table 30. Derived results of series AB3.

Analysis of Adsorption	Series AB4	
CFU Conc. [#/ml] (· 10^6)	2.65	
Shear Stress [N·m^{-2}]:	.75	
Observed Adsorption CFU [#·mm^{-1}·min^{-1}]	18.82	
Observed Ads. Cells [#·mm^{-1}·min^{-1}]	27.33	
Other Important Parameters:		
Geometry of tube [mm]:		
Width:	4.00	
Half Height:	.09	
Transport Parameters:		
Diffusivity [mm^2·s^{-1}]	10^{-3}	
Viscosity [N·s·m^{-1}]	10^{-3}	
Adsorption and Transport CFU		
Adsorption coefficient ϵ:		.01073
Transport rate:		2658.60
Ratio Transp./ Adsorpt. [%]		.71
Adsorption and Transport Cells		
Adsorption coefficient ϵ:		.01563
Transport rate:		2658.60
Ratio Transp./ Adsorpt. [%]		1.03

Table 31. Derived results of series AB4.

Analysis of Adsorption	Series AB5	
CFU Conc. [#/ml] (· 10^6)	6.75	
Shear Stress [N·m^{-2}]:	1.00	
Observed Adsorption CFU [#·mm^{-1}·min^{-1}]	31.33	
Observed Ads. Cells [#·mm^{-1}·min^{-1}]	56.01	
Other Important Parameters:		
Geometry of tube [mm]:		
Width:	4.00	
Half Height:	.09	
Transport Parameters:		
Diffusivity [mm^2·s^{-1}]	10^{-3}	
Viscosity [N·s·m^{-1}]	10^{-3}	

Adsorption and Transport CFU	
Adsorption coefficient ϵ:	.00699
Transport rate:	7453.46
Ratio Transp./ Adsorpt. [%]	.42

Adsorption and Transport Cells	
Adsorption coefficient ϵ:	.01254
Transport rate:	7453.46
Ratio Transp./ Adsorpt. [%]	.75

Table 32. Derived results of series AB5.

Analysis of Adsorption	Series AB6	
CFU Conc. [#/ml] (· 10^6)	6.90	
Shear Stress [N·m^{-2}]:	1.25	
Observed Adsorption CFU [#·mm^{-1}·min^{-1}]	19.69	
Observed Ads. Cells [#·mm^{-1}·min^{-1}]	30.42	
Other Important Parameters:		
Geometry of tube [mm]:		
Width:	4.00	
Half Height:	.09	
Transport Parameters:		
Diffusivity [mm^2·s^{-1}]	10^{-3}	
Viscosity [N·s·m^{-1}]	10^{-3}	

Adsorption and Transport CFU	
Adsorption coefficient ϵ:	.00429
Transport rate:	8207.42
Ratio Transp./ Adsorpt. [%]	.24

Adsorption and Transport Cells	
Adsorption coefficient ϵ:	.00664
Transport rate:	8207.42
Ratio Transp./ Adsorpt. [%]	.37

Table 33. Derived results of series AB6.

Analysis of Adsorption	Series AC1	
CFU Conc. [#/ml] (· 10^6)	4.70	
Shear Stress [N·m^{-2}]:	.50	
Observed Adsorption CFU [#·mm^{-1}·min^{-1}]	35.34	
Observed Ads. Cells [#·mm^{-1}·min^{-1}]	46.29	
Other Important Parameters:		
Geometry of tube [mm]:		
Width:	4.00	
Half Height:	.09	
Transport Parameters:		
Diffusivity [mm^2·s^{-1}]	10^{-3}	
Viscosity [N·s·m^{-1}]	10^{-3}	
Adsorption and Transport CFU		
Adsorption coefficient ϵ:		.01138
Transport rate:		4119.16
Ratio Transp./ Adsorpt. [%]		.86
Adsorption and Transport Cells		
Adsorption coefficient ϵ:		.01494
Transport rate:		4119.16
Ratio Transp./ Adsorpt. [%]		1.12

Table 34. Derived results of series AC1.

Analysis of Adsorption	Series AC2	
CFU Conc. [#/ml] (· 10^6)	3.64	
Shear Stress [N·m^{-2}]:	.50	
Observed Adsorption CFU [#·mm^{-1}·min^{-1}]	27.29	
Observed Ads. Cells [#·mm^{-1}·min^{-1}]	47.61	
Other Important Parameters:		
Geometry of tube [mm]:		
Width:	4.00	
Half Height:	.09	
Transport Parameters:		
Diffusivity [mm^2·s^{-1}]	10^{-3}	
Viscosity [N·s·m^{-1}]	10^{-3}	
Adsorption and Transport CFU		
Adsorption coefficient ϵ:		.01134
Transport rate:		3190.16
Ratio Transp./ Adsorpt. [%]		.86
Adsorption and Transport Cells		
Adsorption coefficient ϵ:		.01992
Transport rate:		3190.16
Ratio Transp./ Adsorpt. [%]		1.49

Table 35. Derived results of series AC2.

Analysis of Adsorption	Series AC3	
CFU Conc. [#/ml] (· 10^6)	6.30	Adsorption and Transport CFU
Shear Stress [N·m^{-2}]:	.75	
		Adsorption coefficient ∈: .01021
Observed Adsorption CFU [#·mm^{-1}·min^{-1}]	42.61	Transport rate: 6320.46
Observed Ads. Cells [#·mm^{-1}·min^{-1}]	74.17	Ratio Transp./ Adsorpt. [%] .67
Other Important Parameters:		Adsorption and Transport Cells
Geometry of tube [mm]:		
Width:	4.00	Adsorption coefficient ∈: .01787
Half Height:	.09	Transport rate: 6320.46
		Ratio Transp./ Adsorpt. [%] 1.17
Transport Parameters:		
Diffusivity [mm^2·s^{-1}]	10^{-3}	
Viscosity [N·s·m^{-1}]	10^{-3}	

Table 36. Derived results of series AC3.

Analysis of Adsorption	Series AC4	
CFU Conc. [#/ml] (· 10^6)	8.70	Adsorption and Transport CFU
Shear Stress [N·m^{-2}]:	1.00	
		Adsorption coefficient ∈: .00716
Observed Adsorption CFU [#·mm^{-1}·min^{-1}]	41.33	Transport rate: 9606.68
Observed Ads. Cells [#·mm^{-1}·min^{-1}]	73.86	Ratio Transp./ Adsorpt. [%] .43
Other Important Parameters:		Adsorption and Transport Cells
Geometry of tube [mm]:		
Width:	4.00	Adsorption coefficient ∈: .01283
Half Height:	.09	Transport rate: 9606.68
		Ratio Transp./ Adsorpt. [%] .77
Transport Parameters:		
Diffusivity [mm^2·s^{-1}]	10^{-3}	
Viscosity [N·s·m^{-1}]	10^{-3}	

Table 37. Derived results of series AC4.

Analysis of Adsorption Series AC5

CFU Conc. [#/ml] ($\cdot 10^6$)	12.20	
Shear Stress [$N \cdot m^{-2}$]:	1.25	
Observed Adsorption CFU [$\# \cdot mm^{-1} \cdot min^{-1}$]	51.76	
Observed Ads. Cells [$\# \cdot mm^{-1} \cdot min^{-1}$]	80.40	
Other Important Parameters:		
Geometry of tube [mm]:		
Width:	4.00	
Half Height:	.09	
Transport Parameters:		
Diffusivity [$mm^2 \cdot s^{-1}$]	10^{-3}	
Viscosity [$N \cdot s \cdot m^{-1}$]	10^{-3}	

Adsorption and Transport CFU

Adsorption coefficient ϵ:	.00639
Transport rate:	14511.67
Ratio Transp./ Adsorpt. [%]	.36

Adsorption and Transport Cells

Adsorption coefficient ϵ:	.00994
Transport rate:	14511.67
Ratio Transp./ Adsorpt. [%]	.55

Table 38. Derived results of series AC5.

APPENDIX F

DISTRIBUTIONS OF "BEHAVIORAL" CHARACTERISTICS

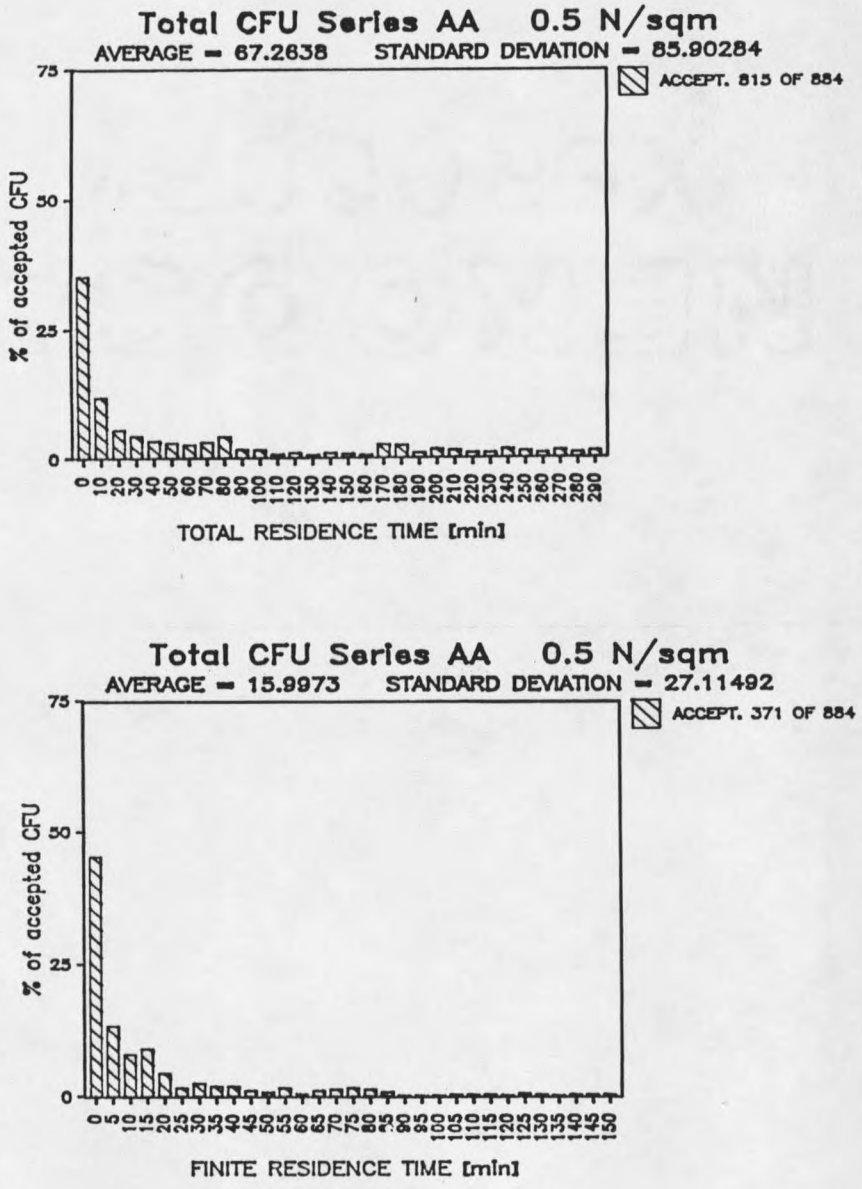

Figure 73. Residence time distribution Series AA (0.5 N m^{-2}). a: Total residence time distribution representing all CFU except the ones entering or exiting. b. Finite residence time of series AA. Only CFU were accepted where adsorption and desorption has directly been observed (no daughter-CFU, entering, exiting, or CFU exceeding last image of the experiments). This distribution represents for reversibly adsorbed CFU the probability in respect to time to remain at the substratum.

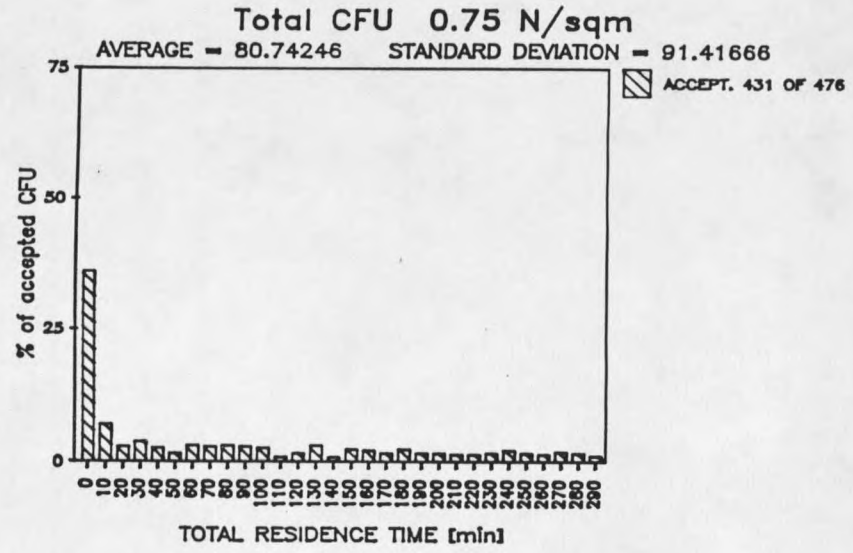

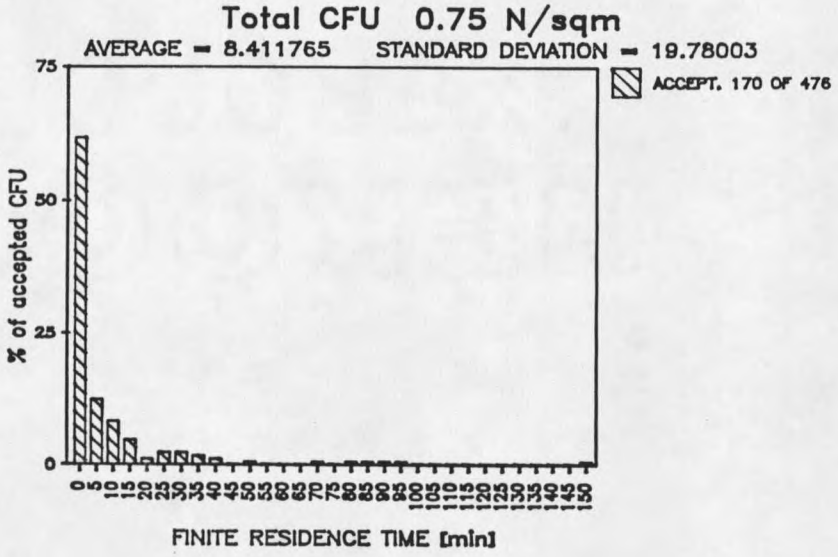

Figure 74. Residence time distribution (0.75 N m^{-2}). a: Total residence time distribution representing all CFU except the ones entering or exiting. b: Finite residence time. Only CFU were accepted where adsorption and desorption has directly been observed (no daughter-CFU, entering, exiting, or CFU exceeding last image of the experiments). This distribution represents for reversibly adsorbed CFU the probability in respect to time to remain at the substratum.

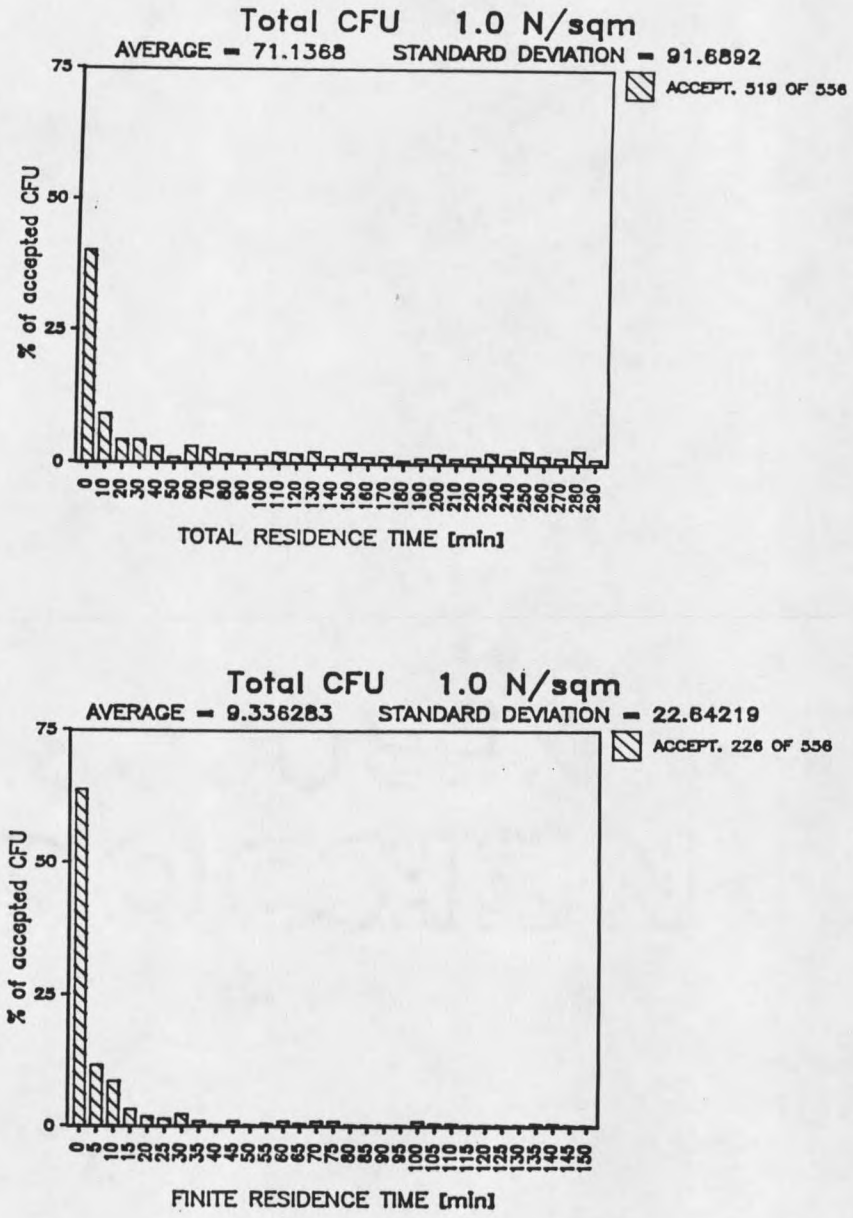

Figure 75. Residence time distribution (1.0 N m^{-2}). a: Total residence time distribution representing all CFU except the ones entering or exiting. b: Finite residence time. Only CFU were accepted where adsorption and desorption has directly been observed (no daughter-CFU, entering, exiting, or CFU exceeding last image of the experiments). This distribution represents for reversibly adsorbed CFU the probability in respect to time to remain at the substratum.

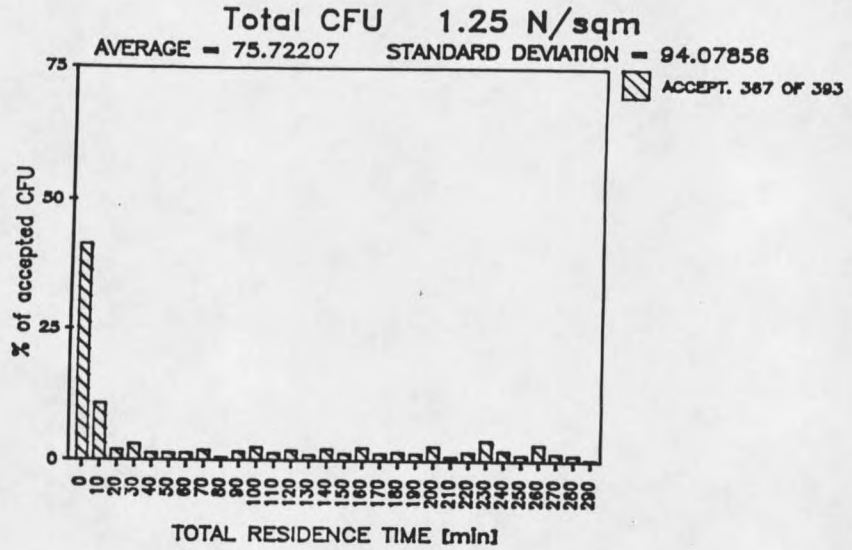

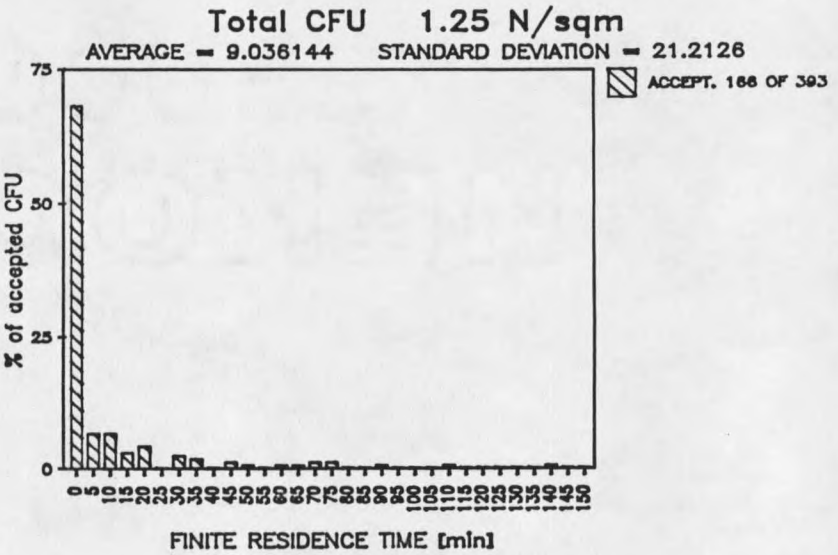

Figure 76. Residence time distribution (1.25 N m^{-2}). a: Total residence time distribution representing all CFU except the ones entering or exiting. b: Finite residence time. Only CFU were accepted where adsorption and desorption has directly been observed (no daughter-CFU, entering, exiting, or CFU exceeding last image of the experiments). This distribution represents for reversibly adsorbed CFU the probability in respect to time to remain at the substratum.

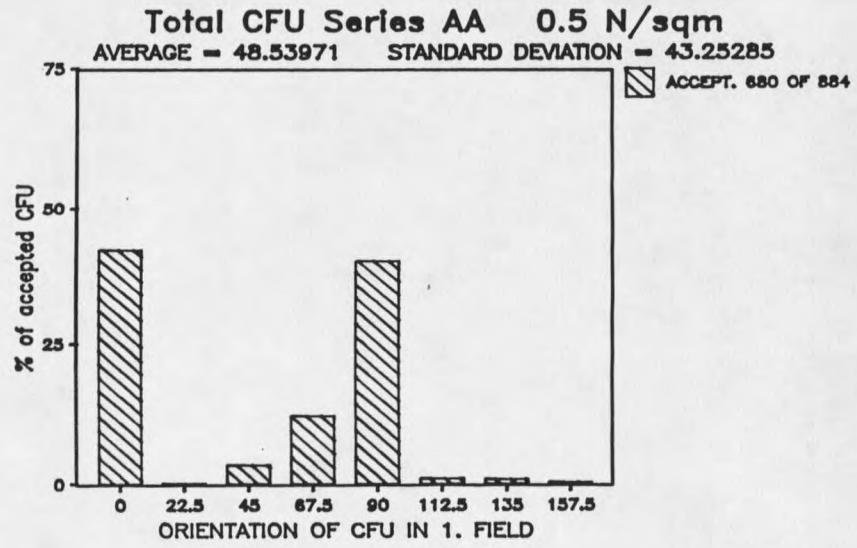

Figure 77. Orientation of CFU after adsorption. Shear stress: 0.5 N/m². Direction of flow: 90°.

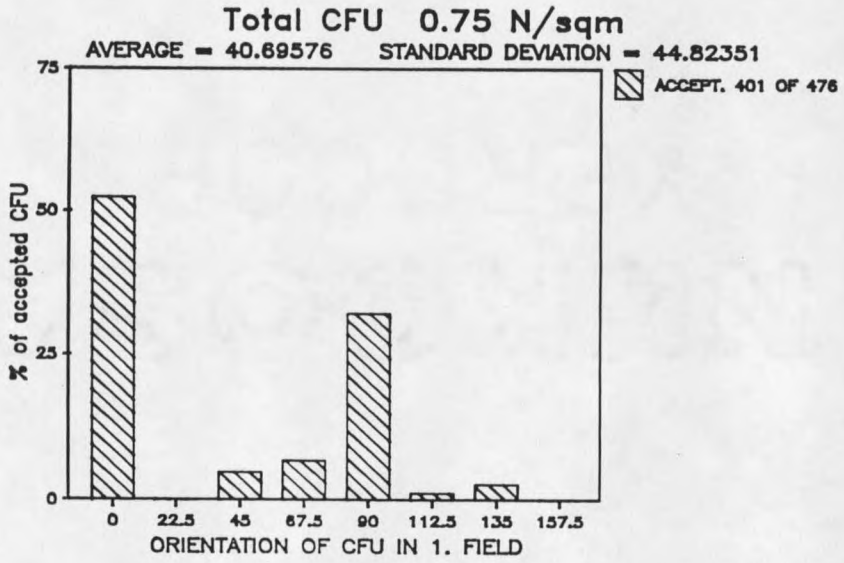

Figure 78. Orientation of CFU after adsorption. Shear stress: 0.75 N/m². Direction of flow: 90°.

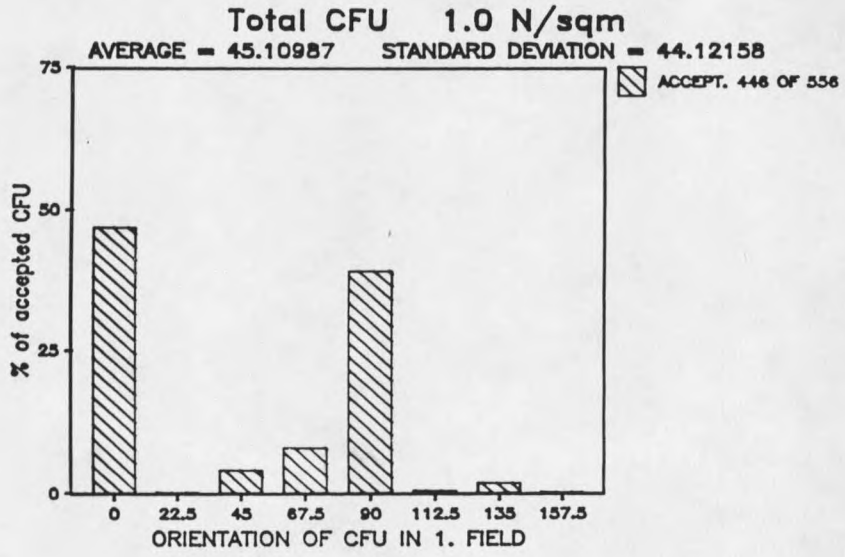

Figure 79. Orientation of CFU after adsorption. Shear stress: 1.0 N/m². Direction of flow: 90°.

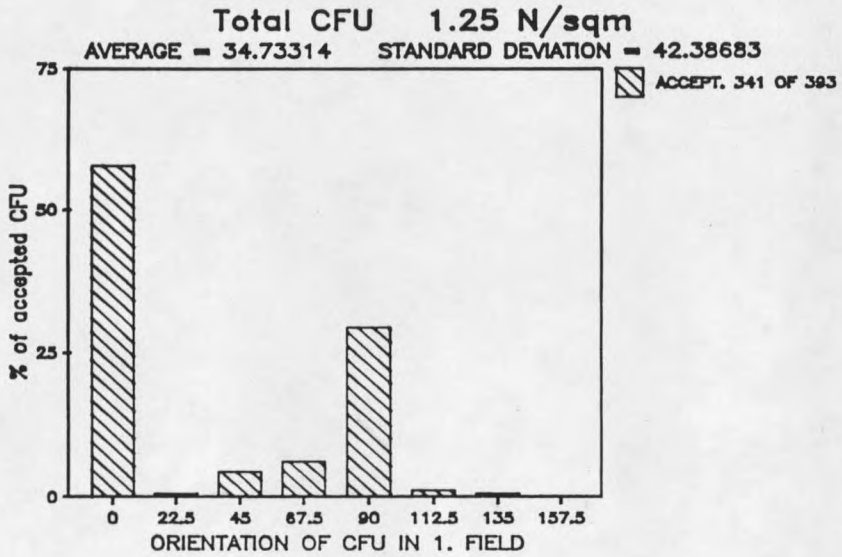

Figure 80. Orientation of CFU after adsorption. Shear stress: 1.25 N/m². Direction of flow: 90°.

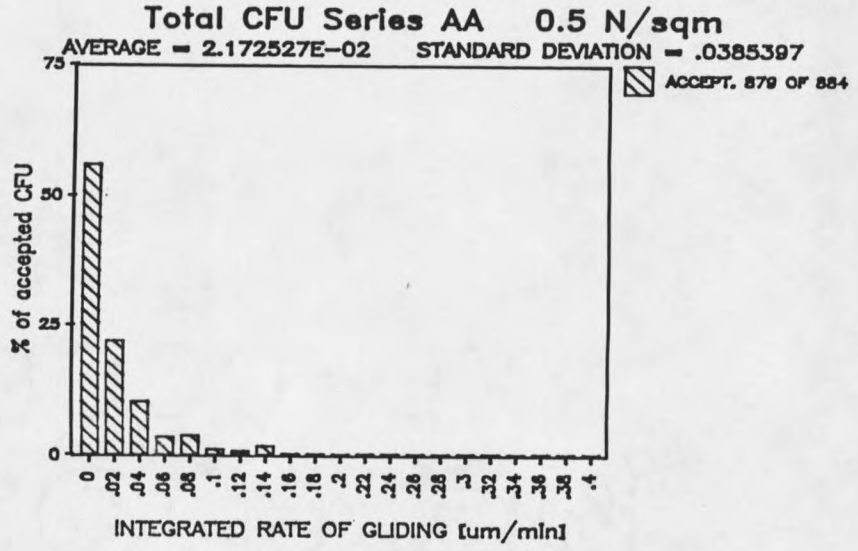

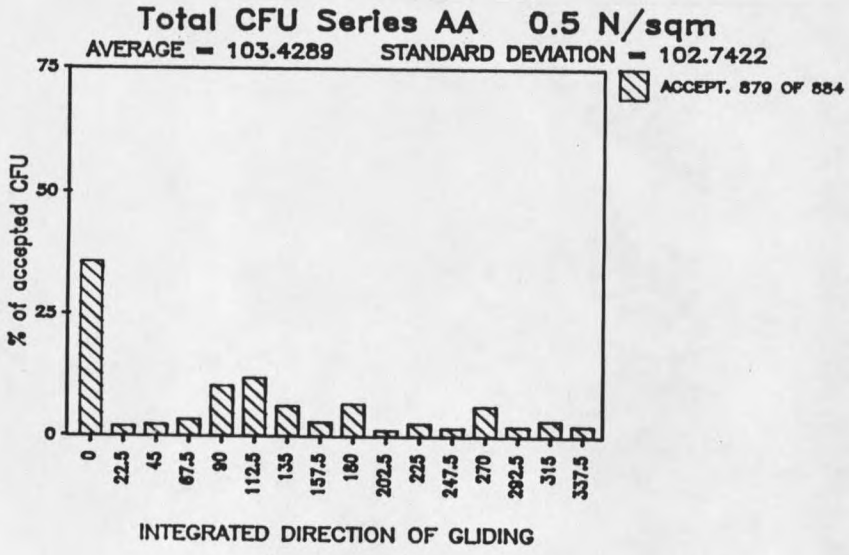

Figure 81. Integrated movement at substratum (Series AA, 0.5 N m^{-2}). a: Integrated rate of gliding of CFU in Series AA. Minimum residence time for this distribution is 15 min. b: Integrated direction of gliding of CFU at substratum. 0° degree direction is associated with no motion. Direction of flow: 90°.

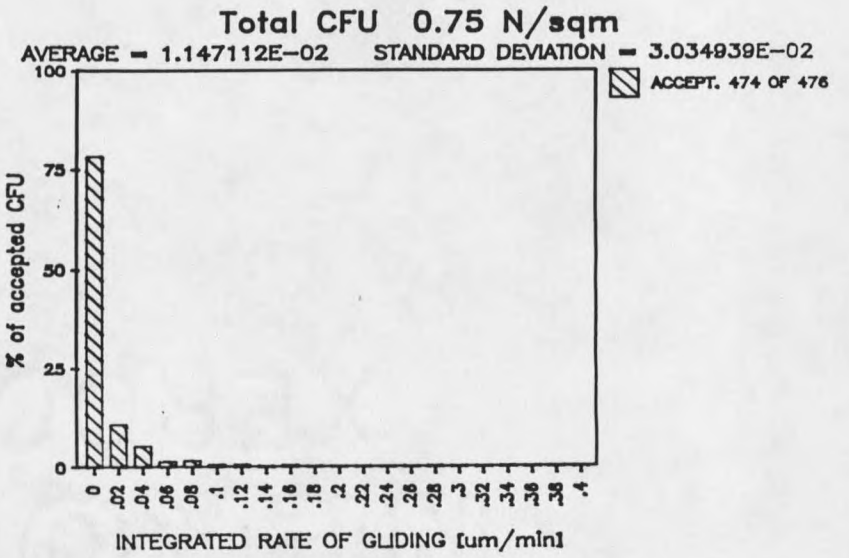

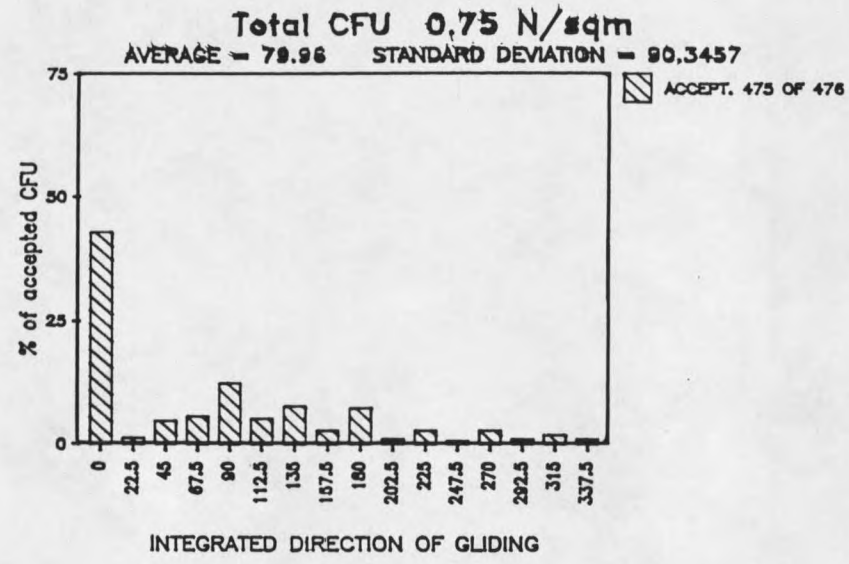

Figure 82. Integrated movement at substratum (0.75 N m^{-2}).
a: Integrated rate of gliding of CFU in Series AA. Minimum residence time for this distribution is 15 min.
b: Integrated direction of gliding of CFU at substratum. 0° degree direction is associated with no motion. Direction of flow: 90°.

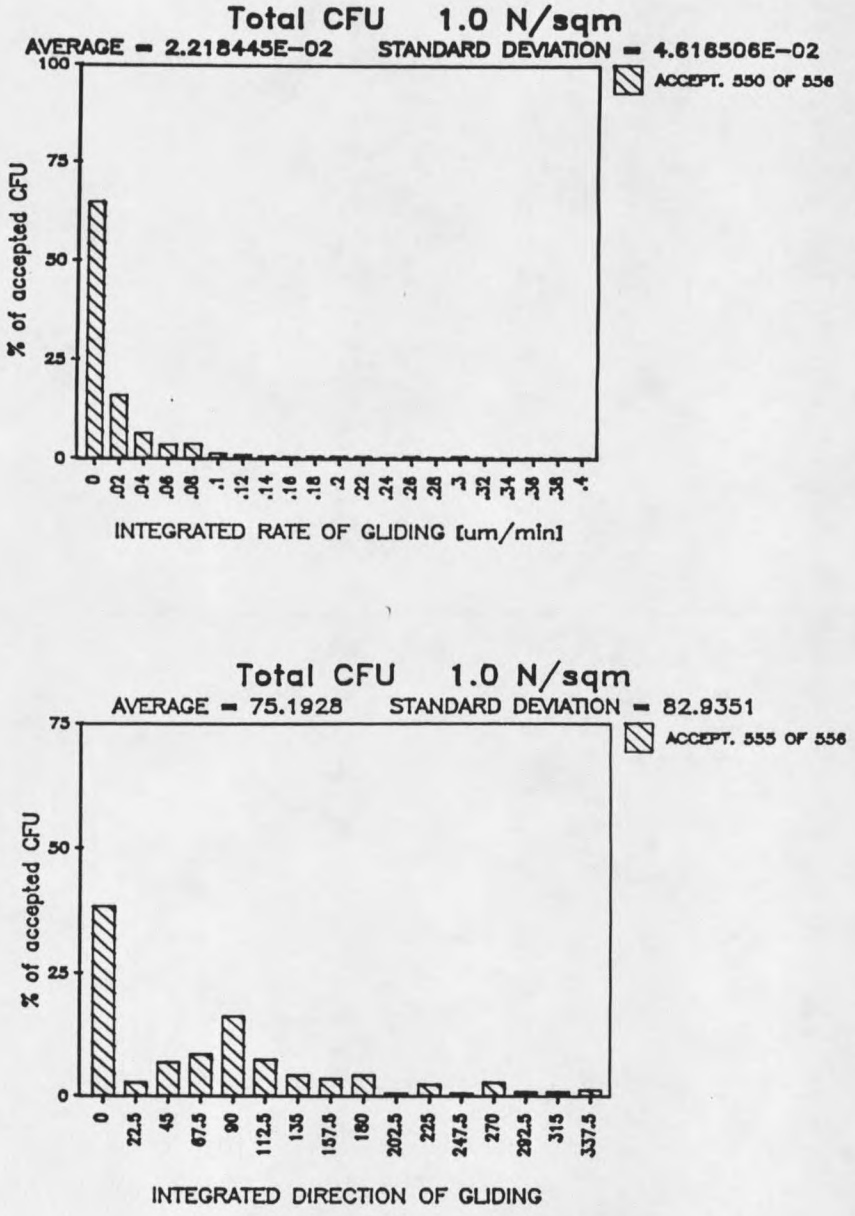

Figure 83. Integrated movement at substratum (1.0 N m^{-2}).
a: Integrated rate of gliding of CFU in Series AA. Minimum residence time for this distribution is 15 min.
b: Integrated direction of gliding of CFU at substratum. 0° degree direction is associated with no motion. Direction of flow: 90°.

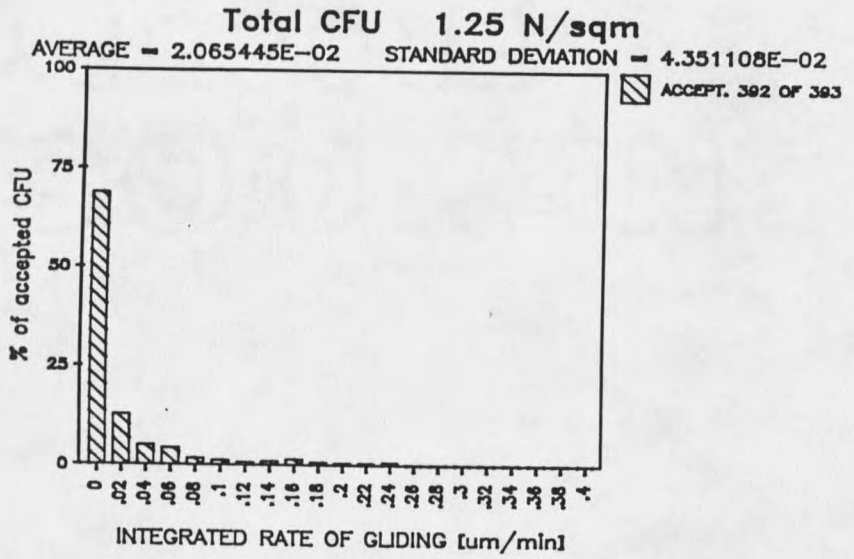

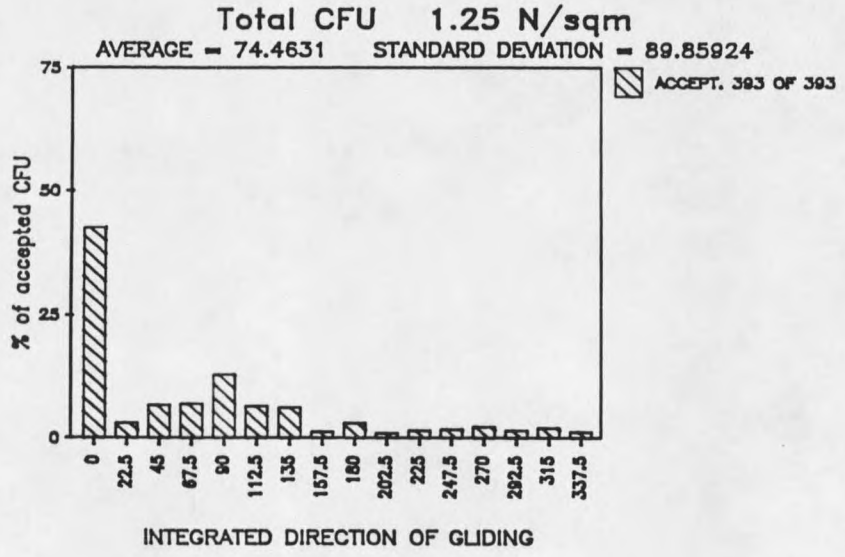

Figure 84. Integrated movement at substratum (1.25 N m^{-2}).
a: Integrated rate of gliding of CFU in Series AA. Minimum residence time for this distribution is 15 min.
b: Integrated direction of gliding of CFU at substratum. 0° degree direction is associated with no motion. Direction of flow: 90°.

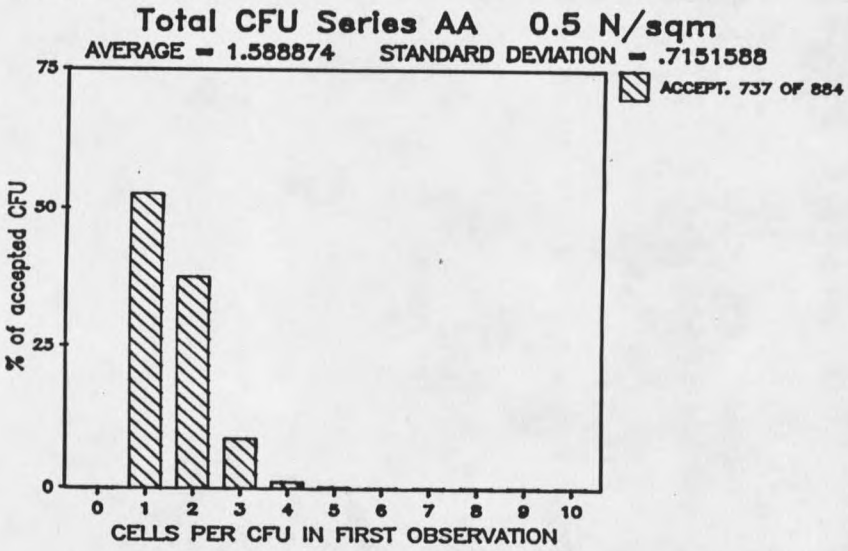

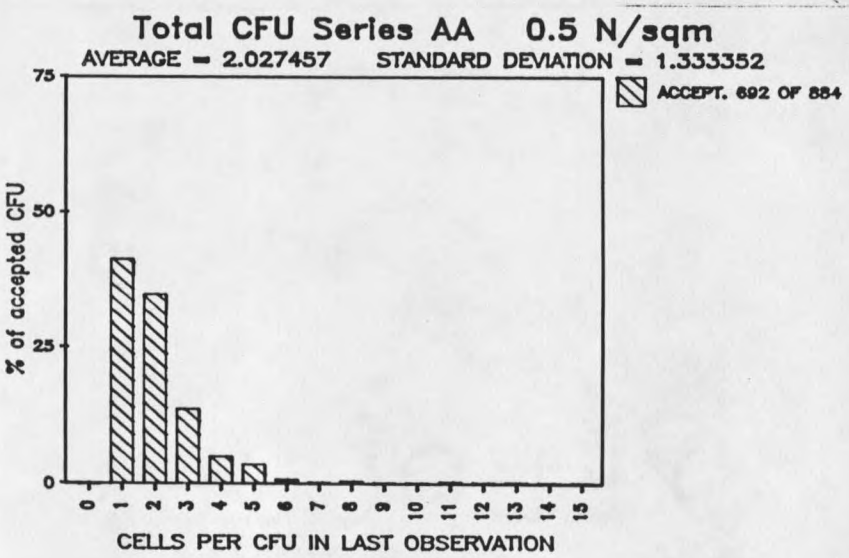

Figure 85. Cells per CFU (Series AA, 0.5 N m^{-2}).
a: Number of cells per CFU during first observation.
b: Number of cells per CFU during last observation.

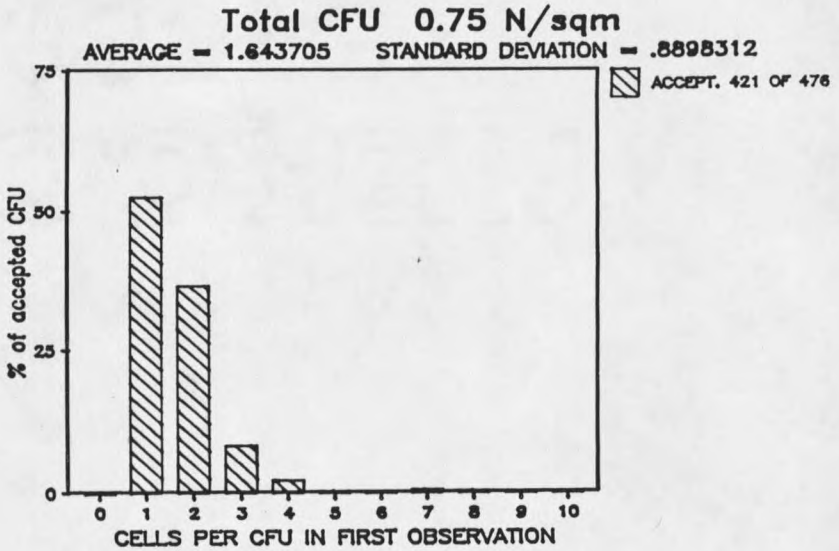

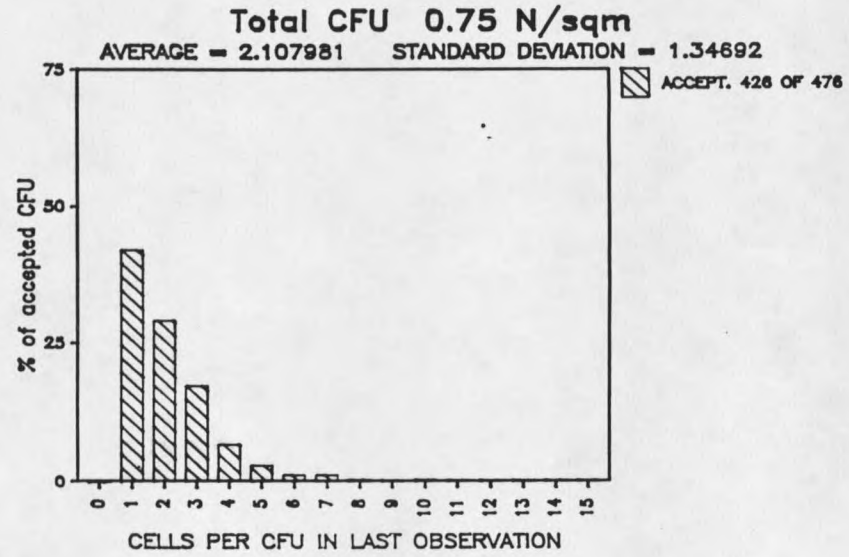

Figure 86. Cells per CFU (0.75 N m^{-2}). a: Number of cells per CFU during first observation. b: Number of cells per CFU during last observation.

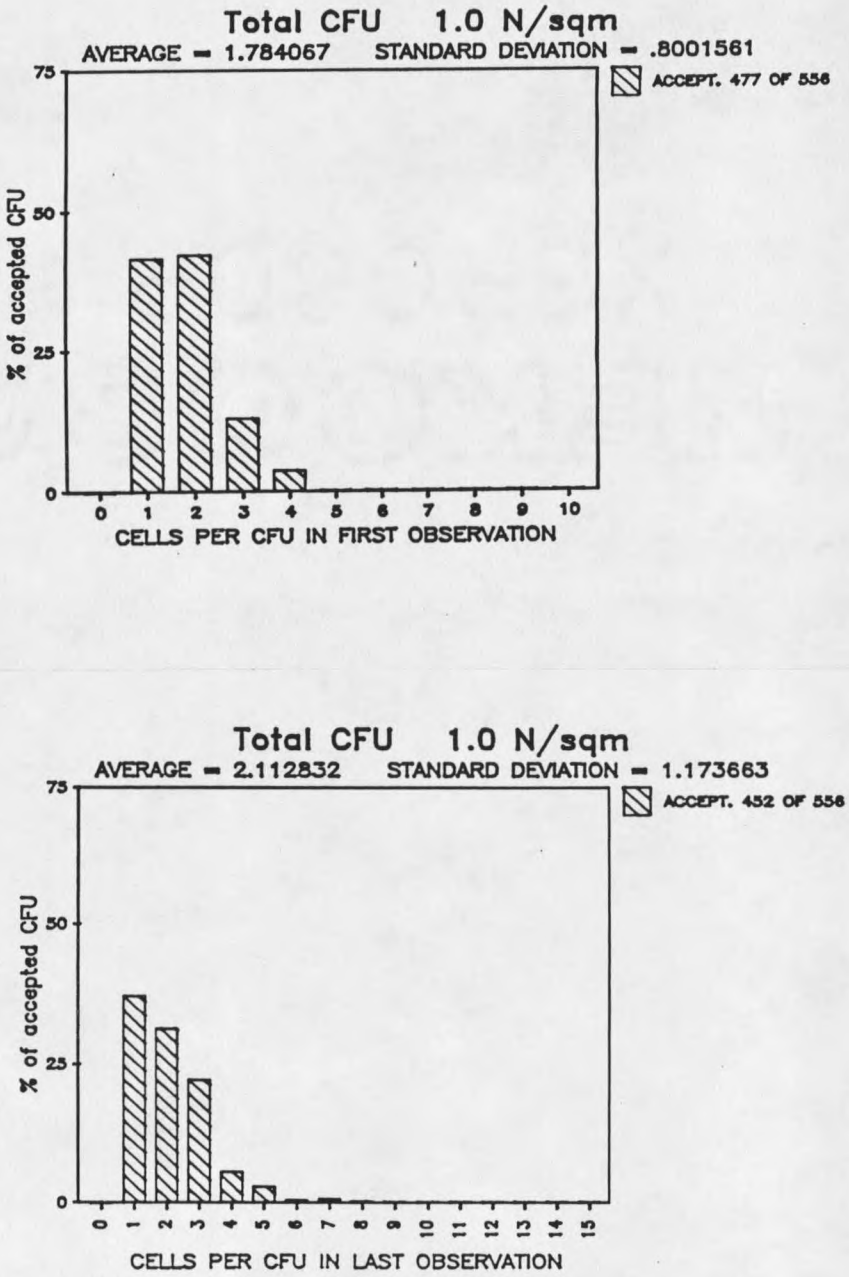

Figure 87. Cells per CFU (1.0 N m^{-2}). a: Number of cells per CFU during first observation. b: Number of cells per CFU during last observation.

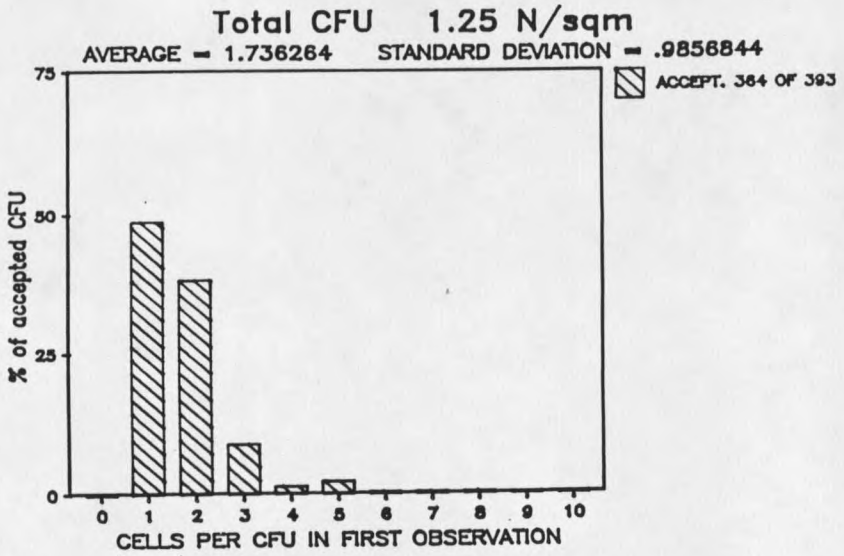

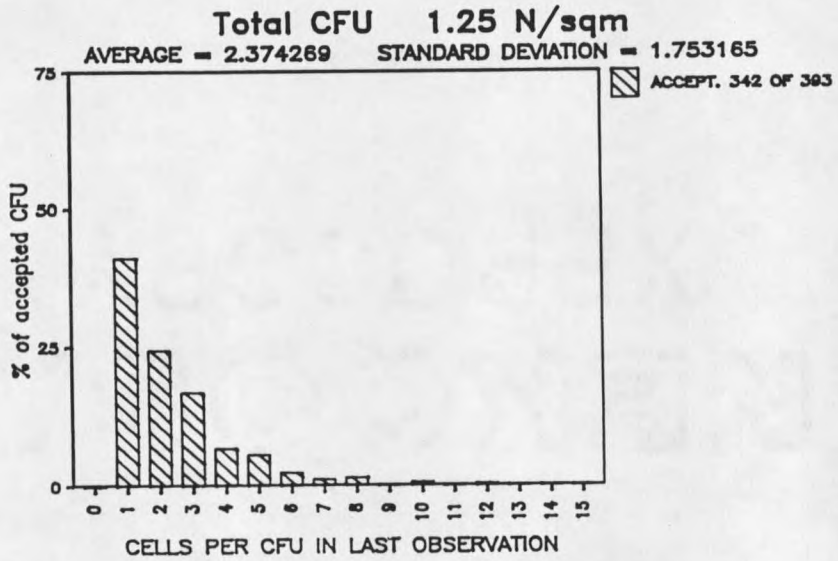

Figure 88. Cells per CFU (1.25 N m^{-2}). a: Number of cells per CFU during first observation. b: Number of cells per CFU during last observation.

APPENDIX G

RESULTS OF SPATIAL DISTRIBUTIONS

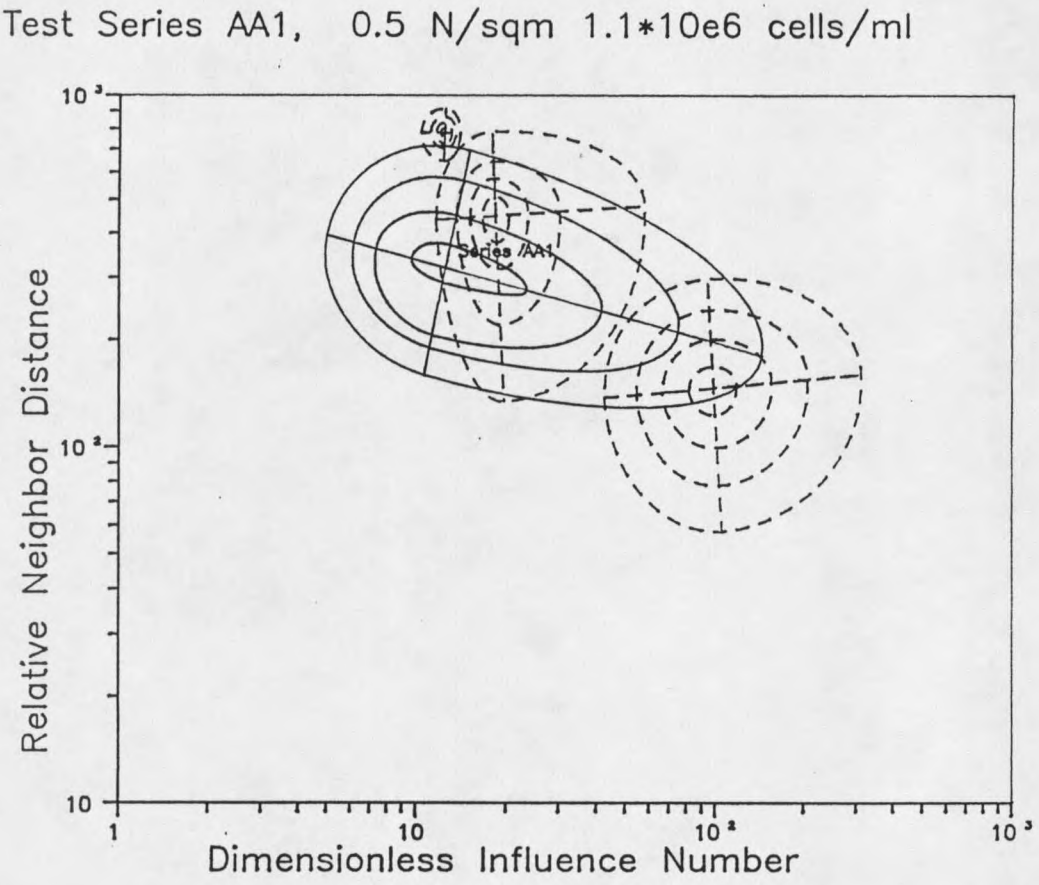

Figure 89. Spatial distribution of adsorbing CFU, Series AA1. The measured distribution is superimposed on the calibration distributions (dotted lines). The calibration distribution in the upper left is for uniform, in the center for random, and in the lower right for aggregated.

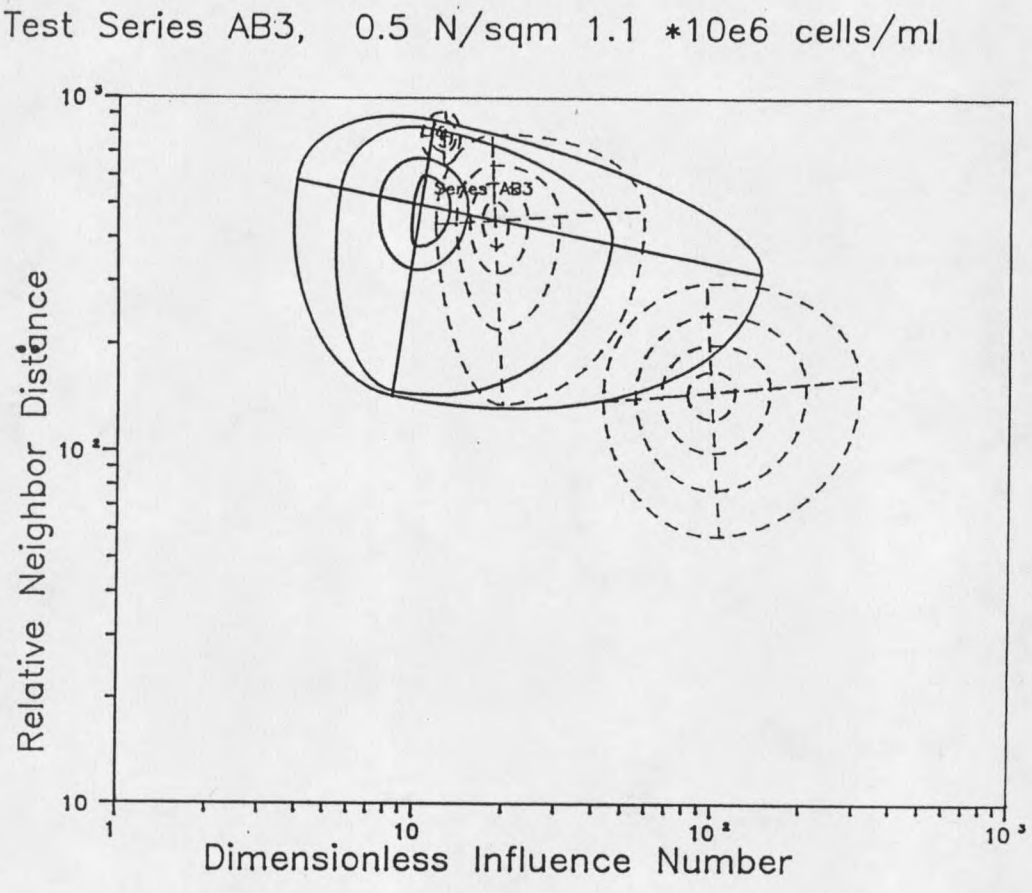

Figure 90. Spatial distribution of adsorbing CFU, Series AB3. The measured distribution is superimposed on the calibration distributions (dotted lines). The calibration distribution in the upper left is for uniform, in the center for random, and in the lower right for aggregated.

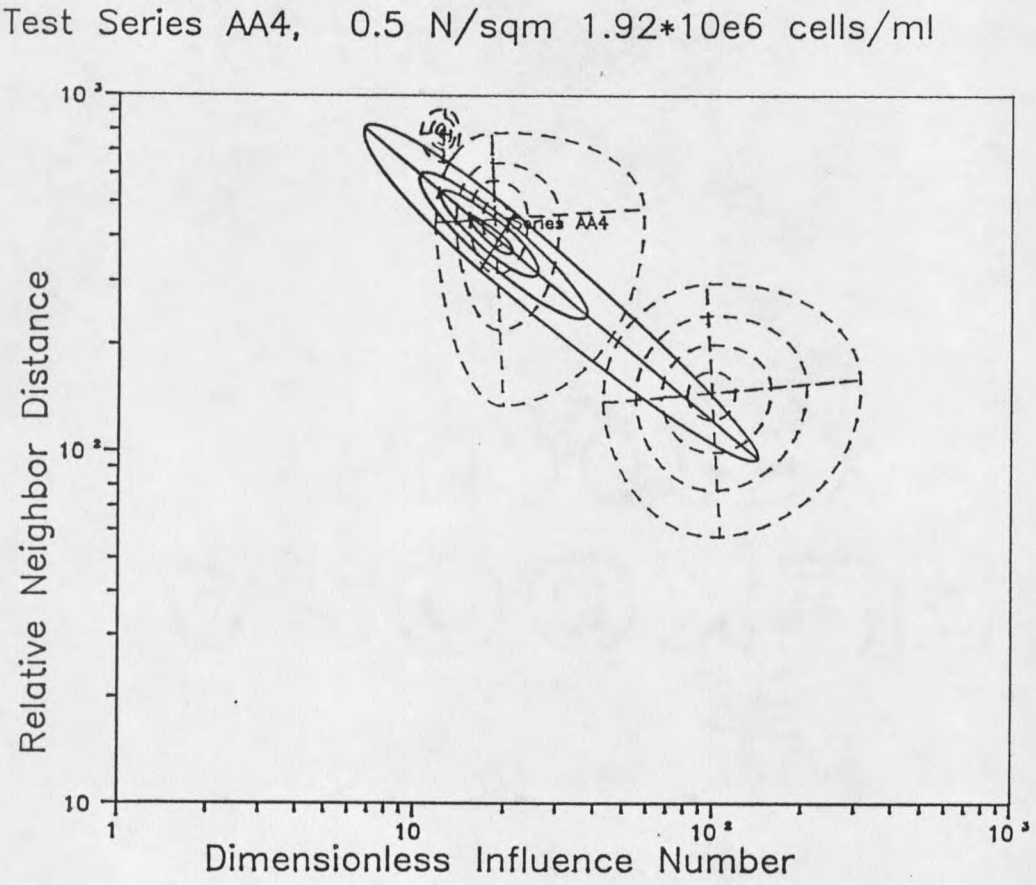

Figure 91. Spatial distribution of adsorbing CFU, Series AA4. The measured distribution is superimposed on the calibration distributions (dotted lines). The calibration distribution in the upper left is for uniform, in the center for random, and in the lower right for aggregated.

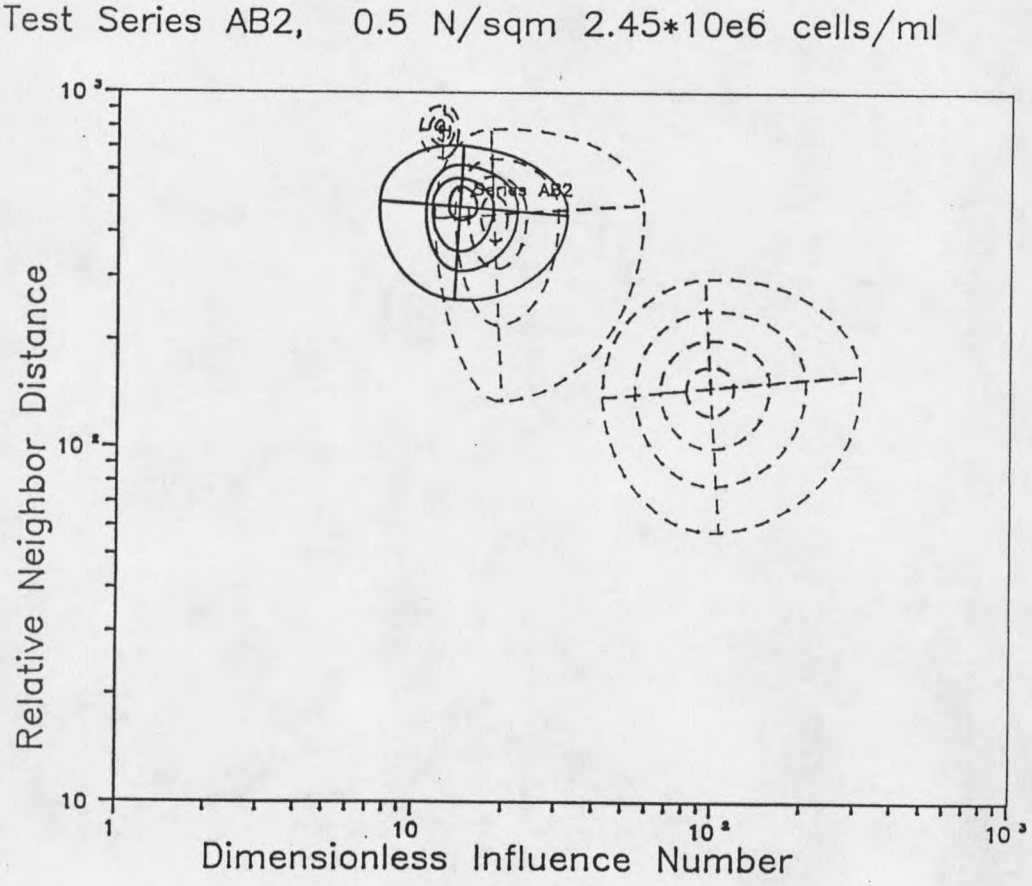

Figure 92. Spatial distribution of adsorbing CFU, Series AB2. The measured distribution is superimposed on the calibration distributions (dotted lines). The calibration distribution in the upper left is for uniform, in the center for random, and in the lower right for aggregated.

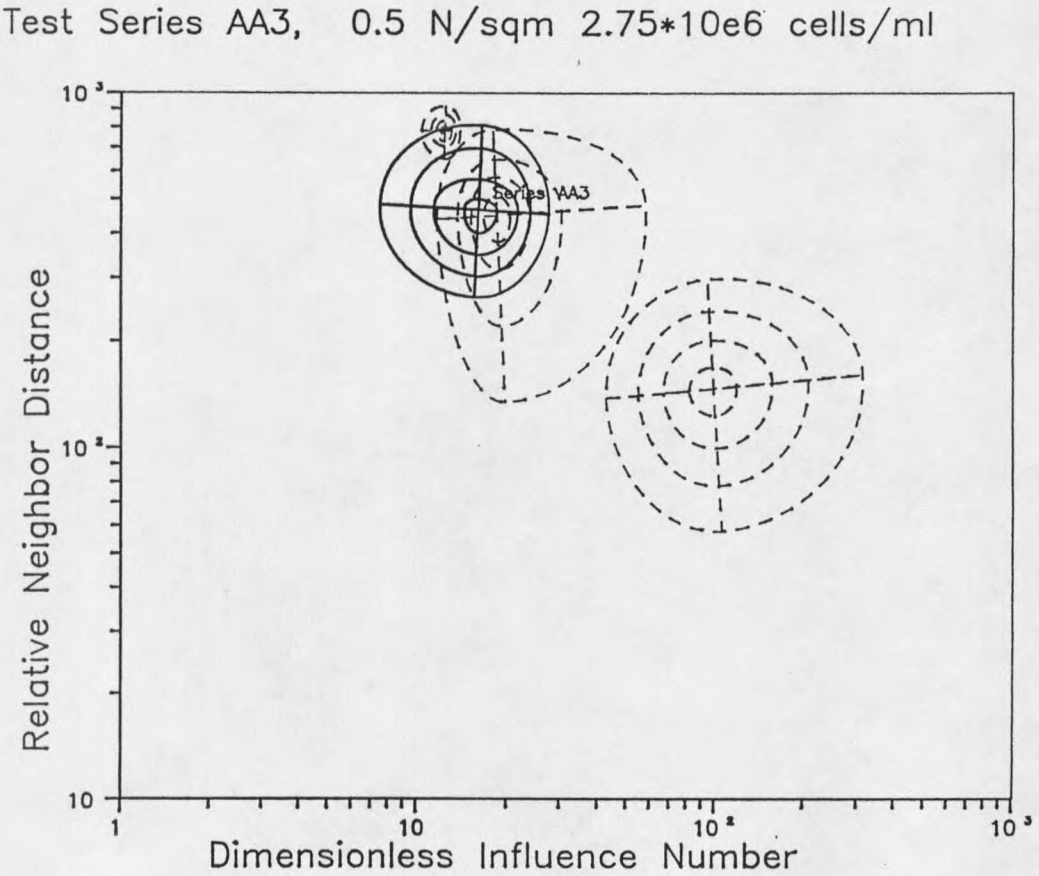

Figure 93. Spatial distribution of adsorbing CFU, Series AA3. The measured distribution is superimposed on the calibration distributions (dotted lines). The calibration distribution in the upper left is for uniform, in the center for random, and in the lower right for aggregated.

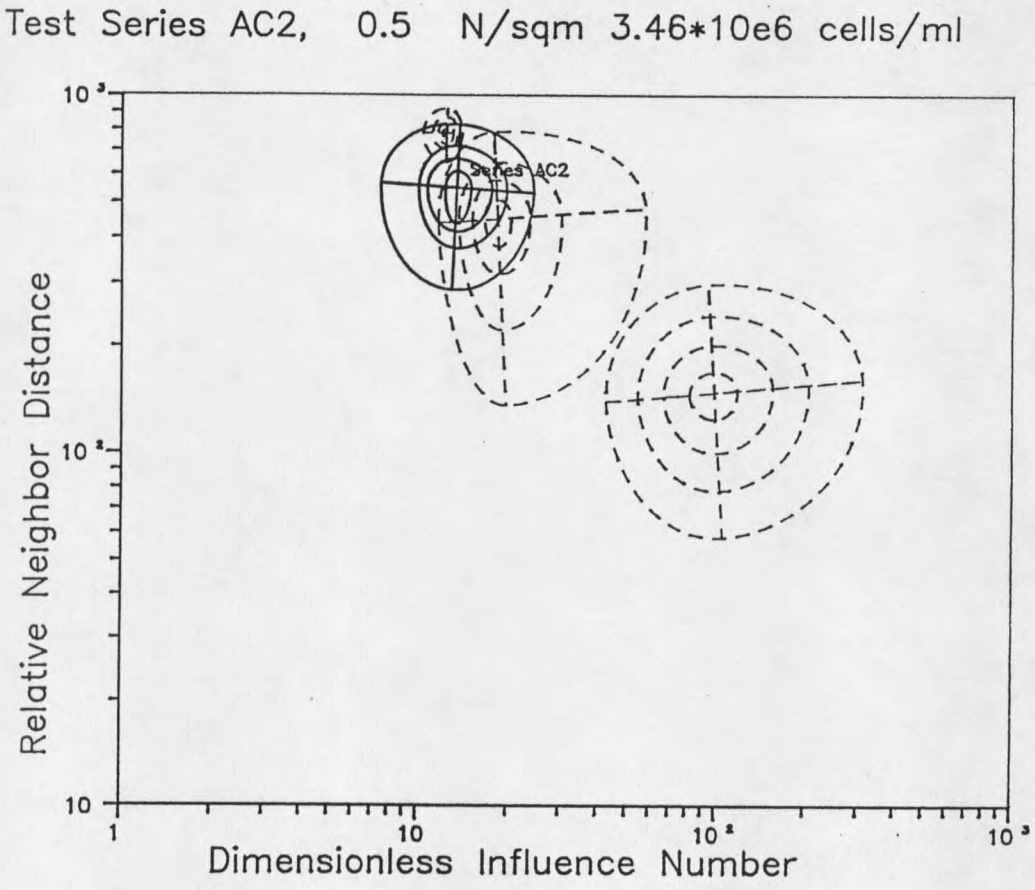

Figure 94. Spatial distribution of adsorbing CFU, Series AC2. The measured distribution is superimposed on the calibration distributions (dotted lines). The calibration distribution in the upper left is for uniform, in the center for random, and in the lower right for aggregated.

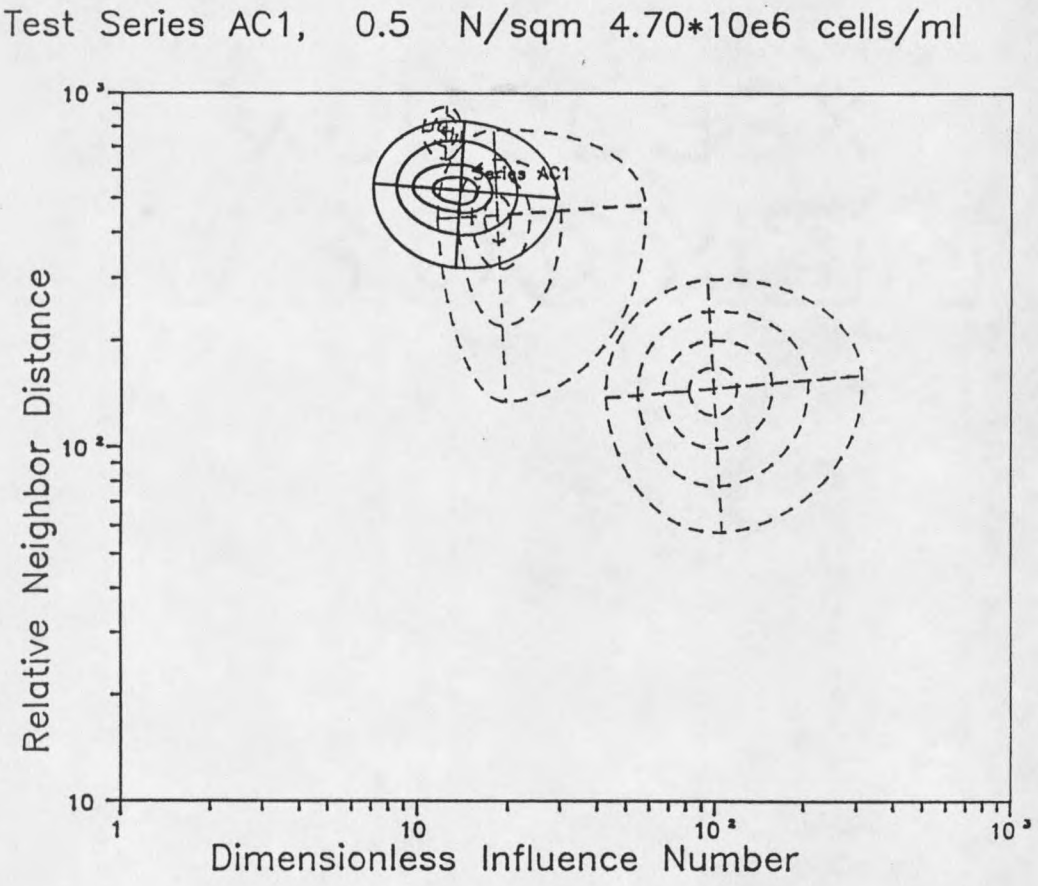

Figure 95. Spatial distribution of adsorbing CFU, Series AC1. The measured distribution is superimposed on the calibration distributions (dotted lines). The calibration distribution in the upper left is for uniform, in the center for random, and in the lower right for aggregated.

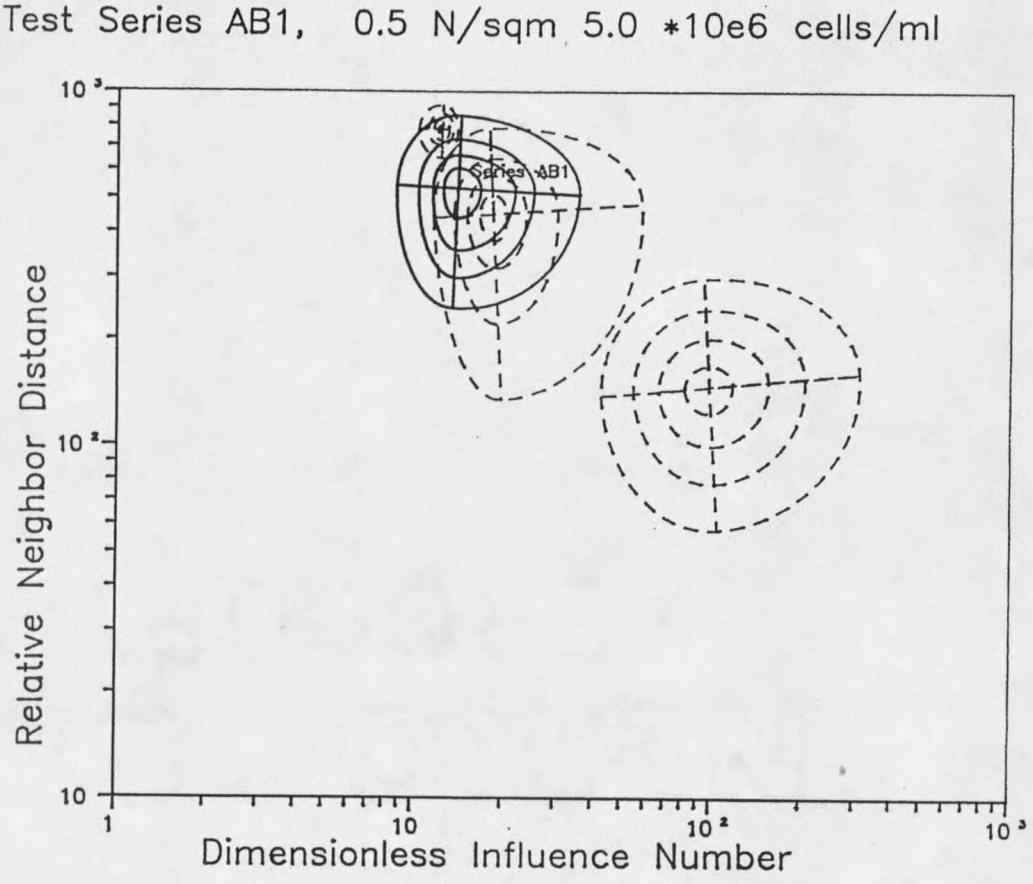

Figure 96. Spatial distribution of adsorbing CFU, Series AB1. The measured distribution is superimposed on the calibration distributions (dotted lines). The calibration distribution in the upper left is for uniform, in the center for random, and in the lower right for aggregated.

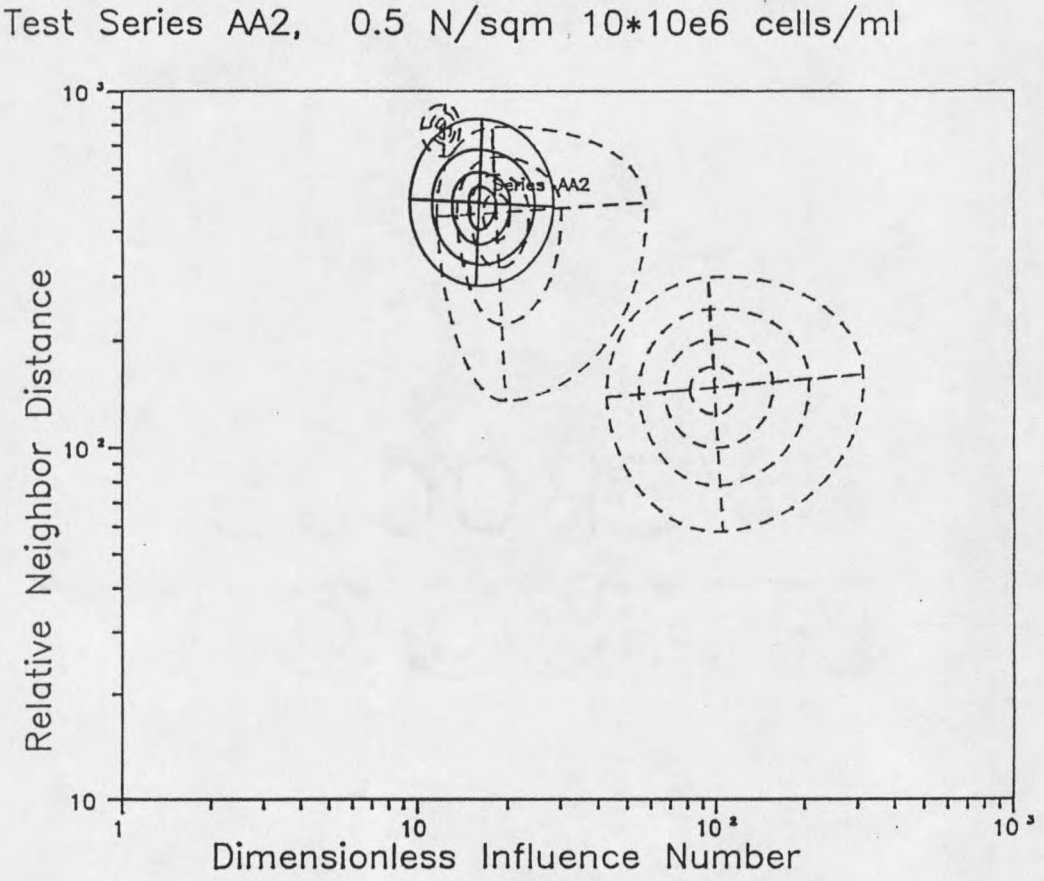

Figure 97. Spatial distribution of adsorbing CFU, Series AA2. The measured distribution is superimposed on the calibration distributions (dotted lines). The calibration distribution in the upper left is for uniform, in the center for random, and in the lower right for aggregated.

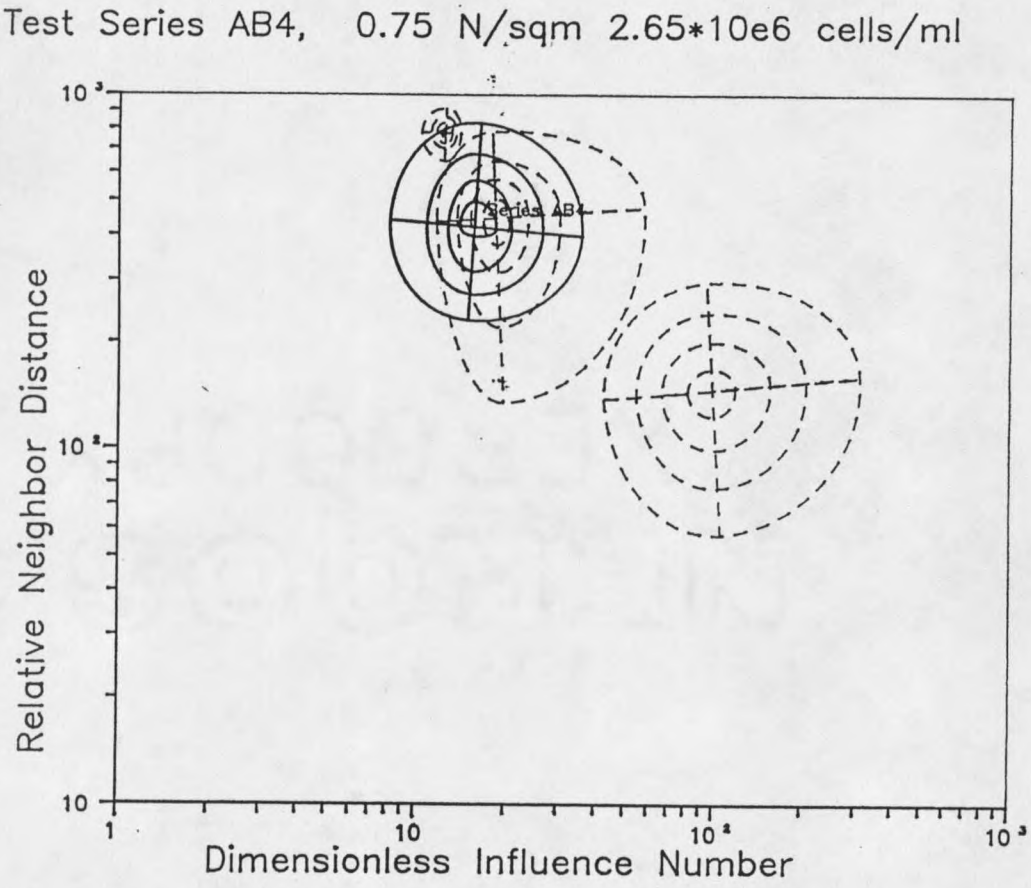

Figure 98. Spatial distribution of adsorbing CFU, Series AB4. The measured distribution is superimposed on the calibration distributions (dotted lines). The calibration distribution in the upper left is for uniform, in the center for random, and in the lower right for aggregated.

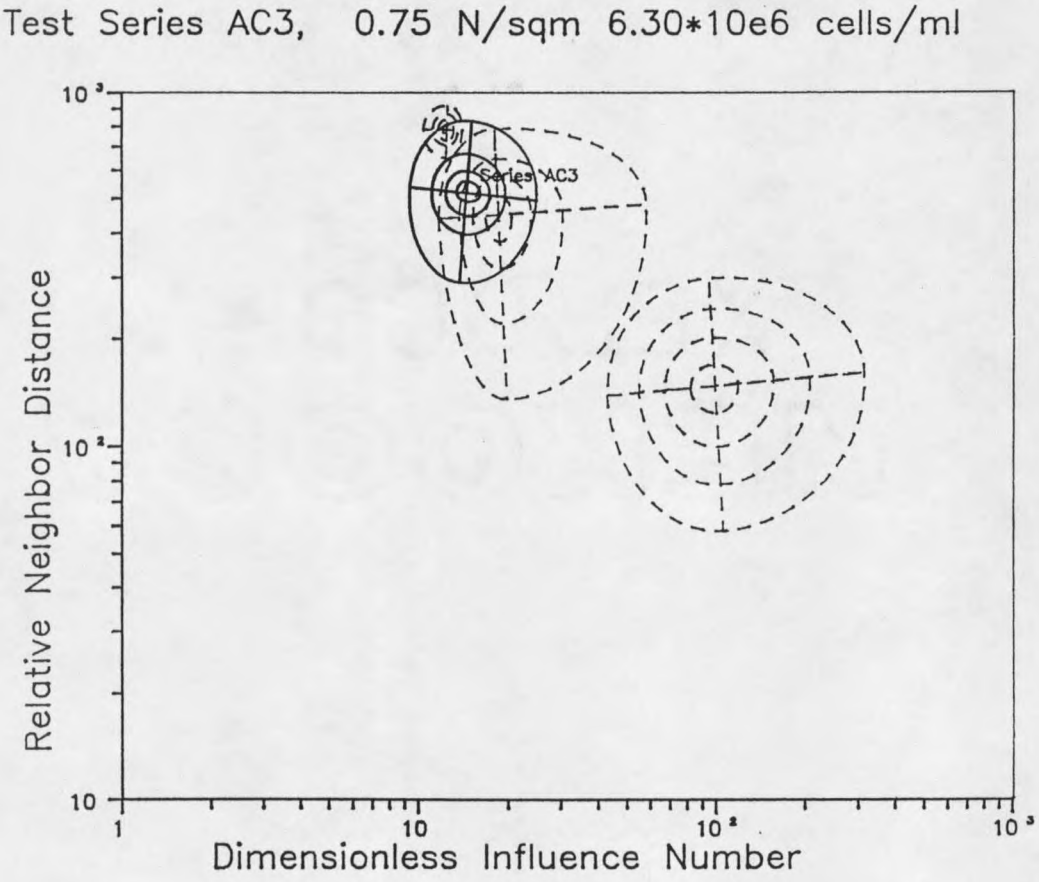

Figure 99. Spatial distribution of adsorbing CFU, Series AC3. The measured distribution is superimposed on the calibration distributions (dotted lines). The calibration distribution in the upper left is for uniform, in the center for random, and in the lower right for aggregated.

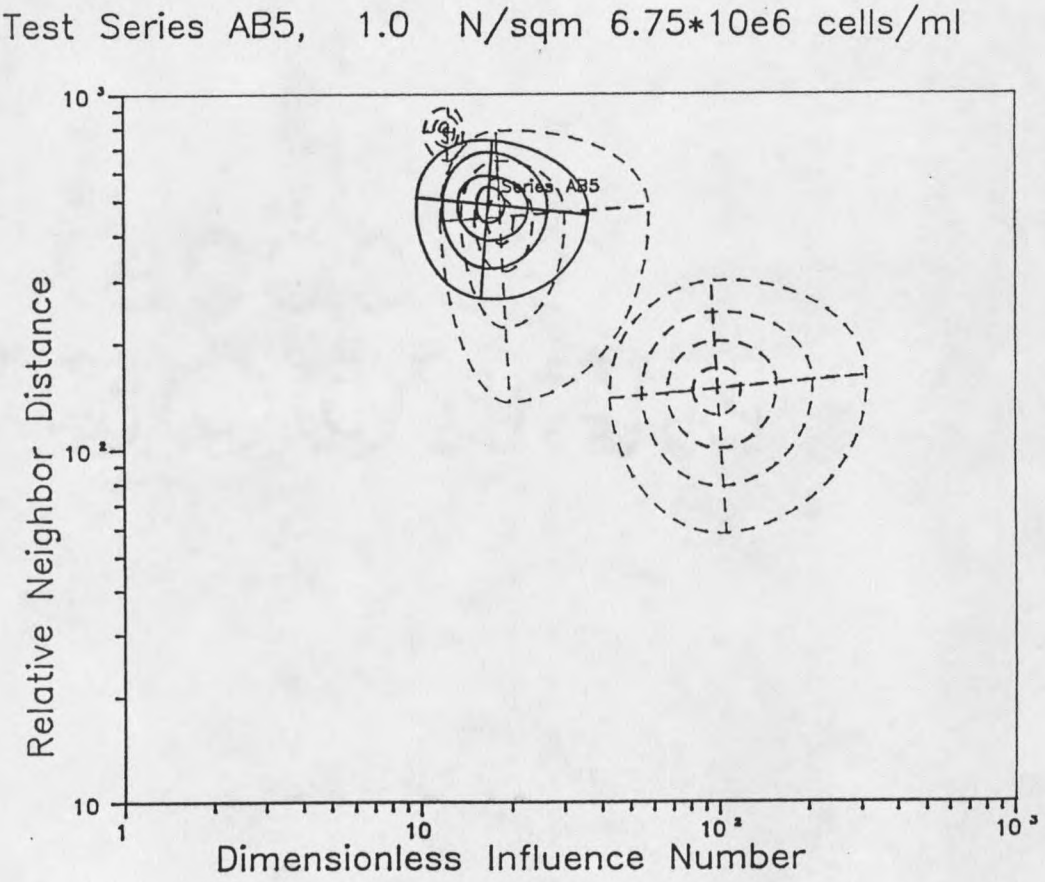

Figure 100. Spatial distribution of adsorbing CFU, Series AB5. The measured distribution is superimposed on the calibration distributions (dotted lines). The calibration distribution in the upper left is for uniform, in the center for random, and in the lower right for aggregated.

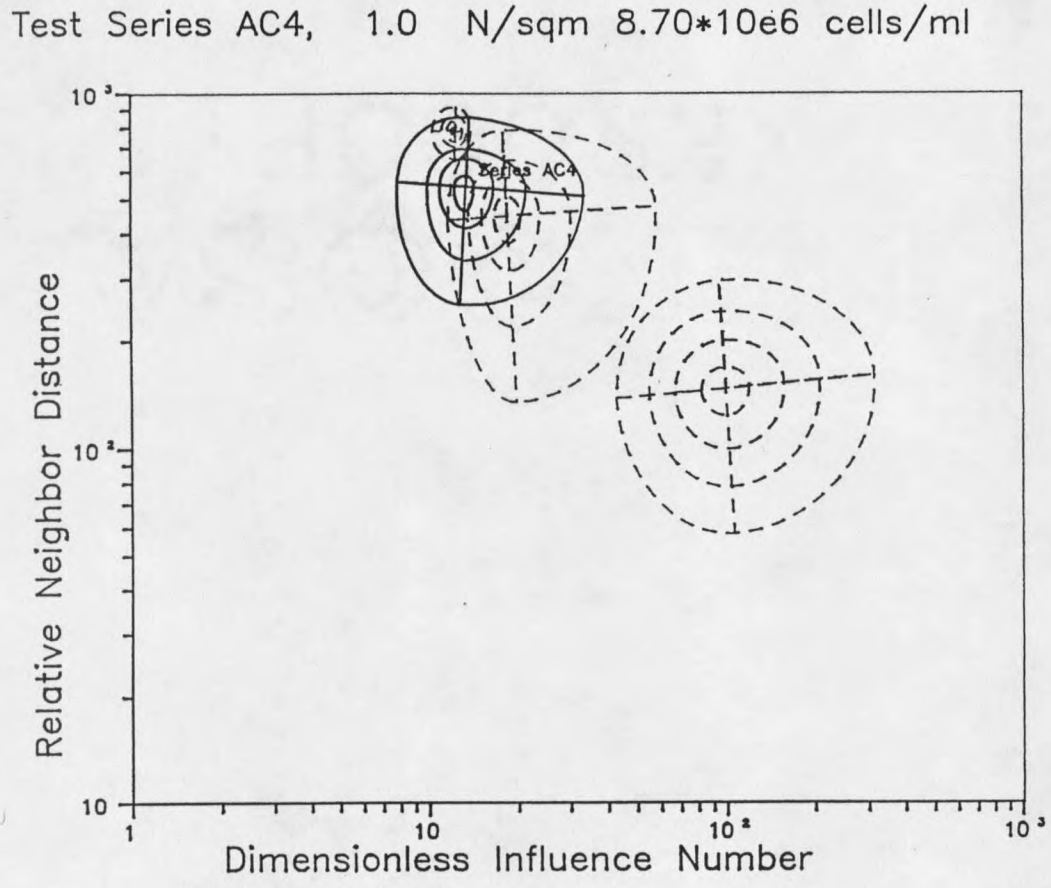

Figure 101. Spatial distribution of adsorbing CFU, Series AC4. The measured distribution is superimposed on the calibration distributions (dotted lines). The calibration distribution in the upper left is for uniform, in the center for random, and in the lower right for aggregated.

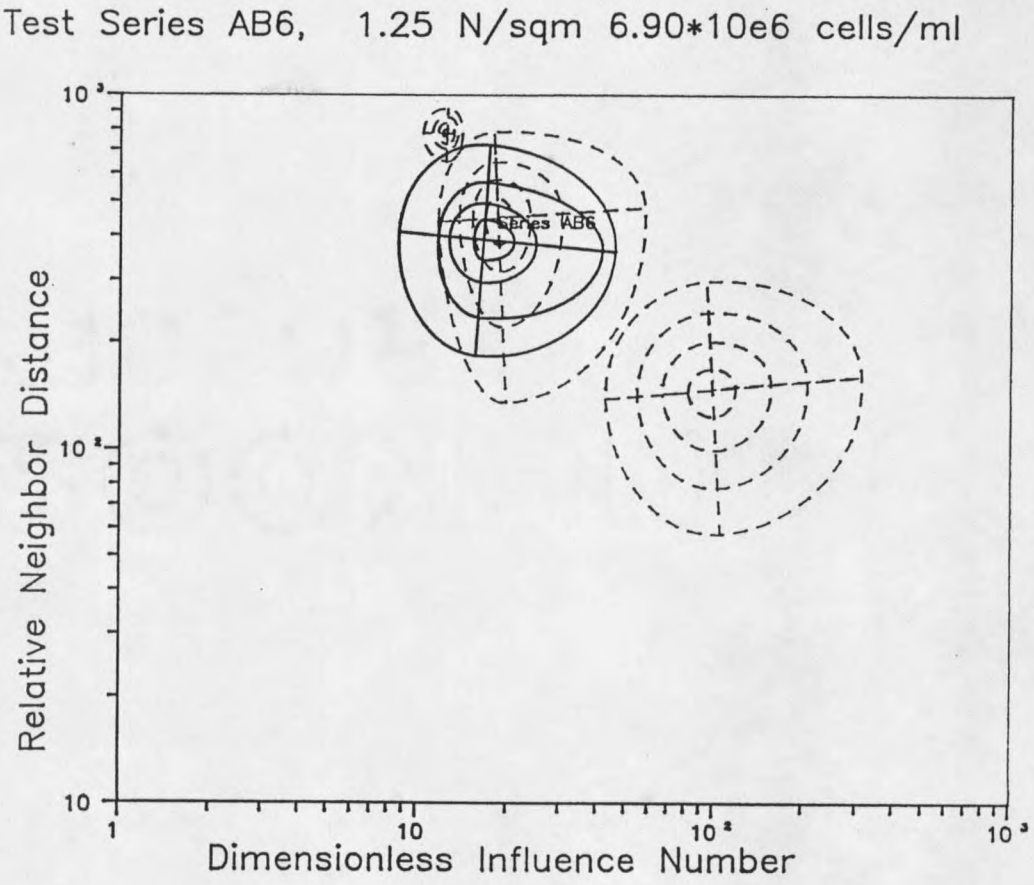

Figure 102. Spatial distribution of adsorbing CFU, Series AB6. The measured distribution is superimposed on the calibration distributions (dotted lines). The calibration distribution in the upper left is for uniform, in the center for random, and in the lower right for aggregated.

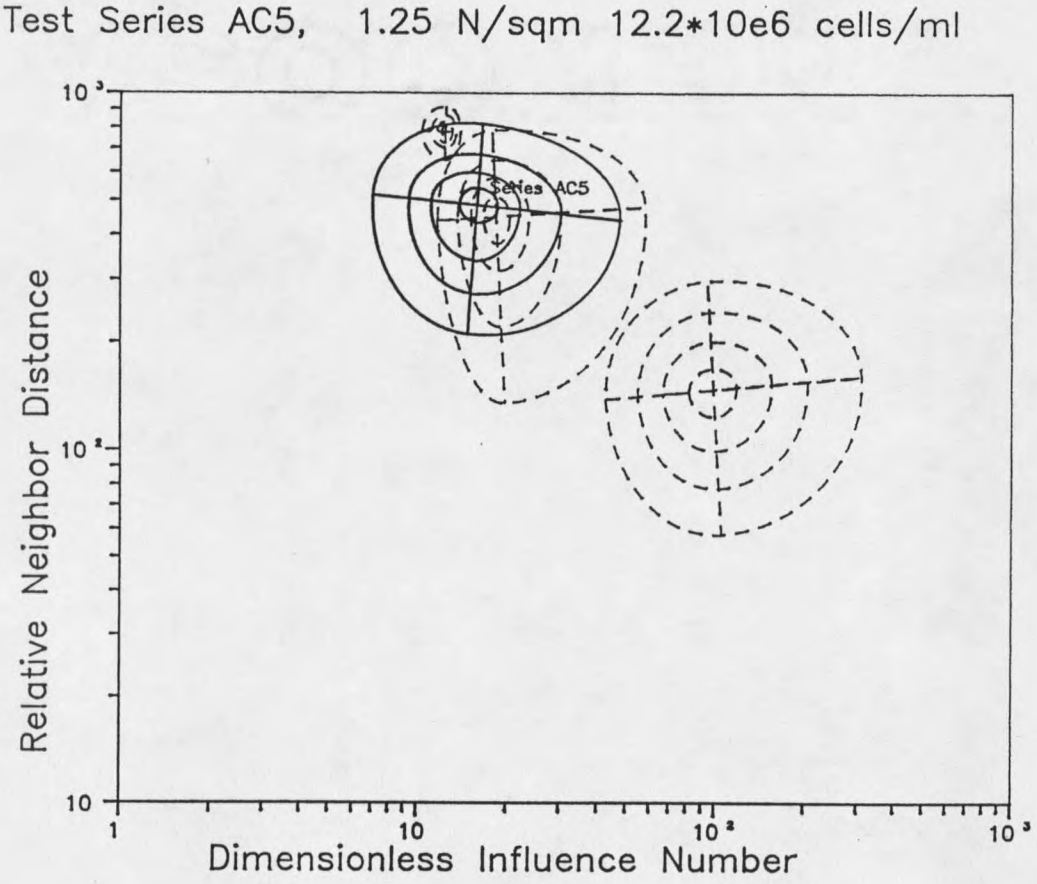

Figure 103. Spatial distribution of adsorbing CFU, Series AC5. The measured distribution is superimposed on the calibration distributions (dotted lines). The calibration distribution in the upper left is for uniform, in the center for random, and in the lower right for aggregated.